



Standardization of Highly Polymer-Modified Asphalt Mixtures (HPMix)

**Normierung von hoch polymermodifizierte
Asphaltbelägen (HPMix)**

**Normalisation des mélanges bitumineux hautement
modifiés par des polymères (HPMix)**

Empa

Dr. Martins Zaumanis

Dr. Martin Arraigada

Canton GR

Gion Dosch

Canton AG

Olga Paperna

Der Inhalt dieses Berichtes verpflichtet nur den (die) vom Bundesamt für Strassen unterstützten Autor(en). Dies gilt nicht für das Formular 3 "Projektabschluss", welches die Meinung der Begleitkommission darstellt und deshalb nur diese verpflichtet. Bezug: Schweizerischer Verband der Strassen- und Verkehrsfachleute (VSS)

Le contenu de ce rapport n'engage que les auteurs ayant obtenu l'appui de l'Office fédéral des routes. Cela ne s'applique pas au formulaire 3 « Clôture du projet », qui représente l'avis de la commission de suivi et qui n'engage que cette dernière. Diffusion: Association suisse des professionnels de la route et des transports (VSS)

La responsabilità per il contenuto di questo rapporto spetta unicamente agli autori sostenuti dall'Ufficio federale delle strade. Tale indicazione non si applica al modulo 3 "conclusione del progetto", che esprime l'opinione della commissione d'accompagnamento e di cui risponde solo quest'ultima. Ordinazione: Associazione svizzera dei professionisti della strada e dei trasporti (VSS)

The content of this report engages only the author(s) supported by the Federal Roads Office. This does not apply to Form 3 'Project Conclusion' which presents the view of the monitoring committee. Distribution: Swiss Association of Road and Transportation Experts (VSS)

Standardization of Highly Polymer-Modified Asphalt Mixtures (HPMix)

**Normierung von hoch polymermodifizierte
Asphaltbelägen (HPMix)**

**Normalisation des mélanges bitumineux hautement
modifiés par des polymères (HPMix)**

Empa

Dr. Martins Zaumanis

Dr. Martin Arraigada

Canton GR

Gion Dosch

Canton AG

Olga Paperna

Research project VSS_2022_337 at the request of the Federal Roads Office

FEDRO

December 2025 | 1816

Imprint

Research centre and project team

Project management

Martins Zaumanis

Members

Martin Arraigada

Gion Dosch

Olga Paperna

Advisory commission

President

Martin Horat

Members

Sandra Dünner

Fabian Traber

Ould Henia Mehdi

Hans-Peter Bucheli

Françoise Beltzung

Adrian Zippo

Co-financing of the research project

Kanton Graubunden

Kanton Aargau

Applicant

Schweizerischer Verband der Strassen- und Verkehrsfachleute VSS

Source

The document can be downloaded free of charge from

<https://www.mobilityplatform.ch/>

December 2025

Table of contents

List of illustrations	9
List of tables.....	16
List of abbreviations	17
Summary	19
Résumé	31
Zusammenfassung.....	45
1 Introduction	59
1.1 Reported performance of high PmB	60
1.2 Potential advantages, use cases and concerns when using high PmB	62
1.3 Project scope	64
2 Methods.....	67
2.1 Binder tests	67
2.1.1 Sampling.....	67
2.1.2 Conventional binder tests.....	67
2.1.3 Reheating experiment.....	67
2.1.4 Binder aging and mass change	68
2.1.5 Rotational viscosity.....	68
2.1.6 Binder fast characterization test (BTSV)	68
2.1.7 Multiple Stress Creep Recovery Test (MSCR)	68
2.1.8 DSR Frequency sweep and Superpave high Performance Grade (PG)	69
2.1.9 Gel Permeation Chromatography (GPC)	70
2.2 Mixture tests	70
2.2.1 Particle size distribution	70
2.2.2 Conventional mixture tests.....	70
2.2.3 Semi-circular bend (SCB) test	70
2.2.4 IDEAL-CT	72
2.2.5 French rutting test	73
2.2.6 Stiffness modulus using Indirect Tensile Test	74
2.2.7 Fatigue using two point bending test.....	75
2.2.8 Thermal Stress Restrained Specimen Test	76
2.2.9 Cantabro test.....	77
2.2.10 Leutner test.....	78
2.2.11 Model Mobile Load simulator (MMLS3).....	78
2.3 Structural capacity of test sections with FWD	87

3	Binder quality control standardization.....	89
3.1	Materials.....	91
3.2	Penetration.....	92
3.3	Softening point.....	93
3.4	Elastic recovery.....	94
3.5	Fraass breaking point.....	95
3.6	Storage stability.....	95
3.7	Mass change.....	96
3.8	Rotational viscosity.....	97
3.9	BTSV.....	98
3.10	MSCR.....	102
3.11	Gel Permeation Chromatography.....	105
3.12	Correlation between test results.....	107
3.12.1	BTSV temperature versus penetration.....	107
3.12.2	MSCR test recovery versus elastic recovery.....	108
3.12.3	GPC peak area versus BTSV delta phase angle.....	109
3.13	Summary of the binder quality control standardization.....	110
3.14	Conclusions.....	113
4	Construction and monitoring of test sections.....	115
4.1	AC B 22 S test section H19 Oberalpstrasse, Tamins - Val Malien, Graubünden.....	115
4.1.1	Mixtures and test section location.....	115
4.1.2	Methodology.....	119
4.1.3	Conventional binder tests.....	119
4.1.4	BTSV.....	122
4.1.5	MSCR.....	124
4.1.6	DSR Frequency Sweep.....	124
4.1.7	Aggregate gradation.....	125
4.1.8	Marshall air voids and Marshall test.....	126
4.1.9	Rutting test.....	126
4.1.10	Semi-circular bend (SCB) test.....	127
4.1.11	IDEAL-CT.....	128
4.1.12	Thermal stress restrained specimen test (TSRST).....	129
4.1.13	Stiffness using indirect tensile test.....	130
4.1.14	Fatigue.....	132
4.1.15	MMLS3.....	133
4.1.16	Structural capacity with FWD.....	135
4.1.17	Summary.....	138
4.2	AC 8 S test section, H27 Engadinerstrasse in St. Moritz Charnadüra, Graubünden.....	139
4.2.1	Mixtures and test section location.....	139
4.2.2	Methodology.....	142
4.2.3	Conventional binder tests.....	142
4.2.4	BTSV.....	144

4.2.5	MSCR.....	146
4.2.6	Aggregate gradation.....	147
4.2.7	Marshall air voids and Marshall test	148
4.2.8	Rutting test	148
4.2.9	Semi-circular bend test.....	149
4.2.10	IDEAL-CT	150
4.2.11	Thermal Stress Restrained Specimen Test (TSRST)	151
4.2.12	Stiffness modulus using indirect tensile test	152
4.2.13	Structural capacity with FWD.....	155
4.2.14	Summary.....	157
4.3	SDA 4-12 test section, K244, Rapperswil IO, Aargau.....	159
4.3.1	Mixtures and test section location	159
4.3.2	Methodology	160
4.3.3	Conventional binder test results.....	160
4.3.4	BTSV results	161
4.3.5	MSCR test results.....	162
4.3.6	Frequency sweep.....	163
4.3.7	Pavement layer tests	165
4.3.8	Marshall air voids and Marshall test	166
4.3.9	Rutting test	166
4.3.10	Semi-circular bend (SCB) test	167
4.3.11	IDEAL-CT	168
4.3.12	Cantabro test.....	169
4.3.13	Stiffness	171
4.3.14	Thermal stress restrained specimen test (TSRST)	172
4.3.15	Leutner test results	173
4.3.16	Summary.....	173
5	Pavement structural design standardization	175
5.1	Pavement dimensioning according to VSS 40 324.....	175
5.2	Methodology	177
5.2.2	Fatigue design.....	179
5.2.3	Rutting verification.....	181
5.3	Material parameters.....	182
5.3.1	Fatigue	182
5.3.2	Stiffness	182
5.3.3	Viscoelastic characterization	182
5.4	Pavement modelling	183
5.4.1	Geometry, material properties and boundary conditions.....	184
5.4.2	Load	187
5.4.3	Output.....	187
5.4.4	Summary of the models	188

5.5	Validation using FWD test data.....	190
5.6	Results and determination of <i>a-values</i>	193
5.7	Impact of the proposed <i>a-values</i> in the expected ESALs	195
5.8	Summary	195
6	Conclusions and recommendations	197
6.1	Binder characterisation	197
6.2	Mixture rutting test	198
6.3	Mixture cracking resistance tests (SCB and IDEAL-CT)	199
6.4	Mixture fatigue and stiffness tests.....	199
6.5	Thermal stress restrained specimen test (TSRST) ...	199
6.6	Pavement dimensioning standardization.....	200
6.7	Research needs.....	200
7	Annexes.....	203
7.1	FWD report H19 Oberalpstrasse, Infralab SA.....	203
7.2	FWD report H27 Engadinerstrasse, Infralab SA.....	212
	Acknowledgements.....	221
	Bibliography	222
	Project conclusion	227

List of illustrations

Figure 1: Structure of binder depending on polymer content (from (Habbouche et al., 2019))	19
Figure 2: Project overview (the abbreviations used in the figure are presented in the methods section)	20
Figure 3: BTSV proposed classes for high PmBs. HH and HS denotes high PmB's while the other letters are for binders with lower polymer content	21
Figure 4: BTSV temperature versus log penetration	22
Figure 5: MSCR test result summary at 10.0 kPa and 64 °C. HH denotes high PmB's while the other letters are for binders with lower polymer content	23
Figure 6: The test temperature of the various methods based on the results of this paper for highly polymer-modified binders. Suggested methods for European specifications are shown above the line.	23
Figure 7: Summary of the AC B 22 S test section test results	25
Figure 8: Summary of the AC 8 S test section test results	27
Figure 9: Summary of SDA test results	28
Figure 10: Structure du liant en fonction de la teneur en polymère (à partir de (Habbouche et al., 2019))	31
Figure 11: Aperçu du projet (les abréviations utilisées dans la figure sont présentées dans la section des méthodes)	32
Figure 12: BTSV a proposé des classes pour les High PmB. HH et HS désignent les High PmB, tandis que les autres lettres correspondent à des liants à plus faible teneur en polymères.	33
Figure 13: Température BTSV par rapport à la pénétration logarithmique	34
Figure 14: Résumé des résultats du test MSCR à 10,0 kPa et 64 °C. HH désigne les High PmB, tandis que les autres lettres correspondent à des liants à faible teneur en polymères.	35
Figure 15: La température d'essai des différentes méthodes basées sur les résultats de cet article pour les liants hautement modifiés par des polymères. Les méthodes suggérées pour les spécifications européennes sont indiquées au-dessus de la ligne.	36
Figure 16: Résumé des résultats des essais de la section d'essai AC B 22 S	38
Figure 17: Résumé des résultats des essais de la section d'essai AC 8 S	40
Figure 18: Résumé des résultats des tests SDA	41
Figure 19: Struktur des Bindemittels in Abhängigkeit vom Polymergehalt (von (Habbouche et al., 2019))	45
Figure 20: Projektübersicht (die in der Abbildung verwendeten Abkürzungen sind im Methodenteil aufgeführt)	46
Figure 21: Vorgeschlagene Klassen für BTSV für High-PmBs. HH und HS bezeichnen hohe PmBs, während die anderen Buchstaben für Bindemittel mit geringerem Polymergehalt stehen	47
Figure 22: BTSV-Temperatur im Vergleich zur logarithmischen Penetration	49
Figure 23: Zusammenfassung der MSCR-Prüfergebnisse bei 10.0 kPa und 64 °C. HH steht für hohe PmB-Werte, während die anderen Buchstaben für Bindemittel mit geringerem Polymergehalt stehen.	50

Figure 24: Die Prüftemperatur der verschiedenen Methoden auf der Grundlage der Ergebnisse dieser Arbeit für hochpolymermodifizierte Bindemittel. Die für europäische Spezifikationen empfohlenen Methoden sind oberhalb der Linie angegeben.....	50
Figure 25: Zusammenfassung der Prüfergebnisse des Testabschnitts AC B 22 S.....	53
Figure 26: Zusammenfassung der Prüfergebnisse des AC 8 S-Testabschnitts.....	54
Figure 27: Zusammenfassung der SDA-Prüfergebnisse	55
Figure 28: Structure of binder depending on polymer content (from (Habbouche et al., 2019))	60
Figure 29: Project overview (the abbreviations used in the figure are presented in the methods section)	65
Figure 30: Location of the test sections.....	66
Figure 31: The principle of preparing SCB test samples.....	71
Figure 32: SCB test setup (a) and typical test result (b)	71
Figure 33: IDEAL-CT test setup and the principle of result expression from the load – displacement curve	73
Figure 34: French Rut Tester (FRT).....	74
Figure 35: The gyratory samples were cut from top and bottom to increase homogeneity.....	74
Figure 36: Stiffness modulus and fatigue test setup.....	75
Figure 37: Dimensions of the fatigue samples.....	75
Figure 38: Mixture fatigue testing apparatus.....	76
Figure 39: TSRST setup and typical TSRST test result	77
Figure 40: Los Angeles testing machine for the Cantabro test.....	78
Figure 41: Testing of the layered composite according to Leutner method	78
Figure 42: View of the MMLS3 with its 4 wheels and working principle.....	79
Figure 43: Roller compactor and specimen production for the MMLS3.....	80
Figure 44: Photo collection of the test preparation process.....	81
Figure 45: View of the thermocouples and data acquisition system	81
Figure 46: MMLS3 cracking test setup and pictures showing the load application area, DIC System, strain gauge and LVDT measuring arrangement	82
Figure 47: Example of two LVDTs records at the center of two different slabs (left) and calculated defl. amplitudes.....	83
Figure 48: Conceptual schema of the MMLS3 test progression (left) and expected evolution of deflection (right)	84
Figure 49: view of the measuring area showing the raw and grinded surface and the surface after painting and speckle application.....	85
Figure 50: Schematic of the tire passing over the notch, showing the opening of an existing crack whereas the bottom graph shows the deflection of the center at different times	85
Figure 51: DIC pattern following over time (from Digital Image Correlation: Theory [PDF]. Source: Michael A. Sutton, Jean Jose Orteu, Hubert W. Schreier Source: Image Correlation for Shape, Motion and Deformation Measurements, LIMESS)....	86
Figure 52: Example of the evolution of the von Mises strains showing the evolution of the cracks vs. the MMLS3 loading; each figure.....	86
Figure 53: View of the Infralab FWD (left) and loading plate and geophones (right)	87

Figure 54: Research overview (the abbreviations used in the figure are presented in the methods section).....	91
Figure 55: Penetration test results (hard binder – left side; soft binder – right side)	93
Figure 56: Softening point test results (hard binder – left side; soft binder – right side)	94
Figure 57: Elastic recovery test results (hard binder – left side; soft binder – right side)	94
Figure 58: Fraass breaking point test results (hard binder – left side; soft binder – right side).....	95
Figure 59: Storage stability test results (hard binder – left side; soft binder – right side)	96
Figure 60: Mass change test results (hard binder – left side; soft binder – right side)	96
Figure 61: Shear sweep results for binder 2MH.....	97
Figure 62: Rotational viscosity results at 100 s ⁻¹	98
Figure 63: BTSV proposed classes for high PmB	99
Figure 64: BTSV aging resistance criteria for high PmB after and 2xPAV (hard binder – left side; soft binder – right side).....	100
Figure 65: Determination of the $\Delta\delta$ BTSV and temperature at the minimum phase angle.....	101
Figure 66: Delta phase angle and the corresponding BTSV temperature (hard binder – left side; soft binder – right side).....	102
Figure 67: MSCR test result summary at 3.2 kPa and 64 °C.....	103
Figure 68: MSCR test results of all binders at 10 kPa and 64 °C test temperature	104
Figure 69: MSCR test results of unaged soft binders at 10 kPa and 58 °C test temperature	105
Figure 70: GPC chromatogram of 9HS at different aging states.....	106
Figure 71: Overlay of polymer region in GPC chromatograms for similar polymer groups	107
Figure 72: BTSV temperature versus log penetration	108
Figure 73: MSCR test recovery and BTSV phase angle VS elastic recovery	109
Figure 74: GPC polymer peak area VS delta phase angle of BTSV.....	109
Figure 75: The test temperature of the various methods based on the results of this research for highly polymer-modified binders. Suggested methods for European specifications are shown above the line.	113
Figure 76: Location of the AC B 22 S test section, H19 Oberalpstrasse, Tamins - Val Maliens, Graubünden	116
Figure 77: Normal profile of the Tamins - Val Maliens test section.....	117
Figure 78: Layer thicknesses of the Tamins – Val Maliens test section (highlighted – the layer used in this research)	118
Figure 79: Construction of the AC T 22 S pavement in Tamins – Vel Mailens test section.....	118
Figure 80: AC T 22 S penetration test results. The demonstrated minimum and maximum requirements are based on the VSS 40 430 standard for the PmB 45/80-65 (CH-E) bitumen. Blue bars are virgin and virgin aged binders, while test section results are shown with orange bars. The minimum requirements are based on SN-	

670210b-NA_EN-14023-E for the virgin unaged binders and based on VSS-40430 for the recovered binders.	119
Figure 81: AC T 22 S softening point test results. The demonstrated minimum requirements are based on the VSS 40 430 standard for the PmB 45/80-65 (CH-E) bitumen. Blue bars are virgin and virgin aged binders, while test section results are shown with orange bars. The minimum requirements are based on SN-670210b-NA_EN-14023-E for the virgin unaged binders and based on VSS-40430 for the recovered binders.	120
Figure 82: AC T 22 S elastic recovery test results. The demonstrated minimum requirements are based on the VSS 40 430 standard for the PmB 45/80-65 (CH-E) bitumen. Blue bars are virgin and virgin aged binders, while test section results are shown with orange bars. The minimum requirements are based on SN-670210b-NA_EN-14023-E for the virgin unaged binders and based on VSS-40430 for the recovered binders.	121
Figure 83: AC T 22 S Fraass breaking point test results. Blue bars are virgin and virgin aged binders, while test section results are shown with orange bars. The minimum requirements are based on SN-670210b-NA_EN-14023-E for the virgin unaged binders.	122
Figure 84: AC T 22 S BTSV result summary.....	123
Figure 85: AC T 22 S BTSV results throughout the test	123
Figure 86: AC T 22 S MSCRT results. Test performed at 64 °C and 10 kPa load ...	124
Figure 87: DSR Frequency sweep test results of AC T 22 S binder (binder recovered from mixtures) at 1.59 Hz frequency.....	125
Figure 88: Recovered aggregate gradation of the AC B 22 S RAPMix and HPMix samples.....	125
Figure 89: Marshall test results and Marshall air voids of the AC B 22 S mixtures	126
Figure 90: French rutting test results of the AC B 22 S mixtures.....	127
Figure 91: SCB test results of the AC B 22 S mixtures. AV is the air void content of the test samples.	128
Figure 92: IDEAL-CT results of the AC B 22 S mixtures. AV is the air void content of the test samples.	129
Figure 93: TSRST results of the AC B 22 S mixtures. AV is the air void content of the test samples.	129
Figure 94: Stiffness modulus of the AC B 22 S mixtures at five different temperatures at 10 Hz (top figure), 1 Hz (middle), and 0.1 Hz (bottom).....	131
Figure 95: Stiffness master curves of the AC B 22 S mixtures. Shifted to 15 °C.	132
Figure 96: Fatigue test regression lines of the AC B 22 S mixtures using the 2-point bending test.....	133
Figure 97: MMLS3 setup	134
Figure 98: MMLS3 loading results.....	134
Figure 99: Layer configuration of the test sections and simplification into three layers for backcalculation (left), and backcalculated asphalt layer E-modulus corrected to 15 °C (right).	135
Figure 100: Boxplots showing the maximum deflection measured at the load center for the RP and HP pavement sections.....	136
Figure 101: Deflection bowl parameters (SCI, BDI, BCI, AREA) calculated from FWD measurements for the RAPMix and HPMix sections.....	137
Figure 102: Summary of the AC B 22 S test section test results.....	138

Figure 103: Location of the AC 8 S test section, H27 Engadinerstrasse in Charnadüra, Graubünden.....	139
Figure 104: Normal profile of the Charnadüra test section	140
Figure 105: Layer thicknesses of the Charnadüra test section.....	141
Figure 106: Construction of the AC 8 S pavement in the Charnadüra test section ..	141
Figure 107: Penetration test results of the binders recovered from the AC 8 S mixtures and for comparison the results of the soft binder grades from section 3. Blue bars are virgin and virgin aged binders, while test section results are shown with orange bars. The minimum requirements are based on SN-670210b-NA_EN-14023-E for the virgin unaged binders and based on VSS-40430 for the recovered binders..	142
Figure 108: Softening point test results of the binders recovered from the AC 8 S mixtures and for comparison, the results of the soft binder grades from section 3. Blue bars are virgin and virgin aged binders, while test section results are shown with orange bars. The minimum requirements are based on SN-670210b-NA_EN-14023-E for the virgin unaged binders and based on VSS-40430 for the recovered binders..	143
Figure 109: Elastic recovery test results of the binders recovered from the AC 8 S mixtures and for comparison, the results of the soft binder grades from section 3. Blue bars are virgin and virgin aged binders, while test section results are shown with orange bars. The minimum requirements are based on SN-670210b-NA_EN-14023-E for the virgin unaged binders and based on VSS-40430 for the recovered binders..	144
Figure 110: BTSV results of the binders recovered from the AC 8 S mixtures. For comparison, the results of the soft binder grades from section 3 are also included..	145
Figure 111: AC 8 S BTSV results throughout the test	145
Figure 112: MSCR results of the binders recovered from the AC 8 S mixtures built in Charnadüra. The test was performed at 3.2 kPa stress at 58 °C temperature. For comparison, the results of the soft binder grades from section 3 are also included..	146
Figure 113: MSCR results of the binders recovered from the AC 8 S mixtures built in Charnadüra. The test was performed at 10 kPa stress at 58 °C temperature. For comparison, the results of the soft binder grades from section 3 are also included..	147
Figure 114: MSCR results throughout the loading cycles for the binders recovered from the AC 8 S mixtures built in Charnadüra. The test was performed at 10 kPa stress at 58 °C temperature.....	147
Figure 115: Recovered aggregate gradation of the AC 8 S Reference and HPMix samples	148
Figure 116: Marshall air voids and Marshall test results of the AC 8 mixture built in Charnadüra test section.	148
Figure 117: Rutting test results of the AC 8 S mixtures built in the Charnadüra test section. The requirement of "S" type asphalt mixtures is to perform the test up to 10,000 cycles.....	149
Figure 118: Semi-circular bend test results of the AC 8 S mixtures built in the Charnadüra test section. AV is the air void content of the test samples.....	150
Figure 119: Load-displacement curves of the semi-circular bend test of the AC 8 S mixtures built in the Charnadüra test section.	150
Figure 120: IDEAL-CT results of the AC 8 S mixtures. AV is the air void content of the test samples.....	151
Figure 121: TSRST results of the AC 8 S mixtures. The result of the HPMix samples is not known since was below the temperature range that is supported by the test device (-40 °C). AV is the air void content of the test samples.	152

Figure 122: Stiffness modulus of the plant-produced, lab-compacted AC 8 S mixtures at five different temperatures at 10 Hz (top figure), 1 Hz (middle), and 0.1 Hz (bottom).....	153
Figure 123: Stiffness master curves of the plant-produced, lab-compacted AC 8 S mixtures. Shifted to 15 °C.....	154
Figure 124: Stiffness modulus of the plant-produced, lab-compacted AC 8 S (denoted as "Gyrator") and road cores from the Charnadüra test section of the same mixtures (denoted as "cores"). Each mixture type is presented in a separate column, and the results are shown for three different temperatures at 10 Hz (top figure), 1 Hz (middle), and 0.1 Hz (bottom). The error bar represents one standard deviation. ..	155
Figure 125: Layer configuration of the test sections and simplification into three layers for backcalculation (left), and backcalculated asphalt layer E-modulus corrected to 15 °C (right).....	156
Figure 126: Boxplots showing the maximum deflection measured at the load center for the RP and HP pavement sections.....	156
Figure 127: Deflection bowl parameters (SCI, BDI, BCI, AREA) calculated from FWD measurements for the Reference and HPMix sections.	157
Figure 128: Summary of the AC 8 S test section test results	158
Figure 129: Location of the SDA test section in Canton AG and the location of the road cores that were taken after the construction.....	159
Figure 130: BTSV results from the SDA test section. For comparison, the recovered binder results from the AC T 22 S test section are as well as the virgin hard binder test results are also included in the figure	161
Figure 131: BTSV results of the recovered binder from the road cores (2024) of the SDA sections (dotted line – phase angle, solid line – complex shear modulus).....	162
Figure 132: BTSV results of the recovered binder from the mixture (2020) of the SDA sections (from Consultest AG report No. 0953-20-4).....	162
Figure 133: MSCR results of the binder recovered from the SDA road cores in 2024. Test conditions: 10 kPa and 64°C.....	163
Figure 134: MSCRT cycles for the 10kPa at 64°C.....	163
Figure 135: Phase angle at 1.59 Hz test results at various temperatures for the binder from SDA mixtures (H- HPMix, R-Reference).....	164
Figure 136: Complex modulus test results at various temperatures for the binder from SDA mixtures (H- HPMix, R-Reference). "Construstr" refers to modulus from extracted binder during construction and "Core" refers to the road cores taken in 2024.	164
Figure 137: Mastercurve of the SDA binder from the year 2024 road cores (H- HPMix, R-Reference).....	165
Figure 138: Marshal test results of lab-mixed SDA mixtures.....	166
Figure 139: Rutting test results of the lab-mixed SDA mixtures.....	167
Figure 140: Semi-circular bend test results of the lab-mixed SDA mixtures and the road cores from 2024. AV is the air void content of the test samples.	168
Figure 141: IDEAL-CT results of the lab-produced SDA mixtures. AV is the air void content of the test samples.....	168
Figure 142: Cantabro test results for lab-produced SDA samples and road cores. AV is the air void content of the test samples.	170
Figure 143: Cantabro test samples. Top: laboratory-prepared specimen	170

Figure 144: Stiffness modulus of the SDA 4-12 road cores from 2024 at four different temperatures at 10 Hz (top figure), 1 Hz (middle), and 0.1 Hz (bottom) ...	171
Figure 145: Stiffness master curves of the SDA 4-12 road cores from 2024. Shifted to 15 °C	172
Figure 146: Summary of SDA test results	174
Figure 147: <i>a-values</i> proposed in VSS 40 324	176
Figure 148: Schematic diagram for the calculation of the <i>a-values</i> for High PmB Mixture	179
Figure 149: Master curves at 15 °C of RP and HP mixtures based on modulus testing and WLF shift factors.....	182
Figure 150: Comparison of measured and Prony-series-calculated complex modulus (real and imaginary components) for RP and HP mixtures	183
Figure 151: Pavement structure of Type 1 (Oberbautyp 1) from the Swiss design catalogue used for the simulations	184
Figure 152: Asphalt layer thicknesses and materials according to VSS 40 430.....	185
Figure 153: View of the 3D pavement model in Comsol Multiphysics.....	186
Figure 154: Representation of the dual-wheel axle load applied in the pavement model.	187
Figure 155: Horizontal strains in the direction and transversal to traffic (ϵ_{11} and ϵ_{22} respectively) and their combination	188
Figure 156: View of the plain to obtain the strains (top) and strain output (bottom)	188
Figure 157: View of the FWD test carried out in the H19 Oberalpstrasse test section.	190
Figure 158: a) average, max. and min. time-dependent load histories used in FEM simulations; b) average, max. and min. measured DO responses for RP and HP sections of H19 Oberalpstrasse.	191
Figure 159: FEM geometry used for FWD validation, with loading plate at the pavement center.....	191
Figure 160: Pavement structure of H19 Oberalpstrasse (left), its 3-layer simplification for Elmod backcalculation (center), and the backcalculated moduli used as seed values in FEM (right).	192
Figure 161: Comparison between measured and simulated DO deflections under FWD loading for RP and HP mixtures.....	193
Figure 162: Calculated structural coefficients (<i>a-values</i>) for High PmB mixtures (a_{HP}) from 36 simulations. Values range between 4.43 and 6.92. The inset shows the frequency distribution of the results.....	194
Figure 163: Proposed methods for highly-polymer modified binder characterisation and the temperature for each test as it was used in this research	197

List of tables

Table 1: Proposed methods and criteria for highly polymer-modified binder quality control	24
Table 2: Méthodes et critères proposés pour le contrôle qualité des liants hautement modifiés par des polymères.....	37
Table 3: Vorgeschlagene Methoden und Kriterien für die Qualitätskontrolle von hochpolymermodifizierten Bindemitteln.....	51
Table 4: Potential advantages and use cases for high PmB mixtures	63
Table 5: Potential concerns when using high PmB and possible risk mitigation strategies	64
Table 6: Comparison of test results for one binder when taking samples from the top or the bottom of the bucket	67
Table 7: Results of reheating the PmB after recovery	68
Table 8: Swiss requirements of select classes of CH-C and CH-E type polymer-modified binders according to SN EN 14023-NA	89
Table 9: Binders used in the research and their characteristics.....	92
Table 10: Comparison of the different binder test methods that might be used for high PmB classification	112
Table 11: Asphalt recipes for Tamins - Val Malians test section	117
Table 12: Fatigue test results of the AC B 22 S mixtures using the 2-point bending test.....	133
Table 13: Asphalt recipes for Charnadüra test section.....	140
Table 14: Binder test results from SDA test section.....	160
Table 15: SDA layer properties in the Canton AG test section	165
Table 16: TSRST results of the SDA mixtures (the construction results are from the Consultest AG report No. 0953-20-4).....	173
Table 17: Leutner test results of the SDA mixtures (the results after construction are from the Consultest AG report No. 0953-20-4).....	173
Table 18: Parameters used for the calculation of the risk coefficient k_r	181
Table 19: Prony series coefficients for RP and HP mixtures.....	183
Table 20: Summary of all layer thicknesses and material properties used in the pavement models.	186
Table 21: Summary of all numerical simulation scenarios considered in this study.....	189
Table 22: Summary of layer thicknesses and material properties used for the calibration	192
Table 23: Comparison of expected ESALs for different standard pavements using current and proposed <i>a-values</i>	195
Table 24: Proposed methods and criteria for highly polymer-modified binder quality control	198

List of abbreviations

%	For void content, % by volume is reported, for PmB, RAP, and other mixture recipe quantities, % by mass is reported.
2PB-TR	Two point bending on trapezoidal specimens
AC	Asphalt Concrete
AG	Aargau
BTSV	Bitumen Fast Characterisation Test
CIT-CY	Cyclic indirect tension to cylindrical specimens
DIC	Digital Image Correlation
DSR	Dynamic Shear Rheometer
EH	Elevated polymer content, hard binder
EME	High Modulus Asphalt Concrete
ES	Elevated polymer content, soft binder
ESAL	Equivalent Standard Axle Load
FEM	Finite Element Method
FI	Flexibility Index
FRT	French Rut Tester
FWD	Falling Weight Deflectometer
GPC	Gel Permeation Chromatography
GR	Graubünden
HH	High polymer content, hard binder
High PmB	Highly Polymer Modified Binder
HPMix	High polymer content mixture
HP	High polymer content mixture
HS	High polymer content, soft binder
IDEAL-CT	Indirect Tensile Asphalt Cracking Test
ITT	Indirect Tensile Test
k_s	Support coefficient
k_r	Risk coefficient
k_c	Adjustment coefficient
LH	Low polymer content, hard binder
LS	Low polymer content, soft binder
LVDT	Linear Variable Differential Transformer
MH	Medium polymer content, hard binder

MMLS ₃	Model Mobile Load Simulator
MS	Medium polymer content, soft binder
MSCR	Multiple Stress Creep Recovery
NE	Admissible number of load repetitions
PAV	Pressure Aging Vessel
PmB	Polymer Modified Binder
RAP	Reclaimed Asphalt Pavement
RP	Reference mixture
RTFOT	Rolling Thin Film Oven Test
SBS	Styrene-Butadiene-Styrene
SCB	Semi Circular Bend Test
SDA	Semi Dense Asphalt
SN	Structural Number
TSRST	Thermal Stress Restrained Specimen Test

Summary

In a typical Polymer Modified Biner (PmB), the polymer dosage ranges between 2.5 % and 3.5 % by mass of asphalt binder, while highly polymer modified binders (High PmBs) typically contain polymer dosages of 6-8 %. Such binders have already been widely used both in research and in full-scale application. Compared to conventional PmBs, the reported benefits of high PmBs include increased pavement service life, improved rutting and cracking resistance, reduced pavement thickness, and increased recycled asphalt content in conventional polymer-modified mixtures (CH-E or CH-C binder type).

The benefits of high PmB over conventional PmB stem from the continuous polymer network. While in a conventional PmB the polymer phase is discontinuous, in a high-PmB the polymer phase forms an extensive polymer network, conferring a rubber-like response to external loads (Habbouche et al., 2020) (see Figure 1). That is, the blend goes from a discontinuous to a continuous polymer phase at approximately a 5 % of polymer by weight of asphalt binder. This inversion enhances the performance and durability of asphalt mixtures. The viscosity of high-PmB is ensured through Styrene-Butadiene-Styrene (SBS) polymer with high vinyl content and reduced molecular size which, when blended with bitumen, swell and increase in volume between 5 to 10 times (Porot et al., 2019a).

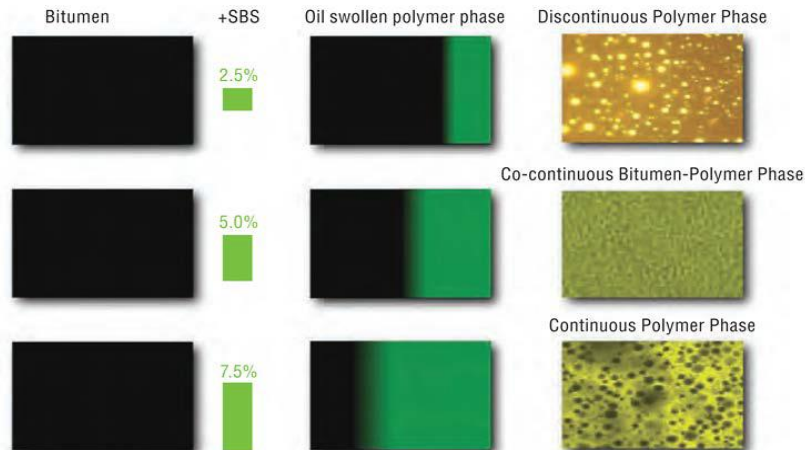


Figure 1: Structure of binder depending on polymer content (from (Habbouche et al., 2019))

As with many new technologies and materials, their benefits have to be weighed against the potential drawbacks and concerns. The high polymer content in high PmB mixtures can increase binder viscosity, making the asphalt difficult to produce at the plant and increasingly unworkable for paving crews. There is also a risk of phase separation and increased potential for microplastic wear. Due to the higher polymer content, high PmB is also more expensive than a conventional PmB thus adding to the up-front costs of production.

Considering the discussion above, the scope of this project was developed. We aimed to capitalize on the existing world-wide knowledge of using high PmB and developed a research plan that would allow to first verify the claims and then propose means for

standardization of high PmB use. The current lack of criteria to standardise the use of high PmBs is limiting their application and causing challenges during quality control.

The core of this project was divided into three parts as shown in Figure 2 and included binder standardization, construction of two test sections, evaluation of one existing test section and modelling to propose necessary means for pavement design standardization when using high PmB. A summary of the core findings of the project is provided in the following sub-sections.

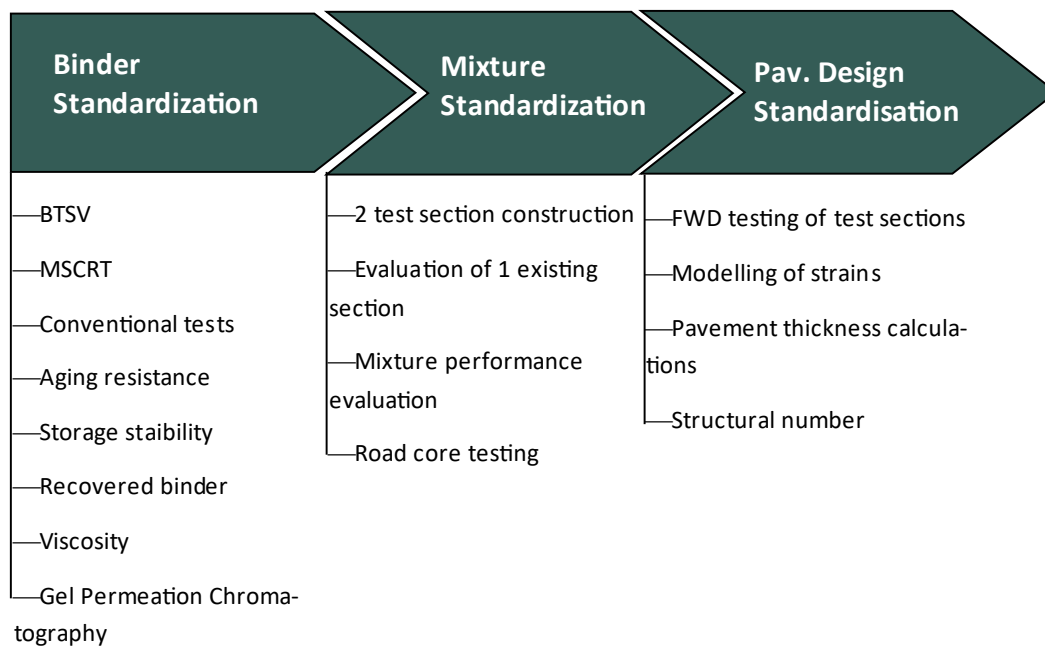


Figure 2: Project overview (the abbreviations used in the figure are presented in the methods section)

Binder Quality Control Standardization

In this section we evaluated a total of 10 different binders from two classes (denoted as soft and hard) using conventional tests as well as multiple stress creep recovery (MSCR) test, binder fast characterization test (BTSV), frequency sweep, and rotational viscosity. Additionally, Gel Permeation Chromatography (GPC) was employed to assess polymers. Binders were selected to reflect a gradient of polymer modification levels, categorized roughly as low (~2 %), medium (~3 %), elevated (~5 %), and high (>6 %).

Conventional Test Results

The penetration test can serve its current purpose also for determining the hardness of high PmB's. However, it is suggested to replace it with a DSR-based test that provides more information about the visco-elastic properties in the intermediate and/or low temperature range.

Softening point temperature did not offer reliable means to classify high PmBs depending on the polymer content and depending on the sample and aging resulted in both reduction and increase of the softening point temperature. For these reasons, the method is not recommended for high PmB classification.

The elastic recovery test at 25°C in most cases did not allow to differentiate between the binders with different polymer contents since the results were close to or above 90 %.

The Fraass breaking point test resulted in unexpected trends - many binders improved low temperature cracking resistance after aging and three of the binders did not fulfill the current breaking point temperature requirements. For these reasons, the test method is not recommended for classification of high PmBs.

Rotational viscosity

Rotational viscosity tests showed that while all binders met the AASHTO M320 requirement of ≤ 3 Pa·s at 135 °C, high PmBs demonstrated non-Newtonian behaviour at this temperature. At 160 °C, binders behaved in a Newtonian fashion, and a proposed additional criterion of ≤ 1 Pa·s at this temperature proposed for ensuring binder workability.

BTSV Characterization

The BTSV test method successfully discriminated binders based on the polymer content. Acceptance criteria were proposed for the soft and hard binders as shown in Figure 3. With aging, a clear increase in BTSV temperature and decrease in phase angle was observed.

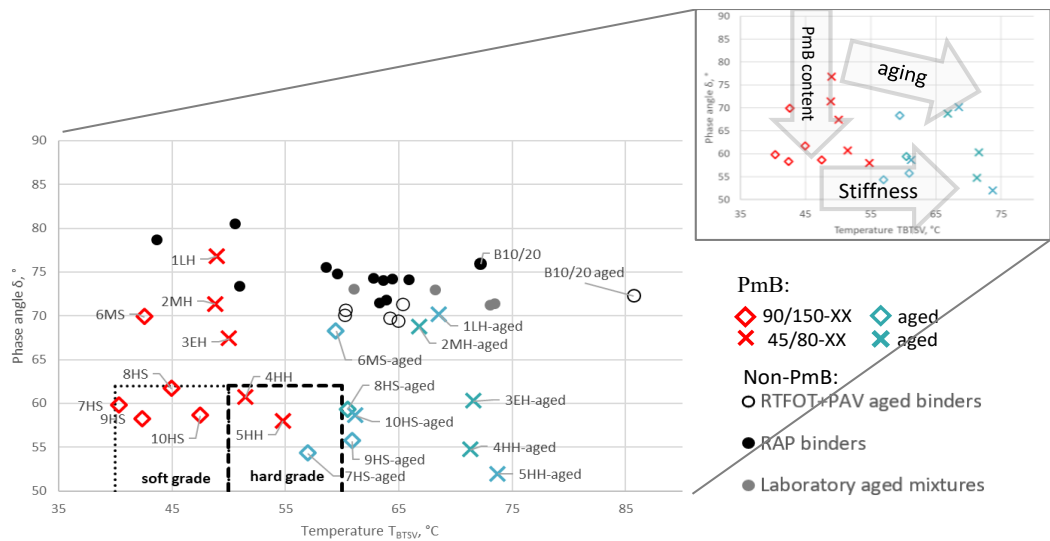


Figure 3: BTSV proposed classes for high PmBs. HH and HS denotes high PmB's while the other letters are for binders with lower polymer content

An extension of the BTSV test to 1 kPa was proposed to enable calculating the "delta phase angle". This parameter characterizes the effect of polymer network at high temperature, and it correlated well with the GPC results of most binders. Gathering more data with this parameter might provide new insights.

The applied aging protocol (RTFOT+2PAV¹ cycles) successfully simulated the aging state of typical binders found in reclaimed asphalt in Switzerland. This aging state is

¹ RTFOT: Rolling Thin Film Oven Test
PAV: Pressure Aging Vessel

therefore proposed to screen binders that are prone to accelerated long-term aging. The proposed BTSV criteria for aging evaluation are summarized in Table 1.

A good exponential relationship ($R^2=0.93$) was found between BTSV temperature versus log penetration as shown in Figure 4. The figure also includes two shaded boxes that demonstrate the overlapping region of the proposed BTSV temperature requirements and the corresponding penetration requirements for the soft and the hard highly modified binders. It can be seen that the high PmB's are always within the boxes, meaning that both the BTSV and the penetration results would include the binders in the same class. This means that if BTSV test results are used for high PmB classification, the penetration test is partially redundant in this case. Of course, unmodified or non-high PmB's can also be located in the boxes, in this case the 6MS and 3EH binders. Testing of binder's elastic properties is necessary to discriminate these binders. If the BTSV limits indicated in Figure 3 would be implemented, these binders would not fall in the same class based on the phase angle criteria.

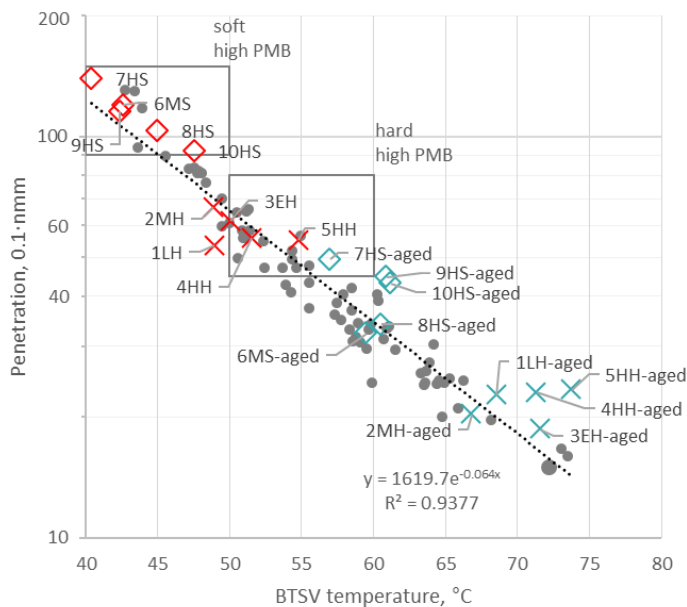


Figure 4: BTSV temperature versus log penetration

MSCR Evaluation

The MSCR test stress of 3.2 kPa was too low to differentiate between the different polymer contents. Increasing the stress to 10 kPa and testing at an appropriate temperature (64 °C for hard binders; 58 °C for soft binders) allowed to clearly classify the binders based on polymer content. As an example, the proposed acceptance criteria for the hard high PmB's is shown in Figure 5. However, selecting the test temperature remains a challenge, as binders for different areas of application (e.g., in the mountains or in lowlands) may require different test temperatures.

It was also recommended to increase the number of cycles per stress level to 30 for better result reproducibility.

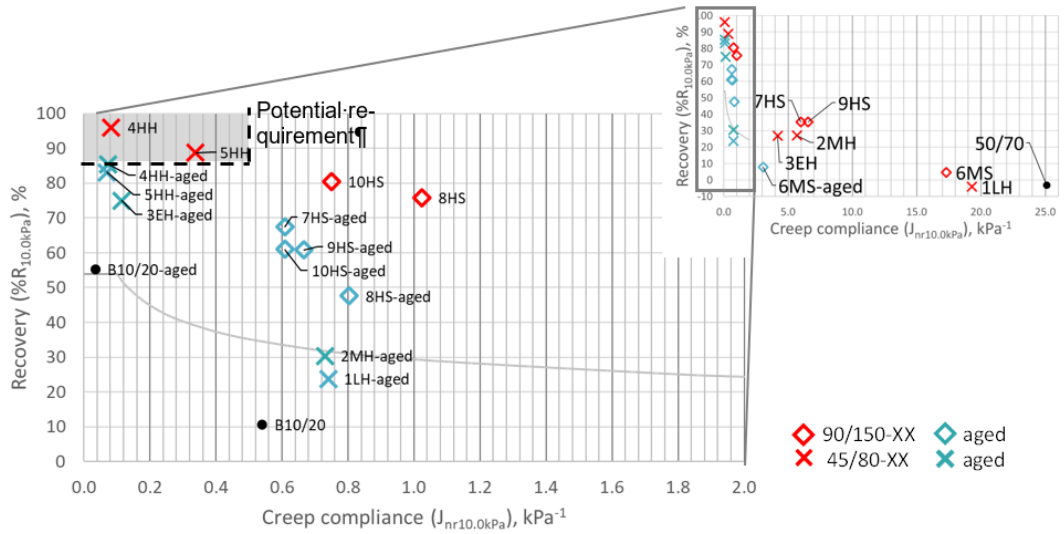


Figure 5: MSCR test result summary at 10.0 kPa and 64 °C. HH denotes high PmB's while the other letters are for binders with lower polymer content

Gel Permeation Chromatography

The peak area in Gel Permeation Chromatography (GPC) is correlated to the amount of polymer used in the binder, as long the polymer was identical. Otherwise, the peak area of different polymer types gives no information neither about the polymer content nor the mechanical performance.

The GPC proved a useful means for research, but it is not suitable for binder classification because the polymer peak area and molecular mass depends on the polymer type and thus cannot be universally applied to any type of binder.

Binder standardization recommendations

Figure 6 summarizes the test temperatures of high PmBs for each method that was used in this research. Based on the results of this research, the test methods that are suitable for high PmB classification are shown above the horizontal axis and the methods below the axis are not recommended.

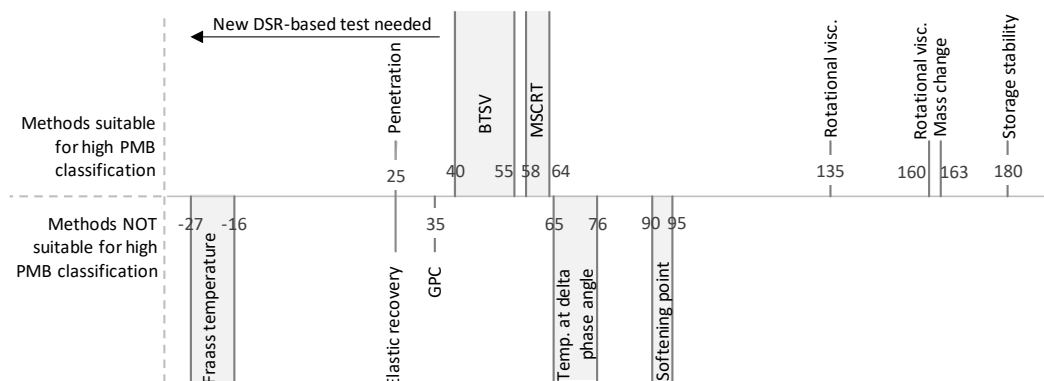


Figure 6: The test temperature of the various methods based on the results of this paper for highly polymer-modified binders. Suggested methods for European specifications are shown above the line.

Table 1 summarizes the proposed methods and criteria for highly polymer-modified binder classification. The methods are suitable for any PmB and also unmodified

binders, but they are especially necessary for highly polymer-modified binder classification since the currently used methods can not adequately distinguish between conventional and highly polymer-modified binders. It is highly recommended re-evaluate the proposed criteria after more data is collected.

Proposed methods for High PmB quality control				
Method	Criteria hard binder	Criteria soft binder	Remarks	Standard
Penetration	45-80 0.1mm	90-150 0.1mm	-	EN 1426
Rotational viscosity	$\leq 3 \text{ Pa}\cdot\text{s @ } 135 \text{ }^\circ\text{C}$ $\leq 1 \text{ Pa}\cdot\text{s @ } 160 \text{ }^\circ\text{C}$	$\leq 3 \text{ Pa}\cdot\text{s at } 135 \text{ }^\circ\text{C}$ $\leq 1 \text{ Pa}\cdot\text{s at } 160 \text{ }^\circ\text{C}$	Validation of the criteria necessary	EN 13302
Storage stability	$\leq 5^\circ\text{C}$	$\leq 5^\circ\text{C}$	Development of MSCR or BTSV-based criteria recommended	EN 13399
Mass change after RTFOT	$\leq 0.5 \%$	$\leq 0.5 \%$	-	EN 12607-1
BTSV	$\delta_{\text{BTSV}} \leq 62^\circ$ & $T_{\text{BTSV}} 50-60 \text{ }^\circ\text{C}$	$\delta_{\text{BTSV}} \leq 62^\circ$ & $T_{\text{BTSV}} 40-50 \text{ }^\circ\text{C}$	Validation of the criteria recommended	EN 17643
Aging resistance using BTSV after RTFOT	Reduction in $\delta_{\text{BTSV}} \leq 6^\circ$ Increase in $T_{\text{BTSV}} \leq 8 \text{ }^\circ\text{C}$	Reduction in $\delta_{\text{BTSV}} \leq 6^\circ$ Increase in $T_{\text{BTSV}} \leq 8 \text{ }^\circ\text{C}$	The proposed criteria based on a German pre-norm. Validation recommended	EN 17643 EN 12607-1
Aging resistance using BTSV after RTFOT+2PAV cycles	Reduction in $\delta_{\text{BTSV}} \leq 10^\circ$ Increase in $T_{\text{BTSV}} \leq 23 \text{ }^\circ\text{C}$	Reduction in $\delta_{\text{BTSV}} \leq 10^\circ$ Increase in $T_{\text{BTSV}} \leq 23 \text{ }^\circ\text{C}$	Two PAV aging cycles suggested for more realistic aging state.	EN 17643 EN 14769
MSCR test	$\geq 85 \%$ recovery $\leq 0.5 \%$ kPa^{-1} Test @ 10 kPa stress, 64 $^\circ\text{C}$	$\geq 85 \%$ recovery $\leq 0.5 \%$ kPa^{-1} Test @ 10 kPa stress, 58 $^\circ\text{C}$	- 10 kPa stress not in standard currently - Test temperature should be selected based on climate - In this research, testing performed on unaged samples	EN 16659

Table 1: Proposed methods and criteria for highly polymer-modified binder quality control

Test section: AC B 22 S on H19 Oberalpstrasse, Tamins - Val Maliens, Graubünden

AC B 22 S asphalt was paved as a binder course in the test site on H19 Oberalpstrasse Tamins – Val Maliens. This site was selected due to the high traffic intensity. Two mixtures were paved: (1) 40% RAP content mixture with added soft highly-polymer modified binder (PmB 90/150-85); (2) 0% RAP mixture with hard highly polymer-modified binder (PmB 45/80-85). The 40 % RAP mixture allowed to evaluate the advantages of using high PmB for compensating the lack of polymers in RAP and the 0 % RAP mixture allowed to evaluate the benefits of using high PmB for increasing the performance and longevity of asphalt as well as to evaluate the potential reduction of layer thickness.

The results of the AC B 22 S test section are summarized in Figure 7. The table allows to qualitatively compare the results of the high polymer content mixture (HPMix) to the 40 % RAP mixture (RAPMix). Overall, both mixtures provided good performance that corresponds to the current specification requirements for mixtures and recovered PmB 45/80-65 (CH-E) binder. This was achieved even with the 40 % RAP mixture thus indicating that at least 40 % RAP content can be successfully used in polymer-modified mixtures. Based on the binder test results, even higher RAP content may allow to satisfy the current specification requirement when high PmB is used and further mix design optimization is performed. However, it has to be noted that the current requirements do not always offer a reliable way to determine the binder performance and therefore the additional test methods were used in this research.

It can be seen in the figure that most test methods, including advanced binder tests and performance-based mixture test indicate a better performance of the HPMix compared to the RAPMix. This was expected, considering that the effective polymer content in the HPMix is higher compared to the RAPMix due to the 40 % RAP content. Overall, these results allow to conclude that the use of highly polymer-modified binder can serve two purposes:

- It is beneficial for performance improvement when used with low RAP content or no RAP².
- It can permit using high RAP content (at least up to 40% in the binder layer mixtures) to ensure performance that is expected from a conventional polymer modified mixture when the target grade is PmB 45/80-60 (CH-E).

Mixture	RAP content	Binder tests				Rutting resistance	Crack propagation resistance		Fatigue		Stiffness	Low temp. cracing resistance
		ER	BTSV	MSCR	FS	FRT	SCB	IDEAL-CT	2PB-TR	MMLS3	ITT	TSRST
AC B 22 S	HPMix	0%	↗	↗	↗	↘	↗ ¹	↗ ¹	↗	↗	↗	→
	RAP Mix	40%	●	●	●	●	●	●	●	●	●	●

Legend:

- reference mixture result
- ↗ significantly better performance
- ↘ slightly better performance
- similar performance
- ↘ slightly worse performance
- ↙ significantly worse performance

- ER Elastic Recovery (binder)
- BTSV Binder fast characterisation test
- MSCR Multiple stress creep recovery test (binder)
- FS Frequency Sweep (binder)
- FRT French Rutting Tester (mixture)
- SCB Semi-circular bend test (mixture)
- IDEAL-CT Indirect tensile asphalt cracking test (mixture)
- 2PB-TR Two point bending on trapezoidal specimen
- MMLS3 Model mobile load simulator (mixture)
- ITT Indirect tensile test (mixture)
- TSRST Tensile stress restrained specimen test

¹ SCB and IDEAL-CT tests are not sensitive to polymer content

Figure 7: Summary of the AC B 22 S test section test results

² Although the mix without recycled content shows the best results, the authors do not recommend abandoning asphalt recycling. The use of RAP should be evaluated in the context of sustainability and resource efficiency. Such an evaluation was not part of this project.

Test section: AC 8 S on H27 Engadinerstrasse in St.Moritz Charnadüra, Graubünden

AC 8 S type asphalt mixture wearing course was paved in the test site on H27 Engadinerstrasse in St. Moritz Charnadüra, Graubünden. This jobsite was selected due to the high traffic intensity and climatic conditions. Two mixtures were paved: HPMix was paved using highly polymer-modified binder (90/150-85) and a reference mixture was paved by adding PmB 90/150-60 (CH-E) type binder. Both mixtures had the same mixture design.

Overall, both mixtures provided good performance that corresponds to the current specification requirements. However, as discussed before, the test methods used for quality control do not always offer a reliable way to evaluate the effect of increased polymer content and therefore several performance-based test methods were used in this research.

The performance-based results of the AC 8 S test section are summarized in Figure 8. The table allows to qualitatively compare the results of the HPMix to the reference mixture. In can be seen in the table that the binder tests and low temperature cracking resistance test (TSRST) show superior performance of the highly polymer-modified binder compared to the reference mixture made using conventional polymer-modified binder. The rutting resistance of both mixtures is similar and very good. Based on the binder test results, it is reasonable to expect better pavement rutting resistance of the HPMix. However, the rutting test conditions were not severe enough to induce significant rutting. Even extending the test did not result in significant damage. Therefore, other changes in test conditions could be considered in the future, for example increasing the test temperature or using another test method (e.g. the cyclic compression test). The stiffness for both mixtures was similar and the crack propagation resistance was slightly worse for the HPMix compared to the reference mixture. However, based on previous research, it is likely that the differences in the crack propagation are not related to the polymer content since the employed test methods are not sensitive towards polymer content.

Overall, the results allow to conclude that the use of highly polymer-modified binder in the wearing course:

- Improves the performance of the wearing course.
- Binder characterisation using conventional tests does not fully demonstrate the benefits of using the highly polymer modified binder. BTVS and MSCR at 10 kPa are suitable means for binder characterisation.
- More severe conditions are required for the rutting resistance test to discriminate between the performance.

Mixture	RAP content	Binder tests			Rutting resistance	Crack propagation resistance		Stiffness	Low temp. cracing resistance
		ER	BTSV	MSCR	FRT	SCB	IDEAL-CT	ITT	TSRST
AC 8 S	HPMix	0%	↗	↕	↕	↘ ¹	↘ ¹	↔	↕
	Reference	0%	●	●	●	●	●	●	●

Legend:

●	reference mixture result	ER	Elastic Recovery (binder)
↕	significantly better performance	BTSV	Binder fast characterisation test
↗	slightly better performance	MSCR	Multiple stress creep recovery test (binder)
↔	similar performance	FRT	French Ruting Tester (mixture)
↘	slightly worse performance	SCB	Semi-circular bend test (mixture)
↙	significantly worse performance	IDEAL-CT	Indirect tensile asphalt cracking test (mixture)
		ITT	Indirect tensile test (mixture)
	¹ SCB and IDEAL-CT tests are not sensitive to polymer content	TSRST	Tensile stress restrained specimen test

Figure 8: Summary of the AC 8 S test section test results

Test section: SDA 4-12 on K244, Rapperswil IO, Aargau

The SDA test section using highly polymer-modified asphalt in Kanton AG was built in 2020 and the relevant test results are included in this report. In 2024 road cores were taken from the built pavement and new lab-produced mixtures were prepared for testing. The lab mixture was produced using the same mixture recipe and materials from the same sources as in 2020.

The test section is located in K244 Rapperswil and the SDA 4-12 reference section was built with binder PmB 45/80-65 (CH-E). The SDA 4-12 HPmix section was built using high PmB 45/80-80.

During this project we tested various sample types tested and we also used the test results of the reports from the original construction. In total, four types of results were used:

- Mixture and binder results from the samples collected during the construction of the test section in 2020.
- Mixture and recovered binder test results from the road cores that were cored soon after construction of the test section in 2020.
- Mixture and recovered binder test results from the road cores that were cored during the HPmix project in 2024.
- Mixture results from the samples produced in the Empa laboratory during the HPmix project in 2024.

The results from the SDA test allow to conclude that there appears to be an advantage of using the highly polymer-modified binder over the conventional polymer-modified binder. This is evident in the binder test results in Figure 9 which qualitatively compares the binder recovered from the HPmix with the binder recovered from the reference mixture. The mixture testing results also show similar or better performance compared to the reference mixture. The interlayer bond resistance of the HPmix samples is lower than required. Since the construction technology and the tack coat material were equal, one hypothesis is that a chemical reaction between the highPmB and the tack coat reduced the adhesion. This needs further verification.

Unfortunately, the Cantabro test (even after modification to make it more severe) did not allow to conclusively demonstrate the potential advantages of high polymer

modification with regard to reducing ravelling of SDA mixtures, even with the variations of the test that were implemented in the project. Other test methods should be considered to evaluate this property.

Mixture	Binder tests				Rutting resistance	Crack propagation resistance		Raveling resistance	Stiffness	Low temp. cracing resistance	Interlayer bond
	ER	BTS	MS	FS	FRT	SCB	IDEAL-	Cantabro	ITT	TSRST	Leutner
SDA HPMix	↑	↑	↑	↑	→	↘ ¹	→ ¹	↘	↘	↑	↓
Reference	●	●	●	●	●	●	●	●	●	●	●

Legend:

- reference mixture result
- ↑ significantly better performance
- ↘ slightly better performance
- similar performance
- ↘ slightly worse performance
- ↓ significantly worse performance

1 SCB and IDEAL-CT tests are not sensitive to polymer content

- ER Elastic Recovery (binder)
- BTSV Binder fast characterisation test
- MSCR Multiple stress creep recovery test (binder)
- FS Frequency Sweep (binder)
- FRT French Ruting Tester (mixture)
- SCB Semi-circular bend test (mixture)
- IDEAL-CT Indirect tensile asphalt cracking test (mixture)
- Cantabro Cantabro test (mixture)
- ITT Indirect tensile test (mixture)
- TSRST Tensile stress restrained specimen test
- Leutner Leutner test (mixture)

Figure 9: Summary of SDA test results

Asphalt mixture standardization proposal

This research has shown that highly polymer-modified binder can bring definite advantages over conventional polymer-modified binder. During the research this was demonstrated both on the binder and mixture-level. For standardization, however, mostly binder-based test methods and criteria are proposed as summarized in Table 1 since on the mixture level, the tests either did not demonstrate a notable difference between the highly polymer-modified binder and a conventional polymer-modified binder or the test execution is too laborious (in the case of the fatigue test). Therefore, even though some of the mixture tests might be beneficial for using in mix design, their use is not necessarily related exclusively to highly polymer-modified binder and therefore no recommendations are provided in this report. Below is a summary of the considerations for pro-posing or not proposing a certain test for standardization.

Mixture rutting test

All the mixtures fulfilled the rutting test requirements and, in most cases, no more than 5% rut depth was observed up to 30,000 loading cycles. Extending the test to 90,000 cycles did not provide any advantage and did not highlight the potential benefits of the high polymer content in the binder since the results even up to 90,000 cycles were similar between the reference and HPMix.

Rutting is a particular problem in slow traffic areas exhibiting significant shear forces (e.g. bus stops and roundabouts). Considering the possibility to achieve very high rutting resistance, it can be considered if the highly polymer-modified binders could provide a solution for such locations. It is therefore recommended to evaluate the use of highly polymer-modified mixtures for such locations (possibly through constructing a trial section) and consider developing harsher test conditions (e.g. higher test

temperature) or using another test method (for example cyclic compression test) for testing rutting resistance.

Mixture cracking resistance tests (SCB and IDEAL-CT)

The cracking resistance tests (SCB using the Illinois method and IDEAL-CT) are suitable means for mixture design since they are sensitive towards parameters that affect the mixture performance: binder content, binder properties, and RAP content. These methods have also demonstrated relatively high correlation with field performance and they are simple and quick to perform. For these reasons, the methods can be considered for use in mix design.

However, based on this and previous Empa research, the methods are not sensitive towards the use of polymers in binder. Therefore, they cannot be relied upon for mixture characterization with the goal of evaluating the elastic properties or effect of polymers.

Mixture fatigue and stiffness tests

The fatigue test demonstrated a distinct advantage of using highly polymer modified binder. However, it is currently not proposed for including in quality control or mixture type testing because the test execution is very laborious and it can reasonably be assumed that the binder characterisation tests are sufficient for assuming sufficient performance of the mixtures, especially for well-established mixture type like AC.

The stiffness test, as expected, did not demonstrate a notable difference between the mixtures containing different polymer contents. Therefore, since the mixture types that were evaluated in this project do not currently require a stiffness test, there is also no need to introduce it when using highly polymer-modified binder.

Thermal stress restrained specimen test (TSRST)

The TSRST showed that there is possibly an advantage of using higher polymer content for increasing the resistance to low temperature cracking. However, even the conventional polymer-modified binder ensured high low temperature cracking resistance. Therefore, even though it might be advantageous to include the TSRST as a criteria for approving asphalt mixtures in cold regions, this is not necessarily related to the use of highly polymer modified binder. For this reason, no criteria for standardization is provided for this test as part of this report.

Pavement structural design standardization

In this work, a methodology was applied to estimate structural coefficients (*a-values*) for High PmB mixtures within the Swiss pavement design framework (VSS 40 324). The calculated values ranged between 4.43 and 6.92. From these results, a conservative value of 4.4 is proposed for design. This confirms the expected structural advantage of High PmB mixtures when compared to conventional materials. In practical terms, this could translate into a reduction of around 10% in asphalt layer thickness. Alternatively, if the thickness remains unchanged, an increase in the equivalent single axle load applications (ESALs) between 39% and 106% can be expected depending on the pavement structure. It has to be noted that the proposed *a-value* refers only to mixtures that have no RAP. In case of using high content of RAP, the goal of using high PmB is to achieve similar performance to mixtures that are currently specified in the standard with the existing *a-values*. Nevertheless, the proposed *a-value* must be validated in real

structures, either reduced-scale trials or full-scale pavement testing, before being adopted in practice.

Research needs

During the HPMix project, several specific needs for future research were identified. A follow-up study on these topics would help the implementation of high PmBs:

- During this research, structural coefficient was proposed for mixtures containing high PmB. A validation of these results is recommended by building a test site for loading with MMLS11 according to the dimensions calculated using the new coefficient.
- It was shown that the current rutting test conditions are not severe enough to demonstrate a difference between a conventional PmB and high PmB mixture. Therefore development of new test conditions or validation of another test method, for example cycling compression, is recommended.

Additionally, several areas of shortcomings were identified during the research that are not necessarily related to the implementation of high PmBs but rather could benefit the sector as a whole:

- High PmB can be especially useful in specialty application with high traffic intensity and high shear forces. This includes bus stops, weigh station, roundabouts, intersections and similar locations. A construction of a test section with a corresponding evaluation could show the potential of high PmB mixtures to replace concrete in such applications.
- The storage stability is currently evaluated using softening point test. Since softening point is not recommended for high PmB evaluation, development of new criteria for binder storage stability evaluation using DSR-based test is recommended.
- The proposed DSR-based method are executed at high service temperatures. A new DSR-based method (or methods) should be developed for intermediate and low-temperature binder characterization.
- Calculation of strains and asphalt dimensioning is very laborious but pavement design optimisation could save materials and resources as well as allow innovations. A simple, free analytical tool for pavement design can be developed using the approach used in VSS 40 324.
- The project revealed potential advantages of using high PmB mixtures. Their use, including their use in combination with asphalt recycling, should also be promoted, considering the sustainability and resource efficiency assessment.

Résumé

Dans un liant bitumineux modifié par des polymères (PmB) classique, la teneur en polymères varie entre 2,5 % et 3,5 % en masse du liant bitumineux, tandis que les liants hautement modifiés par des polymères (High PmB) contiennent généralement entre 6 et 8 % de polymères. Ces liants sont déjà largement utilisés tant dans la recherche que dans des applications à grande échelle. Par rapport aux PmB conventionnels, les avantages rapportés des PmB à haute teneur en polymères comprennent une durée de vie accrue de la chaussée, une meilleure résistance à l'orniérage et à la fissuration, une épaisseur réduite de la chaussée et une teneur accrue en asphalte recyclé dans les mélanges modifiés par des polymères (Type de liant CH-E ou CH-C).

Les avantages des PmB à haute teneur en polymères par rapport aux PmB conventionnels proviennent du réseau polymère continu. Alors que dans un liant conventionnel, la phase polymère est discontinue, dans un liant à haute teneur en polymères, la phase polymère forme un réseau polymère étendu, conférant une réponse semblable à celle du caoutchouc aux charges externes (voir Figure 10). Autrement dit, le mélange passe d'une phase polymère discontinue à une phase polymère continue à environ 5 % de polymère en poids du liant bitumineux. Cette inversion améliore les performances et la durabilité des mélanges bitumineux. La viscosité du PmB élevé est assurée par le polymère styrène-butadiène-styrène (SBS) à haute teneur en vinyle et à taille moléculaire réduite qui, lorsqu'il est mélangé au bitume, gonfle et augmente de volume de 5 à 10 fois (Porot et al., 2019a).

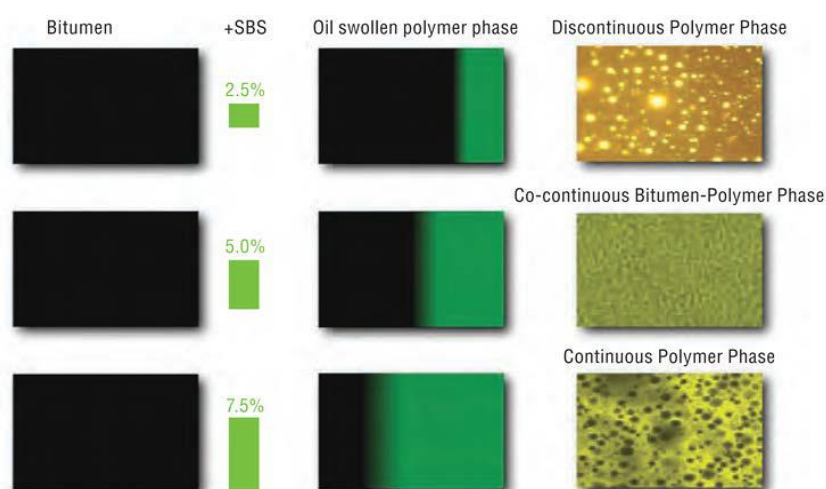


Figure 10: Structure du liant en fonction de la teneur en polymère (à partir de (Habbouche et al., 2019))

Comme pour de nombreuses nouvelles technologies et matériaux, leurs avantages doivent être mis en balance avec leurs inconvénients effectifs et potentiels. La teneur élevée en polymères des mélanges à haute teneur en PmB peut augmenter la viscosité du liant, rendant l'asphalte difficile à produire en usine et de plus en plus difficile à travailler pour les équipes de pose. Il existe également un risque de séparation de phases et un potentiel accru d'usure microplastique. En raison de sa teneur plus élevée en polymères, le PmB à haute teneur est également plus coûteux que le PmB conventionnel, ce qui augmente les coûts initiaux de production.

Compte tenu de la discussion ci-dessus, la portée de ce projet a été définie. Nous avons cherché à tirer parti des connaissances mondiales existantes en matière d'utilisation des PmB à haute teneur et avons élaboré un plan de recherche permettant d'abord de vérifier les affirmations, puis de proposer des moyens de normalisation de l'utilisation des PmB à haute teneur. L'absence actuelle de critères de normalisation de l'utilisation des PmB à haute teneur limite leur application et pose des problèmes lors du contrôle de la qualité.

Le cœur de ce projet a été divisé en trois parties, comme le montre la Figure 11, et comprenait la normalisation des liants, la construction de deux sections d'essai, l'évaluation d'une section d'essai existante et la modélisation afin de proposer les moyens nécessaires à la normalisation de la conception des chaussées lors de l'utilisation de PmB à haute teneur. Un résumé des principales conclusions du projet est présenté dans les sous-sections suivantes.

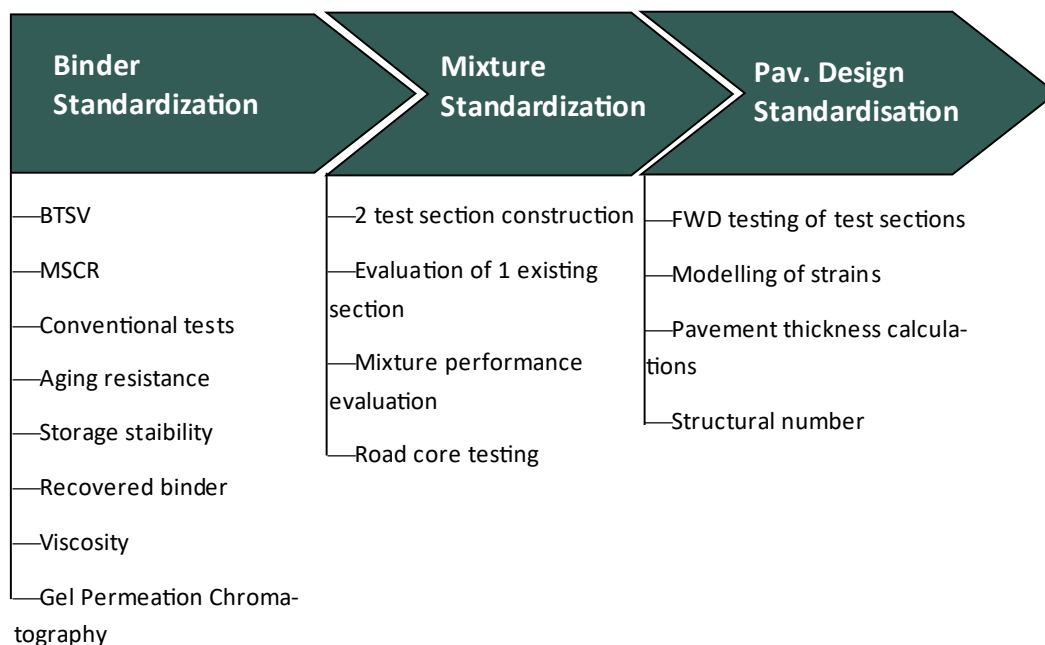


Figure 11: Aperçu du projet (les abréviations utilisées dans la figure sont présentées dans la section des méthodes)

Normalisation du contrôle qualité des liants

Dans cette section, nous avons évalué un total de 10 liants différents appartenant à deux catégories (désignées comme souples et durs) à l'aide de tests conventionnels ainsi que d'un test de fluage-recouvrance sous contraintes répétées (MSCR), d'un test de caractérisation rapide des liants (BTSV), d'un balayage de fréquence et d'une viscosité rotationnelle. De plus, la chromatographie par perméation de gel (GPC) a été utilisée pour évaluer les polymères. Les liants ont été sélectionnés de manière à couvrir une étendue de niveaux de modification des polymères, et ont été classés grossièrement comme faibles ($\sim 2\%$), moyens ($\sim 3\%$), élevés ($\sim 5\%$) et élevés ($> 6\%$).

Résultats des tests conventionnels

Le test de pénétration peut également servir à déterminer la dureté des PmB à haute teneur. Cependant, il est recommandé de le remplacer par un test basé sur le DSR qui

fournit davantage d'informations sur les propriétés viscoélastiques dans la plage de températures intermédiaires et/ou basses.

La température du point de ramollissement n'offrait pas de moyen fiable pour classer les PmB avec des teneurs en polymères élevées et, selon l'échantillon, le vieillissement entraînait soit une réduction ou une augmentation de la température du point de ramollissement. Pour ces raisons, la méthode n'est pas recommandée pour la classification des High PmB.

Dans la plupart des cas, le test de récupération élastique à 25 °C ne permettait pas de différencier les liants ayant des teneurs en polymères différentes, car les résultats étaient proches ou supérieurs à 90 %.

Le test de point de rupture de Fraass a donné des résultats inattendus : de nombreux liants ont amélioré leur résistance à la fissuration à basse température après vieillissement et trois d'entre eux ne répondaient pas aux exigences actuelles en matière de température de point de rupture. Pour ces raisons, cette méthode de test n'est pas recommandée pour la classification des PmB à haute teneur.

Viscosité rotationnelle

Les essais de viscosité rotationnelle ont montré que, bien que tous les liants répondaient à l'exigence AASHTO M320 de ≤ 3 Pa·s à 135 °C, les High PmB présentaient un comportement non newtonien à cette température. À 160 °C, les liants se comportaient de manière newtonienne, et un critère supplémentaire de ≤ 1 Pa·s à cette température a été proposé afin de garantir la maniabilité du liant.

Caractérisation à l'aide du BTSV

La méthode d'essai BTSV a permis de distinguer avec succès les liants en fonction de leur teneur en polymères. Des critères d'acceptation ont été proposés pour les liants souples et durs, comme le montre la Figure 12. Avec le vieillissement, on a observé une augmentation nette de la température BTSV et une diminution de l'angle de phase.

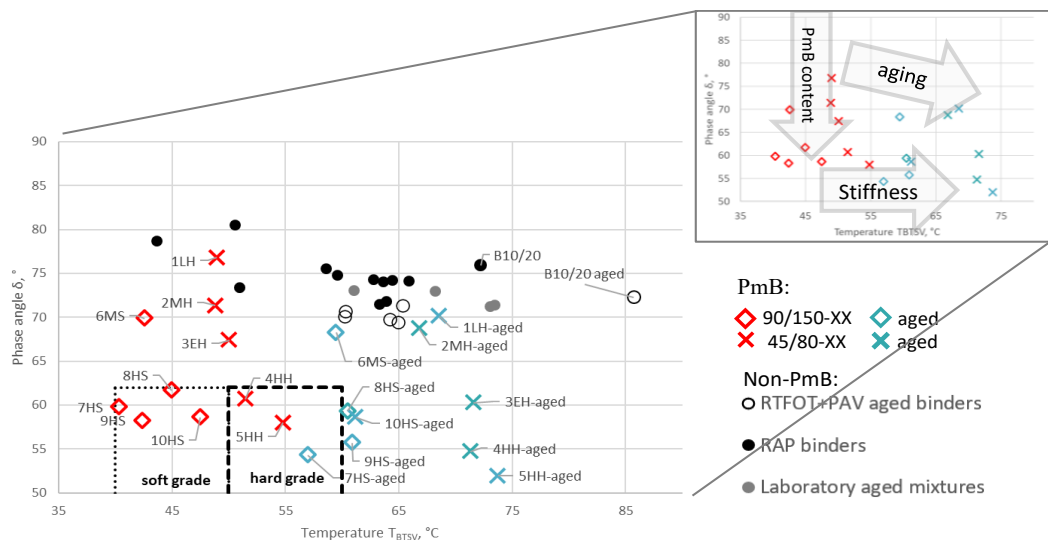


Figure 12: BTSV a proposé des classes pour les High PmB. HH et HS désignent les High PmB, tandis que les autres lettres correspondent à des liants à plus faible teneur en polymères.

Une extension du test BTSV à 1 kPa a été proposée afin de permettre le calcul de l'« angle de phase delta ». Ce paramètre caractérise l'effet du réseau polymère à haute

température et présente une bonne corrélation avec les résultats GPC de la plupart des liants. La collecte de données supplémentaires à l'aide de ce paramètre pourrait fournir de nouvelles informations.

Le protocole de vieillissement appliqué (cycles RTFOT+2PAV³) a permis de simuler avec succès l'état de vieillissement des liants typiques présents dans l'asphalte recyclé en Suisse. Cet état de vieillissement est donc proposé pour sélectionner les liants susceptibles de subir un vieillissement accéléré à long terme. Les critères BTSV proposés pour l'évaluation du vieillissement sont résumés dans le Table 2.

Une bonne relation exponentielle ($R^2 = 0,93$) a été observée entre la température BTSV et la pénétration logarithmique, comme le montre la Figure 13. La figure comprend également deux encadrés ombrés qui montrent la zone de chevauchement entre les exigences de température BTSV proposées et les exigences de pénétration correspondantes pour les liants souples et durs hautement modifiés. On constate que les High PmB se trouvent toujours dans les cases, ce qui signifie que les résultats BTSV et de pénétration incluraient les liants dans la même classe. Cela signifie que si les résultats des tests BTSV sont utilisés pour la classification des High PmB, le test de pénétration est en partie redondant dans ce cas. Bien sûr, des liants non modifiés ou PmB standards peuvent également se trouver dans les cases, dans ce cas les liants 6MS et 3EH. Il est nécessaire de tester les propriétés élastiques des liants pour les distinguer. Si les limites BTSV indiquées dans la Figure 12 étaient appliquées, ces liants n'appartiendraient pas à la même classe sur la base des critères d'angle de phase.

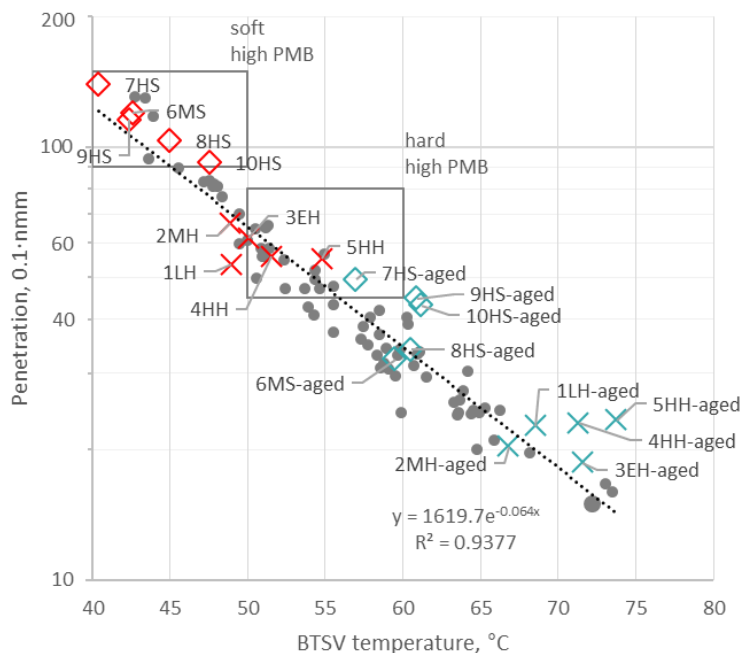


Figure 13: Température BTSV par rapport à la pénétration logarithmique

Evaluation MSCR

³ RTFOT: Rolling Thin Film Oven Test
PAV: Pressure Aging Vessel

La contrainte d'essai MSCR de 3,2 kPa était trop faible pour permettre de différencier les différents teneurs en polymères. L'augmentation de la contrainte à 10 kPa et la réalisation des essais à une température appropriée (64 °C pour les liants durs ; 58 °C pour les liants souples) ont permis de classer clairement les liants en fonction de leur teneur en polymères. À titre d'exemple, les critères d'acceptation proposés pour les liants durs à haute teneur en PmB sont présentés à la Figure 14. Cependant, le choix de la température d'essai reste un défi, car les liants destinés à différents domaines d'application (par exemple, en montagne ou en plaine) peuvent nécessiter des températures d'essai différentes.

Il a également été recommandé d'augmenter le nombre de cycles par niveau de contrainte à 30 pour une meilleure reproductibilité des résultats.

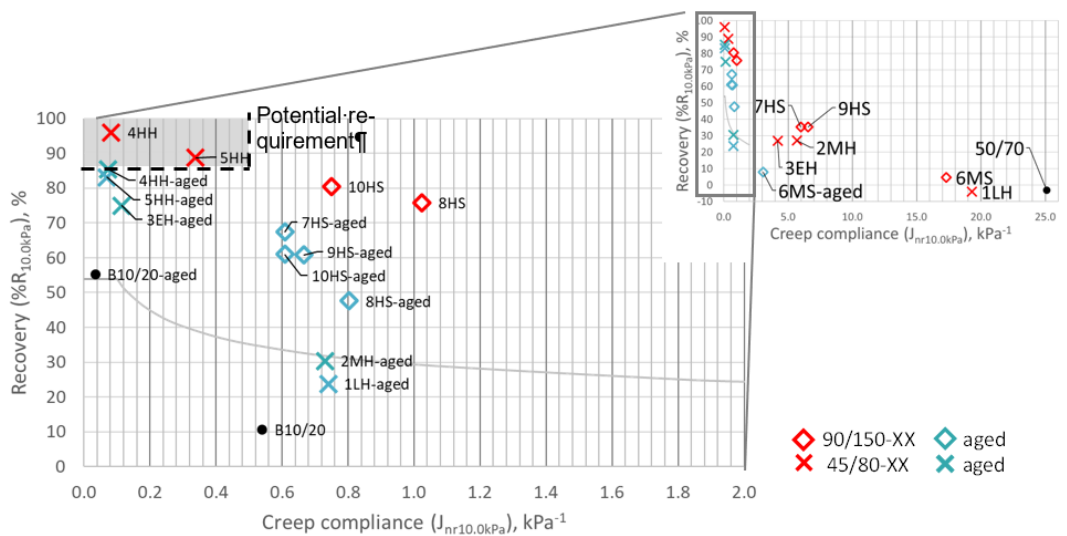


Figure 14: Résumé des résultats du test MSCR à 10,0 kPa et 64 °C. HH désigne les High PmB, tandis que les autres lettres correspondent à des liants à faible teneur en polymères.

Chromatographie par perméation de gel

La surface autour du pic dans la chromatographie par perméation de gel (GPC) est corrélée à la quantité de polymère utilisée dans le liant, à condition que le polymère soit identique. Sinon, la surface du pic de différents types de polymères ne fournit aucune information ni sur la teneur en polymère ni sur les performances mécaniques.

La GPC s'est avérée utile pour la recherche, mais elle ne convient pas à la classification des liants, car la surface du pic du polymère et la masse moléculaire dépendent du type de polymère et ne peuvent donc pas être appliquées de manière universelle à tous les types de liants.

Recommandations relatives à la normalisation des liants

La Figure 15 résume les températures d'essai des High PmB pour chaque méthode utilisée dans cette recherche. Sur la base des résultats de cette recherche, les méthodes d'essai adaptées à la classification des High PmB sont indiquées au-dessus de l'axe horizontal, tandis que les méthodes situées sous l'axe ne sont pas recommandées.

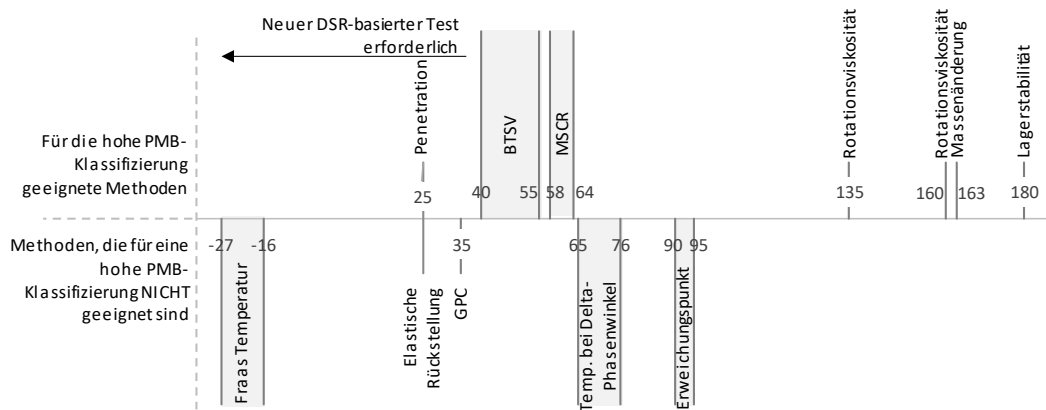


Figure 15: La température d'essai des différentes méthodes basées sur les résultats de cet article pour les liants hautement modifiés par des polymères. Les méthodes suggérées pour les spécifications européennes sont indiquées au-dessus de la ligne.

Table 2 résume les méthodes et critères proposés pour la classification des liants hautement modifiés par des polymères. Ces méthodes conviennent à tous les liants PmB et aux liants non modifiés, mais elles sont particulièrement nécessaires pour la classification des liants hautement modifiés par des polymères, car les méthodes actuellement utilisées ne permettent pas de distinguer de manière adéquate les liants conventionnels des liants hautement modifiés par des polymères. Il est fortement recommandé de réévaluer les critères proposés après avoir recueilli davantage de données.

Méthodes proposées pour le contrôle qualité High PmB

Méthode	Critères liant rigide	Critères liant souple	Remarques	Standard
Penetration	45-80 0.1mm	90-150 0.1mm	-	EN 1426
Viscosité dynamique	≤3 Pa·s @ 135 °C ≤1 Pa·s at 160 °C	≤3 Pa·s at 135 °C ≤1 Pa·s at 160 °C	Validation des critères nécessaires	EN 13302
Stabilité au stockage	≤5°C	≤5°C	Développement de critères basés sur le MSCR ou le BTSV recommandé	EN 13399
Changement de masse après RTFOT	≤0.5 %	≤0.5 %	-	EN 12607-1
BTSV	δ _{BTSV} ≤ 62 ° & T _{BTSV} 50-60 °C	δ _{BTSV} ≤ 62 ° & T _{BTSV} 40-50 °C	Validation des critères recommandés	EN 17643
Résistance au vieillissement avec BTSV après RTFOT	Réduction de δ _{BTSV} ≤ 6 °C Augmentation de T _{BTSV} ≤ 8 °C	Réduction de δ _{BTSV} ≤ 6 °C Augmentation de T _{BTSV} ≤ 8 °C	Les critères proposés sont basés sur une pré-norme allemande. Validation recommandée.	EN 17643 EN 12607-1
Résistance au vieillissement avec BTSV après RTFOT+2PAV cycles	Réduction de δ _{BTSV} ≤ 10° Augmentation de T _{BTSV} ≤ 23 °C	Réduction de δ _{BTSV} ≤ 10° Augmentation de T _{BTSV} ≤ 23 °C	Les critères proposés sont basés sur une pré-norme allemande. Validation recommandée.	EN 17643 EN 14769

Méthode	Critères liant rigide	Critères liant souple	Remarques	Standard
MSCR test	≥85 % de récupération ≤ 0,5 % kPa-1 Test à 10 kPa, 64 °C	Récupération ≥ 85 % ≤ 0,5 % kPa-1 Test à 10 kPa, 58 °C	Contrainte de 10 kPa non conforme à la norme actuelle La température d'essai doit être choisie en fonction du climat Dans cette étude, les essais ont été réalisés sur des échantillons non vieillis	EN 16659

Table 2: Méthodes et critères proposés pour le contrôle qualité des liants hautement modifiés par des polymères

Section d'essai : AC B 22 S sur la H19 Oberalpstrasse, Tamins - Val Maliens, Grisons

L'enrobé AC B 22 S a été posé en couche de liaison sur le site d'essai H19 Oberalpstrasse Tamins – Val Maliens. Ce chantier a été sélectionné en raison de la forte intensité du trafic. Deux mélanges ont été posés : (1) mélange contenant 40 % de RAP avec ajout d'un liant souple hautement modifié par des polymères (PmB 90/150-85) ; (2) un mélange contenant 0 % de RAP avec un liant dur hautement modifié par des polymères (PmB 45/80-85). Le mélange contenant 40 % de RAP a permis d'évaluer les avantages de l'utilisation d'un PmB élevé pour compenser le manque de polymères dans le RAP, tandis que le mélange contenant 0 % de RAP a permis d'évaluer les avantages de l'utilisation d'un PmB élevé pour améliorer les performances et la longévité de l'asphalte, ainsi que d'évaluer la réduction potentielle de l'épaisseur de la couche.

Les résultats de la section d'essai AC B 22 S sont résumés dans le

Mixture	RAP content	Binder tests				Rutting resistance	Crack propagation resistance		Fatigue		Stiffness	Low temp. cracing resistance
		ER	BTSV	MSCR	FS	FRT	SCB	IDEAL-CT	2PB-TR	MMLS3	ITT	TSRST
ACB 22 S	HPMix	↗	↗	↗	↗	↘	↗ ¹	↗ ¹	↗	↗	↗	→
	RAP Mix	●	●	●	●	●	●	●	●	●	●	●

Legend:

- reference mixture result
- ↗ significantly better performance
- ↘ slightly better performance
- similar performance
- ↘ slightly worse performance
- ↘ significantly worse performance
- ER Elastic Recovery (binder)
- BTSV Binder fast characterisation test
- MSCR Multiple stress creep recovery test (binder)
- FS Frequency Sweep (binder)
- FRT French Rutting Tester (mixture)
- SCB Semi-circular bend test (mixture)
- IDEAL-CT Indirect tensile asphalt cracking test (mixture)
- 2PB-TR Two point bending on trapezoidal specimen
- MMLS3 Model mobile load simulator (mixture)
- ITT Indirect tensile test (mixture)
- TSRST Tensile stress restrained specimen test

1 SCB and IDEAL-CT tests are not sensitive to polymer content

Figure 16. Ce tableau permet de comparer qualitativement les résultats du mélange à haute teneur en polymères (HPMix) à ceux du mélange contenant 40 % de RAP (RAP Mix). Dans l'ensemble, les deux mélanges ont fourni de bonnes performances qui correspondent aux exigences actuelles des spécifications pour les mélanges et le liant PmB 45/80-65 (CH-E) récupéré. Ce résultat a été obtenu même avec le mélange contenant 40 % de RAP, ce qui indique qu'une teneur d'au moins 40 % de RAP peut être utilisée

avec succès dans les mélanges modifiés par des polymères. D'après les résultats des essais sur les liants, une teneur en RAP encore plus élevée pourrait permettre de satisfaire aux exigences actuelles des spécifications lorsque du PmB à haute teneur est utilisé et qu'une optimisation supplémentaire de la formulation du mélange est effectuée. Il convient toutefois de noter que les exigences actuelles ne permettent pas toujours de déterminer de manière fiable les performances des liants. C'est pourquoi des méthodes d'essai supplémentaires ont été utilisées dans le cadre de cette recherche.

Comme le montre la figure, la plupart des méthodes d'essai, y compris les essais supplémentaires sur les liants et les essais sur les mélanges basés sur les performances, indiquent que le mélange HPMix offre de meilleures performances que le mélange de référence. Cela était prévisible, étant donné que la teneur effective en polymères du HPMix est plus élevée que celle du RAPMix en raison de la teneur en RAP de 40 %. Dans l'ensemble, ces résultats permettent de conclure que l'utilisation d'un liant hautement modifié par des polymères peut servir deux objectifs :

- Il est bénéfique pour l'amélioration des performances lorsqu'il est utilisé avec un faible taux ou sans RAP⁴.
- Il permet d'utiliser une teneur élevée en RAP (jusqu'à au moins 40 % dans les mélanges de la couche de liaison) afin de garantir les performances attendues d'un mélange modifié par des polymères conventionnels lorsque la qualité cible est PmB 45/80-60 (CH-E).

Mixture	RAP content	Binder tests				Rutting resistance	Crack propagation resistance		Fatigue		Stiffness	Low temp. cracing resistance
		ER	BTSV	MSCR	FS	FRT	SCB	IDEAL-CT	2PB-TR	MMLS3	ITT	TSRST
ACB 22 S	HPMix	0%	↗	↗	↗	↘	↗ ¹	↗ ¹	↗	↗	↗	→
	RAP Mix	40%	●	●	●	●	●	●	●	●	●	●

Legend:

- reference mixture result
 - ↗ significantly better performance
 - ↘ slightly better performance
 - similar performance
 - ↘ slightly worse performance
 - ↘ significantly worse performance
 - ER Elastic Recovery (binder)
 - BTSV Binder fast characterisation test
 - MSCR Multiple stress creep recovery test (binder)
 - FS Frequency Sweep (binder)
 - FRT French Ruting Tester (mixture)
 - SCB Semi-circular bend test (mixture)
 - IDEAL-CT Indirect tensile asphalt cracking test (mixture)
 - 2PB-TR Two point bending on trapezoidal specimen
 - MMLS3 Model mobile load simulator (mixture)
 - ITT Indirect tensile test (mixture)
 - TSRST Tensile stress restrained specimen test
- 1 SCB and IDEAL-CT tests are not sensitive to polymer content

Figure 16: Résumé des résultats des essais de la section d'essai AC B 22 S

Section d'essai : AC 8 S sur la H27 Engadinerstrasse à St. Moritz Charnadüra, dans les Grisons

Un enrobé bitumineux de type AC 8 S a été posé sur le site d'essai situé sur la H27 Engadinerstrasse à St. Moritz Charnadüra, dans les Grisons. Ce site a été choisi en raison de son trafic intense et de ses conditions climatiques. Deux mélanges ont été posés

⁴ Bien que le mélange sans contenu recyclé donne les meilleurs résultats, les auteurs ne recommandent pas d'abandonner le recyclage de l'asphalte. L'utilisation du RAP doit être évaluée dans le contexte de la durabilité et de l'efficacité des ressources. Une telle évaluation ne faisait pas partie de ce projet.

: le mélange HPMix a été posé avec un liant hautement modifié par des polymères (90/150-85) et un mélange de référence a été posé avec un liant de type PmB 90/150-60 (CH-E). Les deux mélanges ont la même composition.

Dans l'ensemble, les deux mélanges ont fourni de bonnes performances qui correspondent aux exigences des spécifications actuelles. Cependant, comme indiqué précédemment, les méthodes d'essai utilisées pour le contrôle de la qualité ne permettent pas toujours d'évaluer de manière fiable l'effet de l'augmentation de la teneur en polymères. C'est pourquoi plusieurs méthodes d'essai basées sur les performances ont été utilisées dans cette recherche.

Les résultats basés sur les performances de la section d'essai AC 8 S sont résumés dans le Figure 17. Ce tableau permet de comparer qualitativement les résultats du HPMix à ceux du mélange de référence. On peut voir dans le tableau que les essais sur le liant et l'essai de résistance à la fissuration à basse température (TSRST) montrent des performances supérieures du liant hautement modifié par des polymères par rapport au mélange de référence fabriqué à partir d'un liant modifié par des polymères conventionnels. La résistance à l'orniérage des deux mélanges est similaire et très bonne. D'après les résultats des essais sur le liant, on peut raisonnablement s'attendre à une meilleure résistance à l'orniérage de la chaussée avec le HPMix. Cependant, les conditions d'essai d'orniérage n'étaient pas suffisamment sévères pour induire un orniérage significatif. Même la prolongation de l'essai n'a pas entraîné de dommages significatifs. Par conséquent, d'autres modifications des conditions d'essai pourraient être envisagées à l'avenir, par exemple en augmentant la température d'essai ou en utilisant une autre méthode d'essai (par exemple, l'essai de compression cyclique).

La rigidité des deux mélanges était similaire et la résistance à la propagation des fissures était légèrement moins bonne pour le HPMix que pour le mélange de référence. Cependant, d'après des recherches antérieures, il est probable que les différences dans la propagation des fissures ne soient pas liées à la teneur en polymères, car les méthodes d'essai utilisées ne sont pas sensibles à la teneur en polymères.

Dans l'ensemble, les résultats permettent de conclure que l'utilisation d'un liant hautement modifié par des polymères dans la couche de roulement:

- Améliore les performances de la couche de roulement.
- La caractérisation des liants à l'aide de tests conventionnels ne permet pas de démontrer pleinement les avantages liés à l'utilisation d'un liant hautement modifié par des polymères. Les tests BTSV et MSCR à 10 kPa constituent des moyens appropriés pour caractériser les liants.
- Des conditions plus sévères sont nécessaires pour le test de résistance à l'orniérage afin de distinguer les différentes performances.

Mixture	RAP content	Binder tests			Rutting resistance	Crack propagation resistance		Stiffness	Low temp. cracing resistance
		ER	BTSV	MSCR	FRT	SCB	IDEAL-CT	ITT	TSRST
AC 8 S	HPMix	0%	↗	↕	↔	↘ ¹	↘ ¹	↔	↕
	Reference	0%	●	●	●	●	●	●	●

Legend:

●	reference mixture result	ER	Elastic Recovery (binder)
↕	significantly better performance	BTSV	Binder fast characterisation test
↗	slightly better performance	MSCR	Multiple stress creep recovery test (binder)
↔	similar performance	FRT	French Ruting Tester (mixture)
↘	slightly worse performance	SCB	Semi-circular bend test (mixture)
↙	significantly worse performance	IDEAL-CT	Indirect tensile asphalt cracking test (mixture)
		ITT	Indirect tensile test (mixture)
		TSRST	Tensile stress restrained specimen test

¹ SCB and IDEAL-CT tests are not sensitive to polymer content

Figure 17: Résumé des résultats des essais de la section d'essai AC 8 S

Section d'essai : SDA 4-12 sur K244, Rapperswil IO, Argovie

La section d'essai SDA utilisant de l'asphalte hautement modifié par des polymères dans le canton d'Argovie a été construite en 2020 et les résultats des essais correspondants sont inclus dans le présent rapport. En 2024, des carottes ont été prélevées sur la chaussée construite et de nouveaux mélanges ont été préparés en laboratoire à des fins d'essai. Le mélange de laboratoire a été produit à partir de la même recette et des mêmes matériaux que ceux utilisés en 2020.

La section d'essai est située à K244 Rapperswil et la section de référence SDA 4-12 a été construite avec le liant PmB 45/80-65 (CH-E). La section SDA 4-12 HPMix a été construite en utilisant du PmB 45/80-80 à haute teneur.

Au cours de ce projet, nous avons testé différents types d'échantillons et nous avons également utilisé les résultats des rapports de la construction d'origine. Au total, quatre types de résultats ont été utilisés :

- Résultats des essais sur les mélanges et les liants provenant des échantillons prélevés lors de la construction de la section d'essai en 2020.
- Résultats des essais sur les mélanges et les liants récupérés provenant des carottes prélevées peu après la construction de la section d'essai en 2020.
- Résultats des essais sur le mélange et le liant récupéré provenant des carottes routières prélevées pendant le projet HPMix en 2024.
- Résultats des essais sur le mélange provenant des échantillons produits dans le laboratoire de l'Empa pendant le projet HPMix en 2024.

Les résultats du test SDA permettent de conclure qu'il semble y avoir un avantage à utiliser le liant hautement modifié par des polymères plutôt que le liant modifié par des polymères conventionnel. Cela ressort clairement des résultats du test de liant présentés dans le Figure 18, qui compare qualitativement le liant récupéré à partir du HPMix avec le liant récupéré à partir du mélange de référence. Les résultats des tests sur les mélanges montrent également des performances similaires ou supérieures à celles du mélange de référence. La résistance d'adhérence intercouche des échantillons HPMix est inférieure à celle requise. Étant donné que la technologie de construction et le matériau de la couche d'accrochage étaient identiques, une hypothèse serait qu'une

réaction chimique entre le highPmB et la couche d'accrochage ait réduit l'adhérence. Cela nécessite une vérification plus approfondie.

Malheureusement, le test Cantabro (même après modification pour le rendre plus sévère) n'a pas permis de démontrer de manière concluante les avantages potentiels d'une modification polymère élevée en ce qui concerne la réduction de la perte de gravillons des mélanges SDA, même avec les variations du test qui ont été mises en œuvre dans le projet. D'autres méthodes d'essai devraient être envisagées pour évaluer cette propriété.

Mixture	Binder tests				Rutting resistance	Crack propagation resistance		Raveling resistance	Stiffness	Low temp. cracing resistance	Interlayer bond
	ER	BTSV	MSCR	FS	FRT	SCB	IDEAL-CT	Cantabro	ITT	TSRST	Leutner
SDA HPMix	↑	↑	↑	↑	→	↗ ¹	↗ ¹	↗	↘	↑	↓
Reference	●	●	●	●	●	●	●	●	●	●	●

Legend:

- reference mixture result
- ↑ significantly better performance
- ↗ slightly better performance
- similar performance
- ↘ slightly worse performance
- ↓ significantly worse performance

1 SCB and IDEAL-CT tests are not sensitive to polymer content

- ER Elastic Recovery (binder)
- BTSV Binder fast characterisation test
- MSCR Multiple stress creep recovery test (binder)
- FS Frequency Sweep (binder)
- FRT French Rutting Tester (mixture)
- SCB Semi-circular bend test (mixture)
- IDEAL-CT Indirect tensile asphalt cracking test (mixture)
- Cantabro Cantabro test (mixture)
- ITT Indirect tensile test (mixture)
- TSRST Tensile stress restrained specimen test
- Leutner Leutner test (mixture)

Figure 18: Résumé des résultats des tests SDA

Proposition de normalisation des mélanges bitumineux

Cette recherche a montré que les liants hautement modifiés par des polymères peuvent présenter des avantages certains par rapport aux liants modifiés par des polymères classiques. Au cours de la recherche, cela a été démontré tant au niveau du liant que du mélange. Toutefois, à des fins de normalisation, ce sont principalement des méthodes d'essai et des critères basés sur le liant qui sont proposés, comme le résume le Table 2, car au niveau du mélange, les essais n'ont pas démontré de différence notable entre le liant fortement modifié par des polymères et un liant modifié par des polymères conventionnels, ou bien la réalisation des essais est trop laborieuse (dans le cas de l'essai de fatigue). Par conséquent, même si certains essais sur les mélanges peuvent être utiles pour la conception des mélanges, leur utilisation n'est pas nécessairement liée exclusivement aux liants fortement modifiés par des polymères et aucune recommandation n'est donc fournie dans le présent rapport. Vous trouverez ci-dessous un résumé des considérations qui ont motivé la proposition ou la non-proposition d'un certain essai pour la normalisation.

Essai d'orniérage sur mélange

Les mélanges ont satisfait aux exigences du test d'orniérage et, dans la plupart des cas, une profondeur d'ornière ne dépassant pas 5 % a été observée jusqu'à 30 000 cycles de charge. L'extension du test à 90 000 cycles n'a apporté aucun avantage et n'a pas mis

en évidence les avantages potentiels de la teneur élevée en polymères du liant, car les résultats, même jusqu'à 90 000 cycles, étaient similaires entre les mélanges de référence et les mélanges HPMix.

L'orniérage est un problème particulier dans les zones à circulation lente où les forces de cisaillement sont importantes (par exemple, les arrêts de bus et les ronds-points). Compte tenu de la possibilité d'obtenir une très grande résistance à l'orniérage, on peut se demander si les liants fortement modifiés par des polymères pourraient constituer une solution pour ces emplacements. Il est donc recommandé d'évaluer l'utilisation de mélanges fortement modifiés par des polymères pour ces emplacements (éventuellement en construisant une section d'essai) et d'envisager de développer des conditions d'essai plus sévères (par exemple, une température d'essai plus élevée) ou d'utiliser une autre méthode d'essai (par exemple, un essai de compression cyclique) pour tester la résistance à l'orniérage.

Essais de résistance à la fissuration des mélanges (SCB et IDEAL-CT)

Les essais de résistance à la fissuration (SCB et IDEAL-CT) constituent des moyens appropriés pour la conception des mélanges, car ils sont sensibles aux paramètres qui influent sur les performances du mélange : teneur en liant, propriétés du liant et teneur en RAP. Ces méthodes ont également démontré une corrélation relativement élevée avec les performances sur le terrain et sont simples et rapides à mettre en œuvre. Pour ces raisons, elles peuvent être envisagées pour la conception des mélanges.

Cependant, d'après cette étude et les recherches précédentes de l'Empa, ces méthodes ne sont pas sensibles à l'utilisation de polymères dans le liant. Elles ne peuvent donc pas être utilisées pour caractériser les mélanges dans le but d'évaluer les propriétés élastiques ou l'effet des polymères.

Essais de fatigue et de rigidité des mélanges

Le test de fatigue a démontré un avantage distinct lié à l'utilisation d'un liant hautement modifié par des polymères. Cependant, il n'est actuellement pas proposé de l'inclure dans le contrôle qualité ou les tests de type de mélange, car la réalisation du test est très laborieuse et on peut raisonnablement supposer que les tests de caractérisation du liant sont suffisants pour garantir les performances des mélanges, en particulier pour les types de mélanges bien établis, comme l'AC.

Comme prévu, l'essai de rigidité n'a pas démontré de différence notable entre les mélanges contenant différentes teneurs en polymères. Par conséquent, étant donné que les types de mélanges évalués dans le cadre de ce projet ne nécessitent pas actuellement d'essai de rigidité, il n'est pas non plus nécessaire de l'introduire lors de l'utilisation d'un liant hautement modifié par des polymères.

Essai sur échantillon soumis à une contrainte thermique (TSRST)

Le TSRST a montré qu'il pourrait être avantageux d'utiliser une teneur en polymères plus élevée pour augmenter la résistance à la fissuration à basse température. Cependant, même le liant modifié par des polymères conventionnels garantissait une résistance élevée à la fissuration à basse température. Par conséquent, même s'il peut être avantageux d'inclure le TSRST comme critère d'homologation des mélanges bitumineux dans les régions froides, cela n'est pas nécessairement lié à l'utilisation d'un liant fortement modifié par des polymères. C'est pourquoi aucun critère de normalisation n'est fourni pour cet essai dans le cadre du présent rapport.

Normalisation du dimensionnement structurel des chaussées

Dans ce travail, une méthodologie a été appliquée afin d'estimer les coefficients structurels (valeurs a) pour les mélanges High PmB dans le cadre de la norme suisse de dimensionnement (VSS 40 324). Les valeurs calculées se situaient entre 4.43 et 6.92, et une valeur conservatrice de 4.4 est proposée pour le dimensionnement. Cela confirme l'avantage structurel attendu des mélanges High PmB par rapport aux matériaux conventionnels. En pratique, cela pourrait représenter une réduction d'environ 10 % de l'épaisseur de la couche d'asphalte. Sinon, si l'épaisseur reste inchangée, on peut s'attendre à une augmentation des charges équivalentes par essieu (ESAL) comprise entre 39 % et 106 % selon la structure de la chaussée. Il convient de noter que la valeur a proposée ne concerne que les mélanges ne contenant pas de RAP. En cas d'utilisation d'une teneur élevée en RAP, l'objectif de l'utilisation d'un PmB élevé est d'obtenir des performances similaires à celles des mélanges actuellement spécifiés dans la norme avec les valeurs a existantes. Toutefois, ces valeurs doivent être validées sur des structures réelles, soit à échelle réduite soit à échelle réelle, avant de pouvoir être introduites en pratique.

Besoins en matière de recherche

Au cours du projet HPmix, plusieurs besoins spécifiques pour les recherches futures ont été identifiés. Une étude de suivi sur ces sujets faciliterait la mise en œuvre de High PmB :

- Au cours de cette recherche, un coefficient structurel a a été proposé pour les mélanges à haute teneur en PmB. Il est recommandé de valider ces résultats en construisant un site d'essai utilisant les dimensions calculées à l'aide du nouveau coefficient.
- Il a été démontré que les conditions actuelles des essais d'orniérage ne sont pas suffisamment sévères pour mettre en évidence une différence entre un mélange PmB conventionnel et un mélange à haute teneur en PmB. Il est donc recommandé de mettre au point de nouvelles conditions d'essai ou de valider une autre méthode d'essai, par exemple la compression cyclique.

En outre, l'étude a identifié plusieurs domaines présentant des lacunes qui ne sont pas nécessairement liées à la mise en œuvre de High PmB, mais qui pourraient plutôt profiter à l'ensemble du secteur :

- Le PmB à haute teneur peut être particulièrement utile dans les applications spécialisées où le trafic est intense et les forces de cisaillement élevées. Cela inclut les arrêts de bus, les stations de pesage, les ronds-points, les intersections et autres emplacements similaires. La construction d'une section d'essai avec une évaluation correspondante pourrait démontrer le potentiel des mélanges à haute teneur en PmB pour remplacer le béton dans de telles applications.
- La stabilité au stockage est actuellement évaluée à l'aide d'un essai de point de ramollissement. Étant donné que le point de ramollissement n'est pas recommandé pour l'évaluation du PmB élevé, il est recommandé de développer de nouveaux critères pour l'évaluation de la stabilité au stockage des liants à l'aide d'un essai basé sur le DSR.
- La méthode proposée basée sur le DSR est exécutée à des températures de service élevées. Une ou plusieurs nouvelles méthodes basées sur le DSR devraient être développées pour la caractérisation des liants à température intermédiaire et basse.

- Le calcul des contraintes et le dimensionnement de l'asphalte sont très laborieux, mais l'optimisation de la conception des chaussées pourrait permettre d'économiser des matériaux et des ressources, tout en favorisant l'innovation. Un outil analytique simple et gratuit pour la conception des chaussées peut être développé en utilisant l'approche utilisée dans la norme VSS 40 324.
- Le projet a révélé les avantages potentiels de l'utilisation de mélanges à forte teneur en PmB. Leur utilisation, y compris en combinaison avec le recyclage de l'asphalte, devrait également être évaluée en tenant compte de la durabilité, du cycle de vie et de l'évaluation des coûts.

Zusammenfassung

In einem typischen polymermodifizierten Bindemittel (PmB) liegt die Polymerdosierung zwischen 2,5 und 3,5 Massenprozent des Asphaltbindemittels, während hochpolymermodifizierte Bindemittel (High-PmBs) typischerweise Polymerdosierungen von 6–8 M.-% enthalten. Solche Bindemittel werden bereits in der Praxis und in der Forschung eingesetzt. Im Vergleich zu konventionellen PmBs werden als Vorteile von hochpolymeren Bindemitteln eine längere Lebensdauer des Belags, eine verbesserte Spurrinnen- und Rissbeständigkeit, eine geringere Belagsdicke und eine Erhöhung des Recycling-Anteils in herkömmlichen polymermodifizierten Mischgütern (Bindemitteltyp CH-E oder CH-C) möglich ist.

Die Vorteile eines hohen PmB-Gehalts gegenüber konventionellem PmB-Gehalt ergeben sich aus dem kontinuierlichen Polymernetzwerk. Während in einem konventionellem PmB die Polymerphase diskontinuierlich ist, bildet die Polymerphase in einem High-PmB ein ausgedehntes Polymernetzwerk, das eine gummiartige Reaktion auf äussere Belastungen bewirkt (Habbouche et al., 2021) (siehe Figure 19). Das bedeutet, dass das Mischgut bei einem Polymeranteil von etwa 5 Gewichtsprozent des Asphaltbinders von einer diskontinuierlichen zu einer kontinuierlichen Polymerphase übergeht. Diese Umkehrung verbessert die Performance und Dauerhaftigkeit von Asphaltmischgutern. Die hohe Viskosität wird durch Styrol-Butadien-Styrol-Polymere (SBS) mit hohem Vinylgehalt und reduzierter Molekülgrössern (Porot et al., 2019a).

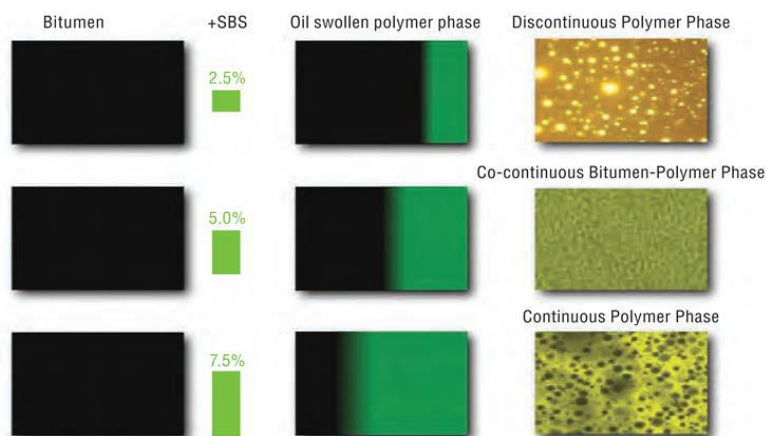


Figure 19: Struktur des Bindemittels in Abhängigkeit vom Polymergehalt (von (Habbouche et al., 2019))

Wie bei vielen neuen Technologien und Materialien müssen ihre Vorteile gegenüber den möglichen Nachteilen und Bedenken abgewogen werden. Der hohe Polymergehalt in Mischgütern mit hohem PmB-Gehalt kann die Viskosität des Bindemittels erhöhen, was die Herstellung des Asphalts in der Anlage erschwert und die Verarbeitung beim Einbau zunehmend unmöglich macht. Auch besteht die Gefahr der Phasentrennung und ein erhöhtes Potenzial für Mikroplastikabrieb bei Strassenverkehr. Aufgrund des höheren Polymeranteils ist ein hoher PmB-Gehalt auch teurer als ein herkömmlicher PmB, was die Materialkosten erhöht.

Das Ziel des vorliegenden Projekts war, das vorhandene Wissen über die Verwendung von PmB zu nutzen und in Anbetracht der obigen Ausführungen einen Forschungsplan

zu entwickeln, der es zunächst ermöglicht, die Annahmen zu überprüfen und anschließend Mittel zur Standardisierung der Verwendung von High-PmB vorzuschlagen. Das derzeitige Fehlen von Kriterien zur Normierung der Verwendung von PmB's mit hohen Polymergehalten schränkt deren Anwendung ein und verursacht Probleme bei der Bewertung der Eigenschaften.

Das Projekt bestand, wie in Figure 20 dargestellt, aus drei Teilen. Es umfasste die Bindemittelnormierung, Mischgutnormierung durch die Erstellung von zwei Teststrecken und die Bewertung eines bestehenden Testabschnitts sowie die Modellierung zur Belagsdimensionierung bei Verwendung von PmB mit hohem Polymergehalt. Eine Zusammenfassung der wichtigsten Ergebnisse des Projekts wird in den folgenden Unterabschnitten gegeben.

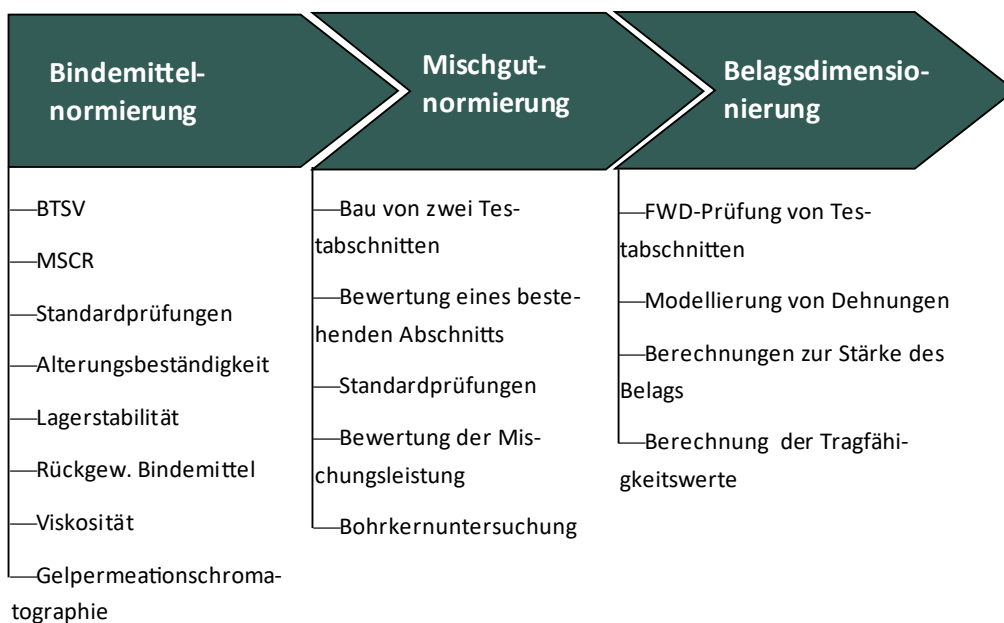


Figure 20: Projektübersicht (die in der Abbildung verwendeten Abkürzungen sind im Methodenteil aufgeführt)

Standardisierung der Bindemittel-Qualitätskontrolle

In diesem Abschnitt wurden insgesamt 10 verschiedene Bindemittel aus zwei Klassen (weich und hart) mit Hilfe konventioneller Prüfungen sowie der MSCR-Prüfungen (Multiple Stress Creep Recovery), der BTSV-Prüfungen (Bitumen-Typisierungsschnell-Verfahren), des Frequenzsweeps und der Rotationsviskosität bewertet. Zusätzlich wurde die Gelpermeationschromatographie (GPC) zur Bewertung der Polymere eingesetzt. Die Bindemittel wurden so ausgewählt, dass sie einen Gradienten der Polymermodifikation widerspiegeln, der grob als niedrig (~2 M.-%), mittel (~3 M.-%), erhöht (~5 M.-%) und hoch (>6 M.-%) eingestuft wurde.

Konventionelle Prüfergebnisse

Die Penetrationsprüfung kann auch zur Bestimmung der Härte von High-PmBs eingesetzt werden. Es wird jedoch vorgeschlagen, die Penetration durch eine dynamisches Scherrheometer (DSR)-basierte Prüfung zu ersetzen, die mehr Informationen über die viskoelastischen Eigenschaften im mittleren und/oder tiefen Temperaturbereich liefert.

Der Erweichungspunkt Ring und Kugel bietet keine verlässliche Möglichkeit, High-PmBs in Abhängigkeit vom Polymergehalt zu klassifizieren. Darüber hinaus kann eine Alterung sowohl zu einer Verringerung als auch zu einer Erhöhung der Erweichungspunkttemperatur führen. Aus diesen Gründen wird die Methode nicht für die Klassifizierung von Bindemitteln mit hohen Polymergehalten empfohlen.

Die Prüfung der elastischen Rückstellung bei 25 °C ermöglicht in den meisten Fällen keine Unterscheidung zwischen den Bindemitteln mit unterschiedlichem Polymergehalt, da die Ergebnisse nahe bei oder über 90 % lagen.

Der Brechpunkt nach Fraass (Bruchfestigkeitsprüfung) ergab unterschiedliche Trends. Viele Bindemittel verbesserten nach der Alterung ihre Beständigkeit gegen Rissbildung bei niedrigen Temperaturen, während drei der Bindemittel die aktuellen Anforderungen an die Bruchfestigkeitstemperatur nicht erfüllten. Aus diesen Gründen wird die Prüfmethode nicht für die Klassifizierung von Bindemitteln mit hohem PmB-Wert empfohlen.

Rotationsviskosität

Die Prüfung der Rotationsviskosität zeigte, dass zwar alle Bindemittel die AASHTO M320-Anforderung von ≤ 3 Pa·s bei 135 °C erfüllten, aber High-PmBs zeigten bei dieser Temperatur nicht-newtonsches Verhalten⁵. Bei 160 °C zeigten die Bindemittel ein Newtonsches Verhalten, und es wurde ein zusätzliches Kriterium von ≤ 1 Pa·s bei dieser Temperatur vorgeschlagen, um die Verarbeitbarkeit der Bindemittel zu gewährleisten.

BTSV-Charakterisierung

Mit der BTSV-Prüfmethode konnten die Bindemittel anhand des Polymergehalts erfolgreich unterschieden werden. Es wurden Akzeptanzkriterien für weiche und harte Bindemittel vorgeschlagen, wie in Figure 21 dargestellt. Mit der Alterung wurde ein deutlicher Anstieg der BTSV-Temperatur und eine Abnahme des Phasenwinkels beobachtet.

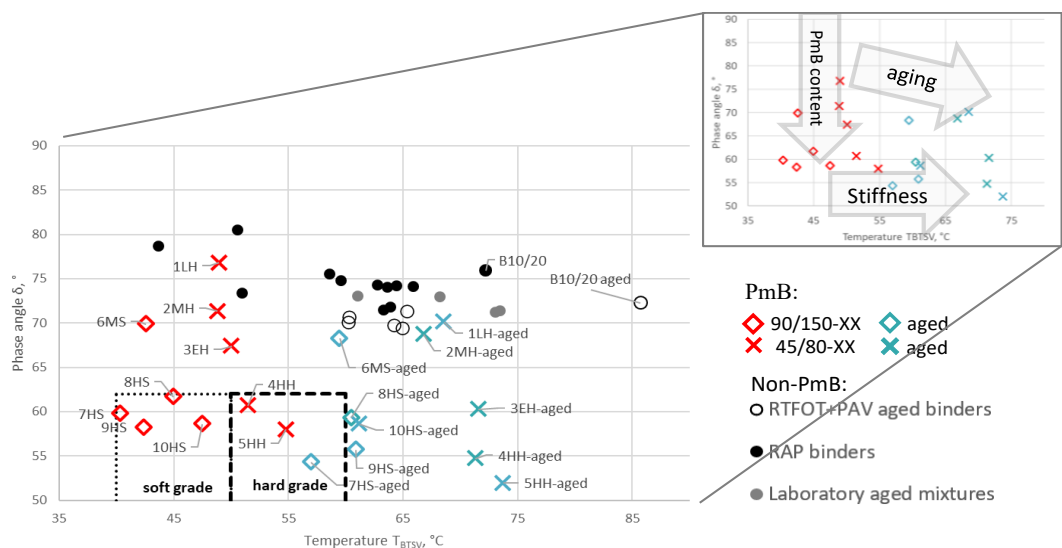


Figure 21: Vorgeschlagene Klassen für BTSV für High-PmBs. HH und HS bezeichnen hohe PmBs, während die anderen Buchstaben für Bindemittel mit geringerem Polymergehalt stehen

⁵ Eine newtonsche Flüssigkeit weist ein lineares viskoses Fließverhalten auf.

Eine Erweiterung der BTSV-Prüfung auf 1 kPa wurde vorgeschlagen (typischerweise wird es bei 10 kPa gestoppt), um die Berechnung des „Delta-Phasenwinkels“ zu ermöglichen. Dieser Parameter charakterisiert die Wirkung des Polymernetzwerks bei hohen Temperaturen und korrelierte gut mit den GPC-Ergebnissen der meisten Bindemittel. Die Erfassung weiterer Daten mit diesem Parameter könnte neue Erkenntnisse liefern. Das angewandte Alterungsprotokoll (RTFOT⁶+2PAV⁷-Zyklen) simulierte erfolgreich den Alterungszustand typischer Bindemittel, die in gefrästem Asphalt in der Schweiz vorkommen. Diese Alterungsmethode wird daher vorgeschlagen, um Bindemittel zu ermitteln, die zu beschleunigter Langzeitalterung neigen. Die vorgeschlagenen BTSV-Kriterien für die Alterungsbewertung sind in Table 3 zusammengefasst.

Es wurde eine gute exponentielle Beziehung ($R^2=0,93$) zwischen der BTSV-Temperatur und der logarithmisch dargestellten Penetration gefunden, siehe Figure 22. Die Abbildung enthält auch zwei schattierte Felder, die den Überlappungsbereich der vorgeschlagenen BTSV-Temperaturanforderungen und die entsprechenden Penetrationsanforderungen für die weichen und harten hochmodifizierten Bindemittel zeigen. Es ist ersichtlich, dass die High-PmB immer innerhalb der Kästchen liegen, was bedeutet, dass sowohl die BTSV- als auch die Penetrationsergebnisse die Bindemittel derselben Klasse umfassen würden. Das bedeutet, dass bei Verwendung der BTSV-Prüfergebnisse für die High-PmB-Klassifizierung die Penetrations-Prüfung in diesem Fall teilweise redundant ist. Natürlich können auch nicht modifizierte oder konventionell-Polymer-modifizierte-Bindemittel in den Kästchen zu finden sein, wie hier die Bindemittel 6MS und 3EH. Um diese Bindemittel unterscheiden zu können, ist eine Prüfung der elastischen Eigenschaften erforderlich. Bei Anwendung der in Figure 21 angegebenen BTSV-Grenzwerte, würden diese Bindemittel aufgrund der Phasenwinkelkriterien nicht in dieselbe Klasse fallen.

⁶ RTFOT (Rolling Thin Film Oven Test)

⁷ PAV (pressure Aging Vessel)

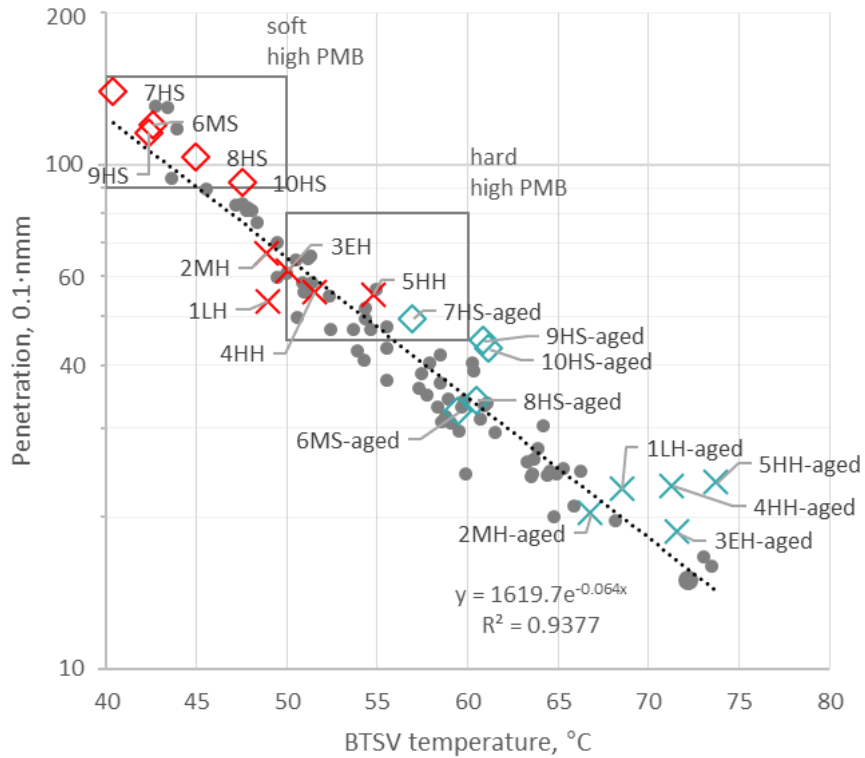


Figure 22: BTSV-Temperatur im Vergleich zur logarithmischen Penetration

MSCR-Bewertung

Die MSCR-Prüfspannung von 3,2 kPa war zu niedrig, um zwischen den verschiedenen Polymergehalten unterscheiden zu können. Durch Erhöhen der Spannung auf 10 kPa und der Prüfung bei einer geeigneten Temperatur (64 °C für harte Bindemittel; 58 °C für weiche Bindemittel) konnten die Bindemittel anhand ihres Polymergehalts eindeutig klassifiziert werden. Als Beispiel ist in Figure 23 das vorgeschlagene Klassifizierungskriterium für die harten PmB-Bindemittel dargestellt. Die Auswahl der Prüftemperatur bleibt jedoch eine Herausforderung, da Bindemittel für unterschiedliche Anwendungsbereiche (z. B. in den Bergen oder im Tiefland) möglicherweise unterschiedliche Testtemperaturen erfordern.

Es wurde auch empfohlen, die Anzahl der Zyklen pro Belastungsstufe auf 30 zu erhöhen, um eine bessere Reproduzierbarkeit der Ergebnisse zu erzielen.

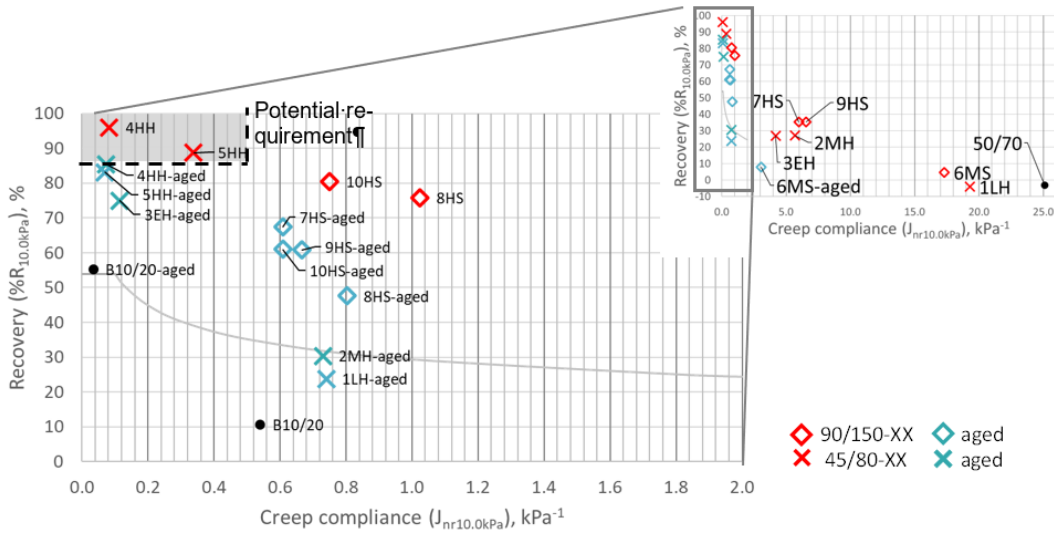


Figure 23: Zusammenfassung der MSCR-Prüfergebnisse bei 10.0 kPa und 64 °C. HH steht für hohe PmB-Werte, während die anderen Buchstaben für Bindemittel mit geringerem Polymergehalt stehen.

Gelpermeationschromatographie

Die Peakfläche in der Gelpermeationschromatographie (GPC) korreliert mit der Menge des im Bindemittel verwendeten Polymers, sofern das Polymertyp identisch ist. Andernfalls gibt die Peakfläche verschiedener Polymertypen weder Auskunft über den Polymergehalt noch über seine mechanischen Eigenschaften.

Die GPC hat sich als nützliches Mittel für die Forschung erwiesen, ist jedoch für die Klassifizierung von Bindemitteln nicht geeignet, da die Polymer-Peakfläche und die Molekülmasse vom Polymertyp abhängen und daher nicht universell auf alle Arten von Bindemitteln angewendet werden können.

Empfehlungen zur Normierung von Bindemitteln

Figure 24 fasst die Prüftemperaturen für hohe PmBs für alle in diesem Projekt verwendeten Methoden zusammen. Basierend auf den Ergebnissen sind die für die Einstufung hoher PmBs geeigneten Prüfmethode oberhalb der horizontalen Achse dargestellt, während die Methoden unterhalb der Achse nicht empfohlen werden.

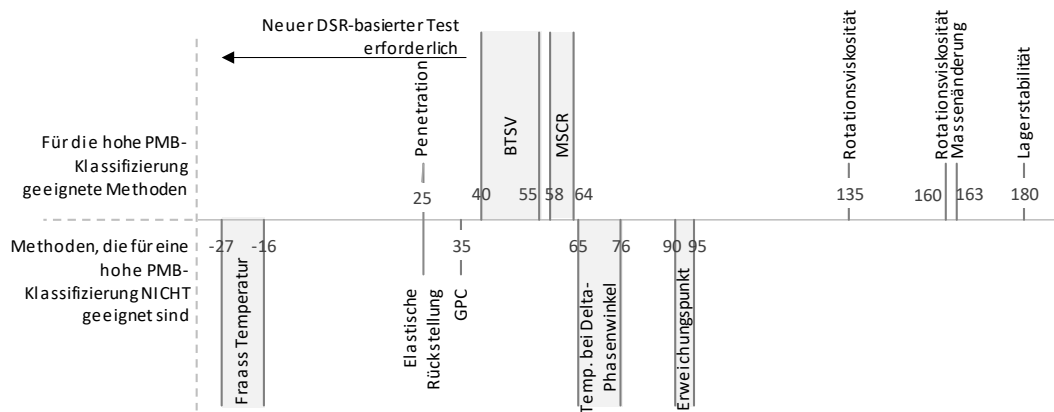


Figure 24: Die Prüftemperatur der verschiedenen Methoden auf der Grundlage der Ergebnisse dieser Arbeit für hochpolymersmodifizierte Bindemittel. Die für europäische Spezifikationen empfohlenen Methoden sind oberhalb der Linie angegeben

Table 3 fasst die vorgeschlagenen Methoden und Kriterien für die Klassifizierung hochpolymermodifizierter Bindemittel zusammen. Die Methoden eignen sich für alle PmBs und auch für nicht modifizierte Bindemittel, sind jedoch insbesondere für die Klassifizierung hochpolymermodifizierter Bindemittel erforderlich, da die derzeit verwendeten Methoden nicht ausreichend zwischen herkömmlichen und hochpolymermodifizierten Bindemitteln unterscheiden können. Es wird empfohlen, die vorgeschlagenen Kriterien nach Erfassung weiterer Daten erneut zu bewerten.

Vorgeschlagene Methoden für die QK von High PmB				
Method	Kriterien für harte Bindemittel	Kriterien für weiche Bindemittel	Bemerkungen	Standard
Penetration	45-80 0.1mm	90-150 0.1mm	-	EN 1426
Rotationsviskosität	$\leq 3 \text{ Pa}\cdot\text{s @ } 135 \text{ }^\circ\text{C}$ $\leq 1 \text{ Pa}\cdot\text{s @ } 160 \text{ }^\circ\text{C}$	$\leq 3 \text{ Pa}\cdot\text{s at } 135 \text{ }^\circ\text{C}$ $\leq 1 \text{ Pa}\cdot\text{s at } 160 \text{ }^\circ\text{C}$	Die Validierung der Kriterien ist erforderlich.	EN 13302
Lagerstabilität	$\leq 5^\circ\text{C}$	$\leq 5^\circ\text{C}$	Entwicklung von MSCR- oder BTVS-basierten Kriterien empfohlen	EN 13399
Massenänderung nach RTFOT	$\leq 0.5 \text{ M.-%}$	$\leq 0.5 \text{ M.-%}$	-	EN 12607-1
BTVS	$\delta_{\text{BTVS}} \leq 62 \text{ }^\circ$ & $T_{\text{BTVS}} 50\text{-}60 \text{ }^\circ\text{C}$	$\delta_{\text{BTVS}} \leq 62 \text{ }^\circ$ & $T_{\text{BTVS}} 40\text{-}50 \text{ }^\circ\text{C}$	Die Validierung der Kriterien ist erforderlich.	EN 17643
Alterungsbeständigkeit mit BTVS nach RTFOT	Reduction in $\delta_{\text{BTVS}} \leq 6^\circ$ Increase in $T_{\text{BTVS}} \leq 8 \text{ }^\circ\text{C}$	Reduction in $\delta_{\text{BTVS}} \leq 6^\circ$ Increase in $T_{\text{BTVS}} \leq 8 \text{ }^\circ\text{C}$	Die vorgeschlagenen Kriterien basieren auf einer deutschen Vornorm. Validierung empfohlen.	EN 17643 EN 12607-1
Alterungsbeständigkeit mit BTVS nach RTFO+ 2xPAV	Reduction in $\delta_{\text{BTVS}} \leq 10^\circ$ Increase in $T_{\text{BTVS}} \leq 23 \text{ }^\circ\text{C}$	Reduction in $\delta_{\text{BTVS}} \leq 10^\circ$ Increase in $T_{\text{BTVS}} \leq 23 \text{ }^\circ\text{C}$	Zwei PAV-Alterungszyklen werden für einen realistischen Alterungszustand vorgeschlagen.	EN 17643 EN 14769
MSCR-Prüfung	$\geq 85 \text{ \% recovery}$ $\leq 0.5 \text{ \% kPa}^{-1}$ Prüfung @ 10 kPa stress, 64 °C	$\geq 85 \text{ \% recovery}$ $\leq 0.5 \text{ \% kPa}^{-1}$ Prüfung @ 10 kPa stress, 58 °C	<ul style="list-style-type: none"> - 10 kPa-Belastung derzeit nicht in der Norm enthalten - Die Prüftemperatur sollte auf der Grundlage des Klimas ausgewählt werden - In dieser Untersuchung wurden die Prüfungen an nicht gelagerten Proben durchgeführt 	EN 16659

Table 3: Vorgeschlagene Methoden und Kriterien für die Qualitätskontrolle von hochpolymermodifizierten Bindemitteln

Testabschnitt: AC B 22 S auf H19 Oberalpstrasse, Tamins – Val Malians, Graubünden

Asphaltbeton vom Typ AC B 22 S wurde als Binderschicht auf der Teststrecke H19 Oberalpstrasse Tamins – Val Malians eingebaut. Diese Baustelle wurde aufgrund der

hohen Verkehrsintensität ausgewählt. Es wurden zwei Mischgüter eingebaut: (1) Mischgut mit 40 M.-% RAP-Anteil und Zusatz von weichem, hochpolymermodifiziertem Bindemittel (PmB 90/150-85); (2) Mischgut mit 0 M.-% RAP und hartem, hochpolymermodifiziertem Bindemittel (PmB 45/80-85). Das Mischgut mit 40 M.-% RAP ermöglichte es, die Vorteile der Verwendung von High-PmB zum Ausgleich des Polymermangels im RAP zu bewerten. Die Mischgut mit 0 M.-% RAP ermöglichte es, die Vorteile der Verwendung von hohem PmB zur Steigerung der Performance und Lebensdauer von Asphalt sowie eine mögliche Verringerung der Schichtdicke zu bewerten.

Die Ergebnisse des AC B 22 S-Testabschnitts sind in Figure 25 zusammengefasst. Die Tabelle ermöglicht einen qualitativen Vergleich der Ergebnisse der HPMix-Mischgut mit der Mischgut mit 40 M.-% RAP (RAP Mix). Insgesamt zeigten beide Mischgüter ein gutes Verhalten, das den aktuellen Anforderungen für das Mischgut und das rückgewonnene PmB 45/80-65 (CH-E)-Bindemittel entspricht. Diese Ergebnisse wurden auch mit der 40 M.-%-RAP-Mischgut erreicht, was darauf hindeutet, dass ein RAP-Gehalt von mindestens 40 M.-% erfolgreich in polymermodifizierten Mischgütern verwendet werden kann. Basierend auf den Ergebnissen der Bindemittelprüfung könnte ein noch höherer RAP-Anteil die aktuellen Anforderungen der Normen erfüllen, wenn ein hoher PmB-Anteil verwendet und die Mischgutzusammensetzung weiter optimiert wird (entweder durch Verwendung eines weicheren Bindemittels oder eines Verjüngungsmittels). Es ist jedoch zu beachten, dass die aktuellen Anforderungen nicht immer eine zuverlässige Methode zur Bestimmung der Bindemittelleistung bieten, weshalb in dieser Untersuchung zusätzliche Prüfmethode verwendet wurden.

Aus der Figure 25 geht hervor, dass die meisten Prüfmethode, einschliesslich der zusätzlichen Bindemittelprüfungen und performancebasierten Mischgütprüfungen, eine bessere Performance der HPMix im Vergleich zur RAP Mix zeigen. Dies war zu erwarten, da der effektive Polymergehalt in der RAP Mix aufgrund des 40-prozentigen RAP-Anteils tiefer ist als in der HPMix. Insgesamt lassen diese Ergebnisse den Schluss zu, dass die Verwendung von hochpolymermodifiziertem Bindemittel zwei Zwecken dienen kann:

- Sie ist vorteilhaft für die Leistungsverbesserung, wenn es mit geringem oder keinem RAP verwendet wird⁸.
- Sie kann die Verwendung eines hohen RAP-Gehalts (mindestens bis zu 40 M.-% in der Binderschicht) ermöglichen, um die gewünschte Leistung zu gewährleisten, die von einem herkömmlichen polymermodifizierten Mischgut erwartet wird, wenn die Klasse des Zielbindemittels PmB 45/80-65 (CH-E) ist. In einem anderen Forschungsprojekt der Empa (Zaumanis, Poulikakos, Boesiger et al., 2023a) und im Kanton ZH werden bei Verwendung von High-PMB 60 % RAP eingesetzt, wobei die herkömmlichen Prüfanforderungen erfüllt werden.

⁸ Obwohl das Mischgut ohne Recyclinganteil die besten Ergebnisse zeigt, die Autoren empfehlen nicht, das Asphaltrecycling aufzugeben. Die Verwendung von RAP sollte im Zusammenhang mit Nachhaltigkeit und Ressourceneffizienz bewertet werden. Eine solche Bewertung war nicht Teil dieses Projekts.

Mischung	RAP-Gehalt	Bindemitteltests				Widerstand gegen Spurrinnen FRT	Widerstandsfähigkeit gegen Rissausbreitung		Ermüdung		Steifigkeit ITT	Tiefemp. Rissbeständigkeit TSRST
		ER	BTSV	MSCR	FS		SCB	IDEAL-CT	2PB-TR	MMLS3		
AC B 22 S	HPMix	0%	↗	↗	↑	↗	↗	↗	↗	↑	↗	→
	RAP Mix	40%	●	●	●	●	●	●	●	●	●	●

Legend:

- Referenzgemisch-Ergebnis
- ↑ deutlich bessere Leistung
- ↗ etwas bessere Leistung
- ähnliche Leistung
- ↘ etwas schlechtere Leistung
- ↓ deutlich schlechtere Leistung
- ER Elastische Rückstellung
- BTSV Bitumen-Typisierungs-Schnell-Verfahren
- MSCR Rückformung und der Nachgiebigkeit von Bitumen
- FS Frequenzdurchlauf
- FRT Spurrinnebildung
- SCB Halbkreisförmige Biegeprüfung
- IDEAL-CT Indirekter Zugversuch zur Prüfung der Rissbildung
- 2PB-TR Zweipunktbiegung an trapezförmigen Prüfkörpern
- MMLS3 Verkehrsbelastungssimulator
- ITT Indirekter Zugversuch
- TSRST Abkühlversuch

1 SCB- und IDEAL-CT-Tests sind nicht empfindlich gegenüber Polymergehalt.

Figure 25: Zusammenfassung der Prüfergebnisse des Testabschnitts AC B 22 S

Testabschnitt: AC 8 S auf der H27 Engadinerstrasse in St. Moritz Charnadüra, Graubünden

Auf der Teststrecke H27 an der Engadinerstrasse in St. Moritz Charnadüra, Graubünden wurde ein Asphaltbeton vom Typ AC 8 S als Deckschicht eingebaut. Diese Teststrecke wurde aufgrund der hohen Verkehrsintensität und der klimatischen Bedingungen ausgewählt. Es wurden zwei Mischgütern eingebaut: Die HPMix-Mischgut mit einem hochpolymermodifizierten Bindemittel (PmB 90/150-85) und eine Referenzmischgut mit Bindemittel vom Typ PmB 90/150-60 (CH-E). Beide Mischgüter hatten die gleiche Zusammensetzung.

Insgesamt zeigten beide Mischgüter ein gutes Verhalten, das den aktuellen Anforderungen entspricht. Wie bereits erwähnt, bieten die für die Qualitätskontrolle verwendeten Prüfmethode jedoch nicht immer eine zuverlässige Möglichkeit, die Auswirkungen eines erhöhten Polymergehalts zu identifizieren. Daher wurden in diesem Projekt mehrere performancebasierte Prüfmethode verwendet.

Die performancebasierten Ergebnisse des AC 8 S-Testabschnitts sind in Figure 26 zusammengefasst. Die Tabelle ermöglicht einen qualitativen Vergleich der Ergebnisse von HPMix mit denen der Referenzmischgut. Aus der Tabelle geht hervor, dass die Bindemittelprüfungen und der Abkühlversuch (TSRST⁹) eine bessere Performance des hochpolymermodifizierten Bindemittels im Vergleich zur Referenzmischgut mit herkömmlichem polymermodifiziertem Bindemittel zeigen. Die Spurrinnenbeständigkeit beider Mischgüter ist ähnlich und sehr gut. Auf der Grundlage der Bindemittelergebnisse ist eine bessere Spurrinnenbeständigkeit der HPMix zu erwarten. Die Bedingungen der Spurbildungsprüfung sind jedoch nicht streng genug, um eine erkennbare Spurrinnenbildung hervorzurufen. Selbst eine Verlängerung der Prüfdauer (erhöhte Zyklenzahl) führte nicht zu einer nennenswert grösseren Spurrinntiefe. Daher sollten in Zukunft Änderungen der Prüfbedingungen in Betracht gezogen werden,

⁹ Thermal Stress Restrained Specimen

beispielsweise eine Erhöhung der Prüftemperatur oder die Verwendung einer anderen Prüfmethode (z. B. der Druckschwellversuch).

Die Steifigkeit war bei beiden Mischgütern ähnlich, die Widerstandsfähigkeit gegen Rissausbreitung war bei HPMix im Vergleich zur Referenzmischgut etwas schlechter. Aufgrund früherer Forschungsergebnisse ist es jedoch wahrscheinlich, dass die Unterschiede in der Rissausbreitung nicht mit dem Polymergehalt zusammenhängen, da die verwendeten Prüfmethode nicht empfindlich auf den Polymergehalt reagieren (Yin, 2023; Zaumanis, Poulikakos, Boesiger, et al., 2023a).

Insgesamt lassen die Ergebnisse den Schluss zu, dass die Verwendung von hochpolymermodifiziertem Bindemittel in der Deckschicht:

- die Leistungsfähigkeit der Deckschicht verbessert.
- Die Charakterisierung des Bindemittels anhand herkömmlicher Prüfungen zeigt nicht vollständig die Vorteile der Verwendung des hochpolymermodifizierten Bindemittels. Somit sind BTSV und MSCR bei 10 kPa geeignete Mittel zur Charakterisierung des Bindemittels.
- Für die Spurbildungsprüfung sind strengere Prüfbedingungen erforderlich, um die Leistungsfähigkeit zu unterscheiden.

Mischung	RAP-Gehalt	Bindemitteltests			Widerstand gegen Spurrinnen	Widerstandsfähigkeit gegen Rissausbreitung		Steifigkeit	Tiefemp. Rissbeständigkeit
		ER	BTSV	MSCR	FRT	SCB	IDEAL-CT	ITT	TSRST
AC 8 S	HPMix	0%	↗	↕	↔	↘ ¹	↘ ¹	↔	↕
	Reference	0%	●	●	●	●	●	●	●

Legend:

- Referenzgemisch-Ergebnis
 - ↕ deutlich bessere Leistung
 - ↗ etwas bessere Leistung
 - ↔ ähnliche Leistung
 - ↘ etwas schlechtere Leistung
 - ↘¹ deutlich schlechtere Leistung
 - ER Elastische Rückstellung
 - BTSV Bitumen-Typisierung-Schnell-Verfahren
 - MSCR Rückformung und der Nachgiebigkeit von Bitumen
 - FRT Spürrinnebildung
 - SCB Halbkreisförmige Biegeprüfung
 - IDEAL-CT Indirekter Zugversuch zur Prüfung der Rissbildung
 - ITT Indirekter Zugversuch
 - TSRST Abkühlversuch
- ¹ SCB- und IDEAL-CT-Tests sind nicht empfindlich gegenüber Polymergehalt.

Figure 26: Zusammenfassung der Prüfergebnisse des AC 8 S-Testabschnitts

Testabschnitt: SDA 4-12 auf K244, Ruppertswil IO, Aargau

Der SDA-Testabschnitt mit hochpolymermodifiziertem Bindemittel im Kanton AG wurde 2020 eingebaut, und die entsprechenden Prüfergebnisse sind in diesem Bericht enthalten. Im Jahr 2024 wurden Bohrkern aus dem Belag entnommen und ausserdem neue, im Labor hergestellte Mischgüter vorbereitet. Die Labormischgüter wurden mit Materialien derselben Herkunft wie im Jahr 2020 unter Verwendung derselben Mischgüterrezeptur hergestellt.

Der Testabschnitt befindet sich auf K244 in Ruppertswil. Im SDA 4-12-Referenzabschnitt wurde das Bindemittel PmB 45/80-65 (CH-E), beim SDA 4-12 HPMix-Abschnitt das PmB 45/80-80 verwendet.

Im Rahmen dieses Projekts haben wir verschiedene Proben typen geprüft und auch die Prüfergebnisse aus den Berichten unmittelbar nach dem Einbau im Rahmen der

Qualitätskontrolle herangezogen. Insgesamt wurden vier Arten von Ergebnissen verwendet:

- Mischgut- und Bindemittel-Ergebnisse aus den Proben, die während des Baus des Testabschnitts im Jahr 2020 entnommen wurden.
- Mischgut- und Bindemittel-Prüfergebnisse aus den Bohrkernen, die kurz nach dem Bau des Testabschnitts im Jahr 2020 entnommen wurden.
- Mischgut- und Bindemittel-Prüfergebnisse aus den Bohrkernen, die während des HPMix-Projekts im Jahr 2024 entnommen wurden.
- Mischgutergebnisse aus den Proben, die im Empa-Labor während des HPMix-Projekts im Jahr 2024 hergestellt wurden.

Die Ergebnisse der SDA-Prüfungen lassen den Schluss zu, dass die Verwendung des hochpolymermodifizierten Bindemittels gegenüber dem herkömmlichen polymermodifizierten Bindemittel Vorteile zu bieten scheint. Dies geht aus den Bindemittelprüfergebnissen in Figure 27 hervor, in denen das aus dem HPMix gewonnene Bindemittel qualitativ mit dem aus der Referenzmischgut gewonnenen Bindemittel verglichen wird. Die Ergebnisse der Mischgutprüfungen zeigen ebenfalls eine ähnliche oder bessere Leistung im Vergleich zur Referenzmischgut. Die Schichtenverbund der HPMix-Proben ist geringer als erforderlich. Da die Bautechnik und das Haftmittel für beide Beläge gleich waren, lautet eine Hypothese, dass eine chemische Reaktion zwischen dem HighPmB und der Haftmittel die Schichtenverbund verringert hat. Leider konnte die Cantabro-Prüfung (Masseverlusttest) selbst nach einer Modifizierung, um den Prüfung anspruchsvoller zu gestalten die potenziellen Vorteile einer hohen Polymermodifizierung hinsichtlich des Ausbruchswiderstandes von SDA-Mischgutoberflächen nicht eindeutig nachweisen, selbst mit den im Projekt durchgeführten Prüfungsvarianten. Zur Bewertung dieser Eigenschaft sollten andere Prüfmethode in Betracht gezogen werden.

Mischung	Bindemitteltests				Widerstand gegen Spurrinnen	Widerstandsfähigkeit gegen Rissausbreitung		Kornverlustbeständigkeit	Steifigkeit	Tiefemp. Rissbeständigkeit	Schichtenverbund
	ER	BTSV	MSCR	FS	FRT	SCB	IDEAL-CT	Cantabro	ITT	TSRST	Leutner
SDA HPMix	↑	↑	↑	↑	→	↗ ¹	→ ¹	↘	↘	↑	↓
Reference	●	●	●	●	●	●	●	●	●	●	●

Legend:

- Referenzgemisch-Ergebnis
- ↑ deutlich bessere Leistung
- ↗ etwas bessere Leistung
- ähnliche Leistung
- ↘ etwas schlechtere Leistung
- ↓ deutlich schlechtere Leistung
- ER Elastische Rückstellung
- BTSV Bitumen-Typisierungs-Schnell-Verfahren
- MSCR Rückformung und der Nachgiebigkeit von Bitumen
- FS Frequenzdurchlauf
- FRT Spürrinnebildung
- SCB Halbkreisförmige Biegeprüfung
- IDEAL-CT Indirekter Zugversuch zur Prüfung der Rissbildung von Asphalt
- Cantabro Cantabro-Test
- ITT Indirekter Zugversuch
- TSRST Abkühlversuch
- Leutner Leutner Test

¹ SCB- und IDEAL-CT-Tests sind nicht empfindlich gegenüber Polymergehalt.

Figure 27: Zusammenfassung der SDA-Prüfergebnisse

Vorschlag zur Standardisierung von Asphaltmischgut

Dieses Projekt hat gezeigt, dass hochpolymermodifizierte Bindemittel gegenüber herkömmlichen polymermodifizierten Bindemitteln eindeutige Vorteile bieten können. Im Rahmen der Forschung wurde dies sowohl auf Bindemittel- als auch auf Mischgutebene nachgewiesen. Für die Standardisierung werden jedoch hauptsächlich bindemittelbasierte Prüfverfahren und Kriterien vorgeschlagen, wie in Table 3 zusammengefasst, da auf Mischgutebene die Prüfungen entweder keinen nennenswerten Unterschied zwischen dem hochpolymermodifizierten Bindemittel und einem herkömmlichen polymermodifizierten Bindemittel zeigten oder die Durchführung der Prüfung zu aufwendig ist (zum Beispiel der Ermüdungsprüfung). Obwohl einige der Mischgutprüfungen für die Gestaltung von Mischgutrezepturen von Vorteil sein könnten, ist ihre Verwendung nicht unbedingt ausschliesslich auf hochpolymermodifizierte Bindemittel beschränkt, weshalb in diesem Bericht keine Empfehlungen gegeben werden. Nachstehend folgt eine Zusammenfassung der Überlegungen, die für oder gegen die Standardisierung einer bestimmten Prüfung sprechen.

Prüfung der Spurbildung am Mischgut

Alle Mischgüter erfüllten die Anforderungen der Spurrinnenprüfung, und in den meisten Fällen wurde bei bis zu 30.000 Belastungszyklen eine Spurrinnentiefe von nicht mehr als 5 % gemessen. Eine Verlängerung der Prüfung auf 90.000 Zyklen brachte keine Vorteile und zeigte auch nicht die potenziellen Vorteile des hohen Polymeranteils im Bindemittel auf, da die Ergebnisse bis zu 90.000 Zyklen zwischen den Referenz- und HPMix-Mischgütern ähnlich waren.

Die Spurrinnenbildung stellt ein besonderes Problem in Bereichen mit langsamem Verkehr dar, in denen erhebliche Scherkräfte auftreten (z. B. Bushaltestellen und Kreisverkehre). Angesichts der Möglichkeit, eine sehr hohe Spurrinnenbeständigkeit zu erreichen, kann geprüft werden, ob hochpolymermodifizierte Bindemittel eine Lösung für solche Standorte sein könnten. Es wird daher empfohlen, den Einsatz hochpolymermodifizierter Mischgüter für solche beanspruchte Flächen zu evaluieren (möglicherweise durch den Bau von Versuchsstrecken- oder Feldern). Auch könnten strengere Prüfbedingungen (z. B. höhere Prüftemperatur) oder die Verwendung anderer Prüfmethoden (z. B. Druckschwellversuch) zur Prüfung der Spurrinnenbeständigkeit in Betracht gezogen werden.

Prüfungen der Rissausbreitung (SCB und IDEAL-CT)

Die Rissausbreitungsprüfungen (SCB¹⁰ unter Verwendung von Illinois Methode und IDEAL-CT¹¹) eignen sich gut zur Entwicklung von Mischgutrezepturen, da sie empfindlich auf Parameter reagieren, die das Verhalten der Mischgüter beeinflussen, wie bspw. Bindemittelgehalt, Bindemittelleigenschaften oder RAP-Gehalt. Diese Methoden sind einfach und schnell durchzuführen und weisen zudem eine relativ hohe Korrelation mit dem In-situ-Verhalten auf.

Aufgrund dieser und früherer Forschungsergebnisse der Empa sind mit diesen Methoden jedoch keine Rückschlüsse auf das von Polymerengehalt im Bindemittel möglich. Daher können sie nicht für die Charakterisierung von Mischgütern herangezogen werden, wenn es darum geht, die elastischen Eigenschaften oder die Wirkung von Polymeren zu bewerten.

Ermüdungs- und Steifigkeitsprüfungen

¹⁰ Semi Circular Bend

¹¹ Indirect Tensile Asphalt Cracking Test

Die Ermüdungsprüfung zeigte einen deutlichen Vorteil der Verwendung von hochpolymermodifiziertem Bindemittel auf. Derzeit wird jedoch nicht vorgeschlagen, diese Prüfung für die Qualitätskontrolle oder die Prüfung von Mischguttypen aufzunehmen, da die Durchführung der Prüfung sehr aufwändig ist. Es kann davon ausgegangen werden, dass die Prüfungen zur Charakterisierung des Bindemittels für eine gute Performance des Mischguts ausreichend sind, dies insbesondere bei etablierten Mischgutsorten wie Asphaltbeton.

Der Steifigkeitsmodulprüfung ergab erwartungsgemäss keinen nennenswerten Unterschied zwischen den Mischgütern mit unterschiedlichem Polymergehalt. Da für die in diesem Projekt bewerteten Mischgutsorten derzeit keine Steifigkeitsprüfung erforderlich ist, besteht auch keine Notwendigkeit, diese bei Verwendung eines hochpolymermodifizierten Bindemittels einzuführen.

Abkühlversuch (TSRST)

Die TSRST-Untersuchung hat gezeigt, dass die Verwendung eines höheren Polymeranteils möglicherweise einen Vorteil hinsichtlich der Erhöhung der Beständigkeit gegen Rissbildung bei niedrigen Temperaturen bietet. Allerdings gewährleistet auch das herkömmliche polymermodifizierte Bindemittel eine hohe Beständigkeit gegen Rissbildung. Daher ist es zwar vorteilhaft, den TSRST als Kriterium für die Zulassung von Asphaltmischgut in kalten Regionen heranzuziehen, dies steht jedoch nicht unbedingt im Zusammenhang mit der Verwendung von hochpolymermodifizierten Bindemitteln. Aus diesem Grund werden in diesem Bericht keine Kriterien für die Standardisierung dieser Prüfung angegeben.

Standardisierung des Belagsbemessung

In dieser Arbeit wurde eine Methodik angewendet, um Strukturkoeffizienten (a-Werte) für High PmB-Mischungen im Rahmen des schweizerischen Bemessungsstandards (VSS 40 324) zu bestimmen. Die berechneten Werte lagen zwischen 4.43 und 6.92, woraus ein konservativer Wert von 4.4 für die Bemessung vorgeschlagen wird. Dies bestätigt den erwarteten strukturellen Vorteil von High PmB-Mischungen im Vergleich zu herkömmlichen Materialien. In der Praxis könnte dies eine Reduktion der Asphaltschichtdicke um rund 10 %. Alternativ kann bei unveränderter Stärke je nach Belagsaufbau mit einer Zunahme der äquivalenten Einzelachslasten (ESAL) zwischen 39 % und 106 % gerechnet werden. Es ist zu beachten, dass sich der vorgeschlagene a-Wert nur auf Mischungen ohne RAP bezieht. Bei Verwendung eines hohen RAP-Anteils besteht das Ziel der Verwendung eines hohen PmB-Werts darin, eine ähnliche Leistung wie bei Mischungen zu erzielen, die derzeit in der Norm mit den bestehenden a-Werten spezifiziert sind. Dennoch müssen diese Werte in realen Strukturen, sei es in verkleinertem Massstab oder im Vollmassstab, validiert werden, bevor sie in der Praxis eingeführt werden können.

Forschungsbedarf

Im Rahmen des HPMix-Projekts wurden mehrere spezifische Anforderungen für die zukünftige Forschung identifiziert. Eine Folgestudie zu diesen Themen würde die Umsetzung von hohen PmBs unterstützen:

- Im Rahmen dieser Forschung wurde ein Tragfähigkeitswert für Mischgut mit hohem PmB-Gehalt vorgeschlagen. Eine Validierung dieser Ergebnisse wird durch den Bau und die Untersuchung einer entsprechenden Teststrecke empfohlen.

- Es hat sich gezeigt, dass die aktuellen Testbedingungen zur Bestimmung der Spurbildung nicht ausreichend, um einen Unterschied zwischen einer herkömmlichen PmB- und einer Mischgut mit hohem PmB-Gehalt nachzuweisen. Daher wird die Entwicklung neuer Testbedingungen oder die Validierung einer anderen Prüfmethode, beispielsweise der Druckschwellversuch, empfohlen.

Darüber hinaus wurden im Rahmen der Untersuchung mehrere Bereiche mit Defiziten identifiziert, die nicht unbedingt mit der Umsetzung High-PmBs zusammenhängen, sondern eher dem gesamten Bereich zugutekommen könnten:

- Ein hoher PmB-Gehalt kann insbesondere bei Spezialanwendungen mit hoher Verkehrsintensität und hohen Scherkräften von Vorteil sein. Dazu gehören Bushaltestellen, Wiegestationen, Kreisverkehre, Kreuzungen und ähnliche Standorte. Die Erstellung und Untersuchung von Teststrecken- oder –abschnitten könnte das Potenzial von Mischgütern mit hohem Polymergehalt als Ersatz für Beton für solche Anwendungen aufzeigen.
- Die Lagerbeständigkeit wird derzeit anhand des Erweichungspunkts R&K bewertet. Da der Erweichungspunkt für die Bewertung von hohem PmB nicht empfohlen wird, wird die Entwicklung neuer Kriterien für die Bewertung der Lagerstabilität von Bindemitteln anhand eines DSR-basierten Prüfungen empfohlen.
- Die vorgeschlagene DSR-basierte Methode wird bei hohen Prüftemperaturen durchgeführt. Es sollte eine neue DSR-basierte Methode (oder Methoden) für die Charakterisierung von Bindemitteln bei mittleren und niedrigen Temperaturen entwickelt werden.
- Die Berechnung von Belastungen und die Dimensionierung von Asphalt sind sehr aufwendig, aber eine Optimierung der Belagskonstruktion könnte Material und Ressourcen einsparen und Innovationen ermöglichen. Eine einfache, kostenlose, web-basierte App zur Dimensionierung sollte unter Verwendung des in VSS 40 324 beschriebenen Ansatzes entwickelt werden.

Das Projekt hat potenzielle Vorteile der Verwendung von Mischgut mit hohem PmB-Anteil aufgezeigt. Die Verwendung solcher Mischgütern, einschliesslich ihrer Verwendung in Kombination mit Asphaltrecycling, sollte auch unter Berücksichtigung der Nachhaltigkeit und der Kostenbewertung aktiv gefördert werden.

1 Introduction

High traffic load and extreme weather conditions lead to premature pavement deterioration. These causes will only intensify in the future because of the expected increase of transported goods and climate change. The main pavement distresses from these effects are cracking, rutting and raveling. Such distresses lead to increased maintenance needs; they make the pavement unsafe and ultimately require pavement rehabilitation, causing high maintenance expenditures and traffic congestions.

One of the most common methods to improve pavement in-service performance is to place pavements containing polymer-modified bitumen (PmB) by blending standard bitumen with elastomeric polymers. PmB was developed several decades ago to enhance rutting, raveling and cracking resistance of top layers as a response to the always-growing traffic load. Nowadays, PmB is increasingly used for structural layers, looking for additional benefits in terms of performance and extended service life (Molenaar et al., 2008a; Porot et al., 2019b).

In a typical PmB, the polymer dosage ranges between 2.5% and 3.5% by mass of asphalt binder, but high-PmB with polymer dosages of 6-8% are increasingly being investigated (Gaspar et al., 2017; Kozłowski & Kucharski, 2015; Ping & Xiao, 2012; Rivera et al., 2021). While in a conventional PmB the polymer phase is discontinuous, in a high-PmB the polymer phase forms an extensive polymer network, conferring a rubber-like response to external loads (Habbouche et al., 2021) (see Figure 28). That is, the blend goes from a discontinuous to a continuous polymer phase at approximately 5% of polymer by weight of asphalt binder. This inversion enhances the performance and durability of asphalt mixtures. The viscosity of high-PmB is ensured through Styrene-Butadiene-Styrene (SBS) polymer with high vinyl content and reduced molecular size which, when blended with bitumen, swell and increase in volume between 5 to 10 times (Porot et al., 2019a). The chemical properties of this polymer lowers the binder viscosity, improving the workability for the asphalt mix. Further, it reduces the sensitivity to the bitumen quality and storage stability issue (Porot et al., 2019a). Apart from SBS, other polymers such as styrene-butadiene-rubber and styrene-butadiene have also been utilized, but in this research the SBS is the primary considered polymer since it has the most widespread use.

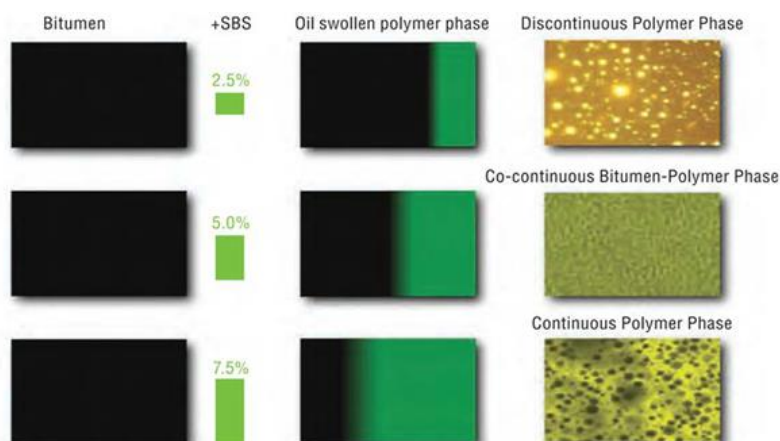


Figure 28: Structure of binder depending on polymer content (from (Habbouche et al., 2019))

The project "Standardization of Highly Polymer-Modified Asphalt Mixtures (HPMix)" aims to provide suggestions for standardization of highly polymer modified binder use. The reported advantages of high PmB over a conventional PmB include superior fatigue resistance, improved rutting resistance, as well as low temperature resistance (Kluttz et al., 2012; Molenaar et al., 2008a). These advantages might allow extending the pavement service life if used instead of conventional PmB. Alternatively, high PmB might allow to reduce the pavement thickness without diminishing the performance or service life expectancy, thus reducing the use of virgin materials (Molenaar et al., 2008a; Willis et al., 2016) and probably sinking environmental footprint of road construction. Finally, high PmB can permit a higher content of reclaimed asphalt in mixtures that require polymer-modified binder since the high polymer content in the high PmB compensates for the lack of (or degraded performance) of polymers in RAP.

Based on the reported literature, high PmB offers a superior fatigue resistance, improved rutting resistance, and low temperature cracking resistance, making high-PmB suitable for highly stressed road pavements, including roundabouts, intersections, rest areas, locations with high thermal gradient and high traffic intensity roads. Due to the performance of pavements containing high-PmB, their use is increasing worldwide and in Switzerland.

As with many new technologies and materials, their benefits have to be weighed against the potential drawbacks and concerns. The high polymer content can increase binder viscosity, making the asphalt difficult to produce at the plant and increasingly unworkable for paving crews. Due to the higher polymer content, high PmB is also more expensive than a conventional PmB, thus adding to the up-front costs of manufacturing and laying down the hot mix asphalt.

Objective

The goal of the HPMIX project is to deliver data and propose recommendations for standardization of highly polymer-modified binder, mixture, and pavement design.

1.1 Reported performance of high PmB

The concept of HiMA has been studied at laboratory scale and in tests sections around the world for around a decade. One of the first works carried out between Delft Technical University in the Netherlands and Kraton Polymers Research (Molenaar et al., 2008b) showed that the addition of 6% and 7.5% of SBS substantially improves mechanical parameters of the modified bitumen and the mixtures as compared to a non-modified reference.

Already in 2009, a full-scale high-PmB test section was built and loaded with 20 million equivalent single axle loads (ESAL) at the National Center for Asphalt Technology test track in USA (Scholten et al., 2011). The pavement with 3 bituminous layers over an unbound base was built using 7.5% SBS modified binder and the damage produced by the traffic load was compared to a pavement without high-PmB, but 20% thicker. After 6 years of observations the high-PmB section resulted in 70 percent less rutting and had no bottom-up fatigue cracking, whereas the control pavement had 18% area

cracks (Willis et al., 2016). Likewise, finite element simulations by TU Delft have shown that the use of high-PmB can lead to substantial thickness reduction in a wide range of flexible pavement structures (Molenaar et al., 2008b).

In a study by the Florida Department of Transportation (Greene et al., 2014), high-PmB with 6% polymer content was used. Laboratory tests were performed on binders and asphalt mixtures with neat bitumen and modified with 3% and 6% SBS polymer. The tests included dynamic shear rheometer (DSR), multiple stress creep recovery (MSCR) and binder fracture energy to characterize the binder properties, and Asphalt Pavement Analyzer (APA), Hamburg wheel tester, and Asphalt Mix Performance Tester (AMPT, testing flow number) were used to evaluate the rut potential of the mixtures in the laboratory. Results showed the enhanced rutting performance of the modified bitumen and mixtures, with the best results for a 6% polymer content. These results were confirmed in full-scale by using the Heavy Vehicle Load Simulator (HVS). A later study (Hyung Lee & Deepak Raghunathan, 2015) showed that high-PmB might provide at least three times more cracking resistance than standard mixtures. In the same work, it was observed that the ride quality of high-PmB is similar to standard wearing courses and that high-PmB was noticeably quieter than the reference pavement.

Researchers of ORLEN Asphalt in Poland have attempted to capitalize on the superior crack resistance of high-PmB by offering a crack resistant layer for heavy duty asphalt pavements (Błazejowski et al., 2016). In another work, the same research group demonstrated how high-PmB can improve the cracking and plastic deformation resistance of SMA (Stone Mastic Asphalt) wearing courses (Wasilewska et al., 2017).

The use of Reclaimed Asphalt Pavement (RAP) in high-PmB is not straightforward. In 2011 the departments of transportation of New Hampshire and Vermont built high-PmB test sections with up to 25% RAP (WALAA S. MOGAWER et al., 2014). The plant produced mixtures and the recovered binder were tested in the laboratory to verify conformance with the standards and mixture performance testing, namely stiffness ($|E^*|$), resistance to rutting, fatigue cracking, reflective cracking and resistance to thermal cracking were carried out to characterize the mixtures. Laboratory results showed mixed results, with one of the HiMA mixtures with RAP failing the rutting requirements and the other failing on the reflexive cracking requirements. In general, the addition of 25% of RAP had negative performance effects that the addition of HiMA binders could not overcome, meaning that special attention to RAP specifications is required. On the other hand, field trials after 2 years showed good performance of HiMA, even in those with RAP content.

In other locations around the world, there are more examples of high-PmB test sections (Global Highways, 2012; Ignacio Kröger & Carlos Pfeiff, 2019). In Switzerland, high-PmB was introduced a few years ago (Lichtsteiner, 2019; Lichtsteiner Felix, 2016) with some sections constructed in areas of heavy vehicle loading and/or high altitude. According to the presentation of Mr. Bucheli in the 2018 Pavono seminar (Bucheli, 2018), test sections have been constructed:

- Roundabout in Andermatt at 1447m altitude.
- Oberalppass in Graubunden at 2046m altitude.
- Agir plant/working area at 380m altitude.
- AO4A Küsnacht-Brunnen in Schwyz at 490m height.

We have not been able to identify any publicly available reports regarding the performance of these test sections.

1.2 Potential advantages, use cases and concerns when using high PmB

Table 4 summarizes the reviewed literature and demonstrates potential use cases of High PmB mixtures.

Advantages and use cases of High PmB	
Scenario	Advantages of High PmB
Low-temperature cracking resistance	The high polymer content of high PmB's typically improves low-temperature crack resistance. In lab studies, High PmB mixes showed higher fracture energy and lower cracking temperatures than conventional mixes, indicating better resistance to thermal cracking (Adriana Vargas-Nordbeck & James A. Musselman, 2022; Kabir et al., 2023). A larger Performance Grade (PG) span is typically required in the US for high PmB's thus showing a broader range of serviceability temperatures (Adriana Vargas-Nordbeck & James A. Musselman, 2022). For a typical PmB the PG span is in the range of 92 to 104 °C while for high PmB it is 104-110 °C.
Rutting resistance	High PmB's increased polymer content typically improves rutting resistance of pavements (Adriana Vargas-Nordbeck & James A. Musselman, 2022; Ohio Asphalt, 2020; Scholten et al., 2011; Wasilewska et al., 2017). For example, in Ohio, USA several heavy trafficked locations that exhibited rutting problems were paved with a High PmB. In all the projects the rutting depth after several years of service is small (Ohio Asphalt, 2020). Due to the high rutting resistance, it can be beneficial to use high-PmB on pavements with heavy traffic load.
Roundabouts, high-traffic intersections and bus stops	Roundabouts, high traffic intersections, weight stations, and bus stops concentrate high shear loads that lead to plastic deformations. High PmB's elasticity can help to resist the associated rutting (Adriana Vargas-Nordbeck & James A. Musselman, 2022; Ohio Asphalt, 2020; Paul Fournier, 2010).
Crack propagation resistance	Multiple reports have shown that high PmB mixtures exhibit better resistance to crack propagation (Błazejowski et al., 2016; Chen et al., 2018; Hyung Lee & Deepak Raghunathan, 2015; Rivera et al., 2022). Some of the references research results suggests that IDEAL-CT, SCB Flexibility Index can show this advantage, but in this project, previous Empa research (Zaumanis, Poulikakos, Boesiger, et al., 2023a) and in research by NCAT (Yin, 2023), however, SCB and IDEAL-CT methods appeared to not be sensitive towards the polymer-modification of binder.
Fatigue resistance	High PmB can improve resistance to repeated-load (fatigue) cracking of asphalt pavement (Adriana Vargas-Nordbeck & James A. Musselman, 2022; Habbouche et al., 2021; Leiva-Villacorta et al., 2017; Scholten et al., 2011; Tran et al., 2019; Willis et al., 2016). The high polymer content increases binder elastic recovery and strain tolerance, so the mixture dissipates stresses more effectively under cyclic loading.
Raveling resistance	High PmB can provide better binder–aggregate adhesion to reduce raveling. This can be especially beneficial for open-graded mixes, including porous asphalt and SDA (Semi-Dense Asphalt). For example, in Florida, High PmB open-graded friction course mixes exhibited reduced raveling (Edith Arámbula-Mercado et al., 2019).
Reduced pavement thickness	High PmB's higher stiffness yields a greater structural layer coefficient, meaning a thinner High PmB layer can provide a similar performance to conventional asphalt (Molenaar et al., 2008b; Tran et al., 2019). For example, research (FDOT/NCAT) found High PmB mixtures' design coefficient ~0.54 vs ~0.44 for a conventional mix (Adriana Vargas-Nordbeck & James A. Musselman, 2022). In practice, this has allowed to pave by 20–25% less thick asphalt.

Scenario	Advantages of High PmB
High PmB + Reclaimed Asphalt Pavement (RAP)	Mixing High PmB can compensate for the lack of polymers in reclaimed asphalt pavement (RAP) and thus permit using RAP in layers where conventional polymer modified binder content is required. Laboratory and field studies (including research by Empa) have shown High PmB mixes with ~20-40 % RAP can fulfil the requirements defined for conventional PmB mixture layers (Porot et al., 2020; Zaumanis, Poulikakos, Boesiger, et al., 2023a). Examples of unsatisfactory performance when using RAP exist as well (WALAA S. MOGAWER et al., 2014; Zaumanis, Poulikakos, Boesiger, et al., 2023a)

Table 4: Potential advantages and use cases for high PmB mixtures

In summary, high-PmB has been studied at laboratory scale and in trial sections around the world for nearly a decade and the results demonstrate the following main advantages:

- High-PmB can extend the pavement life by improving rutting resistance and reducing cracking.
- High-PmB can reduce the pavement thickness.
- High-PmB can compensate for the lack of polymers in RAP.

In most scenarios high PmB can be used to replace conventional PmB without needing adjustment in mix design, production and paving practices. However, some concerns should be considered to achieve the full benefit of the high polymer content. Table 5 provides a summary of the potential concerns and the mitigation measures, as recommended for asphalt producers and construction crew.

Concerns of High PmB use and their mitigation measures		
Concern	Explanation	Mitigation measures
Overheating	Overheating of the binder or excessive production temperature can damage the polymers and therefore compromise the mixture performance.	Keep binder temperature in the range recommended by the manufacturer and ensure circulation or agitation according the manufacturers recommendation. Avoid long storage.
Mix workability difficulties	High PmB's very high polymer content (often 7–8 % SBS) can make asphalt viscous. This can make asphalt less workable for the paving crew. In practice, this means that the mixtures with high PmB might not be suitable for small jobsites requiring manual paving. Use in mixtures with reduced temperature (Warm Mix Asphalt) also should be verified.	High-vinyl SBS or other additives can reduce binder viscosity. Ensure efficient flow for production and coating of aggregates. Binder viscosity tests can be performed to verify this.
Mixing with other binders	Mixing of high PmB with other binders should be avoided as it can degrade the quality of the binder. Even mixing of high PmBs from various manufacturers can lead to unexpected consequences due to incompatibility.	Use dedicated tanks for high PmB or empty tank before filling with high PmB.
Phase separation during storage	Due to the high polymer content high PmB's can be prone to storage stability issues (Manfro et al., 2024).	Ensure the HighPmB has been properly engineered by the manufacturer. Agitation or circulation of the binder is required (follow the manufacturers recommendation). Conduct storage stability tests as part of quality control.

Table 5: Potential concerns when using high PmB and possible risk mitigation strategies

1.3 Project scope

Considering the discussion above, the scope of this project was defined. The aim was to capitalize on the existing world-wide knowledge of using high PmB by developing a research plan that would first verify the claims and then propose approaches for its standardization. The core content of this report is provided in three sections that correspond to the three pillars in Figure 29.

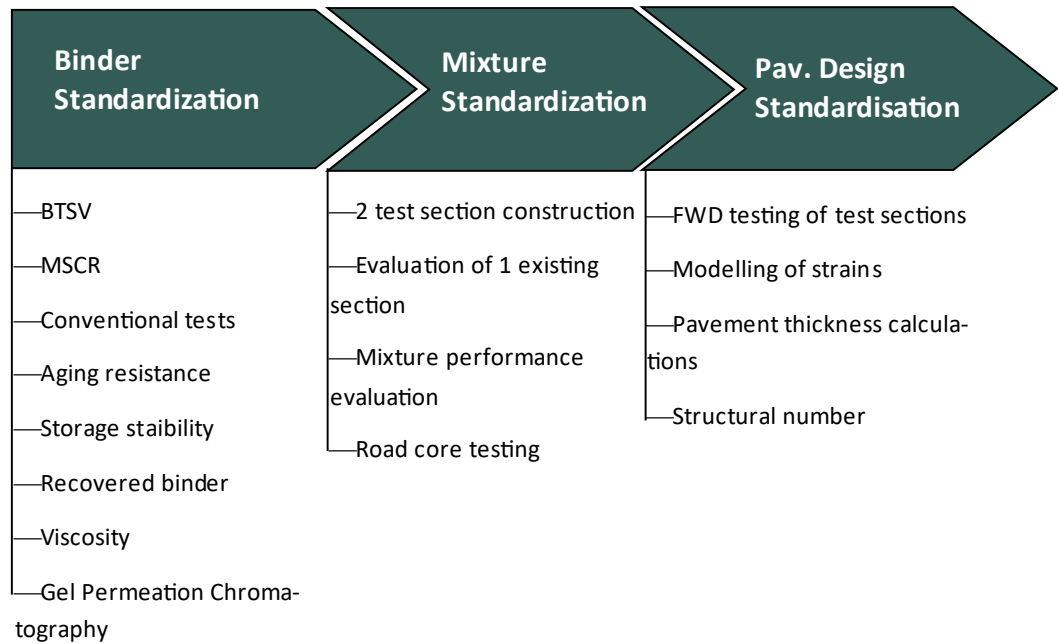


Figure 29: Project overview (the abbreviations used in the figure are presented in the methods section)

In the binder standardization part, 10 binders from different producers were collected, including binders with low, medium and high polymer content. The specific test methods for binder and mixture evaluation were selected to allow thorough evaluation of the properties that the use of high-PmB is expected to affect, including viscoelasticity, cracking resistance, rutting resistance, fatigue resistance, ravelling, and stiffness. In addition, the binders were evaluated for aging resistance and storage stability and were characterized using conventional test methods. Such evaluation was intended to allow proposing the most appropriate methods for standardization of high-PmB in Switzerland.

Early in the project, a commercially available high-PmB binder was used to construct two test sections in roads with high intensity traffic (see Figure 30). Different layers were evaluated in each case. In one of the sections (H27 Engadinerstr.) located at high altitude, the wearing course was evaluated and a soft binder grade was used. On the other section (H19 Oberalstrasse) at low altitude, the binder course with a hard binder grade was studied. The construction of the test sites was carried out early in the project, ensuring enough time to comprehensively evaluate the test section's performance. This included testing of plant-produced mixtures and testing of the pavement using Falling Weight Deflectometer (FWD). The paving of the test sections was executed in close collaboration with Canton Graubunden (GR) and Catram AG. In addition to the construction of the two new test sections, the evaluation of an existing SDA test section was performed in collaboration with Canton AG. This included producing a mixture in the lab using the same material sources that were used in the test section and evaluating the current state of the test section through laboratory testing of road cores.

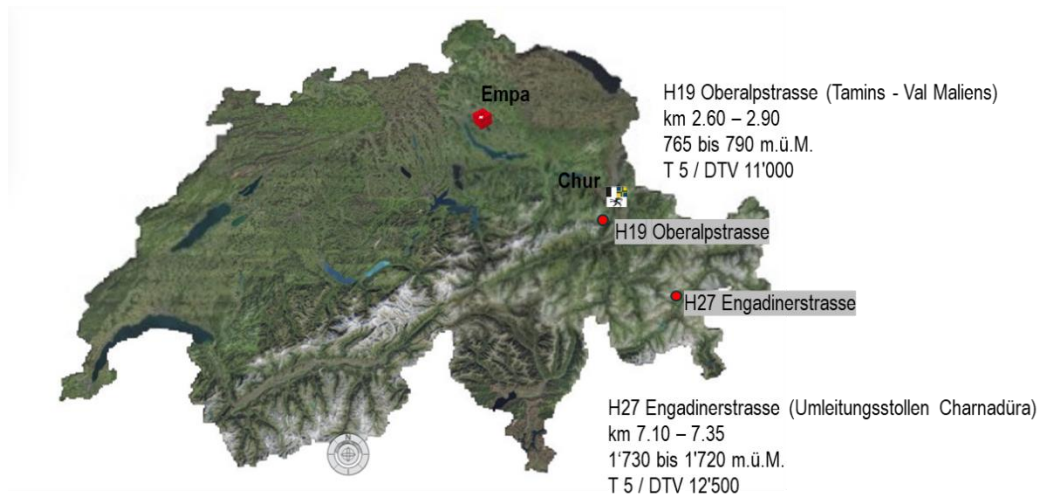


Figure 30: Location of the test sections

The methods for testing the mixtures in the laboratory were selected to verify the reported claims about the performance and benefits of high PmB mixes. At the same time, potential methods for proposing criteria for mixture design and quality control of such mixture were evaluated.

In Switzerland, performance improvement is currently not the main reason for using high PmBs. Rather, high PmBs are primarily used to compensate for the lack of polymers in asphalt mixtures containing Reclaimed Asphalt Pavement (RAP). The high polymer content of high PmB allows achieving the desired elastic properties in the final binder blend of virgin and RAP binders. Therefore, another objective of this project was the evaluation of the use of high PmB with RAP.

Finally, since the use of high-PmB can potentially allow reducing the pavement thickness, the gathered test results were used to model the pavement structures and simulate different loading conditions in order to obtain its deflections and calculate a structural number (a-value) that could be used for pavement structural design.

2 Methods

2.1 Binder tests

2.1.1 Sampling

The binders were collected from the manufacturer plant in large buckets. To sample the required material amount from the bucket (which remained at room temperature) a hot knife was used. At first, the top ~ 5 mm from the top of the binder was removed and discarded. The test sample was then collected.

A small trial experiment using one of the highly modified binders showed that by applying the described procedure, the properties of a sample collected from the top of the bucket were nearly equivalent to the properties of a sample collected from the bottom of the same bucket (see Table 6). Thus, it was assumed that samples collected from the top of the bucket (approx. 5mm below the surface) are representative of the entire bucket.

Results of the binder sampling experiment						
Sampling	Pen, 0.1mm	R&B, °C	TBTSV, °C	δBTSV, °	R3.2kPa, %	Jnr 3.2kPa, kPa-1
From the top of the bucket.	61.7	77.6	50.1	67.4	94.0	0.10
From the bottom of the bucket	62.3	78.1	49.7	67.6	95.0	0.08

Table 6: Comparison of test results for one binder when taking samples from the top or the bottom of the bucket

The described "cold sampling" approach was preferred over the heating of the entire buckets to pour the binder, since heating would induce artificial aging.

2.1.2 Conventional binder tests

Penetration was determined according to EN 1426, Softening point according to EN 1427, Elastic recovery according to EN 13398, Fraass breaking point test according to EN 12593, and storage stability according to EN 13399. The mean of two softening point measurements, two elastic recovery measurements, two breaking point measurements, and three penetration tests measurements is reported.

2.1.3 Reheating experiment

During the project, a discussion was initiated on the best approach for preparing the recovered binder for testing. It was suggested that reheating and blending is necessary to ensure representative test results. For this reason, an experiment was carried out with reheating the binder that was recovered from the binders built in the Oberalpstrasse test section (see section 4.1). The binder was reheated at 190°C for 15 minutes and manually stirred afterwards. The test results are summarized in Table 7. It could be observed, that the results are very similar between the reheated binder and the binder that was used for testing directly after the recovery. For this reason, after this

assessment, all tests on the recovered material were carried out without applying the reheating procedure.

Results of the binder reheating experiment

Material	Pen, 0.1mm	R&B, °C	Elastic rec., %	TBTSV, °C	δ BTSV, °	R _{3.2kPa} , %	J _{nr} 3.2kPa, kPa ⁻¹
High PmB	34.0	78.7	84.7	57.9	60.2	91.7	0.06
High PmB 15min @190°C	34.3	79.6	84.0	58.4	60.1	92.1	0.05
PmB	30.7	73.0	72.8	61.7	59.1	75.4	0.11
PmB 15min @190°C	32.3	73.7	77.6	61.9	58.9	75.9	0.11

Table 7: Results of reheating the PmB after recovery

2.1.4 Binder aging and mass change

Binder short-term aging was performed using the Rolling Thin Film Oven Test () according to EN 12607-1. According to this method, the binder film is exposed for 75 minutes to airflow in an oven set to 163 °C. The change in mass after aging is determined as an indicator for accelerated aging.

The short-term aged binder was then used for long-term using the Pressure Aging Vessel (PAV) according to EN 14769. In this procedure, the binder is exposed to a temperature of 100 °C under an air pressure of 2.1 Pa for 20 h. Originally, the PAV method was intended to simulate the aging that occurs in the binder during pavement use. However, in recent years it has been demonstrated that the procedure is not severe enough and therefore in this research two continuously successive PAV aging cycles (a total of 40 h) were applied to the samples.

2.1.5 Rotational viscosity

The dynamic viscosity at high temperature was measured according to EN 13302 on unaged samples. The test was performed at 135 °C and 160 °C temperatures by applying 100 s⁻¹ shear rate to a cylindrical spindle rotating in a container containing the bitumen. To detect a possible non-Newtonian¹² behavior, a linear shear gradient from 0 to 100 s⁻¹ and back was used.

2.1.6 Binder fast characterization test (BTSV)

The BTSV test was performed according to EN 17643 on unaged samples. The test is performed using a Dynamic Shear Rheometer (DSR) with 25 mm diameter plates having 1 mm gap under a constant shear stress of 500 Pa at 10 rad/s frequency. During the test, the temperature is increased by 1.2 °C/min between 20 °C and 90 °C. The temperature (T_{BTSV}) at which the complex shear modulus reaches 15 kPa along with the corresponding phase angle at this temperature (δ_{BTSV}) is determined. For each binder, two samples were tested to ensure that the variability does not exceed the range specified in the standard.

2.1.7 Multiple Stress Creep Recovery Test (MSCR)

The MSCR was used to determine the resistance to flow and deformation of the asphalt binders. The MSCR was performed using DSR according to EN 16659 on unaged

¹² Non-Newtonian behavior describes a fluid's viscosity which changes depending on the applied stress

samples. Unlike the typical testing at RTFOT aging condition, testing of unaged samples was selected to enable easy comparison with the other test methods used in this research (which also are applied on unaged samples).

The test was performed using 25 mm plate-plate geometry with a 1 mm gap. During the test, stress is applied for 1 second, followed by a 9 second rest period. This cycle is repeated 10 times at 0.1 kPa stress, followed by 10 more cycles at 3.2 kPa stress. Due to the high polymer content, results do not allow to discriminate between the binders (see section 3.10). Therefore, the procedure was extended 10 more cycles at 10 kPa stress. The testing was performed at 64 °C for all binders and additionally at 58 °C for the soft binders.

Two main results are obtained from this test, namely:

- Percent recovery. This value represents the elastic response of binders and can be used to assess the effect of polymers in the binder.
- Non-recoverable creep compliance (J_{nr}). It serves as an indicator of the sensitivity to permanent deformations of the binder under repeated load

2.1.8 DSR Frequency sweep and Superpave high Performance Grade (PG)

Binder rheology was tested using Dynamic Shear Rheometer (DSR) according to EN 14770. A 25mm plate-plate geometry with 1 mm gap was used for the temperature range +40°C to +100°C. For some samples the temperature range was updated, depending on the material properties. Testing was done at 20 different frequencies ranging from 0.1 to 10 Hz at each temperature.

Bitumen is a viscoelastic material and its complex modulus $|G^*|$ is composed by two parts: a viscous part G'' and an elastic part G' as demonstrated in Equation (1).

$$|G^*| = \sqrt{(G')^2 + (G'')^2} \quad (1)$$

In order to obtain $|G^*|$ over a range of frequencies a superposition principle was used to shift the results to a reference temperature of 20°C. To that end, a sigmoidal model was used as proposed by Pallinen (Pallinen et al., 2004), with the shift factors calculated following the Williams-Landel-Ferry (Williams et al., 1955) relation according to Equation (2):

$$\log a_T = \frac{-C_1 (T - T_{ref})}{C_2 + (T - T_{ref})} \quad (2)$$

where

C_1 and C_2 are material constants

a_T is a factor for shifting complex modulus at certain temperature T

T_{ref} is the shifting reference temperature (20°C in this study)

In order to obtain these parameters, a least squares regression was performed.

The results of the DSR frequency sweep were used determine the high Performance Grade (PG) according to ASTM D6373-16.

2.1.9 Gel Permeation Chromatography (GPC)

Gel permeation Chromatography (GPC) was performed according with a GPC-System (Agilent Technology, Santa Clara US) consisting of an isocratic pump, an autosampler and a variable length UV detector (@215 nm). Two 300 mm GPC columns (Agilent Technology, Santa Clara US) PLgel Mixed-C were used at 35°C in a column oven. High purity non-stabilized Tetrahydrofuran (ROMIL, UK) was used as solvent at a flow rate of 1.0 mm/min.

Small bitumen samples of approximately 250 mg were taken from the laboratory sample and dissolved in tetrahydrofuran (THF) with a target concentration of 1.5 mg/ml. About 2 ml of the diluted solution was drawn off with a syringe and filtered directly through a 0.45 micron PTFE disc filter into a glass vial and 50µl was injected for the analysis. Molecular mass determination was performed relative to polystyrene using four standards with peak molecular mass of 556000, 99400, 8130 and 1370 Dalton.

2.2 Mixture tests

2.2.1 Particle size distribution

The gradation of RAP aggregates was performed after binder extraction following the method described in EN 933-1. This includes sieving extracted RAP aggregates for 10 minutes dry, followed by 10 minutes water sieving of the entire tower. The tower, holding 30 cm diameter sieves, was shaken at a frequency of 50 Hz and amplitude of 1.6 mm. Each sieve with the material was then placed in an oven at 110 °C until completely dry. The resulting curve is referred to as the white curve.

2.2.2 Conventional mixture tests

Bulk density of the AC-type asphalt samples was determined using saturated surface dry method, according to EN 12697-6. The void content was calculated according to EN 12697-8. The reported air voids were measured after cutting of the samples, if cutting was performed for the specific test. The density of SDA-type asphalt samples was determined by dimensions according to EN 12697-6. The maximum density was determined according to EN 12697-5 using pycnometers and toluene.

The Marshall test was performed according to EN 12697-34. The samples were compacted at 155 °C with 50 blows from each side.

2.2.3 Semi-circular bend (SCB) test

The Semi Circular Bend (SCB) test was used to determine the susceptibility of the material to crack propagation. The test was performed at 25 °C according to AASH-TO TP 124-16. This test was selected due to its reported sensitivity to mix design parameters, like bitumen content and aging. This test has also proven to be punishing the use of high RAP content, if appropriate measures have not been taken to compensate for the stiff RAP binder. Finally, the result of the test, Flexibility Index (FI), has demonstrated a reasonable correlation with the performance at the FHWA (US Federal Highway Administration) test track. In that study, seven different mixes with various RAP and RAS (reclaimed asphalt shingles) contents and different warm mix asphalt technologies were placed, using equal structural design and tested for cycles to fatigue threshold. The results of this study correlate well with the results of FI (Ozer et al., 2016). Based on these results it was concluded that the FI provides means to identify brittle mixes

that are prone to premature cracking. Further, the FI distinguishes between mixtures more clearly than fracture energy (a parameter that is often used in cracking tests). To prepare samples for the SCB test in laboratory, the asphalt mixture was prepared using the Gyratory compactor. The Gyratory samples were then cut to a height of 50 mm, and cut in half-cylinders as demonstrated in Figure 31. Cutting of the top and bottom was done to avoid the inhomogeneity that is usually present at interfaces. The samples cored from the pavement were prepared by cutting the respective layer to 50 mm. For surface courses instead, and due to these layer thicknesses are below this value, the samples were cut to a high of 30 mm. After cutting to the required height, a notch of 15 mm depth and 3.5 mm width as required by the standard, was cut into half-cylinders to control the crack initiation point.

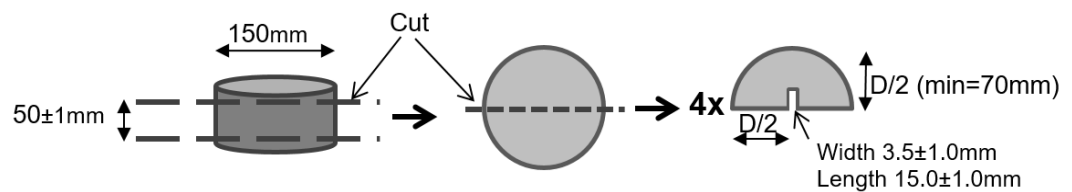


Figure 31: The principle of preparing SCB test samples

The gyratory samples were compacted at the temperature that corresponds to the binder grade: 165 °C for the SDA and AC B 22 S, 155 °C for the AC 8 S. The target air void content in the gyratory compactor was 6 % for the asphalt concrete samples and 12 % for the SDA samples. The reported air voids are measured after cutting of the samples.

During testing, the specimen is positioned in a three-point testing frame as can be seen in Figure 32. Then, a load is applied at a monotonic rate of 50 mm/min along the vertical axis while load and displacement are recorded. For each binder and base course material, six parallel samples were tested, while for each wearing course material, four parallel samples were tested.

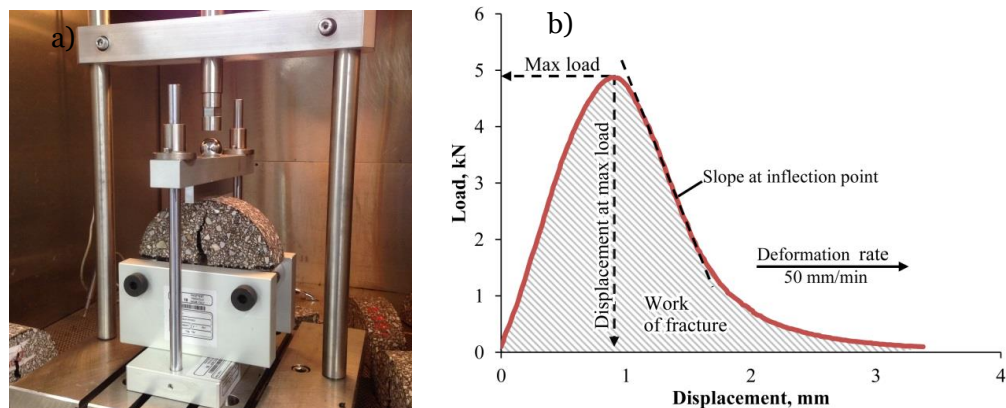


Figure 32: SCB test setup (a) and typical test result (b)

The results are expressed in terms of Flexibility Index (FI) according to Equation (4) and fracture energy according to Equation (3).

$$G_f = \frac{W_f}{Area_{lig}} \times 10^6 \quad (3)$$

where:

G_f – fracture energy in Joules/m²

W_f – work of fracture (calculated as the area under the load versus displacement curve) in Joules

$Area_{lig}$ – ligament length in mm² multiplied by t

t – specimen thickness in mm

$$FI = \frac{G_f}{|m|} \times A \quad (4)$$

where:

FI - flexibility index

G_f - fracture energy in Joules/m²

m - the post-peak slope at the inflection point of the load-displacement curve in kN/mm

A - a scaling factor (0.01)

FI is sensitive to the sample air voids. Therefore, if necessary to correct for air voids, this can be done according to the research described by (Barry, 2016a; Rivera-Pérez et al., 2021) according to Equation (5).

$$FI_{corrected} = \frac{(1 - AV_{target}) * AV_{target}^2}{AV_{measured} - AV_{measured}^2} \quad (5)$$

where:

$FI_{corrected}$ – flexibility index (FI) corrected to AV_{target} , %

AV_{target} – target air voids, %

$AV_{measured}$ – measured air voids, %

Equation (6) from (Barry, 2016b) was used to correct for the different sample heights, considering a nominal thickness of 50 mm. This correction is necessary for road cores from layers with a thickness of less than 50 mm.

$$FI_{50mm} = FI_t \times \frac{t}{50} \quad (6)$$

where t is the sample height.

2.2.4 IDEAL-CT

The Indirect Tensile Asphalt Cracking Test (IDEAL-CT) was used to evaluate the intermediate-temperature cracking resistance of the asphalt mixtures as shown in Figure 33. The test was conducted in accordance with ASTM D8225 at 25 °C using three replicate specimens per mixture. Gyrotory-compacted cylindrical specimens with a nominal diameter of 150 mm and height of approximately 62 mm were prepared at a target

air void content of 6 % for the asphalt concrete specimen and 12 % - for the semi dense asphalt. The reported air voids are measured after cutting of the samples.

Each specimen was positioned in an indirect tensile loading fixture and subjected to a monotonic vertical compressive load at a constant displacement rate of 50 mm·min⁻¹ until the load decreased to the prescribed termination level. From the load–displacement curve, the fracture energy, post-peak slope at 75 % of peak load, and the corresponding displacement were determined, and these parameters were combined to calculate the Cracking Tolerance Index (CTIndex) as defined in ASTM D8225 according to the Equation (7).

$$CT_{index} = \frac{t}{62} \times \frac{l_{75}}{D} \times \frac{G_f}{|m_{75}|} \tag{7}$$

Where:

CT_{index} is the cracking tolerance index

G_f – failure energy, J/m²

m₇₅ – post peak slope around 75 % peak load, N/m

l₇₅ – displacement at 75 % the peak load after the peak, mm

D – specimen diameter, mm

t – specimen thickness, mm

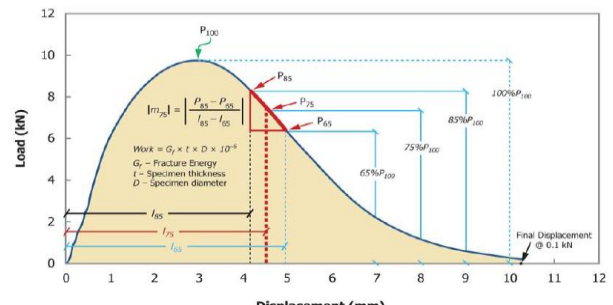


FIG. 1 Recorded Load (P) versus Load-Line Displacement (l) Curve

Figure 33: IDEAL-CT test setup and the principle of result expression from the load – displacement curve

2.2.5 French rutting test

The French rutting test is the standard method in Switzerland to determine the susceptibility of compacted mixtures to rutting. The slabs for the rutting test were compacted using the French wheel compactor according to EN 12697-33 using a steel wheel. For the AC 8 mixture, slabs were compacted to 50 mm height while for the AC 22 mixtures to 100 mm height. All the samples were 500 mm in length, and 180 mm in width. The compaction was carried out at 165 °C for the AC B 22 S and at 165 °C for the AC 8 S samples to a target porosity of 4 % air voids and at 165 °C to 12 % porosity - for the SDA samples.

The rutting resistance was measured using the French Rutting Tester (FRT) according to EN 12697-22. The FRT was run using a rubber pneumatic wheel that moves across the sample with a pressure of 0.60±0.03 MPa and a load of 500±5 kN. A preconditioning load was applied at room temperature for 1,000 cycles. Then, the sample was conditioned at 60°C for about 16 hours in a temperature chamber. For each material, the test was run for two parallel specimens and rut depth was measured after 30, 100, 300,

1,000, 3,000, 10,000, and 30,000 cycles at five pre-defined points along the length of the rut. For some samples, the test was extended to 90,000 cycles to evaluate the effect of the high PmB content.



Figure 34: French Rut Tester (FRT)

2.2.6 Stiffness modulus using Indirect Tensile Test

The stiffness modulus test was performed using the Indirect Tensile Test (ITT) setup according to the German standard AL Sp-Asphalt 09. The specimen diameters were 150 mm for the mixture with maximum aggregate size above 22 mm and 100 mm for the mixture with maximum aggregate size of 16 mm or less. All samples were prepared using the Gyratory compactor using 150 mm molds, followed by coring to 100 mm diameter if necessary. The compaction temperature was 165 °C for the AC B 22 S and the SDA samples, and 155 °C for the SDA 4-12 samples. The target air void content for the gyratory samples was 4.5 % for the AC samples and 12 % for the SDA samples. All samples were cut from top and bottom to increase homogeneity. The height of the 150 mm and 100 mm diameter samples were 60 mm and 40 mm respectively.

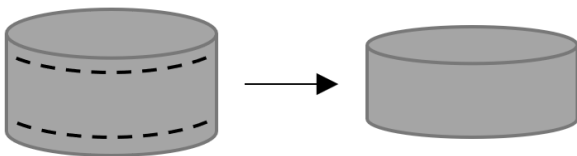


Figure 35: The gyratory samples were cut from top and bottom to increase homogeneity

The samples were tested at 10°C by applying sinusoidal loads at three frequencies: 0.1 Hz, 1 Hz, and 10 Hz. Three replicates were tested for each material. Since the tests were performed in the linear viscoelastic range (which means that no permanent damage was introduced to the specimens), in some cases the same samples were also used for testing fatigue afterward.



Figure 36: Stiffness modulus and fatigue test setup

2.2.7 Fatigue using two point bending test

The fatigue tests were conducted to determine the susceptibility of the material to long-term repeated loading by two-point bending using trapezoidal shaped specimens. The test was conducted according to the SN EN 12697-24 Annex A (2PB-TR).

The samples were prepared by compacting plant-produced asphalt mixtures in laboratory using a French wheel compactor according to EN 12697-33 at 165 °C. The dimensions of the slabs were 60 cm in length, 40 cm in width, and 12 cm in height. The target air void content of the slab was 4.5 %. The trapezoidal samples were cut from the slab to the required dimensions as shown in Figure 37. The air voids of the samples that are reported in this report were measured after cutting the samples.

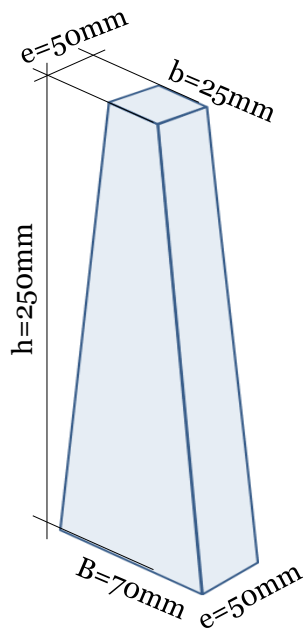


Figure 37: Dimensions of the fatigue samples

To perform the test, the wide base of the specimens was glued to a plate. The fatigue test was performed at 10 °C by applying in a controlled zero-mean stress sinusoidal loading at 25 Hz frequency at the narrow side of the specimen. The applied load was measured by the load cell while the deflection was measured using a displacement transducer. The setup is illustrated in Figure 38.

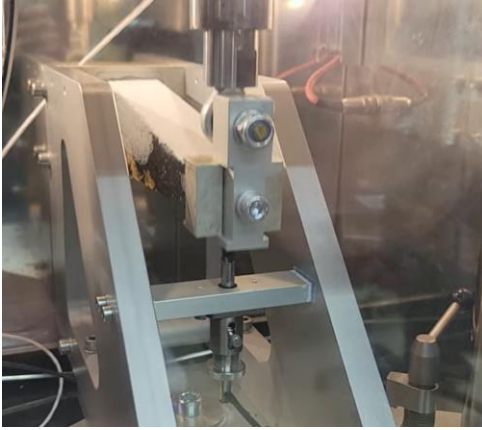


Figure 38: Mixture fatigue testing apparatus

The test was performed at different displacement amplitude levels to enable drawing a fatigue line for fatigue life versus the amplitude level. For each specimen, the fatigue life was defined as the number of load applications for a 50 % reduction from the initial complex stiffness modulus. The initial stiffness modulus was determined as an average of 10 cycles, starting from the 100th cycle. The regression line of the results of the test repetitions at different amplitude levels was calculated according to Equation (8).

$$\lg(N) = a + \left(\frac{1}{b}\right) \cdot \lg(\varepsilon) \quad (8)$$

where

N is number of load cycles to failure

a is the ordinate of the fatigue line

1/b is the slope of the fatigue line

ε is the strain

2.2.8 Thermal Stress Restrained Specimen Test

The Thermal stress restrained specimen test (TSRST) was used to determine the susceptibility of the materials to cold temperature cracking. It was performed according to EN 12697-46 and three repetitive samples were tested per asphalt mix. If the variability between two of the three samples was within the permitted range of 2°C, the result of the third sample was discarded. In other cases, the average result of three samples is reported.

The test specimens were prepared by compacting asphalt slabs and then cutting the beams to the specified dimensions. The specimens were glued to two aluminum plates and mounted in the load frame in an environmental chamber to ensure constant height throughout the test. The test starts at 20°C and the temperature is lowered at a rate of

10°C/h until the sample cracks due to thermal stress exceeding tensile strength. The test set-up and a typical TSRST test result is illustrated in Figure 39. Minor stress is caused at the beginning of the test but as the temperature reduces at 10°C/h an inflection point is reached and stress starts to increase linearly proportionally to the temperature. This cooling rate (specified in the EN 12697-46) does not necessarily reflect the actual conditions in the field and the measured cracking temperature will depend on the applied cooling rate. Therefore, the results should only be considered as an index and compared with samples tested at the same conditions. At sample failure critical stress and cracking temperature are recorded.

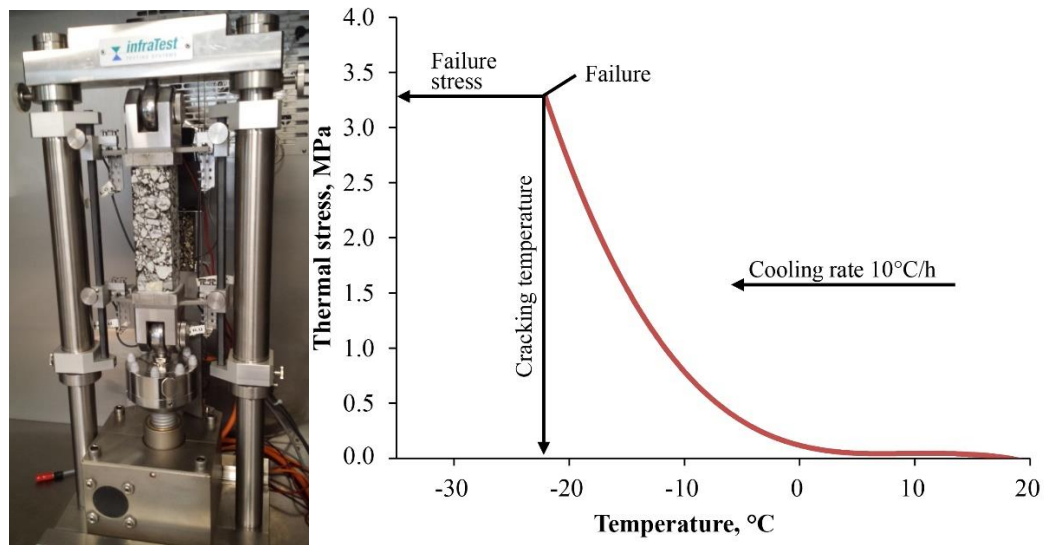


Figure 39: TSRST setup and typical TSRST test result

2.2.9 Cantabro test

The Cantabro test was conducted in accordance with EN 12697-17 to determine the particle loss of asphalt samples. The Marshall compactor was used for the laboratory-mixed samples to prepare specimens of 50 mm height. For road cores, the sample height was defined by the layer thickness. The samples were tested at room temperature (around 20 °C) using the Los Angeles abrasion machine, operated without steel balls. The machine was rotating at a speed of 30–33 revolutions per minute for 300 revolutions. After the test, specimens were removed, gently cleaned to eliminate loose particles, and weighed again to determine the final mass (W_2). The percentage of mass loss (ML) was calculated using Equation (9).

$$PL = [(W_1 - W_2) / W_1] \times 100\% \quad (9)$$

where

PL is the particle loss, %

W_1 is the sample mass before the test, g

W_2 is the sample mass after the test, g



Figure 40: Los Angeles testing machine for the Cantabro test

2.2.10 Leutner test

The Leutner test was used to determine the interlayer shear strength between asphalt pavement layers according to the standard VSS 70 461. Road cores with a diameter of 150mm were placed horizontally in a shear testing device as shown in Figure 41. The tests were performed at 20 °C. During the test, a shear load is applied at a constant displacement rate of 50 mm/min, until failure occurs at the interface. The maximum shear force is recorded and divided by the interface area to calculate the interlayer shear strength.



Figure 41: Testing of the layered composite according to Leutner method

2.2.11 Model Mobile Load simulator (MMLS3)

In order to upscale and validate the results obtained on laboratory samples, an MMLS3 test was performed. The MMLS3 was used to determine the mechanical resistance of slab specimens under rolling tire loading regime against fatigue crack formation and propagation.

The MMLS3 (shown in Figure 42) is a laboratory-scaled accelerated pavement loading device used for pavement trafficking, simulating real pavement loading conditions. The machine is intended to induce pavement distress in a short period of time under the loading of repetitive rolling tires. It consists of a rigid steel frame with four adjustable feet and applies a downscaled load with four single pneumatic tires that simulates

traffic, moving in one direction on a circulating belt. Each tire has a diameter of 0.3 m and a width of ca. 0.10 m and loads the pavement through a spring suspension system over a length of 1.2 m. The tire pressure can be adjusted between 560...800 kPa. The device can be moved laterally during loading to simulate the wandering of the tires in real pavement, or it can be fixed in one position to simulate channelized loading (i.e. the tires apply the loads following the same wheel path). The machine can run at a maximum load of 2.5 kN and a speed of 9 km/h, allowing a maximum of approximately 7200 load applications per hour. This corresponds to a loading frequency rate of nearly 2 Hz. The entire device has a length of 2400mm, a width of 600mm, a height of 1150 mm and a weight of 800 kg. The MMLS3 can be used outside to evaluate real pavement in-situ, or in the laboratory to load slabs in a climatic chamber for precisely controlling the testing temperature. It is usually used to investigate the rutting performance of asphalt mixtures at high temperatures (up to 50 °C) or their crack susceptibility at lower temperatures (10 °C).

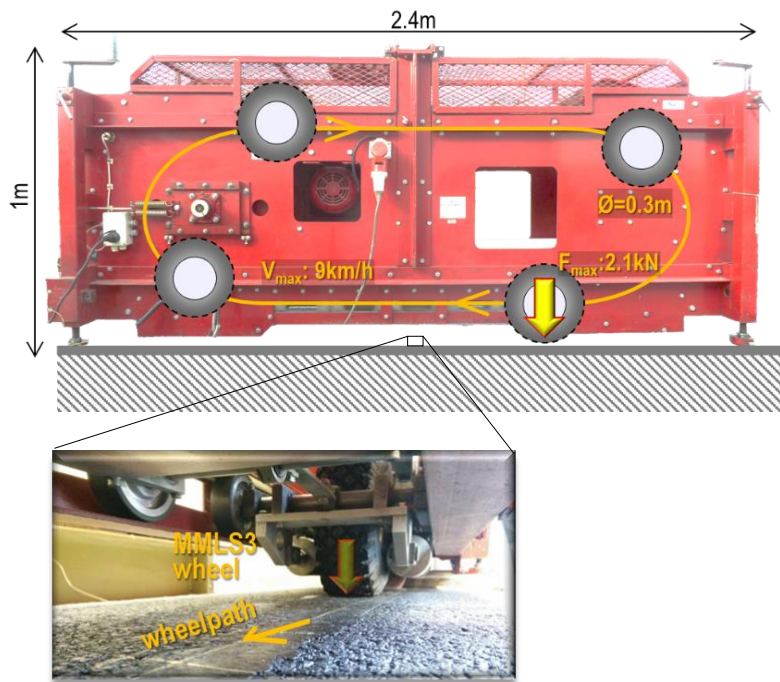


Figure 42: View of the MMLS3 with its 4 wheels and working principle

The advantage of using this type of testing machine over other small scale laboratory tests is the possibility to simulate the complex stress fields that vehicular loading induce in real pavements. As mentioned earlier, the MMLS3 can be used in-situ on existent roads or in combination with plate shaped specimens cut from a real pavement or slabs compacted in the laboratory using a reduced scale roller compactor (see Figure 43). This allows the testing of more representative samples, compared to cylindrical Marshall, gyratory, beam or trapezoidal specimens.



Figure 43: Roller compactor and specimen production for the MMLS3

Experimental setup

In this research, the machine was run at its maximum load (2.5 kN) and at a speed of 4.5 km/h, allowing approximately 3600 load applications per hour. This corresponds to a loading frequency rate of nearly 1 Hz. The tires were inflated at a pressure of 6 bar. In order to prepare the slab specimens, the plant-produced mixtures were heated in an oven, mixed and compacted using the medium size Empa rolling compactor (see Figure 43) with the dimensions of 1.6 m x 0.45 m x 6 cm thickness. After compaction, a 3 cm deep transverse notch was cut in the centre of the bottom face to initiate cracking. The short edges of the slabs were placed on steel profiles (supports) to induce bending under load. Between the steel profiles, and below the slab, a rubber mat was placed to model a soft elastic foundation, simulating the subgrade. The whole setup was fixed onto a stiff concrete plate to anchor the MMLS3 and placed in the temperature chamber for a controlled loading temperature situation. One slab per mixture was loaded. Under these conditions, the bending should be able to generate a tension stress at the tip of the notch, without reaching the failure immediately but high enough to create a fatigue failure over several loading cycles. A photo collection of the construction process and testing setup is shown in Figure 44.

The failure criteria used to terminate the test was when a crack initiated on the tip of the notch reached the surface of the slab. An important aspect to consider for the organization of the experiments was that each test would not take longer than 5 days, i.e. a working week starting on Monday and finishing at the latest on Friday evening.

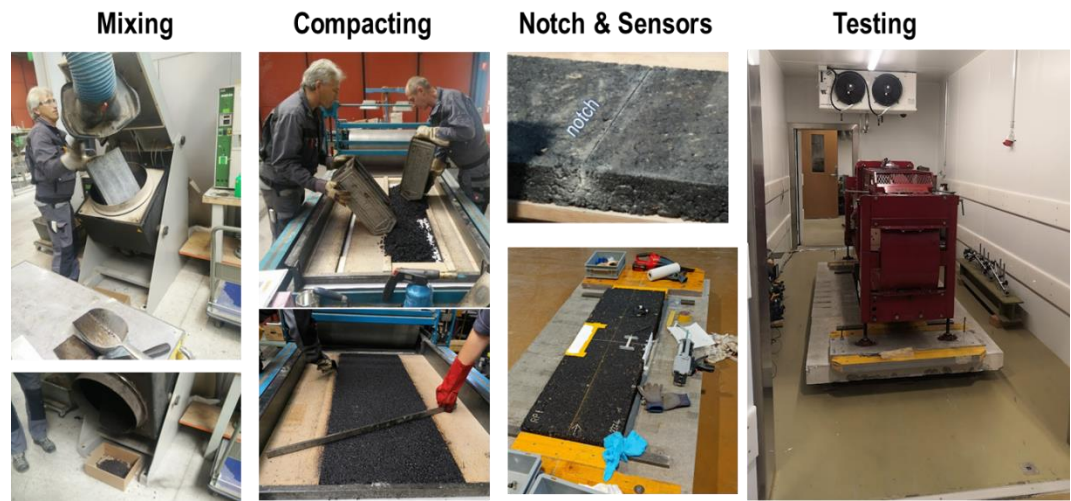


Figure 44: Photo collection of the test preparation process

The temperature during loading was measured inside the slabs and the values were recorded with their timestamps every 2 min. To that end, a thermocouple was installed by drilling a 10 cm hole on one side of the slabs (see Figure 45). The temperature in the specimen was controlled through manually setting the air temperature in the chamber. The target temperature inside the slab was set to 10°C.



Figure 45: View of the thermocouples and data acquisition system

Measurements and data analysis

In order to measure how the cracks generate at the tip of the notch and grow through the specimens, different methods were used. Figure 46 shows a schema and pictures of the measuring methods, which will be described in detail in the following chapters.

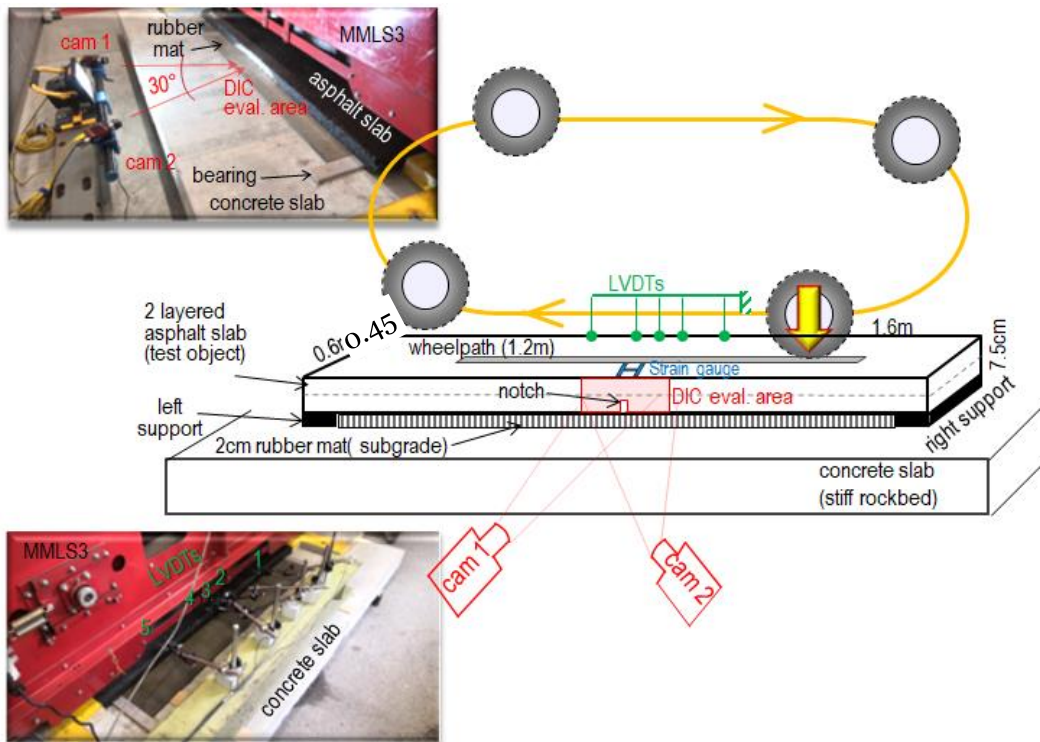


Figure 46: MMLS3 cracking test setup and pictures showing the load application area, DIC System, strain gauge and LVDT measuring arrangement

LVDTs

To measure the deflection of the slab during loading, Linear Variable Differential Transformers (LVDTs) were installed close to the edge along the span of the sample. An LVDT was placed in the middle of the span, two LVDTs 50 mm from the center on either side and another two LVDTs 400 mm from the center (see Figure 46). The deflection was periodically recorded to indirectly determine the crack development. In this case, files containing 10 s deflection information of the five LVDTs were stored every 2 min. An example of the time records for the LVDTs located at the center of the slabs is shown in Figure 47, for two different slabs. Each valley of the curves corresponds to the situation where the tire is in the middle of the wheel path passing close to the LVDT at the center, forming a valley in the time series plot. When the tire reaches the end of the wheel path and the next tire is approaching, the plots form a peak. Once all records are stored, an algorithm calculates the deformation amplitude as the average distance between peaks and valley for each measurement file. Then, these results are plotted versus the amount of MMLS3 load cycles. In this example, it is possible to see that the deflection of slab 1 are higher than in slab 2, meaning that slab 2 is stiffer than slab 1. Further, the deflection amplitudes tend to increase with the MMLS3 load cycles, giving a hint of the degree of damage of a slab, as explained below.

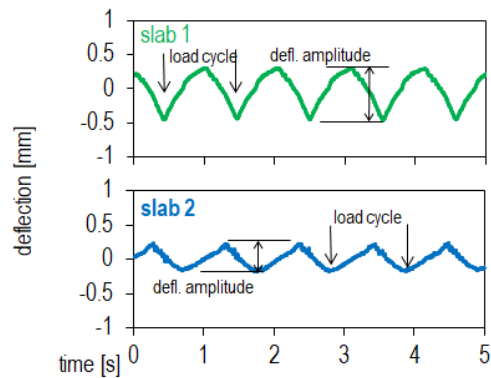


Figure 47: Example of two LVDTs records at the center of two different slabs (left) and calculated defl. amplitudes

Different typical phases of the deflection curves vs. MMLS3 load cycles are shown in Figure 48, and they represent different damage stages. As previously explained, the deflection amplitudes (def, as shown in the left side of Figure 48) are defined as the difference between the LVDT reading when a MMLS3 wheel is passing over the sensor (i.e. maximum vertical deformation) and when no wheel is touching the slab (i.e. the slab is not loaded). Due to the damage the deflection amplitude will increase with the accumulation of MMLS3 load applications. A certain initial value def_0 will increase to a final value def_{END} when a fatigue crack progresses from the bottom to the top of the slab. Ideally, the process can be divided into three phases.

- Phase I is marked by a rapid rise in deflection amplitude, caused by the settlement of the system under load.
- Phase II begins with the propagation of a micro-crack from the notch tip, extending until it reaches the interlayer plane. These cracks are not directly visible to the naked eye but they reduce the stiffness of the slab. This phase is characterized by a relatively low, linear, but steady increase in deflection amplitude.
- Phase III is characterized by a sudden, sharp increase in deflection amplitude, signaling the formation of a macro-crack that are visible to the naked eye. This crack, which began as a micro-cracks at the notch during Phase II, progresses vertically through the top layer of the slab, eventually causing complete failure and separating the slab into two parts, thereby marking the end of the test.

It should be noted that this idealized three-phase damage mechanism may differ, with certain phases potentially not being clearly distinguishable.

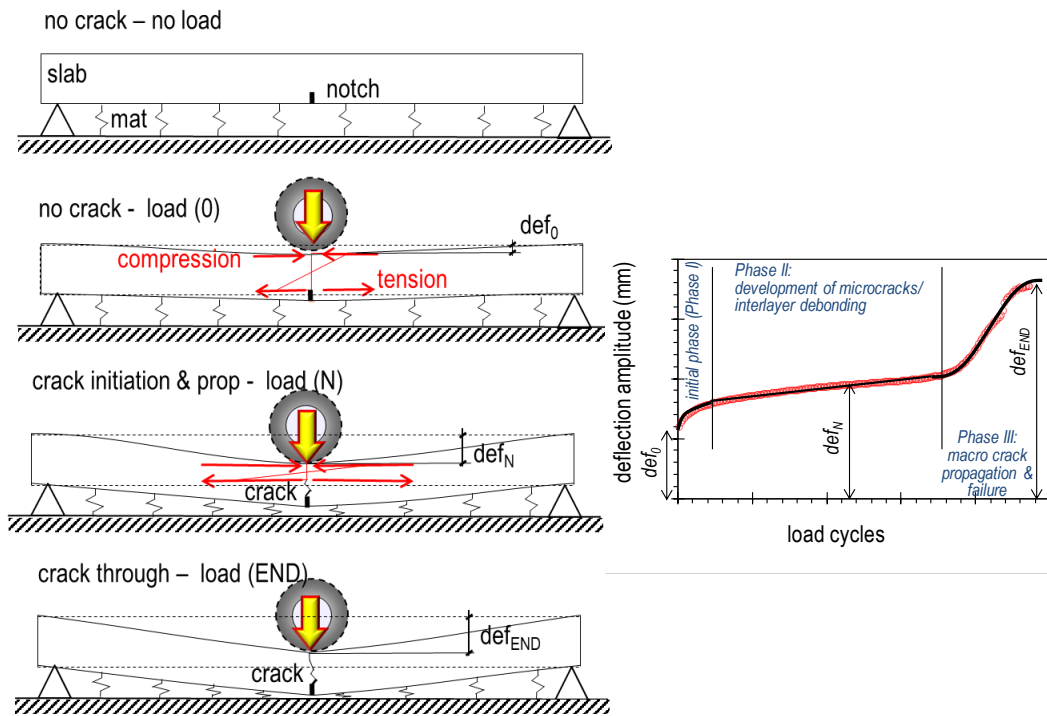


Figure 48: Conceptual schema of the MMLS3 test progression (left) and expected evolution of deflection (right)

Strain gauge

Similarly, as with the LVDTs, a strain gauge was glued to the surface of the slabs in the center and parallel to the wheel loading path, 10 cm from the slab border. The strains produced in the slab's surface by the tires loading was periodically recorded to indirectly determine the crack development. The measurements were stored in the same files containing the LDVTs recordings and the data was analyzed using a similar approach.

Digital Image Correlation (DIC)

In addition to the measurement of deflection, the crack development was monitored by digital image correlation (DIC). As explained in the previous chapter, this non-contact optical technique measures the deformation of a body under load by tracking. The lateral surface around the notch, about 15 cm in each direction, was grinded to make it smooth and was painted with white color to provide high contrast. A black dotted pattern was sprayed with a high-pressure nozzle to create the DIC speckles (see Figure 49). Two cameras placed at an angle of about 30° and pointing at the notch monitored this area (see bottom picture in Figure 47). Image recording was triggered periodically, every ca. 1200 MMLS3 load cycles. Each image recording comprised 50 frames taken in a 2 s window, i.e. enough to capture the passing of the MMLS3 wheels with a sampling rate of 25 Hz as shown in Figure 50. This figure displays five different situations, where one of the tires starts to touch the slab surface, then rolls towards the center of the slab and reaches it after 0.5s. At this time, the bending of the slab is maximum, and a potential crack opens. Then, the tier continues its travel toward the end of the wheel path and after 1 s the slab is again and for an instant not loaded and the bending is minimum, closing any crack. The deflection of the slab center is also presented at the bottom graph of Figure 50.

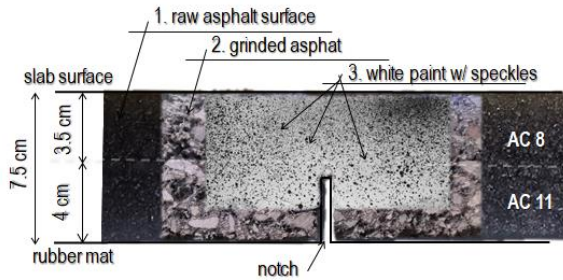


Figure 49: view of the measuring area showing the raw and grinded surface and the surface after painting and speckle application

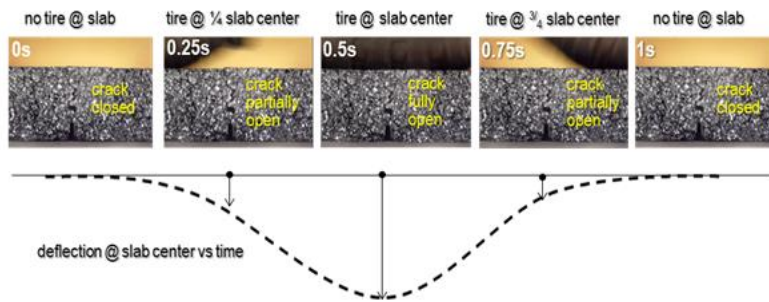


Figure 50: Schematic of the tire passing over the notch, showing the opening of an existing crack whereas the bottom graph shows the deflection of the center at different times

The software used for image acquisition and post-processing was the Istra4D (v. 4.4.2). In order to detect a crack, images of the non-loaded state (when no wheel is touching the slab, see 0 s and 1 s frames in Figure 50) were compared with the loaded state (see 0.5 s frame in Figure 50). The deformation of the surface is obtained by recognizing a pattern- speckle followed throughout time (Figure 51). By doing this, it is possible to evaluate displacement and deformation present in the pattern studied. To be able to recognize a dot pattern, the image captured by the DIC cameras was converted into binary data. In this process each pixel color is converted into a number. Once the image is transcript in memory through numerical values, it is possible for the DIC software to compare it to the next image after a time interval (Figure 43). In this new image, the program will try to find the pattern identified in this first image using a correlation function. By doing so, it will be possible to know if the pattern moved or not, thus knowing if deformations or rigid body displacements occurred. To find the subset pattern in the new image, a correlation function is used. By testing multiple values in this function, different possible locations of the pattern are tested until the function determines which pattern location has the smallest error when compared to the original one. This location is thus saved as the n+1 location. When comparing the n and n+1 locations, it is possible to determine the displacement of the pattern matching the original pattern with a relative displacement. Perfect matches rarely occur due to distortions in the material and image noise slightly modifying the colors from one image to another. In most cases, the selected location is the one that gives the smallest error through the correlation function. As a result, the relative displacements can be displayed over the image of the observed element through a color code. Moreover, starting from the relative displacements the program offers visualization also in terms of strains. As an

example in Figure 52, the von Mises strains obtained by comparing the non-loaded state and the loaded state for different number of MMLS3 loads is presented, clearly showing the progression of the cracks. It can also be observed that the cracks tend to grow wider and the strains in this area tend to increase. This is due to the progression of other cracks in the slab and due to the fact, that because of the relative movement of the crack walls, any interlocking between the aggregates on both sides of the crack tend to grind reducing the stiffness of the slab.

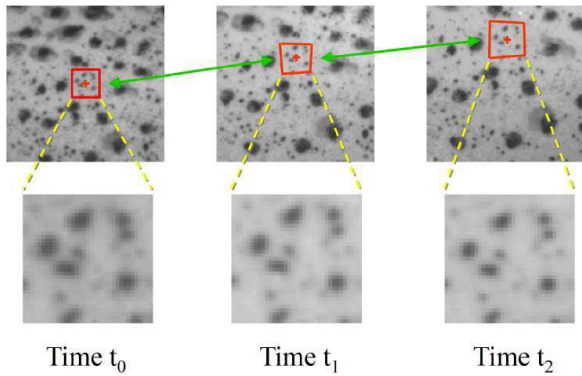


Figure 51: DIC pattern following over time (from Digital Image Correlation: Theory [PDF]. Source: Michael A. Sutton, Jean Jose Orteu, Hubert W. Schreier Source: Image Correlation for Shape, Motion and Deformation Measurements, LIMESS)

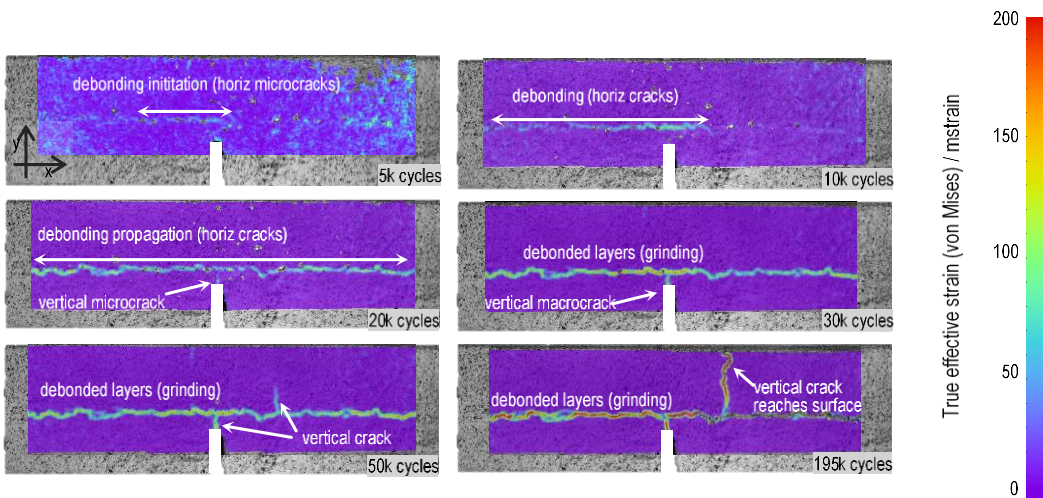


Figure 52: Example of the evolution of the von Mises strains showing the evolution of the cracks vs. the MMLS3 loading; each figure

In order to compare the susceptibility of the different materials to the crack formation and propagation, the images obtained through the test progress were visually compared, until a full crack was observed through the entire slab thickness or until the test reached 5 days of load.

2.3 Structural capacity of test sections with FWD

To evaluate the structural capacity of the test sections constructed with high-PmB and standard bitumen, Falling Weight Deflectometer (FWD) measurements were conducted. The objective of these tests was to determine whether the use of high-PmB produces a measurable effect on the load-bearing capacity of the pavement as assessed through FWD measurements.

This device simulates the load of a passing vehicle wheel by dropping a heavy weight onto a "buffer" which shapes the pulse and then transmitted to the pavement through a circular load plate. The dynamic properties of the load are controlled by means of a spring. The momentary impulse causes a deflection depression on the pavement surface, which is registered by a series of surface-mounted geophones. The velocities of the pavement deformations are recorded at several points and converted into deflections. The amplitudes and deflections that can be measured with this device are used as indicators of the condition of the pavement. In this study, the measurements were carried out by the company Infralab SA from Lausanne (see Figure 53).



Figure 53: View of the Infralab FWD (left) and loading plate and geophones (right)

For the FWD tests conducted at the end of September 2024, a load of 110 kN was applied through a circular plate with a diameter of 30 cm. Surface deflections were measured using 13 geophones positioned at 0, 0.2, 0.3, 0.4, 0.5, 0.6, 0.75, 0.9, 1.05, 1.24, 1.5, 1.7, and 1.9 m from the load center. The drops were performed approximately every 10 m along the test sections, covering both the high-PmB and conventional PmB sections. After testing, Infralab SA provided the raw data and a report, in which the data was processed using the ELMOD software to back-calculate the elastic moduli of the pavement layers (see section o).

3 Binder quality control standardization

Currently there are no standardized test methods and criteria to classify high PmBs, thus limiting their application and causing challenges during quality control. In this section we evaluated a total of 10 different binders from two classes using conventional tests as well as multiple stress creep recovery (MSCR) test and binder fast characterization test (BTSV). The results confirmed earlier reports that the softening point, elastic recovery, and the Fraass breaking point do not allow to characterize polymer-modified binders confidently.

Switzerland has already introduced two PmB types in the standards, CH-C and CH-E for binders with low and medium polymer content respectively. Table 8 summarizes part of the current requirements from the standard SN EN 14023-NA for two of the most used PmB classes. It includes only the properties that, according to our understanding, possibly require modification and are therefore included in this study. However, experience has shown that high PmB considerably overfills these requirements, even of the CH-E type. The elastic recovery and softening point are, for example, typically much higher than required in Table 8. For these reasons, we believe that an additional PmB type with higher requirements is required to classify high PmB.

Requirements for CH-C and CH-E binder types					
Property	Test standard	Low polymer content (CH-C)		Medium polymer content (CH-E)	
		PmB 45/80-50	PmB 90/150-40	PmB 45/80-65	PmB 90/150-60
Penetration (0.1mm)	EN 1426	45-80	90-150	45-80	90-150
Softening point (°C)	EN 1427	≥50	≥40	≥65	≥60
Fraass breaking point (°C)	EN12593	≤-10	≤-20	≤-15	≤-20
Elastic recovery at 25°C (%)	EN 13398	≥50	≥50	≥80	≥80
Storage stability (°C)	EN13399	≤5	≤5	≤5	≤5
Mass change (m%)	EN 12607-1	≤0.5	≤0.8	≤0.5	≤0.8

Table 8: Swiss requirements of select classes of CH-C and CH-E type polymer-modified binders according to SN EN 14023-NA

The current European product standard EN 14023:2010 does not permit using DSR-based test methods for PmB classification. Therefore, softening point and elastic recovery are two methods that can be used for discriminating high PmB. For example, in select paving projects in Switzerland a binder with a softening point of above 80 °C and elastic recovery above 80% has been required. In Poland, a separate binder class has

been introduced for high PmB (PN-EN 14023:2011/Ap2:2020), requiring softening point above 80 °C and elastic recovery above 70 %. However, we consider that such requirements are not sufficient for reliably discriminating high PmB from conventional polymer-modified binders. In the updated EN 14023 standard, DSR-based methods and criteria that allow to reliably classify high PmB should be included.

The Performance Grading system (PG) used in the United States of America is more closely related to binder performance. Nevertheless, this system was primarily intended for characterization of unmodified binders. The high PG temperature parameter $G^*/\sin \delta$ has proven to be inadequate for PmB classification due to its nonlinear rheological behavior of PmB (D'Angelo et al., 2007; Southern, 2015).

In the absence of suitable methods for high PmB classification, road owners and asphalt producers are unable to reliably order a specific binder class¹³ and perform quality control. This leads to limited use of high PmB in road pavements.

With this research, we aim to develop means for classification of high PmBs in Europe. The simplest approach would be to increase the requirements for the currently used empirical tests. However, recognizing the potential problems with this approach, we also included two of the most promising methods for binder classification that employ the Dynamic Shear Rheometer (DSR): the Multiple Stress Creep Recovery (MSCR) test and the Binder Fast Characterization (BTSV) test. Both tests have been reported to effectively be able to characterize PmB (Alisov et al., 2020; Porot, Zhu, Wang, & Falchetto, 2022; Southern, 2015; Zeiada et al., 2022). Further, the methods are already standardized in Europe, allowing relatively quick uptake. In this research we also considered it important to evaluate the effect of long-term aging on high PmBs to determine if aging should be included as part of product specification. Finally, to better understand the fundamental mechanisms of polymer modification, we also performed the Gel Permeation Chromatography (GPC) test to study the molecular composition of the materials.

Ten binders were tested at unaged state, followed by aging and testing at an aged state. The research plan overview along with the test methods used is summarized in Figure 54.

Objective

Considering the limitations described in the introduction, the objective of the research is to propose test methods and test criteria for classification of highly polymer-modified binders (high PMBs).

¹³ The term "binder class" is used in this report according to the EN 14023. It is used as a synonym to the term "binder grade".

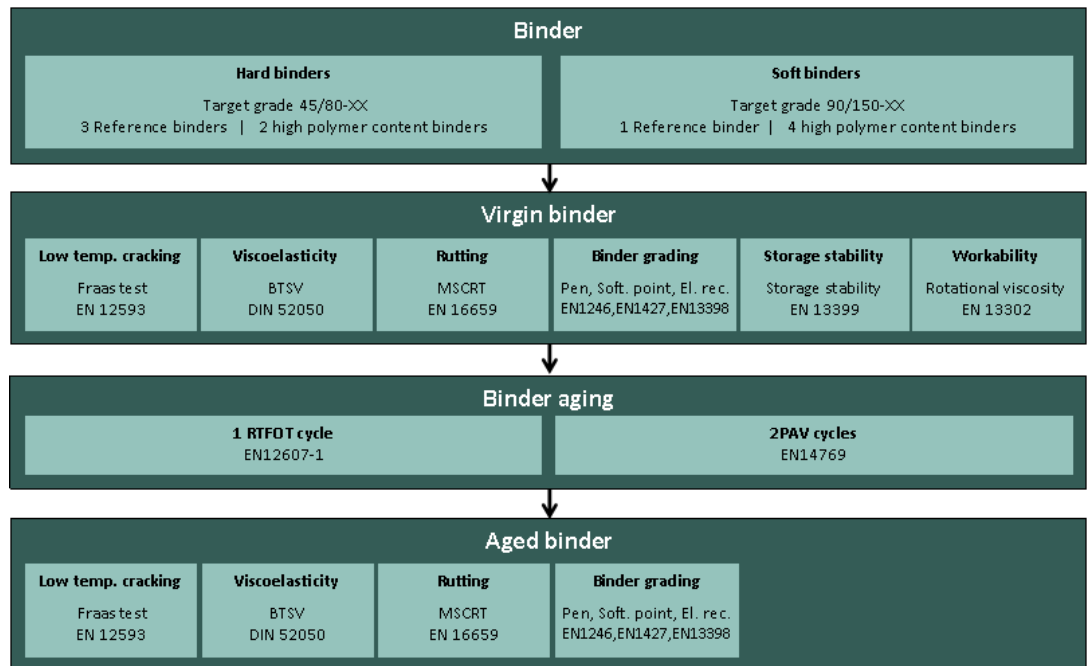


Figure 54: Research overview (the abbreviations used in the figure are presented in the methods section)

3.1 Materials

Table 9 summarizes the elastomer-modified binders analyzed in the research. The binders categorized as high PmB were delivered by four different companies. The table is structured primarily based on the binder's penetration values, which are divided into two main categories: "hard" and "soft," positioned at the top and bottom of the table, respectively.

The approximate polymer content in each binder was provided by the binder manufacturers and since the polymer content of each binder can vary between manufacturers and it was not always precisely disclosed, we roughly classified the binders using descriptors such as "high", "elevated", "medium," and "low". The category "high" corresponds to a polymer content of about 6 % or more, whereas the category "low" corresponds to approximately 2 % or less polymer. The categories "medium" and "elevated" are between these limits and can be linked to progressively increasing polymer contents. The last column of the table specifies whether each binder serves as a reference, i.e. if the results obtained from these materials are a benchmark representing binders with lower polymer content.

To ease the presentation of sample properties throughout the text and figures, the sample ID includes two letters next to the number of the sample: the first letter refers to the polymer content (L-Low; M-Medium; E-Elevated, H-High) while the second letter refers to the sample group (H-Hard, S-Soft).

Including a range of reference binders allows assessing what test methods are the most suitable for binder classification to discriminate high PmBs from those that have lower polymer content. At the same time, it has to be noted that the polymer content alone is not a sufficient classifier of the expected binder performance. The polymer type, base binder properties, and other additives included in the formulation are also important.

Table 9 also includes the manufacturer's declared binder class. Note that in the case of high PmBs, the test results are expected to significantly overfill the minimum softening point value required (the third number in the class name). It is also important to mention that the 10HS binder is classified as having lower penetration compared to the other soft binders but as later shown in the test results, it still corresponds to the same 90/150 penetration and therefore is considered in the same group of soft binders.

Binders used in the research				
Group	Sample ID	Polymer Content	Class (manufacturer declared)	Use in this research
Hard binders	1LH	Low (~2%)	45/80-50	Reference
	2MH	Medium (~3%)	45/80-65	Reference
	3EH	Elevated (~5%)	45/80-80	Reference
	4HH	High (>6%)	45/80-80	High PmB
	5HH	High (>6%)	45/80-80	High PmB
Soft binders	6MS	Medium (~3%)	90/150-65	Reference
	7HS	High (>6%)	90/150-80	High PmB
	8HS	High (>6%)	90/150-75	High PmB
	9HS	High (>6%)	90/130-80	High PmB
	10HS	High (>6%)	65/105-80	High PmB

Table 9: Binders used in the research and their characteristics

3.2 Penetration

The penetration results in Figure 55 show that all the binders in the unaged state fulfil the respective requirements for the binder classes PmB 45/80-80 and -85. The results also show that considerable aging has occurred during the RTFOT+2PAV cycle laboratory aging. After aging, the binder penetration is on par with the penetration that is typically found in binders extracted from reclaimed asphalt in Switzerland (Zaumanis, Poulidakos, Arraigada, et al., 2023a; Zaumanis, Poulidakos, Boesiger, et al., 2023b). Thus, the goal of simulating long-term aging has been achieved.

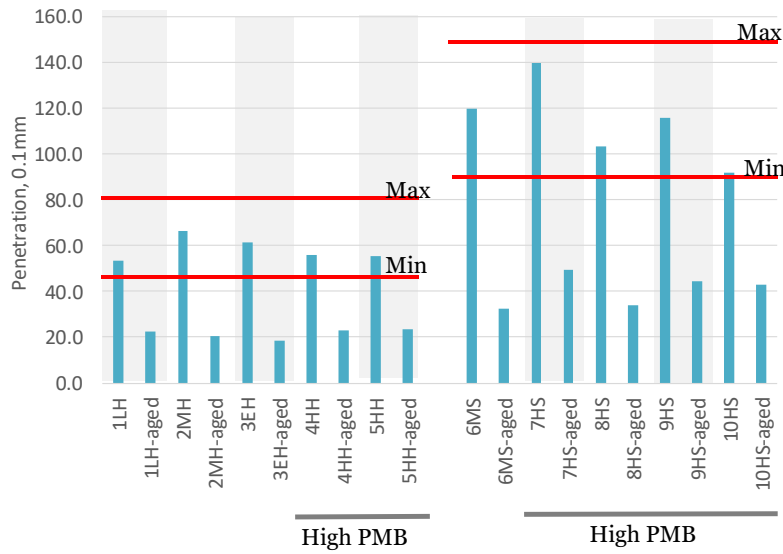


Figure 55: Penetration test results (hard binder – left side; soft binder – right side)

3.3 Softening point

The softening point results in Figure 56 demonstrate that in most cases aging caused the softening point to reduce. In two cases (1LH and 3EH), however, the softening point increased after aging. This demonstrates that the softening point result after aging is affected by a combination of two parameters: (1) the increase of base binder viscosity causing a softening point temperature increase and (2) the change in polymer matrix or polymer degradation causing a softening point temperature reduction. The average softening point reduction as a result of aging is higher for the soft binders compared to the hard binders. This can be explained by the fact that the polymer network (and hence – its degradation) plays a more pronounced role in softer binders.

The current Swiss requirements for medium PmB grade (CH-E) are included in Figure 56. The unaged high PmBs all surpass 85°C softening point temperature, which is the highest class that can be assigned to binders according to the daft European standard for polymer modified binders prEN 14023:2021 (in the current EN 14023 the highest requirement is 80 °C). However, the conventional PmB 6MS also passes this threshold indicating that the classification based on the softening point alone can lead to low polymer-content binders being mistaken for high PmB. Moreover, the softening point also does not discriminate between the binders 2MH and 3EH as well as between most of the unaged soft binders.

The problems of the softening point test to adequately characterize polymer-modified binders are well known (Southern, 2015). For these reasons, softening point is not recommended as a criterion for classification of high PmBs.

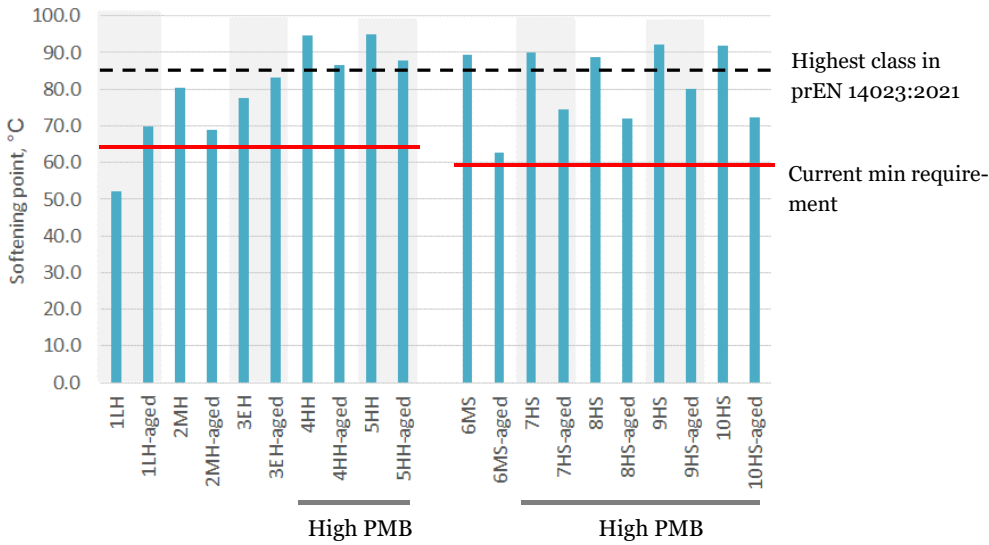


Figure 56: Softening point test results (hard binder – left side; soft binder – right side)

3.4 Elastic recovery

The elastic recovery results at 25 °C are summarized in Figure 57 and show that all the high PmBs have elastic recovery above 95 %. The conventional PmBs, except for the 1LH also have high elastic recovery, in all cases exceeding 90 % and even 95% for 6MS. These results demonstrate that it would be challenging to classify the high PmBs using elastic recovery since the results are very close to the maximum and the testing variability (repeatability defined as 4 % in EN 13398) would make it impossible to discriminate between the binders. For these reasons, the elastic recovery at 25 °C is not recommended as a classification test of high PmBs. A possible alternative would be to perform the test at 10°C where a more pronounced difference between the results depending on the polymer content might be evident.

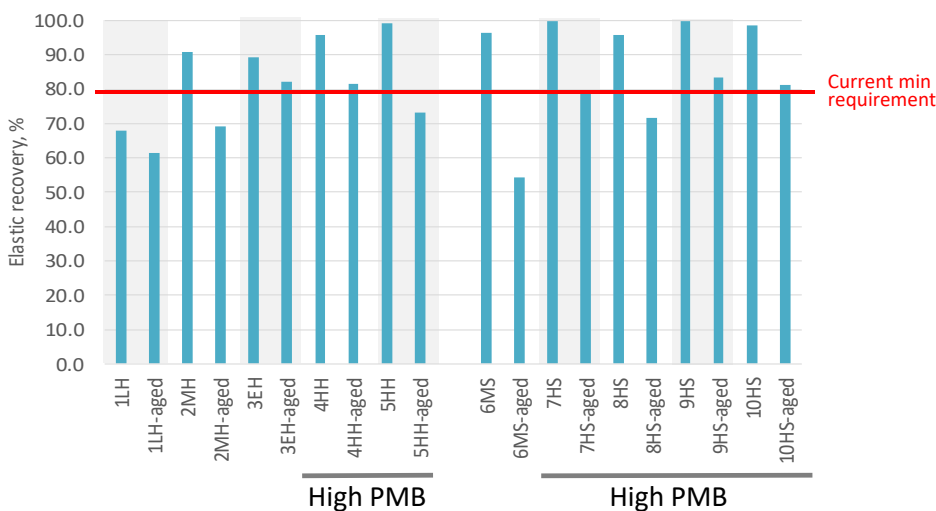


Figure 57: Elastic recovery test results (hard binder – left side; soft binder – right side)

3.5 Fraass breaking point

The Fraass breaking point test results are summarized in Figure 58 and show that the softer binder class, as expected, provides a lower breaking point temperature. Most of the unaged binders fulfil the respective maximum breaking point temperature requirement: -15°C for the hard binder class and -20 °C for the soft class. The individual results, however, are difficult to explain. In particular for the soft binders, aging has reduced the breaking point temperature. This is contrary to what is expected to take place in practice. These results confirm the widely accepted conclusion that the Fraass test is not suitable for characterization of polymer-modified binders.

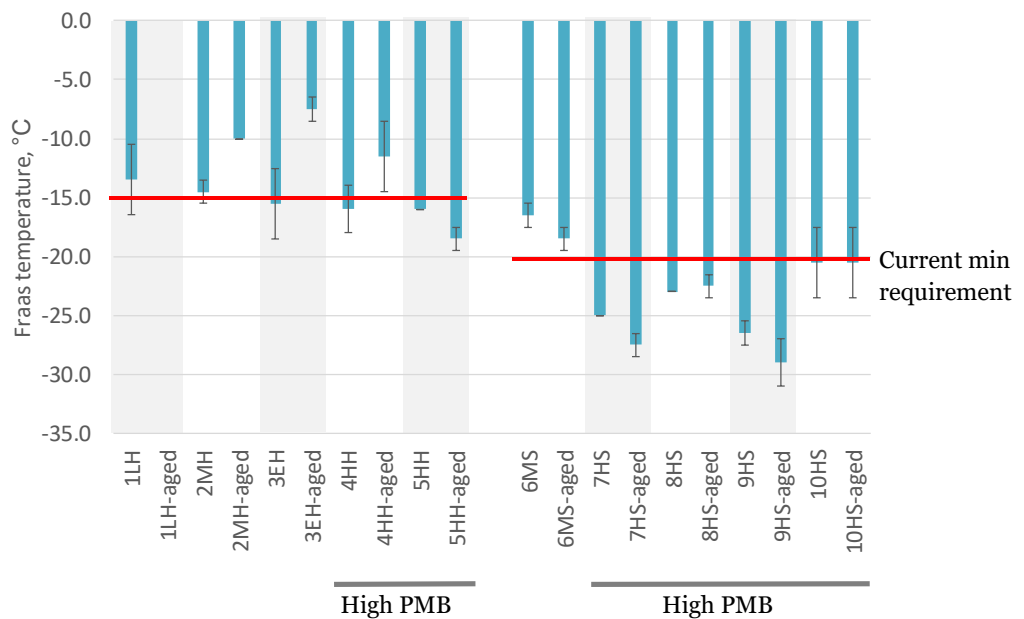


Figure 58: Fraass breaking point test results (hard binder – left side; soft binder – right side)

3.6 Storage stability

The storage stability results are summarized in Figure 59. The SN-EN-14023-E defines that the softening point difference between the upper and lower part of the tube should be no more than 5 °C. The results confirm that all the binders fulfil this requirement. This is an important observation since it demonstrates that even with a high polymer content the binder's storage stability can be ensured.

It must be noted that the storage stability is based on the changes in softening point and we do not recommend using the softening point test method for highly polymer-modified binder characterization. It is therefore suggested to develop criteria for storage stability testing using one of the suggested test methods: MSCR or BTSV.

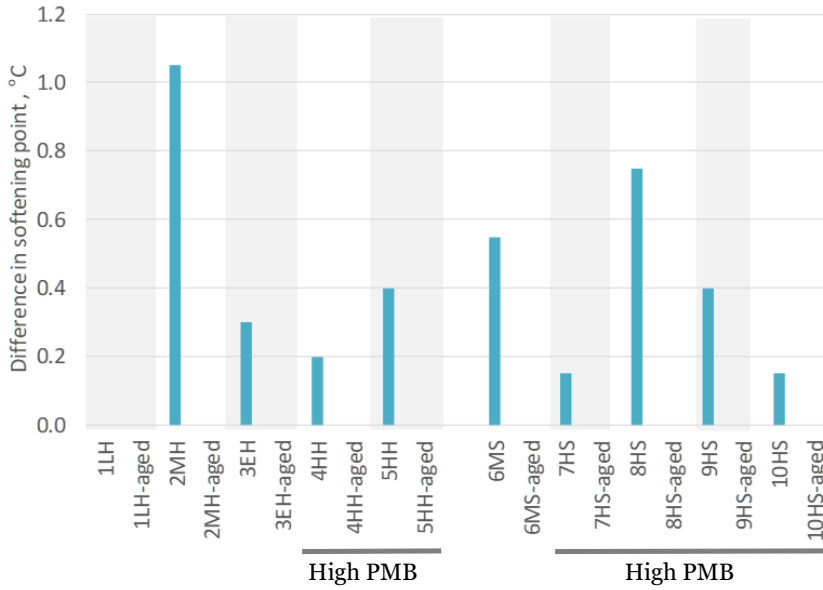


Figure 59: Storage stability test results (hard binder – left side; soft binder – right side)

3.7 Mass change

The mass change results, summarized in Figure 60, show that overall the binders experience a small mass change. The 9HS binder exhibits mass increase which is known to occur due to forming of oxidative products during the test (Roberts et al., 1996). The maximum permitted mass change is 0.5 % for the hard binder and 0.8 % for the soft binder (according to SN EN 14023 E). No particular trend related to the PMB content can be observed and therefore adherence to the limit of 0.5 % is proposed.

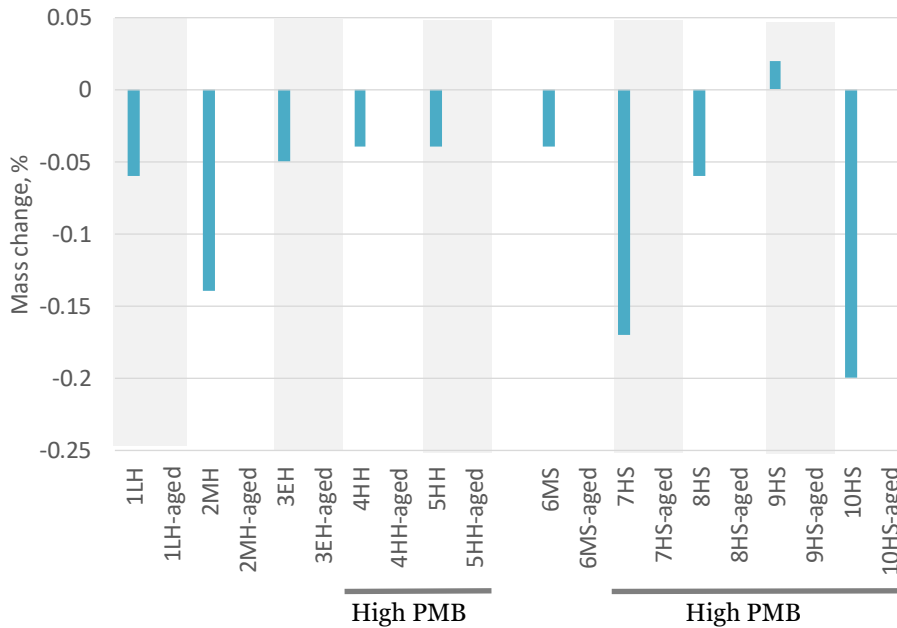


Figure 60: Mass change test results (hard binder – left side; soft binder – right side)

3.8 Rotational viscosity

The viscosity at production and paving temperatures is currently not provided as a classification parameter in the EN 14023. However, the high content of polymers in high PmB (the dominant polymer phase) can cause the asphalt to become unworkable at high temperatures. At the same time the temperature increase can not be used as means to improve workability, since above a certain limit (according to manufacturer's recommendations, typically around 190 °C) the polymer are damaged. Therefore, we have tested the rotational viscosity according to EN 13302 using rotational viscosimeter.

As an example, a shear sweep result of one binder (2MH) is provided in Figure 61. During the test, the shear rate was increased from 0 to 130 s⁻¹ within 15 minutes and then back to 0, again within 15 minutes. This was done to evaluate if the material exhibits a Newtonian-like behavior. It can be seen in Figure 61 that at 135°C the apparent viscosity is non-Newtonian while at 160 °C the binder exhibits Newtonian behavior. This pattern repeated for all the tested samples.

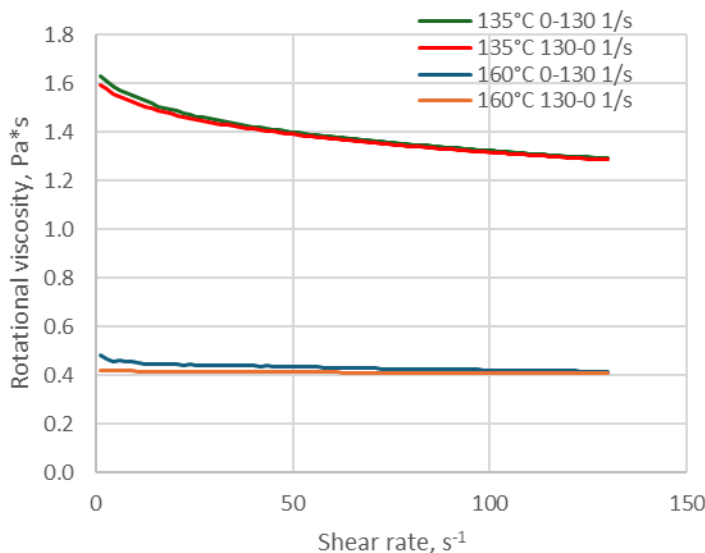


Figure 61: Shear sweep results for binder 2MH

The rotational viscosity results at 100 s⁻¹ are presented in Figure 62. As expected, the viscosity at 135 °C is significantly higher as compared to 160 °C but the difference between the soft (right side in the figure) and the hard binders (left side) is not notable. It can also be seen in Figure 62 that the high PmBs typically exhibit a higher viscosity compared to the binders with lower polymer content. This is true even though vinyl is typically used in high PmBs to improve workability (Porot et al., 2019b).

It is important to ensure acceptable binder viscosity at mixing and compaction temperatures and for this reason the USA standard AASTO M320 specifies that binders should have a viscosity ≤ 3Pa·s at 100 s⁻¹ and 135 °C test temperature. As can be seen, this requirement is ensured in all the tested cases. Until further data is gathered, this limit is recommended as a specification requirement also for high PmB.

Furthermore, since the viscosity at 135 °C exhibited non-Newtonian behavior due to the polymer presence, it is recommended to also test viscosity at 160 °C. This

temperature is typical for production and flowing of the binder is required. The proposed requirement of ≤ 1 Pa·s, similar to the requirement at 135 °C, classified all the tested binders as suitable for use.

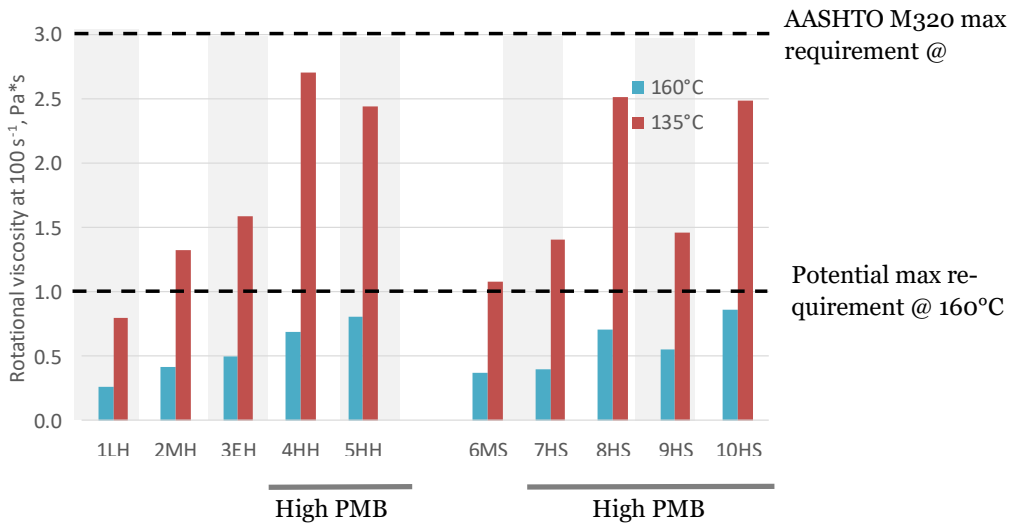


Figure 62: Rotational viscosity results at 100 s⁻¹

3.9 BTSV

The BTSV results in Figure 63 demonstrate that an increase in polymer content leads to a reduction of the BTSV phase angle while a harder base binder class increases the BTSV temperature. A general trend can be observed that with aging the BTSV temperature increases and the phase angle decreases. Similar observations have been found by other researchers (Alisov, 2017; A. Koyun et al., 2022).

Figure 63 demonstrates the preliminary limit values we propose for the BTSV phase angle and temperature for the high PmBs. The proposed limits are defined to group the high PmBs and discriminate the PmBs with lower polymer content. It can be seen that indeed at unaged state all the highly polymer modified binders fall within the dashed boxes while the PmBs with lower polymer contents are outside them.

Figure 63 also includes different non-polymer modified binders that are typical for the region and include penetration grades 10/20, 20/35, 35/50, 50/70, 70/100, and 100/150. These binders are either recovered from RAP, recovered from laboratory aged mixtures or binders that are aged using short (RTFOT) plus long-term (PAV) aging methods. Only aged, non-polymer modified binders are demonstrated in the figure since according to prior research, aging typically reduces the BTSV phase angle and increases the BTSV temperature. This shift in properties could potentially lead to misclassification of an aged non-polymer modified binder as polymer-modified binder. However, it can be seen in Figure 63 that none of the 22 tested non-polymer modified binders falls in the proposed high PmB boxes. At the same time, it has to be recognized that only select non-polymer modified binders are included in the chart and it may well be that in some cases aged binder properties can be similar to PmB when tested using BTSV. It also should be noted observed that using recycling agents often reduces the BTSV temperature of RAP binder without increasing the phase angle (Walther et al.,

2019). Therefore, it is possible that extremely hard rejuvenated RAP binders may be misclassified as PmB. Such binders are not presented in the figure.

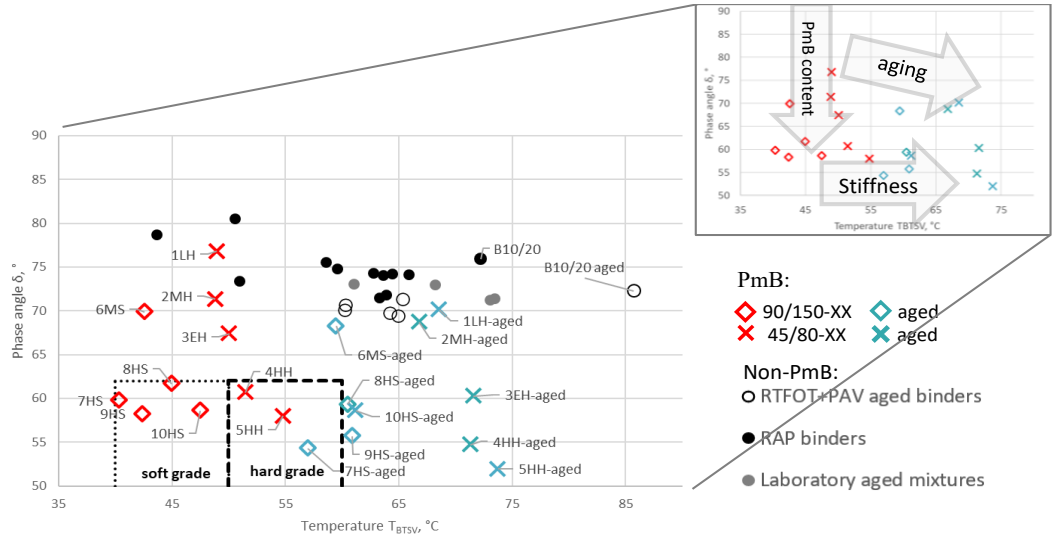


Figure 63: BTSV proposed classes for high PmB

After aging the highly modified binders shift to the right and down in the BTSV chart (see Figure 63). Based on this observation, criteria can be defined to discriminate binders that are prone to accelerated aging. To illustrate this clearly, Figure 64 demonstrates the increase in BTSV temperature and reduction in BTSV phase angle after plus 2 PAV cycles. The tested binders, including conventional PmB and high PmB demonstrate similar changes in phase angle and T_{BTSV} indicating that the aging resistance requirements could be the same for any polymer content. For this reason, the proposed preliminary criteria shown in the figure is defined to ensure that all of the tested binders pass it. Further testing of more PmB's is required to refine the threshold.

Requirements for evaluating resistance against short term aging using are also recommended. Since no testing after RTFOT was done in this research, we suggest adapting the German draft specifications which for polymer-modified binders recommend ≤ 8 °C increase in BTSV temperature and ≤ 6 ° decrease in BTSV phase angle.

The above observations demonstrate that the BTSV test is well suited for classification of the high PmBs. The reduction of phase angle is particularly important for discriminating between binders with various polymer contents. More binders, however, should be tested to refine the limit values.

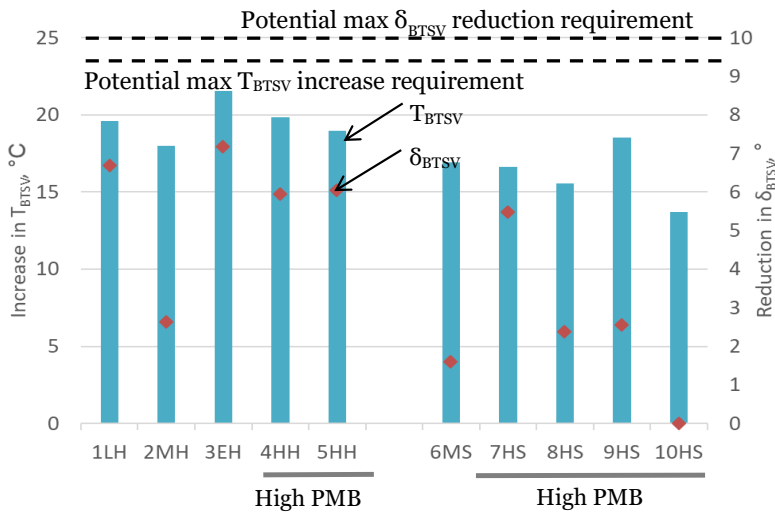


Figure 64: BSV aging resistance criteria for high PmB after and 2xPAV (hard binder – left side; soft binder – right side)

Typically, the BSV test is terminated after the complex shear modulus drops to 10 kPa. However, we performed the test to 1 kPa. This extension allowed observing the material behavior at higher temperature where the effect of the polymer network is progressively more pronounced compared to the effect of the base binder. An interesting preliminary observation was that at high temperature, the phase angle reduced below the BSV temperature, forming a "valley" as shown in Figure 65. This "valley" is related to the non-linear rheological behavior that is a key benefit of polymer modification, allowing binder to maintain elastic behavior also at high temperatures. It can be seen in Figure 65 that after aging the valley disappears, indicating reduced effect of the polymer network on the visco-elastic properties of the binder.

We consider that the "valley" created by the PmB might be a valuable indicator of the polymer effect on the binder performance. To quantify the depth of the "valley", the "delta phase angle" ($\Delta\delta_{BTSV}$) was calculated as shown in Equation (10). The temperature that corresponds to the delta phase angle was also determined as shown in Figure 65.

$$\Delta\delta_{BTSV} = \delta_{BTSV} - \delta_{min} \tag{10}$$

$\Delta\delta_{BTSV}$ – difference between the BSV phase angle at T_{BTSV} and the lowest post- T_{BTSV} phase angle, °

δ_{BTSV} – BSV phase angle, °

δ_{min} – the lowest BSV phase angle after the T_{BTSV} , °

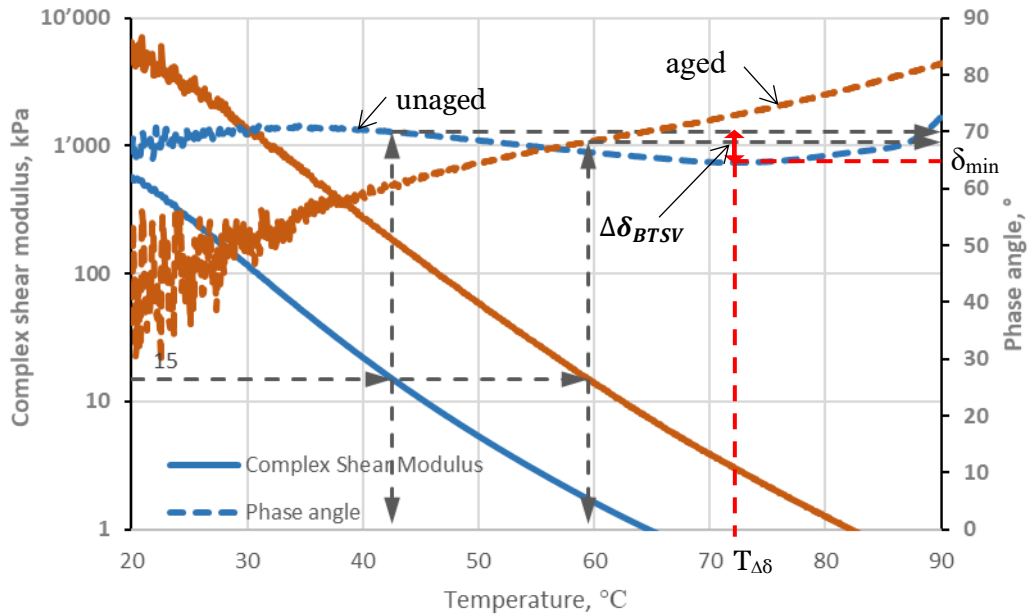


Figure 65: Determination of the $\Delta\delta_{BTSV}$ and temperature at the minimum phase angle

The delta phase angle of each binder and the corresponding temperature are summarized in Figure 66. For all the binders aging caused the phase angle "valley" to disappear similar to what is shown in Figure 65. Therefore, the delta phase angle of only unaged binders is shown in Figure 66.

Figure 66 shows that for the harder binder classes the high PmBs also have a higher delta phase angle (the 1LH binder with low polymer content did not have a delta phase angle even at unaged state). For the softer binders, however, two of them (8HS and 10HS) have a lower delta phase angle compared to the reference. Therefore, it can not be stated that the delta phase angle is directly related to the polymer content. Rather, the polymer type and the cross linking probably play a role in defining the delta phase angle. This is further explored later in section 3.12.3 along with the GPC results.

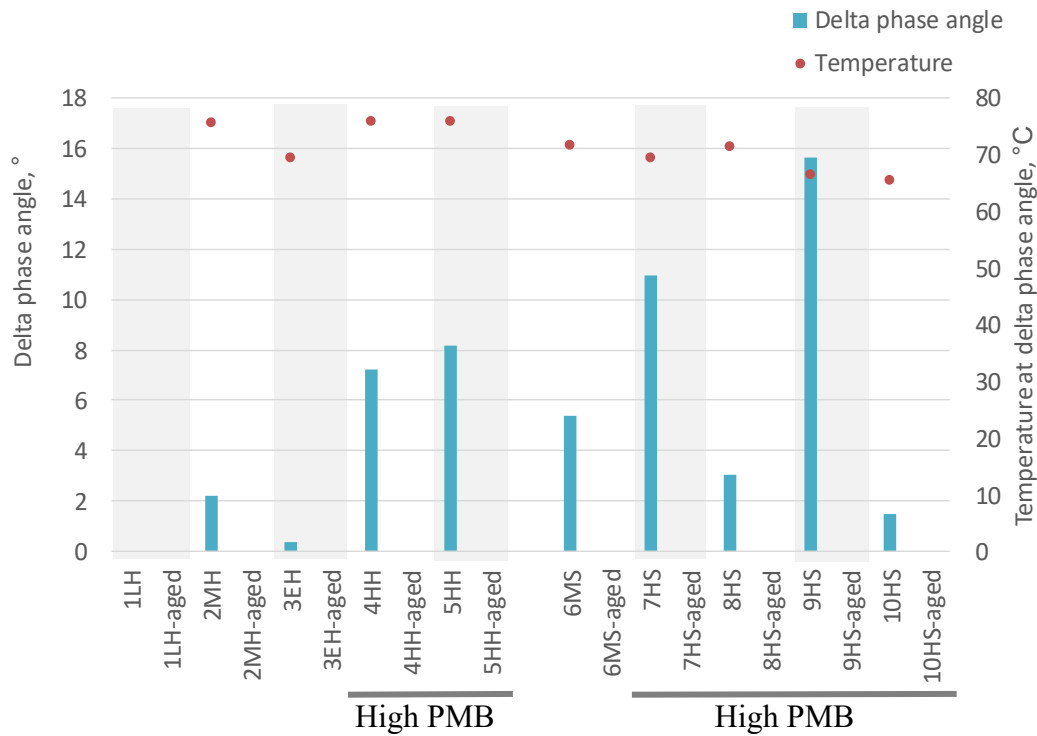


Figure 66: Delta phase angle and the corresponding BTSV temperature (hard binder – left side; soft binder – right side)

3.10 MSCR

The MSCR test results in Figure 67 demonstrate that all the unaged binders having high and elevated polymer-modified binder content have a small none-recoverable creep compliance ($J_{nr3.2kPa}$) and a high creep recovery ($\%R_{3.2kPa}$) at 64 °C and 3.2 kPa stress. The results are close to the top left corner and the small difference between the results does not reliably allow discriminating one material from another (the reproducibility according to EN 16659 is 12 % for recovery and 43 % for creep compliance). The PmB with low polymer content 1LH demonstrates results that are considerably far away from the rest of the results. This shows that at an unaged state, the 1LH has a considerably worse performance compared to the other binders, having a high creep compliance and almost no recovery. This was expected, considering that the test was performed at 64 °C while the softening point temperature of this binder is only 52 °C. In other words – the MSCR test results show that this binder is not suitable for use at 64 °C service temperature. The aging process increases the stiffness of the base binder, thus increasing the recovery and reducing the creep compliance, which is why after aging the 1LH binder results are more similar to the other binders.

Along with the PmBs, two recovered unmodified binders (50/70 & 10/20) are demonstrated in this and the following MSCR result figures. These unmodified binders serve to demonstrate if the MSCR test can discriminate between unmodified hard and/or RAP binders and the polymer-modified binders. It can be seen in the figures that a recovered 50/70 binder can be clearly discriminated. The unaged 10/20 binder has a low creep compliance. After RTFOT+2PAV aging, the 10/20 binder also has a relatively high recovery at different the test conditions that are reported in Figure 67 through

Figure 69. This shows that the MSCR alone cannot be used to clearly differentiate between different binder classes and another test (e.g. penetration test) is required as well.

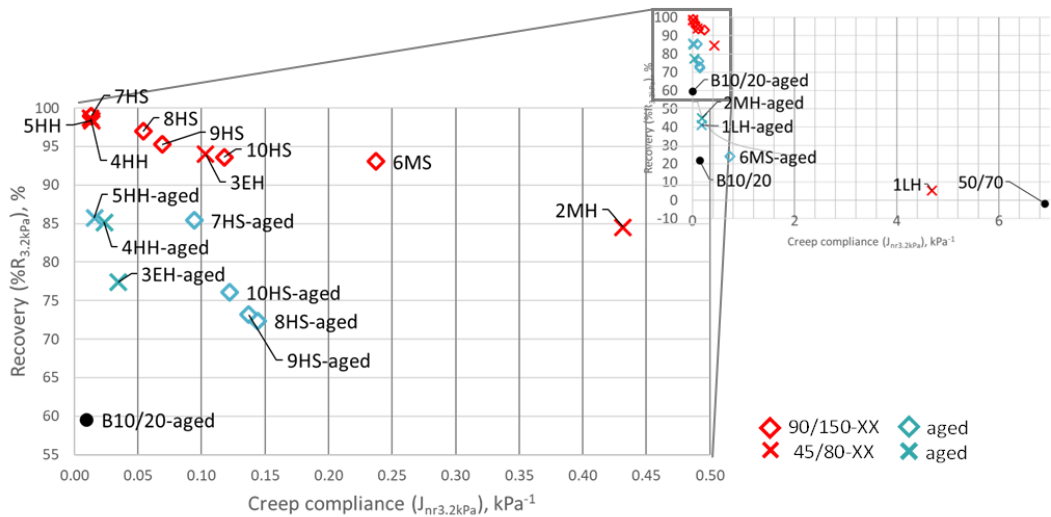


Figure 67: MSCR test result summary at 3.2 kPa and 64 °C

To induce a higher creep that would allow differentiating high PmB from binders with lower polymer content, an increased stress is necessary. The micromechanical modeling by Arshadi showed that at heavy traffic load binders on average exhibit 8.2 to 11.9 kPa stress (Arshadi, 2014). The research by Golalipour et al. therefore suggests using 10 kPa stress in the MSCR test (Golalipour et al., 2017)). This stress level is similar to what other researchers have suggested (Liu et al., 2020).

A different approach for inducing a higher creep and thus potentially discriminate the high PmB would be to increase the test temperature; however, this is not preferred since a high test temperature would not realistically simulate the expected in-service conditions for where the binders will be used.

The results of all binders at 10 kPa and 64 °C are summarized in Figure 68. For reference, the figure also includes a curve that is recommended by AASTHO TP 70 for discriminating elastomeric-modified binders (above the curve).

It can be seen in Figure 68 that for the hard binders all three high PmBs are grouped in the left top corner. The difference between the highly modified binders and the other hard binders (1LH, 2MH, and 3EH) is sufficient to allow clearly discriminating between the PmBs and creating a separate class for the high PmBs. This conclusion is supported by the observations of the RILEM PIM TG1 which concluded that among the evaluated methods (BTSV, softening point temperature, high temperature PG, $|G^*| / \sin\delta$) the MSCR test was able to best differentiate between polymer-modified binders (Porot, Zhu, Wang, Falchetto, et al., 2022).

The soft binders, however, have a lower recovery and higher creep compliance at these test conditions compared to testing at 3.2 kPa. The high PmBs 7HS and 9HS, for example, have a creep compliance of 6 kPa⁻¹ or more, which can be considered high. Such a high compliance would indicate that these binders are not suitable for use at 64 °C service temperature. Indeed, these soft binders are intended for high altitude in Switzerland where the pavement temperature would not reach 64 °C.

Moreover, the soft binder test results show a progressive reduction of recovery during the test. For example, for the binder 7HS the creep compliance in the first 10 kPa cycle was 0.25 kPa⁻¹ while in the tenth cycle it was 11.9 kPa⁻¹. It might therefore be useful to adapt a higher number of cycles to achieve a steady-state response throughout the test as, among others, recommended by Wang et al. (Wang et al., 2023) and Golalipour et al. (Golalipour et al., 2017). For example, the research by Golalipour (Golalipour et al., 2017) suggests applying 30 cycles and using only the last five for the analysis. To enable classifying the soft binders, the MSCR test was repeated at 10 kPa and 58 °C for the unaged soft binders and the results are summarized in Figure 69. It can be seen that the highly modified binders are grouped in the top left corner while the binder with medium polymer content (6MS) has a relatively higher creep compliance and lower recovery. This shows that at an adequate test temperature and at 10 kPa the MSCR test allows differentiating between high PmBs and binders with lower polymer content. On the contrary, at 3.2 kPa and 58 °C the soft PmB's all had >95 % recovery and <0.1 kPa⁻¹ creep compliance thus not allowing to differentiate between the different polymer contents.

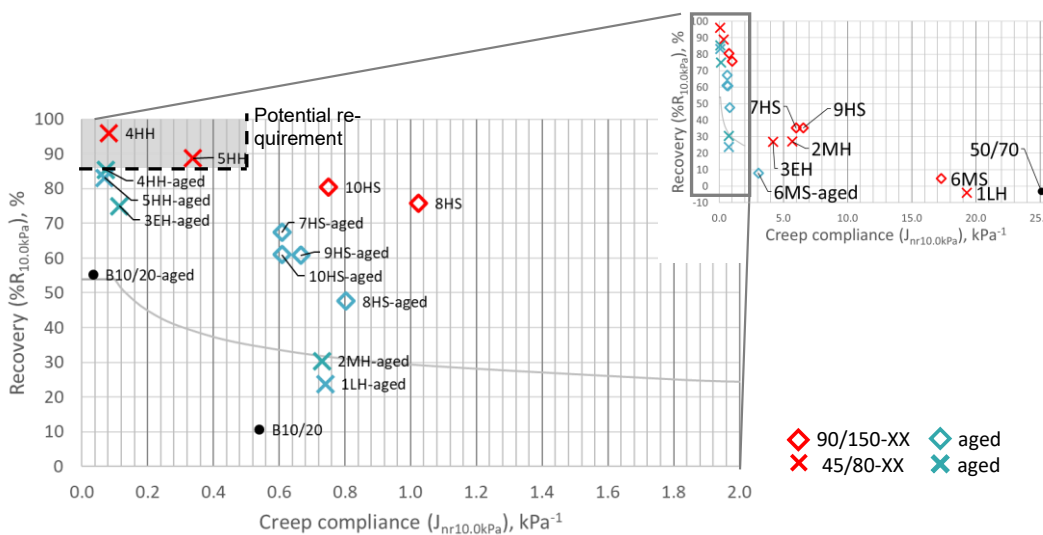


Figure 68: MSCR test results of all binders at 10 kPa and 64 °C test temperature

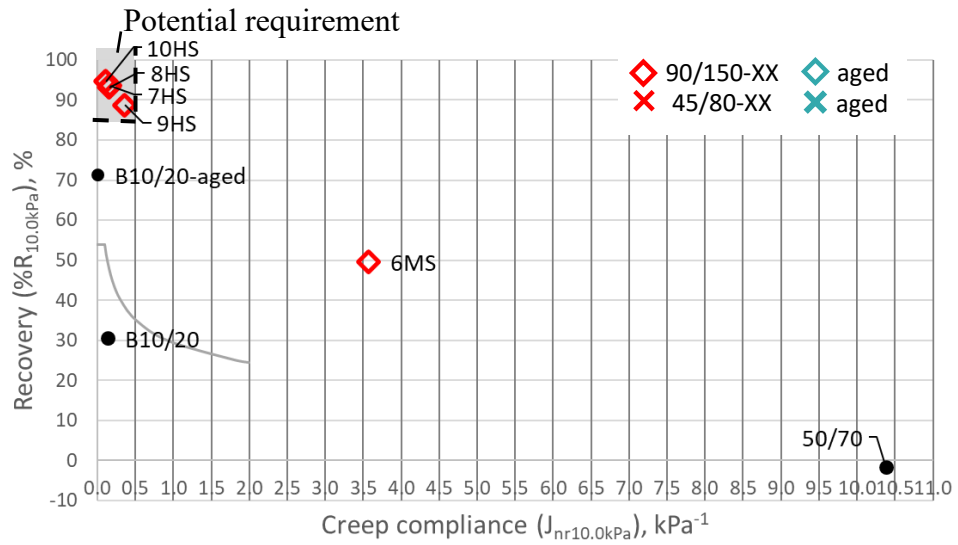


Figure 69: MSCR test results of unaged soft binders at 10 kPa and 58 °C test temperature

The aged polymer-modified binder results in Figure 68 and Figure 67 are shown using blue color and it can be seen that aging in most cases causes a drop in the recovery and increase in compliance, indicating a degradation of the polymer network. However, in the cases with high compliance at unaged state (e.g. 3EH), the results show the opposite trend: an increase in recovery and reduction in creep compliance. This suggests that in these cases aging of the base binder is the primal cause of the changes in MSCR test. The change in the relative performance after aging is similar to the softening point test where some binders exhibited increase while others – a decrease of the softening point temperature after aging. These assumptions are further elaborated in the context of the GPC results discussed in section 3.11.

3.11 Gel Permeation Chromatography

In Figure 70 a typical Gel Permeation Chromatography (GPC) chromatogram before and after aging is shown. In the figure, the time axis is proportional to the logarithm of the molecular mass. The largest peak derives from bitumen with a peak molecular mass (MP) around 1000 Dalton. On the left at lower retention time, two polymer peaks are visible with peak molecular masses of 260'000 and 140'000 Dalton respectively. Note that the molecular mass is only an approximation and would only be accurate if the polymer was made of pure polystyrene.

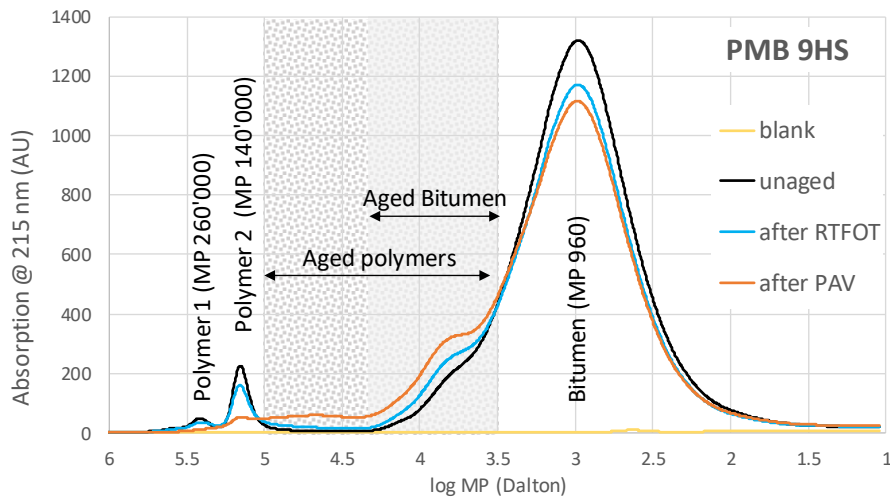


Figure 70: GPC chromatogram of 9HS at different aging states

The effect of aging can be observed both on the bitumen and on the polymers. The bitumen peak decreases with aging and forms a shoulder between log MP of 3.5 and 4.3. This region is attributed to newly formed asphaltene compounds, which are known to be the largest molecules in bitumen.

For the polymer peaks, the height of the peaks decreases with aging. In contrast to bitumen, the aging through PAV is much more severe compared to short-term aging in the RTFOT. After long-term aging, the peak of polymer 2 is only a fraction of its unaged state and polymer peak 1 has completely disappeared. Obviously, the double bonds in SBS have been attacked by oxidative species and cleaved, resulting in two or more smaller degraded polymers. This shows that the double bonds are split randomly resulting in a wide range of degraded polymer sizes, which are visible in the region between log MP of 3.5 and 5, overlapping with the asphaltene shoulder of the bitumen. The two observed aging mechanisms of bitumen and SBS results in non-uniform behavior of the softening point ring and ball or MSCR test. The aging of the base bitumen increases the binder stiffness, whereas the degradation of long chain polymers in smaller chunks lowers the binder viscosity. Depending on which aging mechanism dominates, the softening point ring and ball becomes higher or lower. The same is true for the MSCR results.

The 10 different PmB studied in this research show that a wide range of different SBS-like polymers have been used. They vary not only in molecular mass, but also in concentration and number of peaks (Figure 71). Apparently, in some PmB the same polymer type in varying concentration has been used. This observation shows that the proposed rheological binder test methods and criteria can successfully be used to characterize binders with different polymer types and different polymer concentrations.

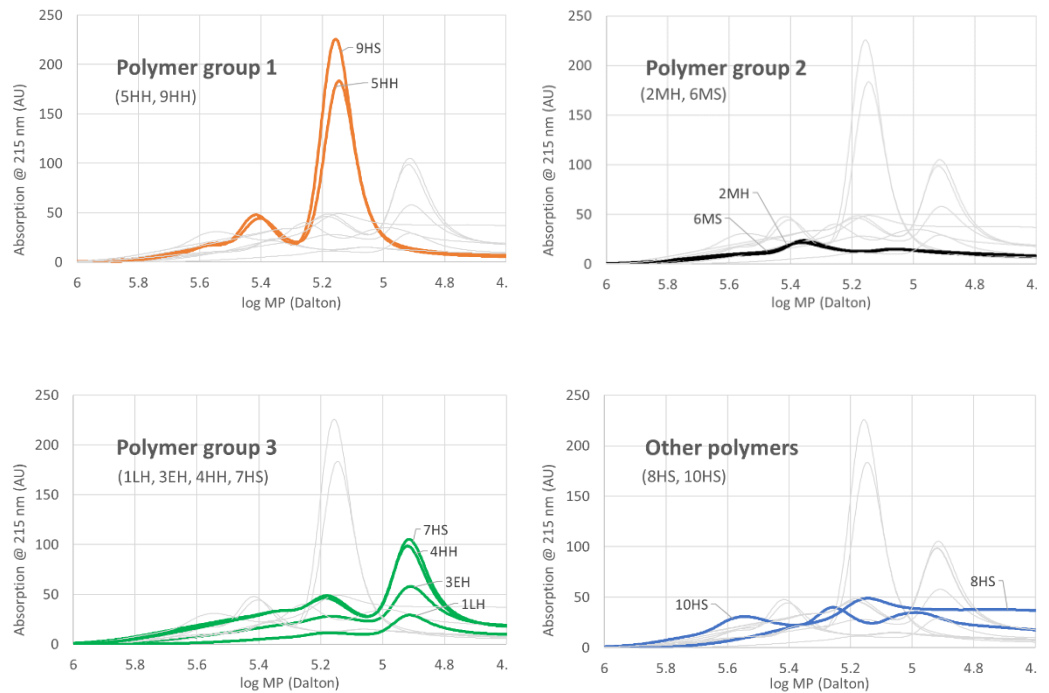


Figure 71: Overlay of polymer region in GPC chromatograms for similar polymer groups

3.12 Correlation between test results

In this section the correlations that provided the highest coefficient of determination (R^2) between the measured parameters are provided along with discussing the significance of these observations.

3.12.1 BTVS temperature versus penetration

The BTVS temperature versus log penetration results are presented in Figure 72. Similarly to the observation by Alisov (Alisov, 2017), a good exponential relationship ($R^2=0.93$) is found between both values.

Figure 72 also includes two shaded boxes that demonstrate the overlapping region of the proposed BTVS temperature requirements (as presented earlier in Figure 63) and the corresponding penetration requirements for the soft and the hard highly modified binders. It can be seen that the high PmB's are always within the boxes, meaning that both the BTVS and the penetration results would include the binders in the same class. This means that if BTVS test results are used for high PmB classification, the penetration test is partially redundant in this case. However, it has to be considered that, depending on the temperature susceptibility of the binders, the relationship may not hold true, especially for air rectified or waxy bitumen.

Of course, unmodified or non-high PmB's can also be located in the boxes, in this case the 6MS and 3EH binders. Testing of binder's elastic properties is necessary to discriminate these binders. If the BTVS limits indicated in Figure 63 would be implemented, these binders would not fall in the same class based on the phase angle criteria.

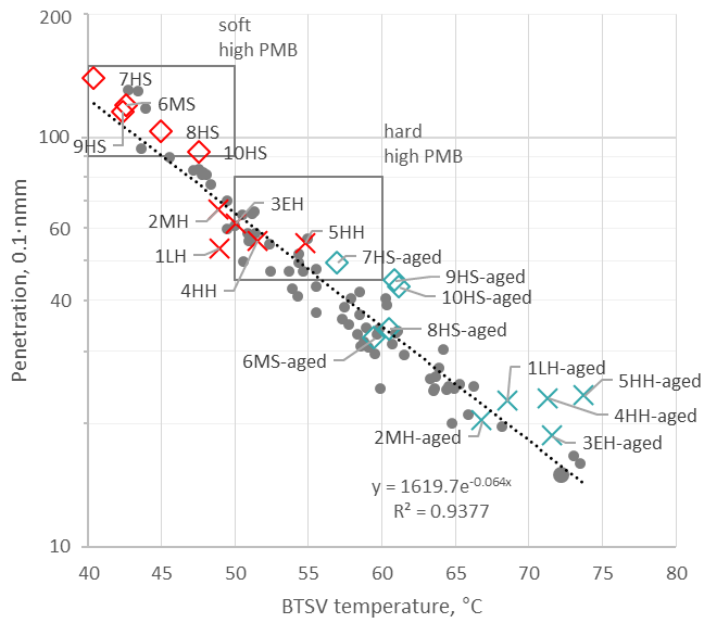


Figure 72: BTVS temperature versus log penetration

3.12.2 MSCR test recovery versus elastic recovery

The correlation between the elastic recovery and the MSCR test recovery at 10 kPa is shown in Figure 73. Note that the MSCR test recovery includes test results at the respective test temperature of each binder: 64 °C for the hard binders and 58 °C for the soft binders.

The correlation shows that both test methods classify the high PmB's close to 100 % recovery. However, only the MSCR test recovery allows clearly discriminating the unaged binders having lower polymer content. The reason for these differences seems to be the test temperature: elastic recovery test was performed at 25 °C irrespective of the binder class and at this temperature even binders with low, medium, and elevated polymer content have a relatively high elastic recovery of more than 65 %. When testing at the high service temperature (as in the case of MSCR test results), the effect of the polymer network is more pronounced. This allows making a better discrimination among the different binders.

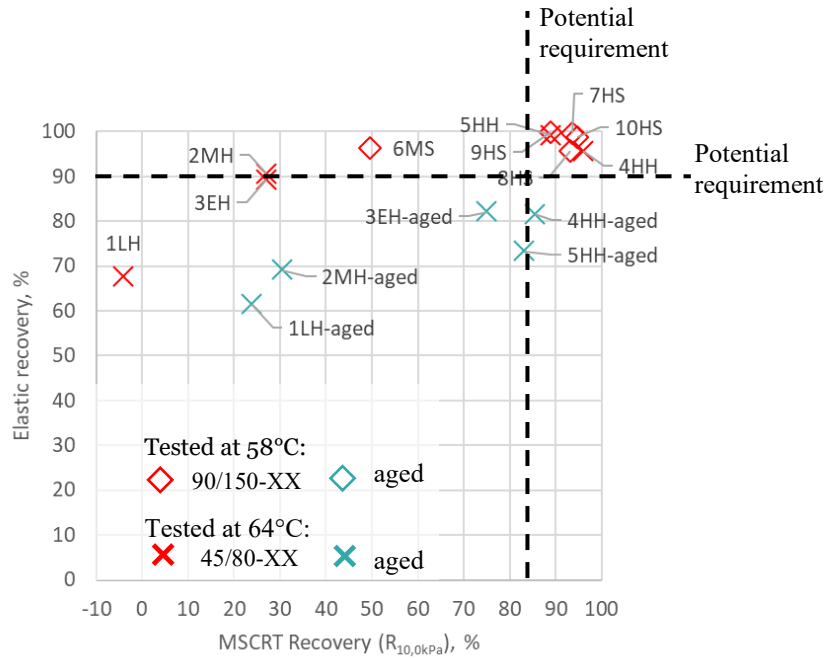


Figure 73: MSCRT test recovery and BTSV phase angle VS elastic recovery

3.12.3 GPC peak area versus BTSV delta phase angle

We expected a good correlation between the elastic recovery or the MSCRT test recovery and the amount of polymers in the binders, manifested by the area of the polymer peaks in the chromatograms. However, this was only true for the PmB containing the same polymer type 3 (see section 3.11). PmB produced with other polymer types resulted in high elastic recovery even though the polymer peak area was very low. Nevertheless, good correlation was found between the GPC polymer peak area and delta phase angle of BTSV for the different polymer types, which corresponds to the elastic benefit of using PmB at elevated temperatures (Figure 74). Only polymer type 2 binders fall outside the trend suggesting that the PmB are produced in a different way or that the polymers are of a different chemistry and therefore the peak area does not correlate with the delta phase angle.

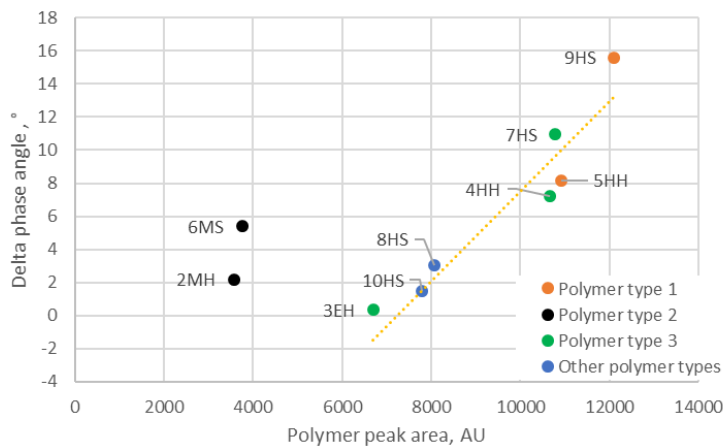


Figure 74: GPC polymer peak area VS delta phase angle of BTSV

3.13 Summary of the binder quality control standardization

This section presented the evaluation of test methods and development of preliminary acceptance criteria for classification of highly polymer modified binders (high PmBs). Two binder classes (defined as "soft" and "hard") with five samples in each class were used in the research including reference samples and high PmBs. Table 10 presents a comparison of the different test methods that were used in the study. For each test, the table holds the proposed criteria for high PmB classification (if any), the benefits and drawbacks of the methods, the test duration and comments based on observations from this research.

Comparison of the methods that could be used for High PmB classification

Test method	Proposed criteria for high PmB (hard & soft binder)	Benefits	Drawbacks	Approx. test time (incl. sample prep.)	Comments based on this research
Penetration	45-80 0.1mm 90-150 0.1mm	Simple and widely used method, the existing criteria can be adapted	Does not reflect the polymer effect	3 h	High correlation with BTSV temp for binders used in this research.
Softening point	Not recommended	Simple and widely used method	Unreliable for polymer-modified asphalt	2 h	-
Elastic recovery	Not recommended at 25 °C	Widely used method	Does not allow to differentiate between high PmB and binders with lower polymer content	5 h	Testing at 10 °C can be explored to classify high PmBs
Fraass temperature	Not recommended	Widely used method	Unreliable for polymer-modified asphalt	4 h	Other low temperature test methods should be explored
Rotational viscosity	≤ 3 Pa·s at 135 °C ≤ 1 Pa·s at 160 °C	DSR can be used Short test duration	Non-Newtonian behavior for PmB at 135 °C.	1 h	Further testing recommended to refine the criteria
Storage stability	$\leq 5^\circ\text{C}$	Widely used method, the existing criteria can be adopted	-	75 h	DSR-based criteria should be developed.
Mass change after RTFOT	$\leq 0.5\%$	Widely used method, the existing criteria can be adopted	-	4 h	-
BTSV	$\delta\text{BTSV} \leq 62^\circ$ & TBTSV 40-50 °C for soft binders. $\delta\text{BTSV} \leq 62^\circ$ & TBTSV 50-60 °C for hard binders.	Simple test execution Reliably discriminates high PmB's No need to define test temperature Aging results in a clear test result change (temperature increase)	The test result is defined at a temperature that is not representative of the high service temperature Some aged non-modified binders may have similar results to PmB.	3 h	Further testing recommended to refine the criteria Delta phase angle is a promising parameter for PmB characterization. Further research is recommended.

Test method	Proposed criteria for high PmB (hard & soft binder)	Benefits	Drawbacks	Approx. test time (incl. sample prep.)	Comments based on this research
Aging resistance using BTSV after RTFOT	Reduction in δ BTSV $\leq 6^\circ$ Increase in TBTSV $\leq 8^\circ\text{C}$	Widely adapted aging methods	-	4 h	The proposed criteria based on a German pre-norm.
Aging resistance using BTSV after RTFOT +2PAV cycles	Reduction in δ BTSV $\leq 10^\circ$ Increase in TBTSV $\leq 23^\circ\text{C}$	Widely adapted aging methods	Unrealistic simulation of chemical aging reported in the literature (Hofer et al., 2023; A. N. Koyun et al., 2021)	44 h	-
MSCR test	$\geq 85\%$ recovery $\leq 0.5\%$ kPa-1 Test @ 10 kPa stress Test temperature depending on climate (here 64°C for hard binders & 58°C for soft binders)	Testing at 10 kPa and appropriate temperature allowed clearly discriminating high PmBs from other binders	Unrepresentative test temperature will not allow discriminating high PmB's In countries without climatic zoning maps, it is challenging to define the test temperature.	1 h	Unaged binders were tested; testing of aged binder can be considered Standardization of testing at 10 kPa necessary Extension to 30 cycles per stress would improve repeatability
GPC	Not recommended	Qualitative information on aging	Virgin binder is needed as a reference	5 h	-

Table 10: Comparison of the different binder test methods that might be used for high PmB classification

Figure 75 summarizes the test temperatures of high PmBs for each method that was used in this research. Based on the results of this research, the test methods that are suitable for high PmB classification are shown above the horizontal axis and the methods below the axis are not recommended.

It can be seen in Figure 75 that while penetration could still be used, it would be highly beneficial to develop DSR-based test methods for temperature range below 40 °C. Polymer-modified binder properties are highly non-linear at different temperatures and therefore to achieve the desired performance, it is important to determine the viscoelastic binder properties also at intermediate and/or low temperatures. Using a DSR-based test method would ensure that all the tests can be done using the same device.

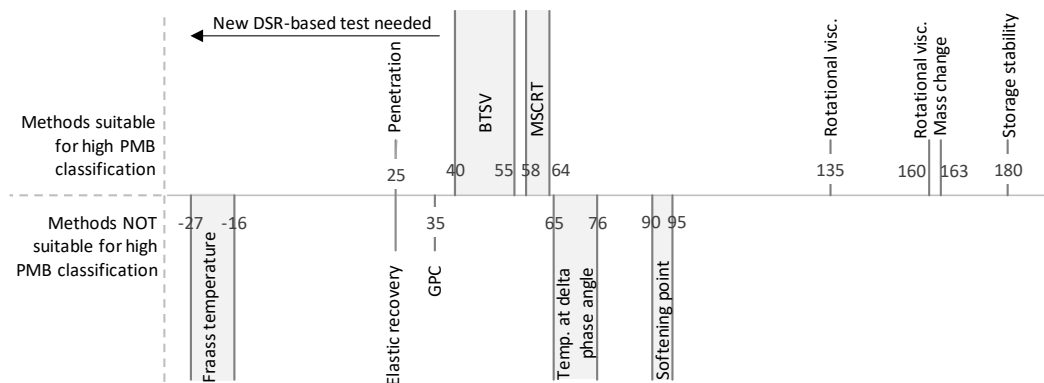


Figure 75: The test temperature of the various methods based on the results of this research for highly polymer-modified binders. Suggested methods for European specifications are shown above the line.

3.14 Conclusions

The following conclusions are drawn from the study:

- The BTSV test method successfully discriminates binders based on the polymer content. Acceptance criteria were proposed for the soft and hard binders as shown in Table 10.
- The applied aging protocol (RTFOT+2PAV cycles) successfully simulated the aging state of typical binders found in reclaimed asphalt in Switzerland. This aging state is therefore proposed to screen binders that are prone to accelerated long-term aging, whereas the proposed BTSV criteria are summarized in Table 10. In addition, short-term aging resistance should be determined by testing BTSV after RTFOT.
- An extension of the BTSV test to 1 kPa was proposed to enable calculating the "delta phase angle". This parameter characterizes the effect of polymer network at high temperature, and it correlated well with the GPC results of most binders. Gathering more data with this parameter might provide new insights.
- The MSCR test stress of 3.2 kPa was too low to differentiate between the different polymer contents. Increasing the stress to 10 kPa and testing at an appropriate temperature (64 °C for hard binders; 58 °C for soft binders) allowed to clearly classify the binders. The proposed acceptance criteria for highly modified binders are shown in Table 10. The test temperature selection, however, remains a challenge especially in countries that do not have clear temperature zoning.

- The penetration test could serve its current purpose also for determining the hardness of high PmB's. However, the results are often redundant with the BTVS temperature. Therefore, it is suggested to replace it with a DSR-based test that provides more information about the visco-elastic properties in the intermediate and/or low temperature range.
- Testing of rotational viscosity is proposed to ensure a workable binder. Preliminary criteria for testing at 135°C and 160 °C are summarized in Table 10.
- Softening point temperature did not offer reliable means to classify high PmBs depending on the polymer content and depending on the sample, aging resulted in both reduction and increase of the softening point temperature. For these reasons, the method is not recommended for high PmB classification.
- The elastic recovery test at 25°C in most cases did not allow to differentiate between the binders with different polymer contents since the results were close to or above 90 %.
- The Fraass breaking point test resulted in unexpected trends - many binders improved low temperature cracking resistance after aging and three of the binders did not fulfill the current breaking point temperature requirements. For these reasons, the test method is not recommended for classification of high PmBs.
- The existing storage stability requirement of $\leq 5^\circ\text{C}$ was fulfilled for all the binders, demonstrating that even for high PmBs the requirement can be ensured. However, the storage stability is currently measured using penetration or softening point. Since these methods are not recommended for high PmBs, new criteria for storage stability should be considered, possibly using a DSR-based test.
- All the binders exhibited a small mass change after aging. The adaptation of the existing ≤ 0.5 % maximum mass change requirement is therefore recommended.
- The peak area in GPC is correlated to the amount of polymer used in the binder, as long as the polymer was identical. Otherwise, the peak area of different polymer types gives no information neither about the polymer content nor the mechanical performance.
- The GPC proved a useful means for research, but it is not suitable for binder classification because the polymer peak area and molecular mass depends on the polymer type and thus cannot be universally applied to any type of binder.
- Further research is recommended to verify the proposed criteria and establish classification criteria for other base binder types.
- It is recommended to develop a low and intermediate temperature binder test method using DSR. Some methods are already in development and could be considered, including Shear-Relaxation (SRV) test and others.

4 Construction and monitoring of test sections

4.1 AC B 22 S test section H19 Oberalpstrasse, Tamins - Val Maliens, Graubünden

AC B 22 S asphalt was paved as a binder course in the test site on H19 Oberalpstrasse Tamins – Val Maliens on 16.08.2023. This jobsite was selected due to the high traffic intensity. Two mixtures were paved: (1) 40% RAP content mixture with added soft highly-polymer modified binder; (2) 0% RAP mixture with hard highly polymer-modified binder. The 40 % RAP mixture allowed to evaluate the advantages of using high PmB for compensating the lack of polymers in RAP and the 0 % RAP mixture allowed to evaluate the benefits of using high PmB for increasing the performance and longevity of asphalt as well as to evaluate the potential reduction of layer thickness (discussed in section 5).

Objective

The objective of the test section on the Tamins – Val Maliens was to determine the potential to improve binder-course mixture performance through the use of high PMB and to evaluate the potential benefits of using high PMB in polymer-modified mixtures with high RAP content.

4.1.1 Mixtures and test section location

The test site is located on H19 Oberalpstrasse Tamins – Val Maliens (km 1.316-1.532) at approximately 790 m above the sea level. Only the right lane in the direction from Tamins to Trin (mountain side) was used in the research since it has no disturbances below the asphalt. The traffic intensity is classified as T 5 with DTV 11,000.

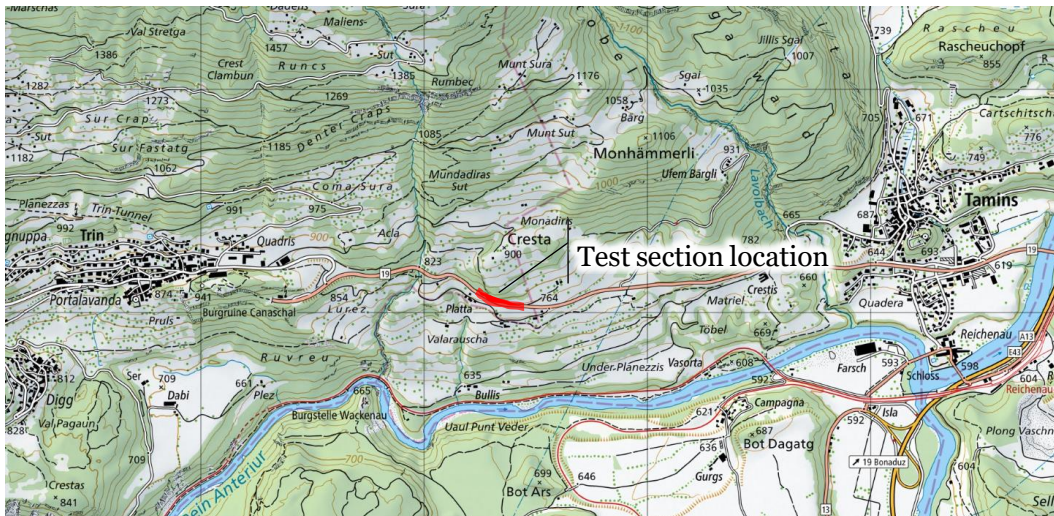


Figure 76: Location of the AC B 22 S test section, H19 Oberalpstrasse, Tamins - Val Maliens, Graubünden

The normal profile of the jobsite is shown in Figure 77 and the layer thicknesses are shown in Figure 78. Only the 7 cm thick AC B layer (Binderschicht) was used in the research. The two recipes were used for the AC B layer are summarized in Table 11. The reason for using these mixtures can be summarized as follows:

- The RAP Mix mixture was constructed with 40% RAP content (size 0/22 mm) and a soft highly polymer-modified binder. 40 % RAP content is typically used in this asphalt type and it is assumed that the RAP has no polymers (or they do not contribute to the elastic properties of the binder). Considering this, the polymer content in the final mixture is lower compared to the initial polymer content in the added binder. Therefore, it was evaluated if using high polymer content can still allow to achieve performance that would be equivalent to a mixture with PmB 45/80-65 CH-E binder as the target grade even when using 40 % RAP content. For these reasons in this report the target grade is defined as PmB 45/80-65 CH-E. In other words, this mixture allows evaluating the advantages of using highly polymer modified binders to compensate for the lack of polymers in RAP.
- For the HPMix no RAP was added and therefore the target grade is equivalent to the added binder grade. This is not a typical mixture, due to not using any RAP. This fact also means that the manufacturer did not have the mixture recipe and hence it is not fully optimized. Using no RAP in the mixture serves to evaluate the potential advantages of the high polymer content in terms of mixture performance and pavement design. It is not the recommendation of the authors to stop asphalt recycling. RAP use is part of a complex issue and should be evaluated in the context of sustainability, pavement life cycle and costs. Such an evaluation was not part of this project.

The added binders are from the same manufacturer that provided binders for the binder research described in section 0. In section 0 these binders had the ID 7HS (soft binder) and 4HH (hard binder).

Asphalt was produced by Catram AG at the production facility in Kieswerkstrasse 4, 7204 Untervaz. This location is approximately 15 minutes from the jobsite.

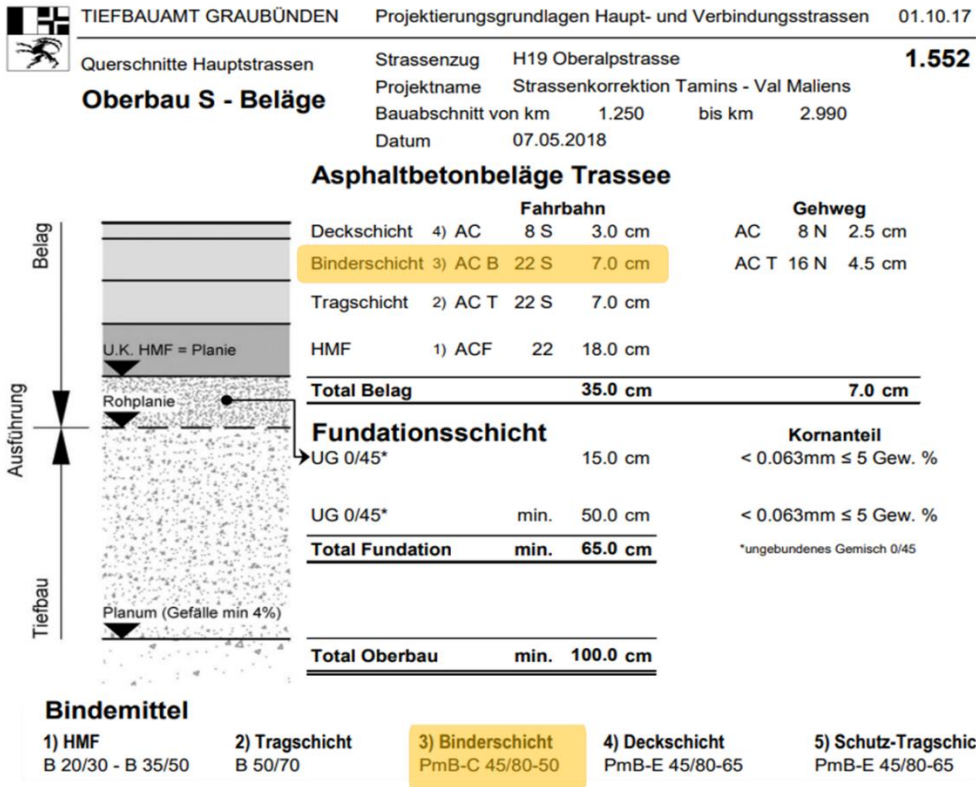


Figure 78: Layer thicknesses of the Tamins – Val Maliens test section (highlighted – the layer used in this research)

Images from the construction of the test section are shown in Figure 79.



Figure 79: Construction of the AC T 22 S pavement in Tamins – Val Maliens test section

4.1.2 Methodology

Asphalt mixture samples were collected from the production plant and road cores were gathered soon after construction. The following methods were used to evaluate the performance of the collected samples:

- The plant-produced samples were used for binder recovery as well as for testing the mixture using the following methods: aggregate gradation, Marshall test, Wheel tracking test, Semi Circular Bend (SCB) test, IDEAL-CT, Low temperature cracking test (TSRST), stiffness modulus test, and fatigue tests using two point prismatic specimen, and fatigue testing using vehicle load simulator (MMLS3).
- The recovered binder was tested using penetration, softening point, elastic recovery, Fraas breaking point, BTSV, MSCRT, and DSR frequency sweep.

Description of each method is provided in section 2.

4.1.3 Conventional binder tests

The penetration results of the binder recovered from the AC T 22 S test section mixtures are summarized in Figure 80. For comparison, the figure also contains the binder test results of this same binder grade that were presented earlier in section 0.

It can be seen that the binder recovered from the test section mixtures has a lower penetration compared to the virgin binders. This is expected due to the aging that takes place during construction. Overall, it can be seen that both test section binders have a similar penetration and it is within the expected range, considering the binder grade. Since the RAPmix contains 40 % RAP, it can be concluded that the binder has been sufficiently softened through the addition of the soft highly polymer modified binder.

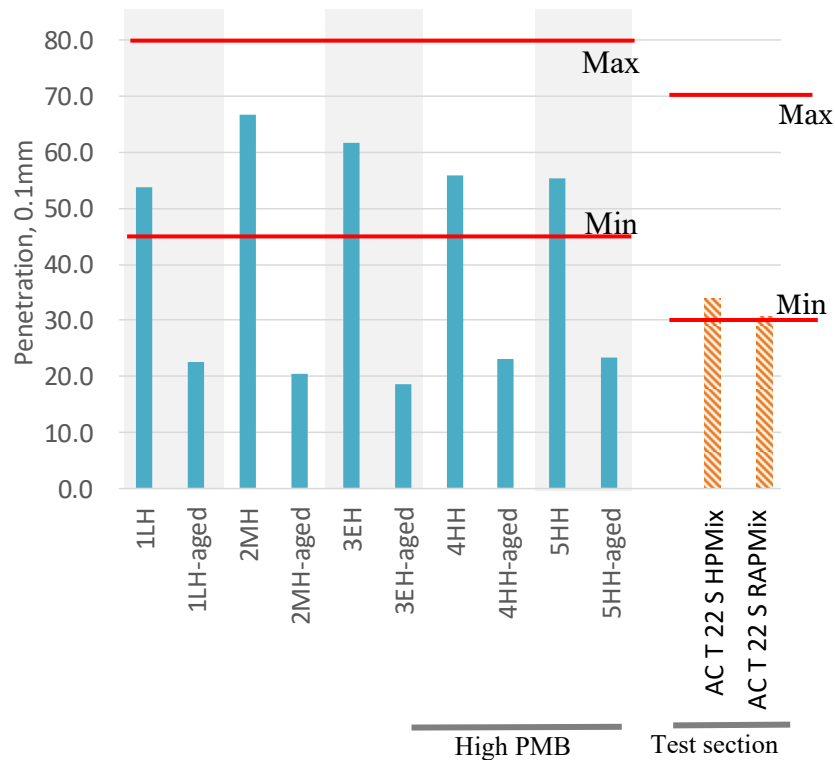


Figure 80: AC T 22 S penetration test results. The demonstrated minimum and maximum requirements are based on the VSS 40 430 standard for the PmB 45/80-65 (CH-E) bitumen. Blue bars are virgin and virgin aged binders, while test section results are shown with orange bars. The minimum requirements are based on SN-670210b-NA_EN-14023-E for the virgin unaged binders and based on VSS-40430 for the recovered binders.

The softening point results are shown in Figure 81 and for comparison, the virgin binder results from section 0 are also included in the figure. Overall, it can be seen that the results are within the expected range and that the HPMix binder has a slightly higher softening point compared to the RAPMix mixture. It should be noted that both mixtures exceed the softening point requirement that is currently imposed on recovered binder for the grade PmB 45/80-65 (CH-E) of minimum 60 °C, showing that the use of highly polymer modified binder can ensure the correspondence to the current requirements for polymer modified mixtures even when 40 % RAP is used. This demonstrates an advantage of using highly polymer modified binder since currently in Canton GR, the requirements for binder grade PmB 45/80-65 (CH-E) require the minimum softening point of 60 °C and this is ensured as well by the 40 % RAP mixture. At the same time, as discussed in section 0, softening point results should not be considered a reliable indicator of the binder performance for highly polymer-modified mixtures.

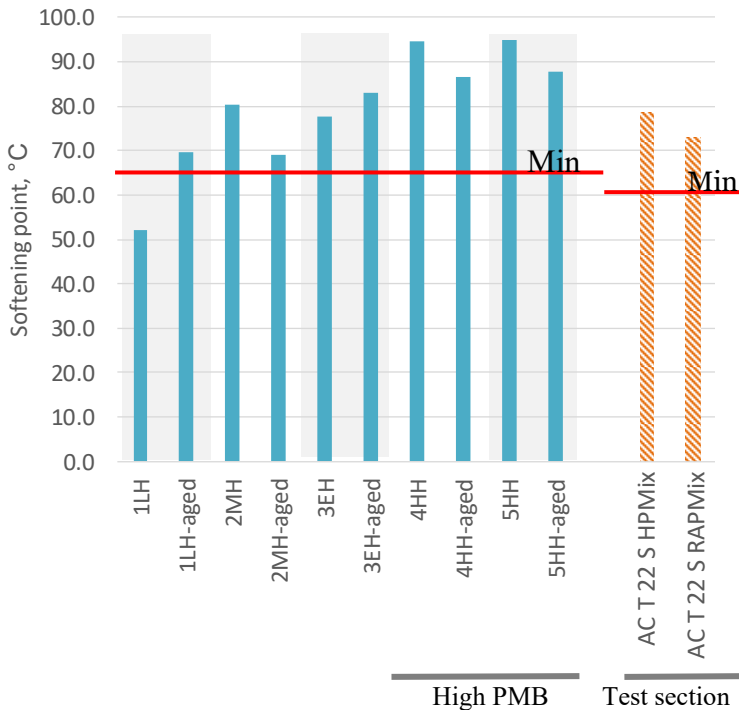


Figure 81: ACT 22 S softening point test results. The demonstrated minimum requirements are based on the VSS 40 430 standard for the PmB 45/80-65 (CH-E) bitumen. Blue bars are virgin and virgin aged binders, while test section results are shown with orange bars. The minimum requirements are based on SN-670210b-NA_EN-14023-E for the virgin unaged binders and based on VSS-40430 for the recovered binders.

The elastic recovery test results are summarized in Figure 82. For comparison, the figure also includes the elastic recovery results of the same grade of the virgin binders (discussed in section 0). It can be seen in the results that the elastic recovery remains high for the binders recovered from the test section mixtures despite the additional aging during production and construction. The elastic recovery of the HPMix binder is by approximately 10 % higher compared to the RAPMix mixture. This is likely the result of the 40 % RAP addition in the RAPMix mixture. At the same time, it has to be noted that even with the 40 % RAP content, the elastic recovery remains high and

significantly exceeds the minimum requirement for the PmB 45/80-65 (CH-E) grade as defined in the VSS 40430 standard.

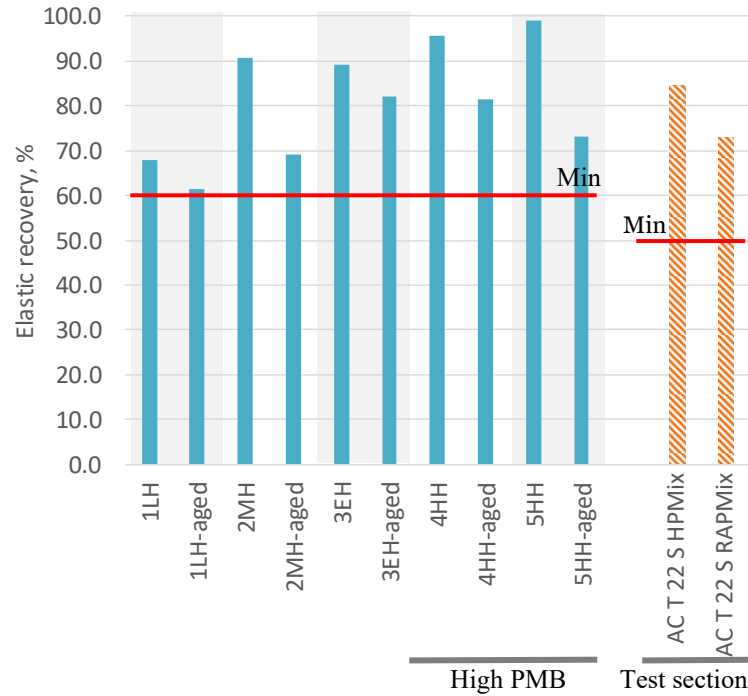


Figure 82: ACT 22 S elastic recovery test results. The demonstrated minimum requirements are based on the VSS 40 430 standard for the PmB 45/80-65 (CH-E) bitumen. Blue bars are virgin and virgin aged binders, while test section results are shown with orange bars. The minimum requirements are based on SN-670210b-NA_EN-14023-E for the virgin unaged binders and based on VSS-40430 for the recovered binders.

Figure 83 summarizes the Fraas breaking point test results of the AC T 22 mixtures as well as presents the virgin binder test results from section 0. As discussed in section 0, the test is considered unsuitable for evaluation of PmB cracking resistance and therefore the results in this figure are presented for information purposes since there is a current norm requirement for using this test.

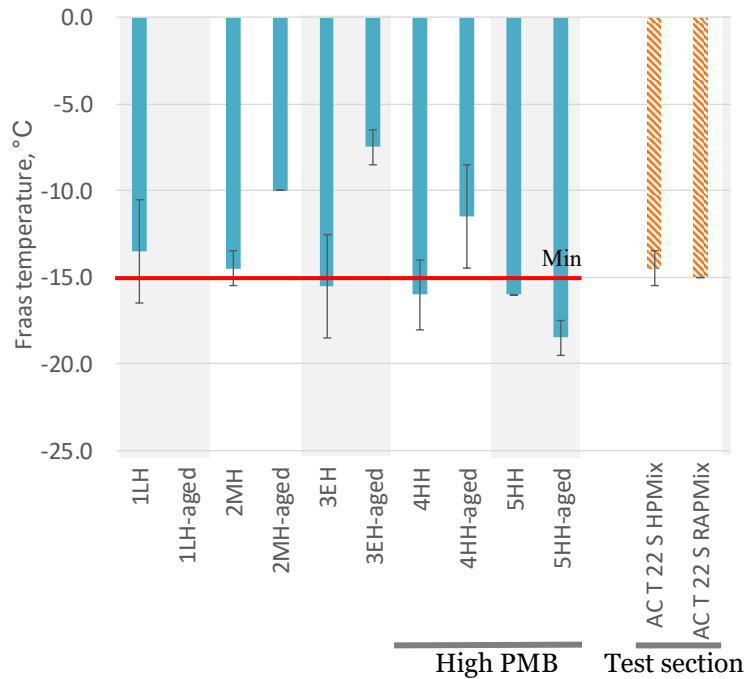


Figure 83: AC T 22 S Fraass breaking point test results. Blue bars are virgin and virgin aged binders, while test section results are shown with orange bars. The minimum requirements are based on SN-670210b-NA_EN-14023-E for the virgin unaged binders.

As can be seen from the conventional binder test results, the VSS 40430 requirements for recovered PmB 45/80-65 (CH-E) binder were fulfilled using 40 % RAP content. For the softening point and elastic recovery the minimum requirements were significantly exceeded while for the penetration the result was close to the minimum requirement of 30 dmm. This indicates that further optimization of the mixture could allow to even increase the RAP content above 40 % while still fulfilling the PmB 45/80-65 (CH-E) requirements for recovered binder. This could be achieved by, for example, adding a recycling agent to increase the penetration without significantly lowering the softening point temperature and elastic recovery. For example, in another research project conducted by Empa (Zaumanis, Poulidakos, Boesiger, et al., 2023a) and in the canton of Zurich, 60% RAP is used with high PMB, while still meeting conventional binder testing requirements. At the same time, it should be considered that the conventional tests might not provide sufficient evidence about the binder performance. Further information about using high PmB in mixtures with high RAP content is provided in the research project (Zaumanis, Poulidakos, Boesiger, et al., 2023a) and in the paper (Zaumanis, Poulidakos, Arraigada, et al., 2023b).

4.1.4 BTSV

The BTSV results of the binder recovered from the AC T 22 S mixtures are summarized in Figure 84. For comparison the figure also contains the results of the hard binder grade of the virgin binders from section o.

One can see in the figure that the HPMix binder from the ACT 22 S mixture falls within the phase angle and temperature requirements that were proposed in section o. The RAPMix binder is outside the box. However, it is surprising that the BTSV phase angle of the RAPMix binder is similar to the phase angle of the HPMix binder. Based on the

results of the section o, binders with lower polymer content typically have higher phase angle. Considering that the RAPMix mixture contains 40 % RAP (and therefore lower polymer content in the recovered binder), we expected phase angle to be higher than that of the HPMix binder and above the proposed 62°. One explanation of this result is that as seen in this and other research results, aged binder also reduces the phase angle and therefore the 40% RAP addition along with the use of the soft high polymer-content binder contributed to the low phase angle. This situation, however, requires to be cautious when evaluating the results of binders containing RAP using the BTSV.

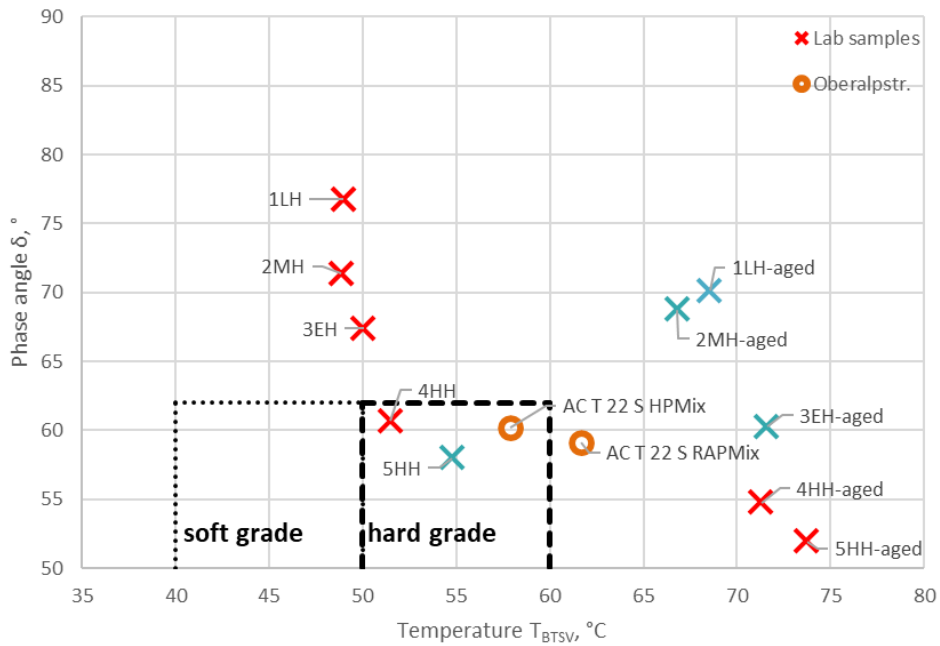


Figure 84: AC T 22 S BTSV result summary

To demonstrate the differences between the two binders, Figure 85 demonstrates the BTSV results over the entire measured test range. One can see that indeed the curves are quite similar despite the difference in the RAP content (40 % in RAPMix and 0 % in HPMix).

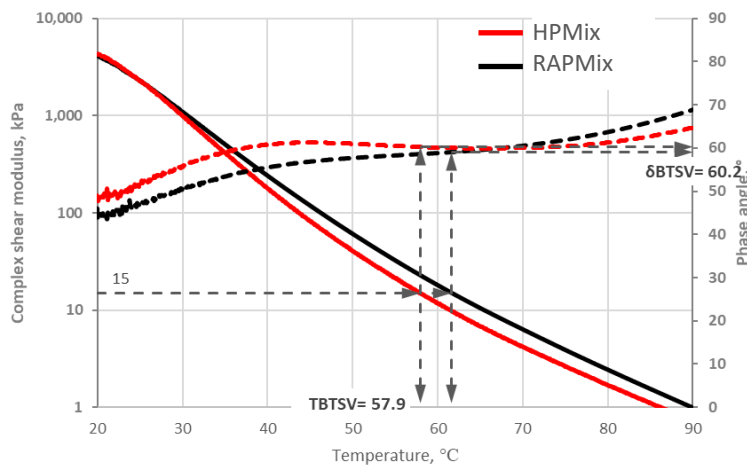


Figure 85: AC T 22 S BTSV results throughout the test

4.1.5 MSCR

The MSCRT results of the ACT 22 S binder are presented in Figure 86. According to the conclusions from section 0, only the results using 10 kPa load are shown here (the results at 3.2 kPa do not allow distinguishing between the binders). The test was done at 64 °C. For comparison, the results of the hard binder grade are also presented in the figure (some results are not in the figure because they had a creep compliance outside of the range presented in the figure).

It can be seen in the figure that there is a significant difference between the results obtained for the binders of the HPMix and the binder from the RAPMix mixture. The HPMix sample has a high recovery and a low creep compliance whereas the RAPMix binder has a lower result in both tests. This is likely the result of the 40 % RAP content in the sample. However, it can be stated that RAPMix mixture still exhibits elastic response that at the test conditions is better than that of the virgin unaged binders having medium and elevated polymer content. Partially this may be related to the aging that the binders exhibited during production and paving since aging can increase binder recovery and reduce compliance.

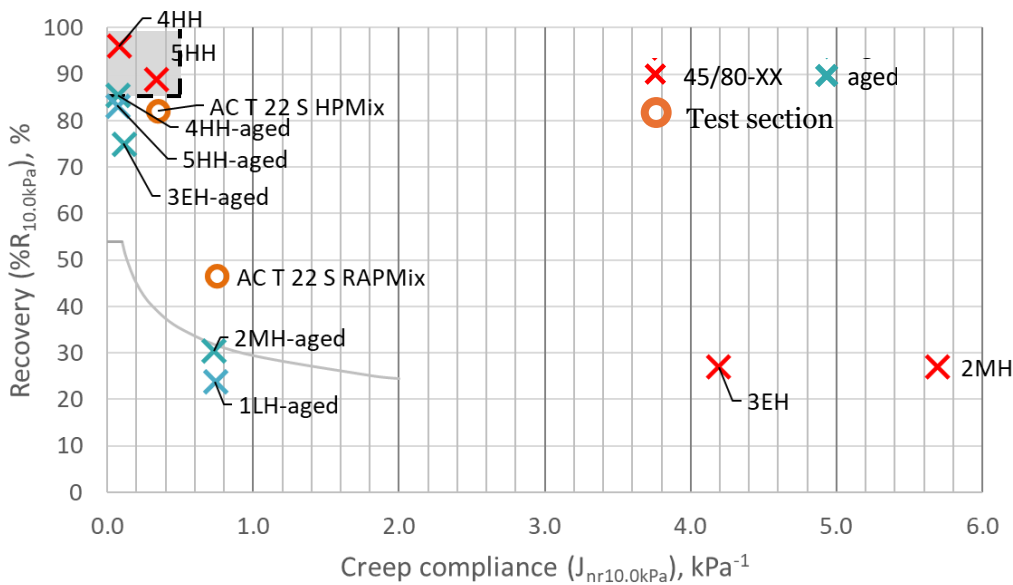


Figure 86: ACT 22 S MSCRT results. Test performed at 64 °C and 10 kPa load

4.1.6 DSR Frequency Sweep

The DSR frequency sweep results of the binder recovered from the ACT 22 S mixtures are summarized in Figure 87. These are results at 1.59 Hz frequency over a range of test temperatures.

The complex modulus of the RAPMix mixture are higher compared to the HPMix binder. The phase angle, however, of the RAPMix binder has a higher temperature dependency compared to the HPMix binder. This is illustrated by the "flatter" curve and is a desirable property in binder.

Based on the frequency sweep results, the Performance Grade (PG) was calculated for each binder. The results are similar for both mixtures: 88.1 °C for the HPMix binder and 90.8 °C for the RAPMix binder.

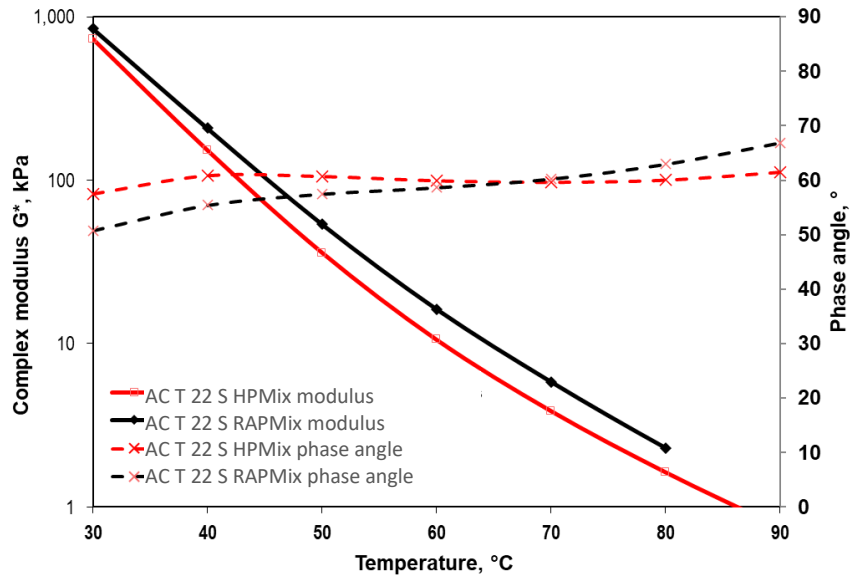


Figure 87: DSR Frequency sweep test results of AC T 22 S binder (binder recovered from mixtures) at 1.59 Hz frequency

4.1.7 Aggregate gradation

The recovered aggregate gradations of the AC B 22 S RAPMix and AC B 22 S HPMix samples are shown in Figure 115 and both are within the max and min grading curve limit values for this asphalt type. It was intended to have the gradations as close as possible but due to the use of 40 % RAP in the RAPMix and no RAP in the HPMix, some differences were expected. It can be seen in the figure that the HPMix is slightly finer below the 8 mm sieve and it has by 1.6 % higher filler content. The differences, however, are not expected to have a major influence on the discussion of the mixture properties. The recovered binder content is 4.6% for the HPMix and 4.3% for the RAP-Mix.

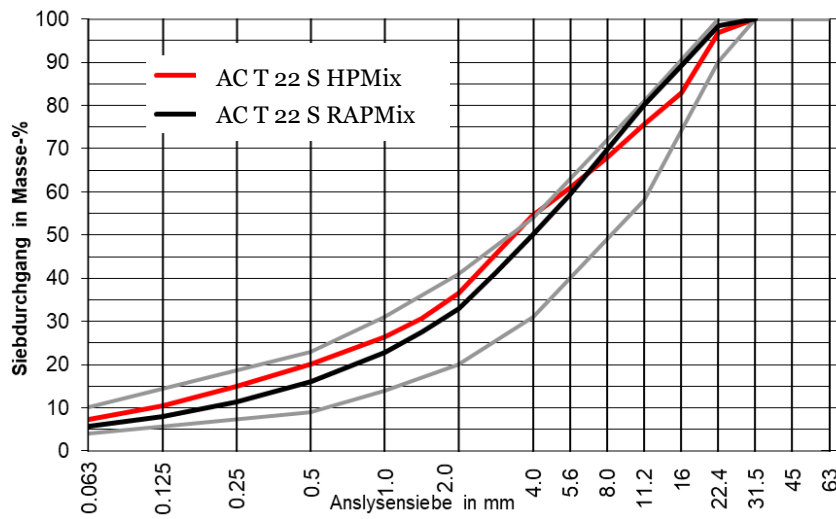


Figure 88: Recovered aggregate gradation of the AC B 22 S RAPMix and HPMix samples

4.1.8 Marshall air voids and Marshall test

Marshall test results of the plant-produced, lab-compacted mixtures are summarized in Figure 89. The Marshall air voids is the most important parameter in the figure and it can be seen that the requirements are fulfilled by both mixtures. The HPMix has lower air voids, which is probably explained by the finer gradation.

The Marshall stability and Marshall flow are not required for "S" type asphalt mixtures, however, the results are provided for information. One can see that both mixtures have a high and similar stability while the flow is slightly higher for the HPMix compared to the RAPMix.

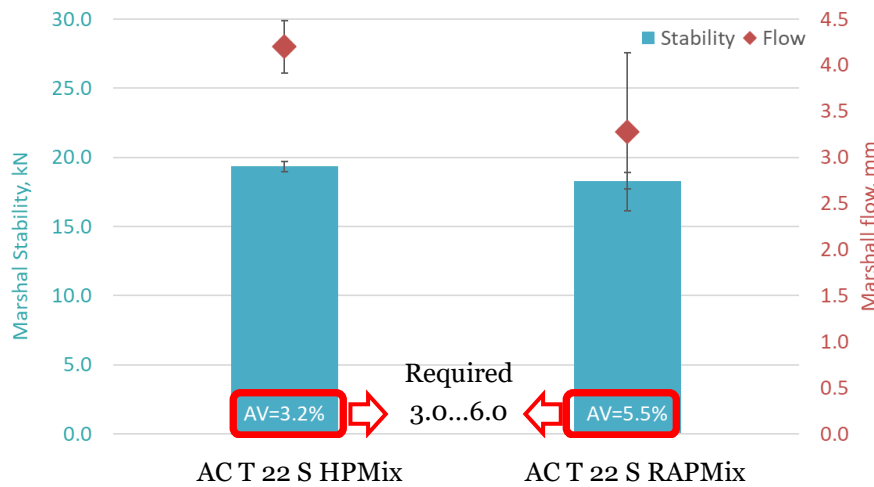


Figure 89: Marshall test results and Marshall air voids of the AC B 22 S mixtures

4.1.9 Rutting test

The French rutting test results of the of the plant-produced, lab-compacted AC B 22 S mixtures are summarized in Figure 90. The requirement according to the Swiss norm is to perform the test up to 30,000 cycles. However, to evaluate the effect of highly modified binder, the test was extended to 90,000 cycles.

It can be seen in the figure that the HPMix sample has a high difference between the two test replicate samples. However, the requirement of less than 7.5 % rut depth up to 30,000 cycles is clearly fulfilled by both mixtures. Extending the test to 90,000 cycles does not appear to provide any added benefit since the trend can be seen already in the phase up to 30,000 cycles.

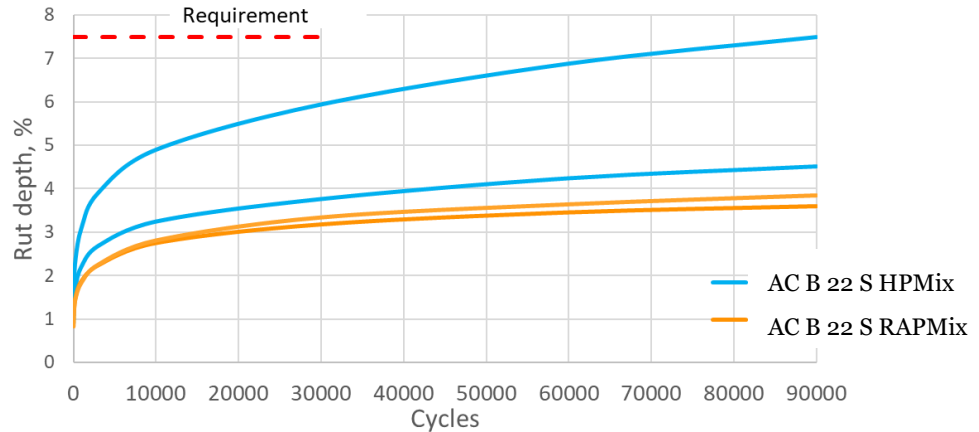


Figure 90: French rutting test results of the AC B 22 S mixtures

4.1.10 Semi-circular bend (SCB) test

The SCB results, including the Flexibility Index (FI) and the fracture energy, of the plant-produced, lab-compacted AC T 22 S mixtures are summarized in Figure 91. The minimum FI of 2.0 was proposed in an earlier research project titled HighRAP at Empa (Zaumanis, Poulidakos, Boesiger, et al., 2023a). The requirement was proposed for binder and base layers.

It can be seen in the figure that the HPMix demonstrates a higher FI and fracture energy compared to the RAPMix. These results indicate that the HPMix has a better resistance to crack propagation. However, it must be noted that according to prior research, the FI is not sensitive towards the use of polymer modified binder (Yin, 2023; Zaumanis, Poulidakos, Boesiger, et al., 2023a). For this reason, we assume that the result is not related to the polymer content and rather related to other factors. Most notably, based on previous research, the binder properties and binder content typically have a high impact on the FI. RAP content, if not accounted for in the mixture design, can also reduce the FI. The RAPMix's binder content is slightly lower (4.3 % versus 4.6 %) and the penetration is slightly lower (31 dmm versus 34 dmm). It is possible these factors, along with the higher RAP content contribute toward the lower FI of the Reference mixture compared to the HPMix.

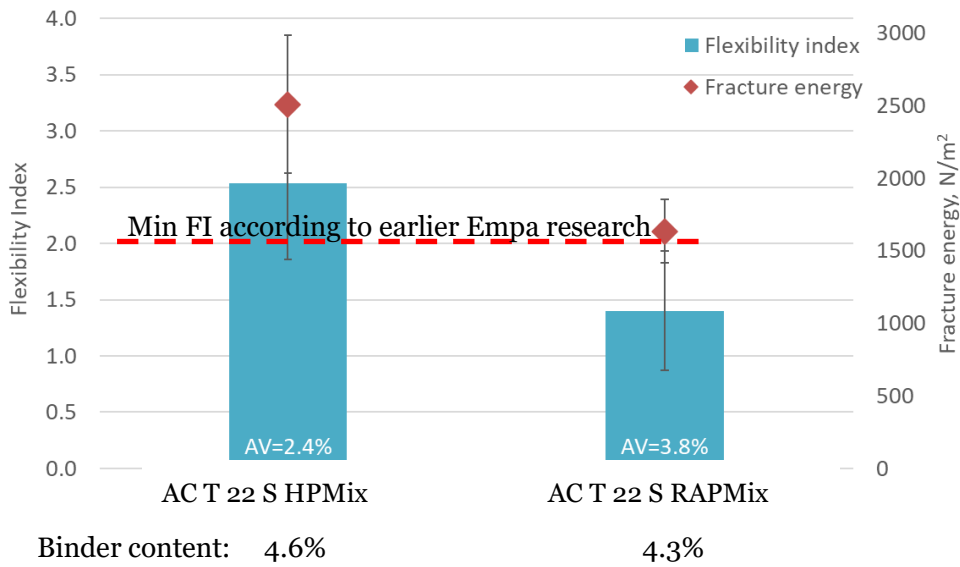


Figure 91: SCB test results of the AC B 22 S mixtures. AV is the air void content of the test samples.

4.1.11 IDEAL-CT

The CTIndex is a crack propagation test that reflects both the fracture energy absorbed by the specimen and its post-peak ductility, with higher values indicating greater resistance to crack initiation and propagation. The procedure offers a relatively rapid and repeatable means of assessing cracking resistance, making it suitable for incorporation into balanced mix design and quality assurance frameworks.

The IDEAL-CT results of the plant-produced, lab-compacted mixtures, including the CT index and failure energy, are summarized in Figure 92. The results demonstrate a similar trend to the SCB results discussed in the previous section and show that the HPMix has a higher CT index as well as a higher failure energy. This indicates a higher resistance to crack propagation. It must be noted that RAPMix mixture has a significantly higher air void content compared to the RAPMix even though both were compacted to the same target air void content (by dimensions 6%) using gyratory compactor. A higher air void content typically leads to lower CT index and thus at least partially the difference in the results can be attributed to the difference in the air void content. Similar to the SCB Flexibility Index, the CT Index has been shown not to be sensitive toward the polymer content (Yin, 2023).

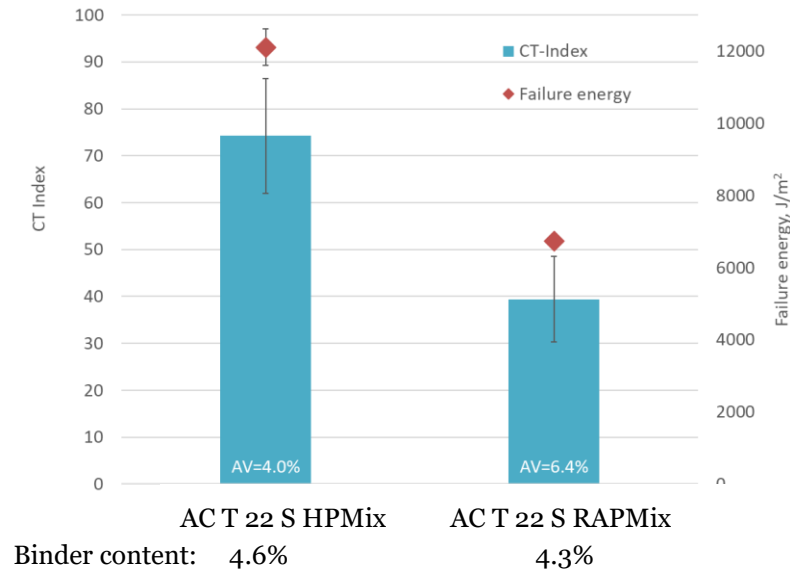


Figure 92: IDEAL-CT results of the AC B 22 S mixtures. AV is the air void content of the test samples.

4.1.12 Thermal stress restrained specimen test (TSRST)

The TSRST results, including the cracking temperature and failure stress, of the of the plant-produced, lab-compacted AC T 22 S mixtures are summarized in Figure 93. The results show that the HPMix has a slightly lower cracking temperature and higher failure stress compared to the RAPMix, which indicates a higher resistance to low temperature cracking. The average air void content of the HPMix samples was 2.8 % and the average air void content of the RAPMix was 4.0 %. A higher air void content can sometimes lead to lower TSRST performance (Zaumanis et al., 2018) and therefore it may be that at least partially the difference in the results between the samples can be attributed to the different sample air voids.

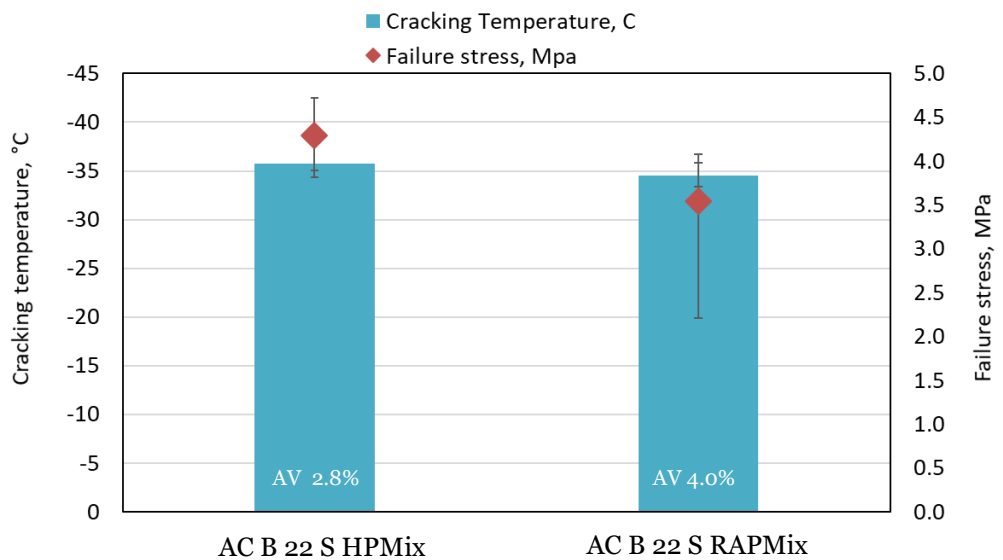


Figure 93: TSRST results of the AC B 22 S mixtures. AV is the air void content of the test samples.

4.1.13 Stiffness using indirect tensile test

The stiffness was measured using Indirect Tensile test method at 5 different temperatures (-10 °C, 0 °C, 10 °C, 15 °C, and 20 °C). At each temperature, the testing was done at three different frequencies (0.1, 1, and 10 Hz). The samples were prepared from plant-produced asphalt mixtures. This test method was selected since it allows testing both road cores and laboratory compacted samples (which is not possible using the 2-point bending test using trapezoidal specimen).

The test results at the five different temperatures and three frequencies at each temperature are demonstrated in Figure 92. It can be seen that the HPMix samples typically have a slightly higher stiffness compared to the RAPMix sample at most temperatures and frequencies. The difference is higher at the low temperatures and smaller or none at high temperature. In principle, considering sufficient stiffness of the bottom layers, a higher stiffness of a particular asphalt layer is a desirable property since it allows less deformations and thus less fatigue damage in the layer. However, this depends on the pavement as a whole.

It must be noted that the average air void content of the HPMix samples was 1.7 % and for the RAPMix samples it was 3.7 %. The samples were prepared using gyratory compactor with the target air void content of 4.5 %. After cutting it is expected that the air void content decreases but the HPMix samples show a lower-than-expected air void content. A lower air void content typically (up to a certain level) leads to a higher stiffness modulus (Zaumanis et al., 2018) and therefore part of the difference in the stiffness results between the two mixtures can be attributed to the difference in the air void content (possibly originating from the differences in the grading curves).

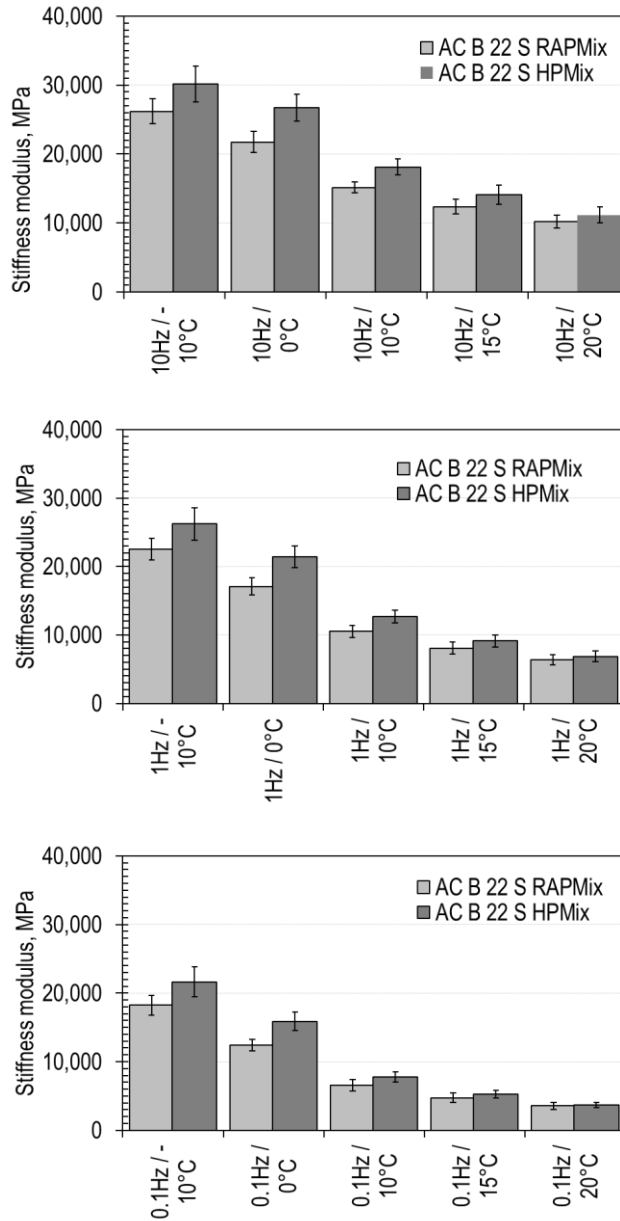


Figure 94: Stiffness modulus of the AC B 22 S mixtures at five different temperatures at 10 Hz (top figure), 1 Hz (middle), and 0.1 Hz (bottom)

The testing of stiffness at a range of temperatures and frequencies allowed to construct a master curve. Master curve uses the principle of time-temperature superposition to shift data at multiple temperatures and frequencies to a reference temperature so that the stiffness data can be viewed without temperature as a variable. This method of analysis allows for visual relative comparisons to be made between mixes.

A sigmoidal model was used as proposed by Witzack and Fonseca (Witzack & Fonseca, 1996), with the shift factors calculated following the Williams-Landel-Ferry (Williams, Landel, & Ferry, 1955) relation shown in Equation (11):

$$\log a_T = \frac{-C_1 (T - T_{ref})}{C_2 + (T - T_{ref})} \tag{11}$$

Where a_T is a factor for shifting stiffness at certain temperature T to a reference temperature T_{ref} (15 °C in this study). C_1 and C_2 are material constants and a least squares regression was performed to obtain the parameters.

The master curves of the RAPMix and the HPMix AC B 22 S mixtures are plotted in Figure 95. It can be seen in the figure that the tested results have a high overlap with the prediction results thus showing the successful application of the time-temperature superposition principle. The results show that at a given temperature HPMix asphalt has a higher stiffness modulus throughout the frequency range, with the difference higher at high frequencies (corresponding to high traffic speed) and lower at low frequencies (corresponding to slow traffic speed).

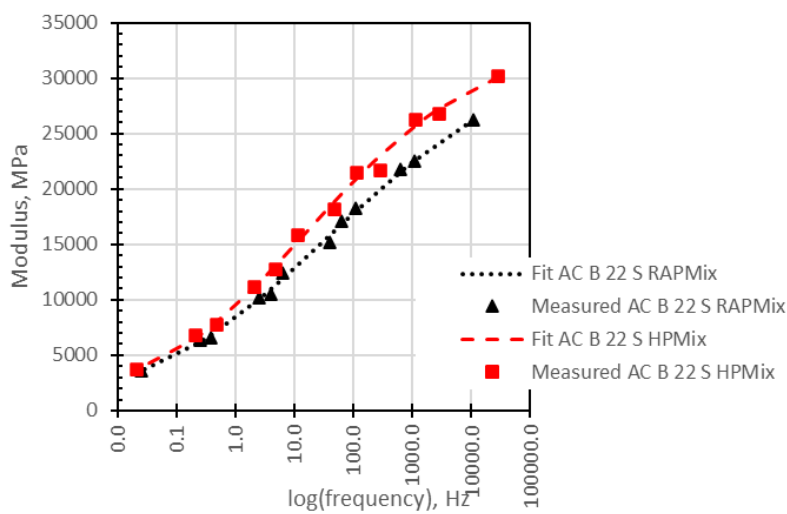


Figure 95: Stiffness master curves of the AC B 22 S mixtures. Shifted to 15 °C.

4.1.14 Fatigue

Fatigue resistance of the plant-produced, lab-compacted mixtures was measured using trapezoidal specimen at 10 °C and 25 Hz frequency. The results are expressed visually in Figure 96 where the vertical axis shows the number of cycles to failure (50 % reduction in complex modulus) and the horizontal axis represents the applied strain.

It can be seen that the variability of both tests is relatively high and does not form a clear fatigue line. However, the HPMix results tend to have a higher number of cycles to failure both at low and at high strains compared to the RAPMix. This behavior is likely the result of the increased elasticity due to the use of higher content of polymers that form a continuous polymer matrix in the binder.

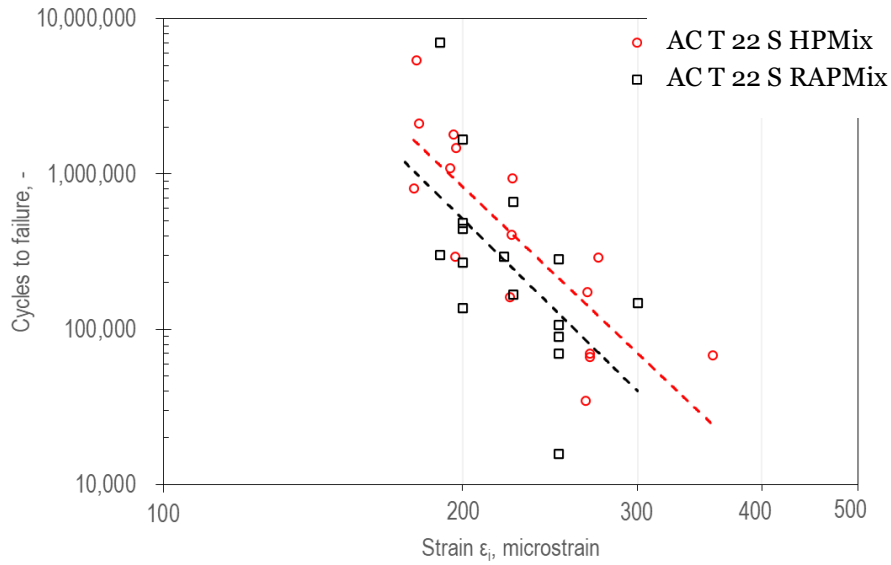


Figure 96: Fatigue test regression lines of the AC B 22 S mixtures using the 2-point bending test

The numerical results of the fatigue test are summarized in Table 12. A typical way to interpret fatigue results is to determine the strain to reach one million cycles (ϵ_6) using the fatigue line. It can be seen in the table that the ϵ_6 is higher for the HPMix sample thus confirming the positive effect of the increased polymer content on the extension of fatigue life of the asphalt mixture. However, it can also be seen in the table that the coefficient of determination and the quality indexes are low for both mixtures thus these results should be interpreted with caution.

Fatigue results of the AC B 22 S mixture					
Mixture	Strain at 10^6 cycles (ϵ_6)	Quality index ($\Delta \epsilon_6$)	Slope (1/b)	Residual standard deviation (S_N)	Linear correlation coefficient (r_2)
AC B 22 S HPMix	194.0	22.61	-6.09	0.47	0.68
AC B 22 S RAPMix	160.49	15.30	-6.16	0.56	0.36

Table 12: Fatigue test results of the AC B 22 S mixtures using the 2-point bending test

4.1.15 MMLS3

The loading using vehicle load simulator MMLS3 was done for the plant-produced, lab-compacted RAPMix and the HPMix AC B 22 S samples that were compacted to 6 cm thickness. The test was performed in a fatigue-inducing mode at 10 °C with the crack propagation expected from the 3 cm deep transversal notch at the middle of the slab as summarized in Figure 97.

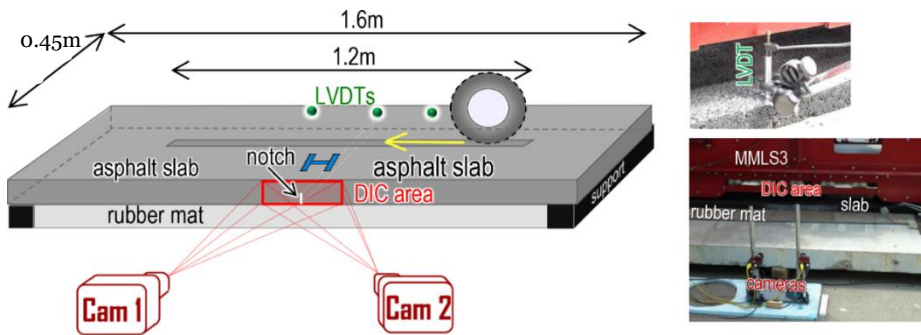
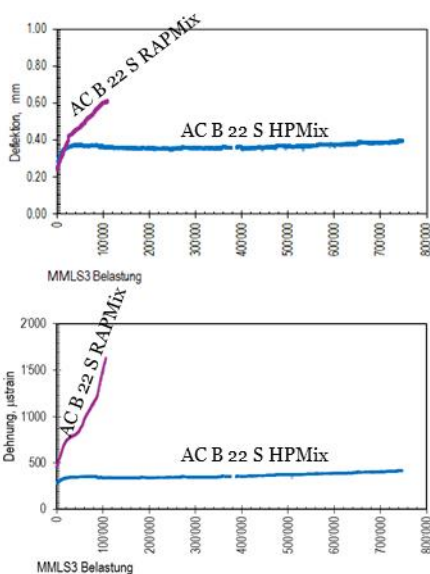


Figure 97: MMLS3 setup

The MMLS3 loading results are summarized in Figure 98. It can be seen that both sample exhibit initial settling during the first 20,000 cycles, manifested by an increasing deflection. Following the initial phase, the crack in the RAPMix propagated quickly and at about 100,000 cycles it had reached the surface of the slab. This is evident both from the increased deflection as measured using the LVDTs, the strains recorded by the strain gauges and from the digital image correlation (DIC) images.

In contrast, the HPMix sample was loaded for up until nearly 80,000 load cycles without exhibiting any crack propagation as measured using DIC. After the initial settling, the deflection as measured by the LVDTs did not increase and remained constant throughout the loading. A similar trend is observed from the Strain Gauges results. The loading was discontinued after the week of testing.

These results demonstrate the superior fatigue resistance of the HPMix sample in comparison with the RAPMix sample. Furthermore, these results support the conclusion from the fatigue testing where the HPMix sample also exhibited better performance in comparison with the RAPMix.



cracks at the end of the tests

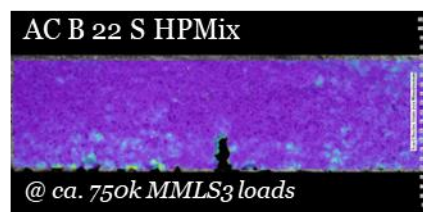


Figure 98: MMLS3 loading results

4.1.16 Structural capacity with FWD

After construction, the structural capacity of the test sections was evaluated through a Falling Weight Deflectometer (FWD) campaign carried out by Infralab SA in September 2024, as described in section 2.3. The post-processing involved the back-calculation of layer stiffnesses from the measured deflection bowls using the software ELMOD. Since the method allows a maximum of three layers, the bituminous layers were combined into a single equivalent layer, the hydraulically bound and unbound layers were grouped as a second, and the natural subgrade was treated as a third, as shown in the left side of Figure 99. The back-calculated asphalt layer E-modulus—where the HPMix layer containing high PmB represents 41% of the total asphalt thickness—corrected to 15°C, are shown the right side of Figure 99 for the RAPMix and HPMix sections. The average temperature in the pavement during the tests measured by the FWD was 16.0 °C for the RAPMix pavement and 16.1 °C for HPMix. As expected, the HPMix section exhibits slightly higher asphalt stiffness. Correspondingly, the maximum deflections obtained from the FWD (see Figure 100) are smaller for HPMix, confirming its higher structural stiffness due to the use of the High PmB in the base layer.

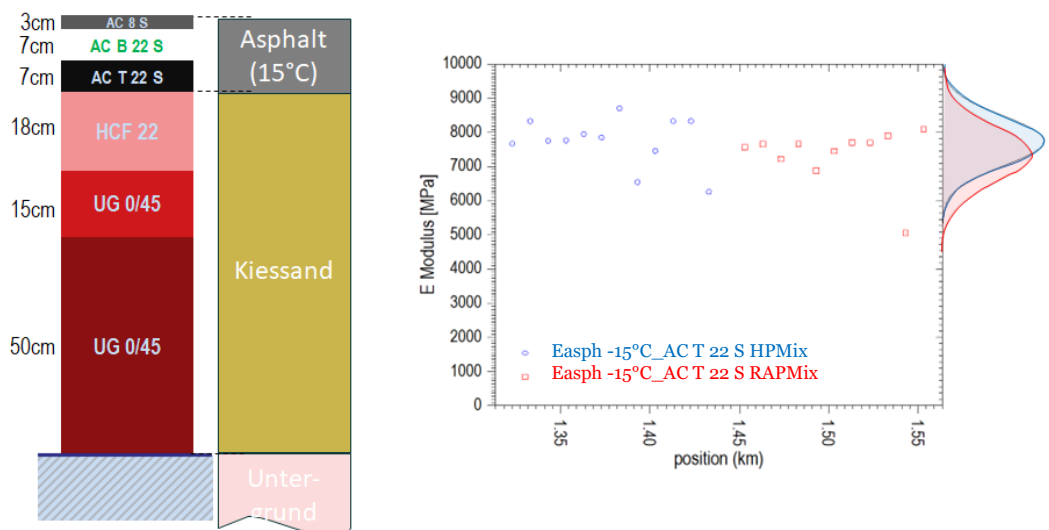


Figure 99: Layer configuration of the test sections and simplification into three layers for backcalculation (left), and backcalculated asphalt layer E-modulus corrected to 15 °C (right).

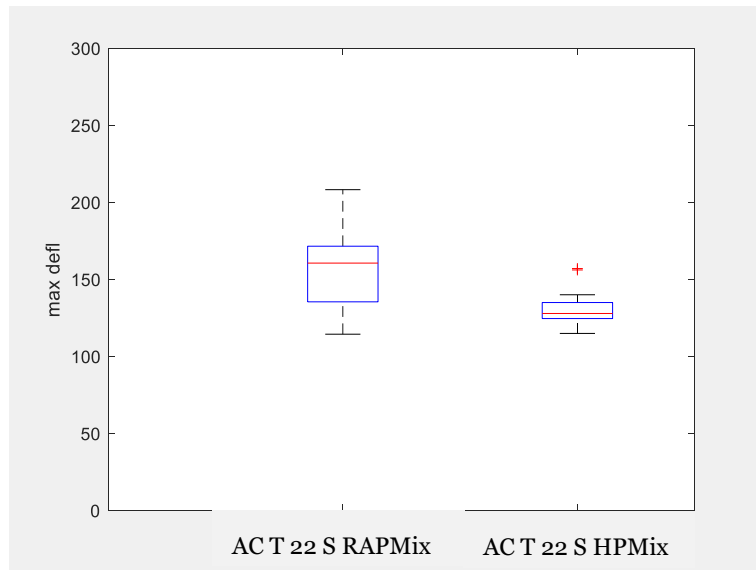


Figure 100: Boxplots showing the maximum deflection measured at the load center for the RP and HP pavement sections.

To quantify the differences in the shape of FWD deflection bowls, several deflection-based indices can be calculated. These parameters provide a straightforward means of comparing structural responses between test sections. The Surface Curvature Index (SCI), is defined as:

$$SCI = D_0 - D_{220} \quad (12)$$

It represents the curvature near the surface and reflects the stiffness of the upper asphalt layers. Lower SCI values indicate a stiffer surface layer.

The Base Damage Index (BDI) can be calculated as:

$$BDI = D_{300} - D_{600} \quad (13)$$

It characterizes the load transfer between the base and subbase layers. A lower BDI suggests a stronger base or better bonding between layers.

The Base Curvature Index (BCI), is calculated through the following equation:

$$BCI = D_{600} - D_{900} \quad (14)$$

it reflects the deformation occurring in deeper layers, with lower values indicating a stronger subbase or subgrade.

Finally, the AREA parameter is expressed as:

$$AREA = \frac{6(D_0 + 2D_{200} + 2D_{300} + D_{500})}{D_0} \tag{15}$$

It provides an overall indicator of the deflection bowl shape. Larger AREA values correspond to stiffer or thicker pavements and improved load distribution.

In summary, high SCI, BDI, and BCI values are associated with weaker surface, base, or subgrade layers, respectively, while a larger AREA indicates better load-spreading efficiency. Therefore, a reduction in SCI and BDI for the improved material compared to the reference section would demonstrate its enhanced ability to distribute loads more effectively.

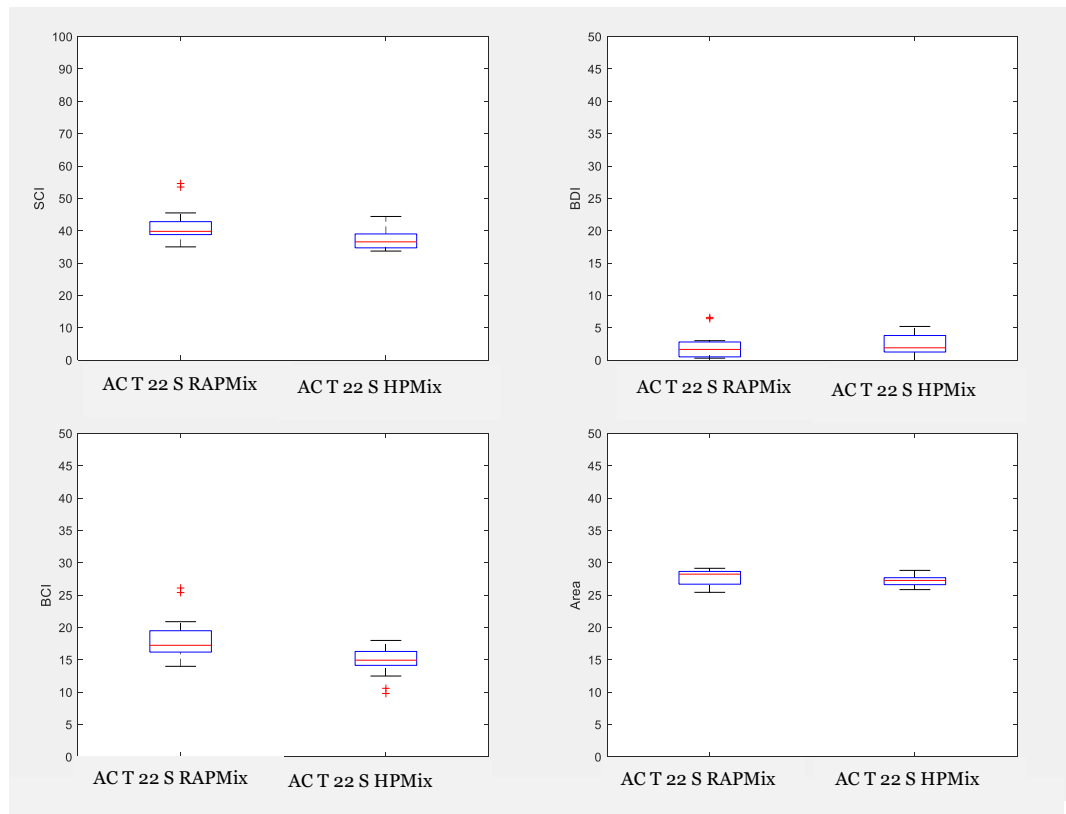


Figure 101: Deflection bowl parameters (SCI, BDI, BCI, AREA) calculated from FWD measurements for the RAPMix and HPMix sections

The comparison of deflection indices shows that the HP section exhibits slightly lower SCI and BCI values than the RAPMix section, indicating a stiffer surface layer and improved load distribution to the lower layers. BDI values are low in both sections, with marginally lower values in HPMix, suggesting good interlayer bonding. The AREA parameter is similar for both structures, confirming comparable overall stiffness. Overall, the HPMix section demonstrates enhanced load-spreading efficiency and more uniform structural performance compared to the pavement with a RAPMix section.

4.1.17 Summary

The results of the AC B 22 S test section are summarized in Figure 102. The table allows to qualitatively compare the results of the HPMix to the RAPMix samples. The HPMix was produced using a highly polymer-modified binder (referred to as PmB 45/80-85) and no RAP while the RAPMix was produced using a soft highly modified binder (PmB 90/150-85) and 40 % RAP.

Overall, both mixtures provided good performance that corresponds to the current specification requirements for the PmB 45/80-65 (CH-E) binder. This performance was achieved even with the 40 % RAP mixture thus indicating that 40 % RAP content can be successfully used in polymer-modified mixtures. Even more so: based on the results it is possible that even a higher RAP content can be used while still achieving the PmB 45/80-65 (CH-E) performance, if adequate mix design measures are implemented (for example recycling agent use).

However, it has to be noted that the currently used methods do not always offer a reliable way to determine the binder performance and therefore additional test methods were used in this research.

In can be seen in the figure that most test methods, including the additional binder tests and performance-based mixture tests indicate a better performance of the HPMix compared to the RAPMix. This was expected, considering that the effective polymer content in the mixture is higher compared to the RAPMix mixture due to the 40 % RAP content. Overall, these results allow to conclude that the use of highly polymer-modified binder can serve two purposes:

- It is beneficial for performance improvement when used with low or no RAP content¹⁴.
- It can permit using high RAP content of at least 40% or more in binder layer mixtures to ensure performance that is expected from a polymer modified mixture where CH-E type binder is required.

Mixture	RAP content	Binder tests				Rutting resistance	Crack propagation resistance		Fatigue		Stiffness	Low temp. cracing resistance
		ER	BTSV	MSCR	FS	FRT	SCB	IDEAL-CT	2PB-TR	MMLS3	ITT	TSRST
AC B 22 S	HPMix	↗	↗	↕	↗	↘	↗ ¹	↗ ¹	↗	↕	↗	→
	RAP Mix	●	●	●	●	●	●	●	●	●	●	●

Legend:

- reference mixture result
- ↕ significantly better performance
- ↗ slightly better performance
- similar performance
- ↘ slightly worse performance
- ↘ significantly worse performance

- ER Elastic Recovery (binder)
- BTSV Binder fast characterisation test
- MSCR Multiple stress creep recovery test (binder)
- FS Frequency Sweep (binder)
- FRT French Ruting Tester (mixture)
- SCB Semi-circular bend test (mixture)
- IDEAL-CT Indirect tensile asphalt cracking test (mixture)
- 2PB-TR Two point bending on trapezoidal specimen
- MMLS3 Model mobile load simulator (mixture)
- ITT Indirect tensile test (mixture)
- TSRST Tensile stress restrained specimen test

¹ SCB and IDEAL-CT tests are not sensitive to polymer content

Figure 102: Summary of the AC B 22 S test section test results

¹⁴ Although the mix without recycled content shows the best results, the authors do not recommend abandoning asphalt recycling. The use of RAP should be evaluated in the context of sustainability and resource efficiency. Such an evaluation was not part of this project.

4.2 AC 8 S test section, H27 Engadinerstrasse in St. Moritz Charnadüra, Graubünden

AC 8 S type asphalt mixture wearing course was paved in the test site on H27 Engadinerstrasse in St. Moritz Charnadüra, Graubünden. This jobsite was selected due to the high traffic intensity and the climatic conditions. Two mixtures were paved: (1) on 04.07.2024 the HPMix was paved using highly polymer-modified binder; (2) on 05.07.2024 the reference mixture was paved by adding PmB 90/150-60 (CH-E) type binder. Both mixtures had the same mixture design and thus comparison of the two mixtures allows to evaluate the potential benefits of using highly polymer-modified binder for improving the performance and longevity of the asphalt.

Objective

The objective of the test section in Charnadüra was to determine the potential to improve wearing-course mixture performance through the use of high PMB.

4.2.1 Mixtures and test section location

The test site is located on H27 Engadinerstrasse in Charnadüra, Graubünden (km 7.032-7.377) at approximately 1725 meters above the sea level. Only the pavement line on the side of the river was used in the research (right side of the direction St. Moritz – Celerina) due to no disturbances below the asphalt. The traffic intensity of the road is classified as T5 with DTV 11,000.

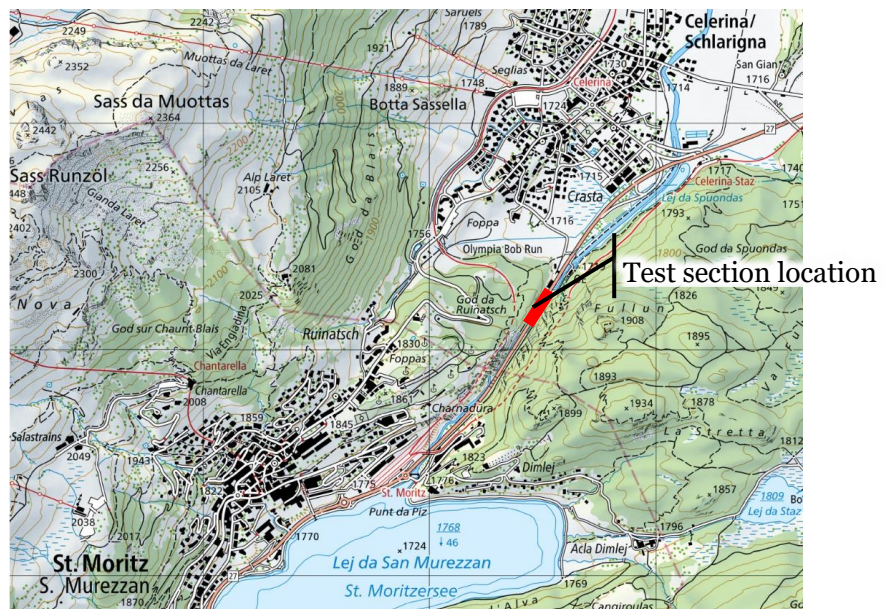


Figure 103: Location of the AC 8 S test section, H27 Engadinerstrasse in Charnadüra, Graubünden

The normal profile of the jobsite is shown in Figure 104 and the layer thicknesses are shown in Figure 105. Only the 3 cm thick wearing course was used in the research project. The two recipes used for the AC 8 wearing course are summarized in Table 11. The reason for using these mixtures can be summarized as follows:

- The Reference mixture uses a conventional recipe and is designed using PmB 90/150-60 (CH-E) binder grade. The soft binder grade is required due to the high

altitude of the road (1725 meters above the sea level). The average production temperature of the mix was 165 °C.

- The HPMix recipe the standard binder was replaced with a highly modified binder. No other changes were made compared to the reference mixture. The average production temperature of the mix was 170 °C.

The properties of the binder used in the HPMix recipe are described in section o. In section o the binder has the ID 6MS.

The asphalt was produced by Catram AG at the production plant in Cho d'Punt 72, 7503 Samedan. The production plant is located approximately 10 minutes from the construction site.

Mixtures used in the Charnadüra test section

Mixture type	Function	RAP content	Target binder	Added binder grade	Binder ID	Location, km
AC 8 S	Reference	0 %	PmB 90/150-60 (CH-E)	PmB 90/150-60 (CH-E)	Not tested	7.217-7.377 (valley side)
AC 8 S	HPMix	0 %	PmB 90/150-85	PmB 90/150-85	6MS	7.032-7.217 (valley side)

Table 13: Asphalt recipes for Charnadüra test section

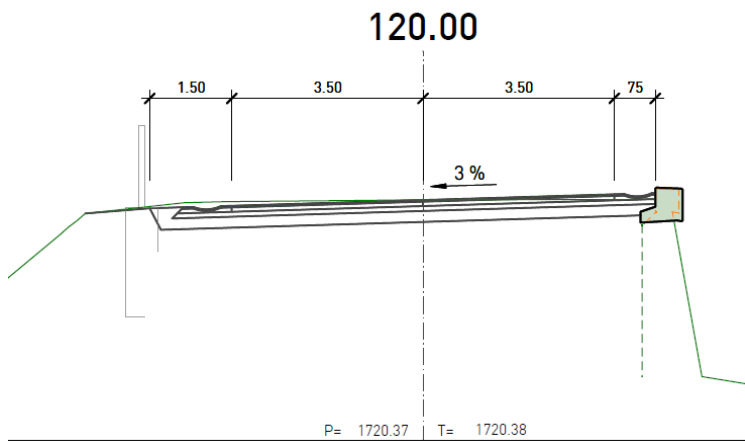


Figure 104: Normal profile of the Charnadüra test section

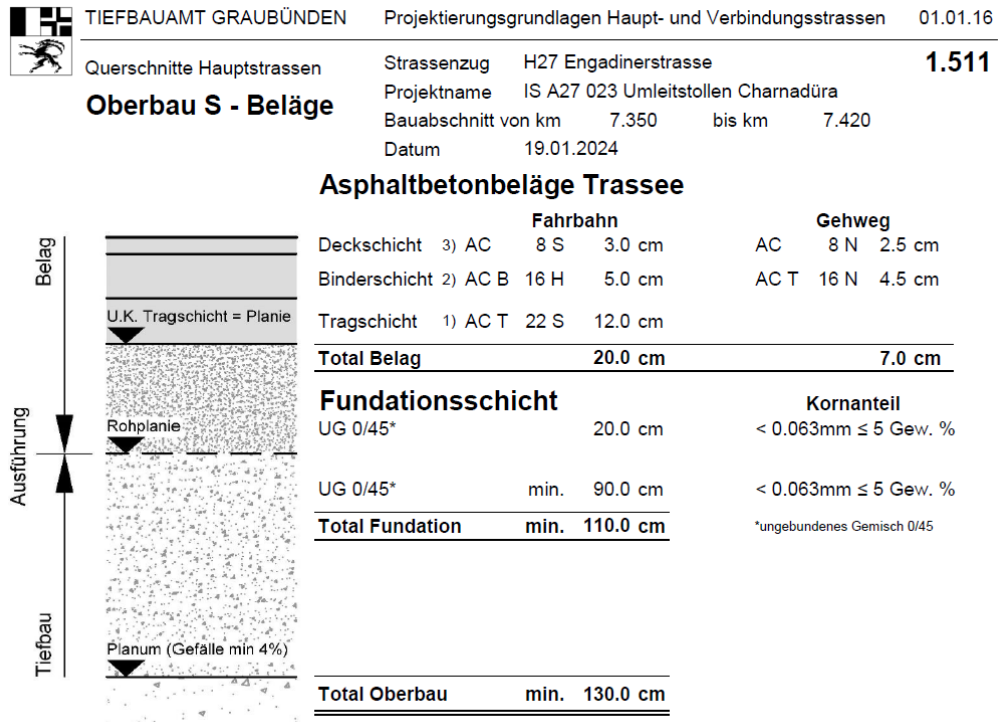


Figure 105: Layer thicknesses of the Charnadüra test section

Images from the construction of the test section are shown in Figure 106.



Figure 106: Construction of the AC 8 S pavement in the Charnadüra test section

4.2.2 Methodology

Asphalt mixture samples for laboratory testing were collected from the production plant and road cores were gathered soon after construction. The following methods were used to evaluate the performance of the collected samples:

- The plant-produced samples were used for binder recovery as well as for testing the mixture using the following methods: aggregate gradation, Marshall test, Wheel tracking test, Semi Circular Bend (SCB) test, IDEAL-CT, low temperature cracking test (TSRST), and stiffness modulus test.
- The recovered binder was tested using penetration, softening point, elastic recovery, BTSV, and MSCRT.
- The road cores were tested to determine the stiffness modulus.

A complete description of each test method is provided in section 2.

4.2.3 Conventional binder tests

The penetration tests of the binder recovered from the AC 8 S mixtures are summarized in Figure 107. For comparison, the figure also contains the binder test results of this same soft binder grade that were presented earlier in section 0.

It can be seen in the figure that the binder recovered from the test section mixtures has a lower penetration compared to the virgin binders. This is expected due to the aging that takes place during construction. Overall, it can be seen that both test section binders have a similar penetration and it is within the expected range for recovered binders.

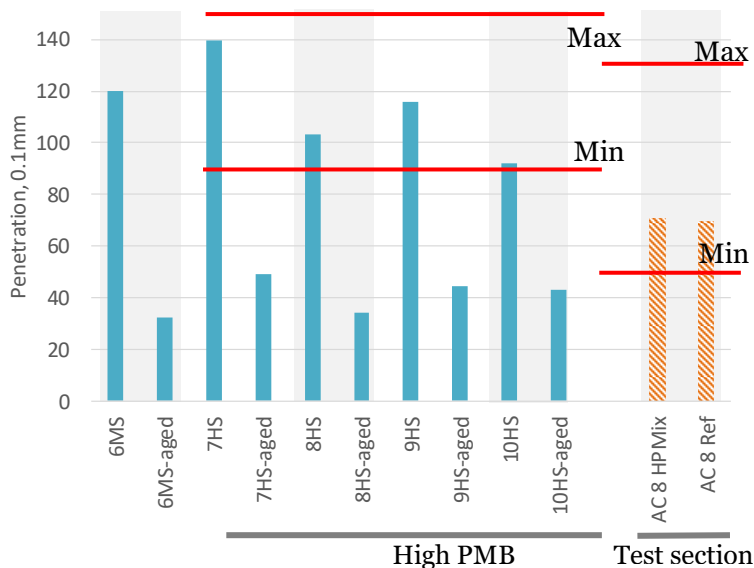


Figure 107: Penetration test results of the binders recovered from the AC 8 S mixtures and for comparison the results of the soft binder grades from section 0. Blue bars are virgin and virgin aged binders, while test section results are shown with orange bars. The minimum requirements are based on SN-670210b-NA_EN-14023-E for the virgin unaged binders and based on VSS-40430 for the recovered binders.

The softening point results are shown in Figure 108 and for comparison, the virgin soft binder results from section 0 are also included in the figure. Overall, it can be seen that the results of the recovered binders are within the expected range for the recovered binder of the grade PmB 90/150-60. However, it can be seen that the HP Mix binder has a significantly higher softening point compared to the reference mixture. At the

same time, as discussed in section o, softening point results should not be considered a reliable indicator of the binder performance for highly polymer-modified mixtures.

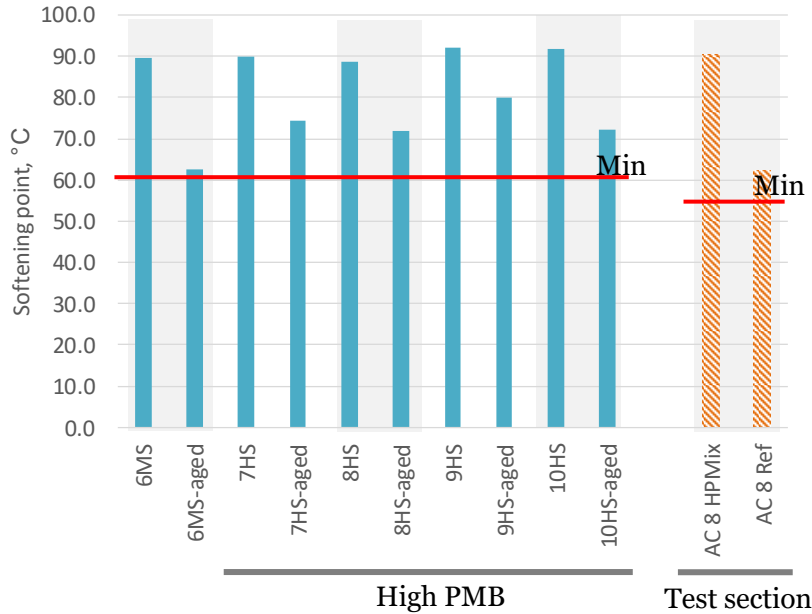


Figure 108: Softening point test results of the binders recovered from the AC 8 S mixtures and for comparison, the results of the soft binder grades from section o. Blue bars are virgin and virgin aged binders, while test section results are shown with orange bars. The minimum requirements are based on SN-670210b-NA_EN-14023-E for the virgin unaged binders and based on VSS-40430 for the recovered binders.

The elastic recovery test results are summarized in Figure 109. For comparison the figure also includes the elastic recovery results of the same grade of the virgin binders (discussed in section o). It can be seen in the results that the elastic recovery remains high for the binders recovered from the test section mixtures even considering the mixtures underwent aging during production and construction.

The elastic recovery of the HPMix binder is only slightly higher compared to the reference mixture supporting the conclusion from section o that elastic recovery at 25 °C likely can not be used as a reliable criteria for discriminating the binders based on polymer content.

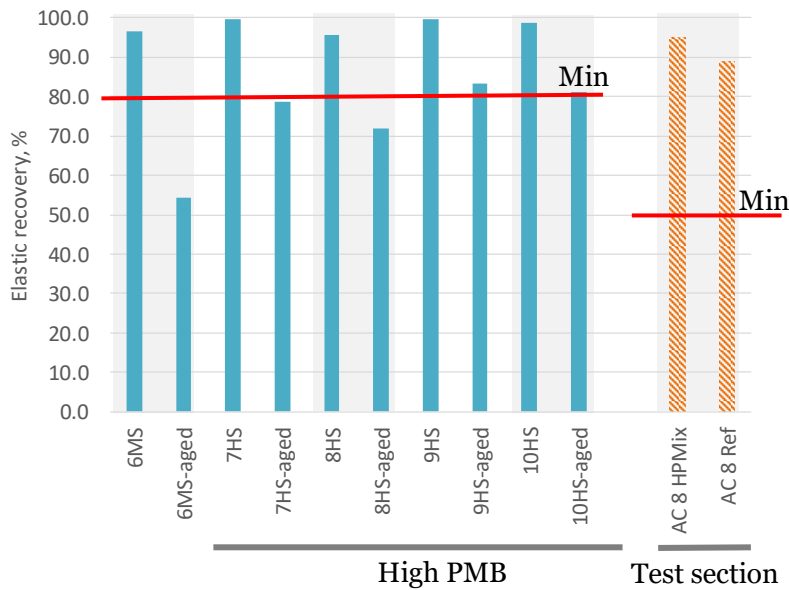


Figure 109: Elastic recovery test results of the binders recovered from the AC 8 S mixtures and for comparison, the results of the soft binder grades from section 0. Blue bars are virgin and virgin aged binders, while test section results are shown with orange bars. The minimum requirements are based on SN-670210b-NA_EN-14023-E for the virgin unaged binders and based on VSS-40430 for the recovered binders.

4.2.4 BTSV

The BTSV results of the binders recovered from the AC 8 S mixtures are summarized in Figure 110. For comparison, the figure also contains the results of the soft binder grade of the virgin binders from section 0 (including aged and virgin binders). One can see in the figure that the HPMix binder from the AC 8 S mixture falls within the phase angle and temperature requirements that were proposed in section 0. The binder recovered from the reference mixture is outside the box. At the same time, it has to be noted that the difference in phase angle of the reference binder compared to the proposed requirement is not large. One can also see that the HPMix binder has a lower phase angle than any other of the tested binders. The lower-than-expected phase angle of both of the recovered binders might be an indication that the aging that takes place during production and paving has caused the phase angle to reduce (the fact that the BTSV phase angle reduces after aging was discussed in section 3.9). This might be an indication that for recovered binder the criteria need to be adjusted. More data collection, however, is needed to define the criteria.

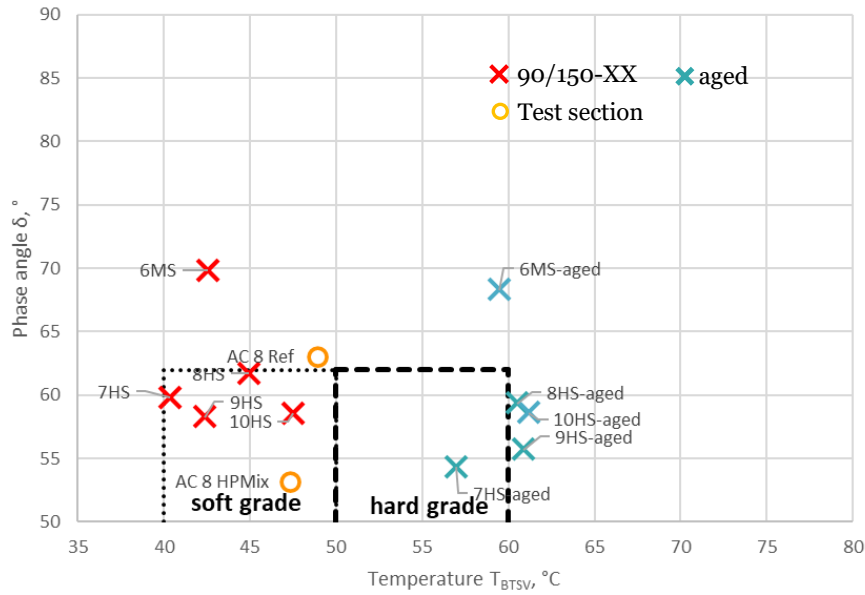


Figure 110: BTSV results of the binders recovered from the AC 8 S mixtures. For comparison, the results of the soft binder grades from section 0 are also included.

Figure 111 summarizes the BTSV results of the binders recovered from the AC 8S mixtures throughout the temperature sweep. It can be seen that the complex shear modulus results are fairly similar while the difference in the phase angle between the HPmix binder and the reference binder increases with higher temperature. This is likely the result of the higher polymer content creating a stronger polymer network and thus higher elasticity. It is thus evident that the HPmix binder holds an advantage over the reference binder, especially at higher temperatures. Higher elasticity at high temperatures increases the resistance to plastic deformations, given that all other parameters remain constant. For example, in Zurich region, a high pavement temperature can reach 60-65 °C in summer. The phase angle difference between the binders at this temperature is higher than at the BTSV temperature that corresponds to the 15 kPa complex shear modulus (which is the typical test result).

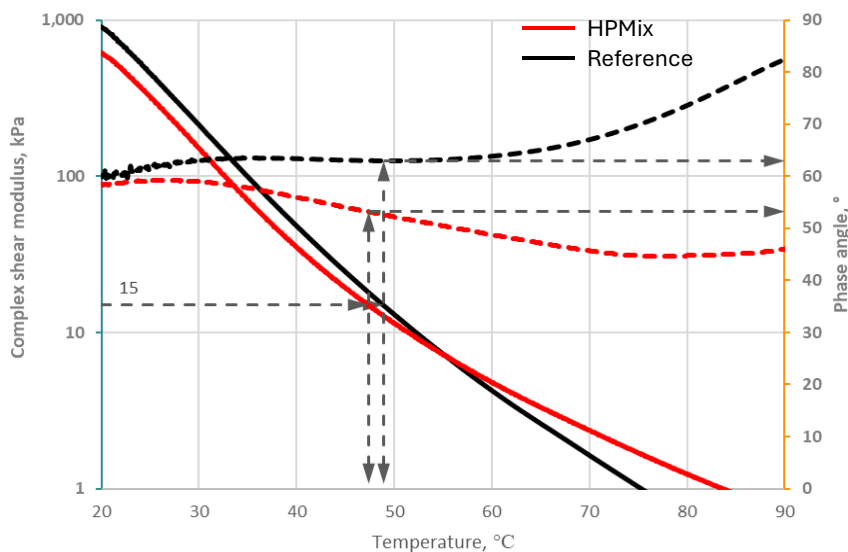


Figure 111: AC 8 S BTSV results throughout the test

4.2.5 MSCR

The MSCR test was performed at 58 °C. The results at 3.2 kPa stress are summarized in Figure 112 and at 10 kPa – in Figure 113. For comparison, the figures also include the respective binder test results of the same grade (soft binders) that were already presented in 0.

Figure 112 shows that the binder recovered from the highly polymer-modified mixture (HPMix) has a lower creep compliance and elastic recovery compared to the reference binder. However, it can be seen in Figure 113 that the difference is more pronounced at the stress of 10 kPa. The binder recovered from the highly polymer-modified mixture (HPMix) is exhibiting a high recovery and low creep compliance even at 10 kPa stress. At the 10 kPa stress, the HPMix binder results fall within the proposed acceptance range (see section 0). In comparison, the reference binder exhibits a recovery of 38 % and a creep compliance of approximately 2.2 kPa⁻¹ which is outside the proposed range.

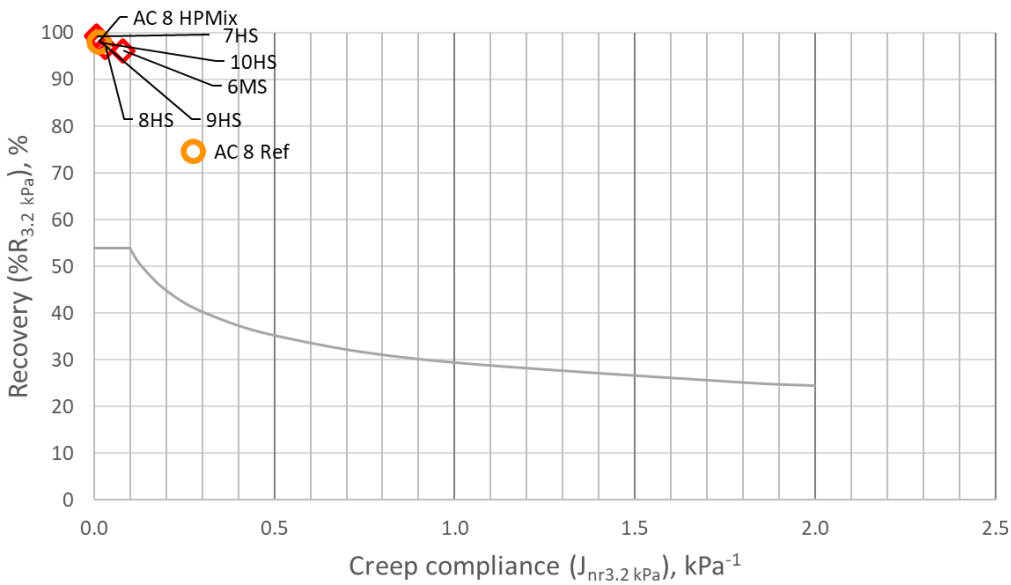


Figure 112: MSCR results of the binders recovered from the AC 8 S mixtures built in Charnadūra. The test was performed at 3.2 kPa stress at 58 °C temperature. For comparison, the results of the soft binder grades from section 0 are also included.

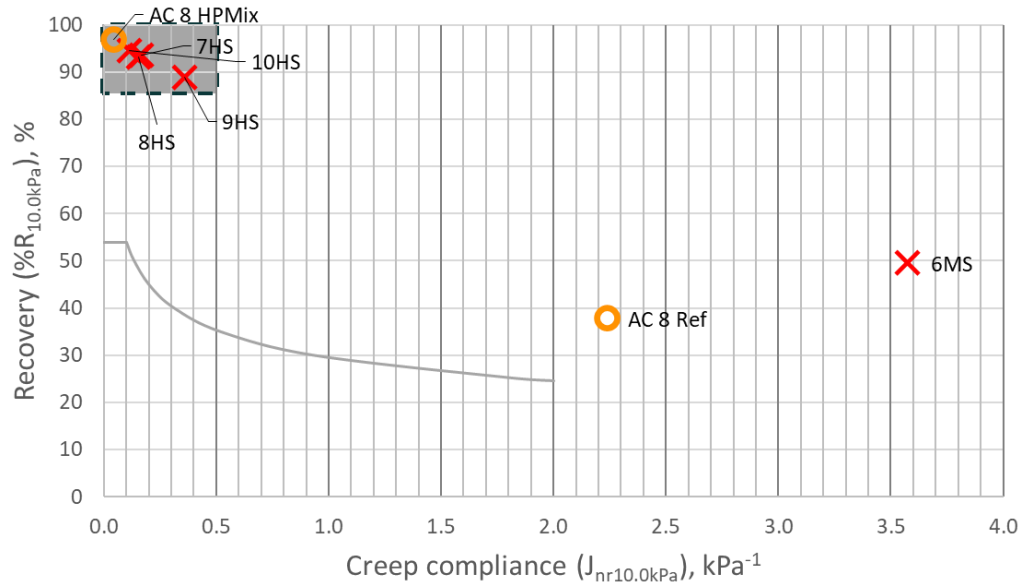


Figure 113: MSCR results of the binders recovered from the AC 8 S mixtures built in Charnadúra. The test was performed at 10 kPa stress at 58 °C temperature. For comparison, the results of the soft binder grades from section 0 are also included.

Figure 114 demonstrates the test results throughout the MSCR loading cycles at the 10 kPa stress at 58 °C. This figure is included to demonstrate the significant difference in the elastic recovery and the creep compliance between the reference polymer-modified binder and the highly modified binder (HPMix).

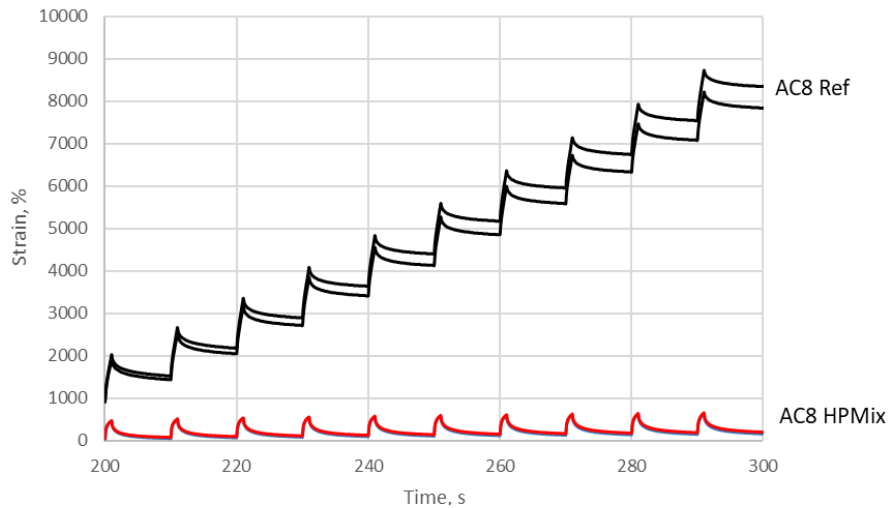


Figure 114: MSCR results throughout the loading cycles for the binders recovered from the AC 8 S mixtures built in Charnadúra. The test was performed at 10 kPa stress at 58 °C temperature..

4.2.6 Aggregate gradation

The recovered aggregate gradations of the AC 8 S Reference and AC 8 S HPMix are shown in Figure 115 and both are within the max and min grading curve limit values for this asphalt type. It can be seen that, as intended, the differences are very small and therefore can be neglected in further discussion of the results.

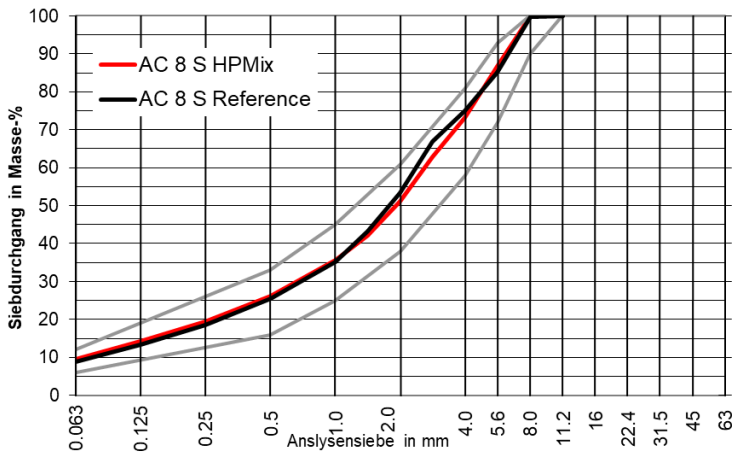


Figure 115: Recovered aggregate gradation of the AC 8 S Reference and HPMix samples

4.2.7 Marshall air voids and Marshall test

Marshall test results of the plant-produced, lab-compacted AC 8 S mixtures built in Charnadüra test section are summarized in Figure 116. The Marshall air voids is the most important parameter in the figure and it can be seen that the results are close to the minimum requirement but are fulfilled by both mixtures.

The Marshall stability and Marshall flow are not required for "S" type asphalt mixtures, however, the results are provided for information. It can be seen that the HPMix has a higher stability and flow compared to the reference mixture.

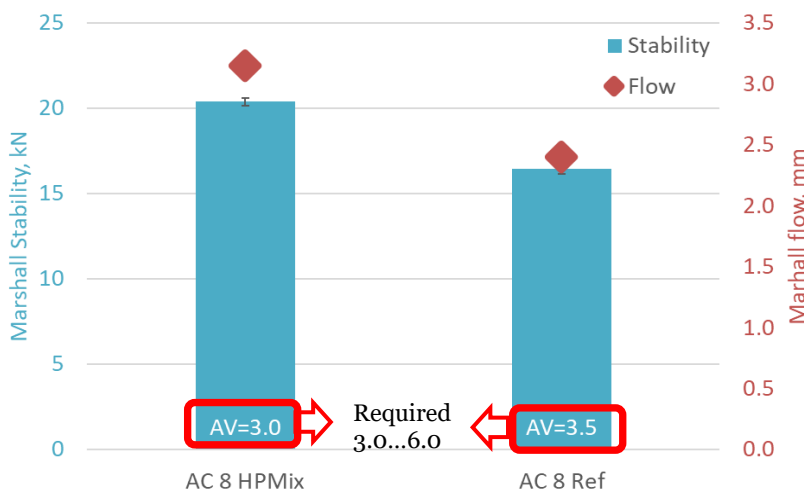


Figure 116: Marshall air voids and Marshall test results of the AC 8 mixture built in Charnadüra test section.

4.2.8 Rutting test

The rutting test results of the of the plant-produced, lab-compacted AC 8 S mixtures are summarized in Figure 117. The requirement according to the Swiss norm SN EN 13108-1 is to perform the test up to 30,000 cycles for "H" asphalt types and up to 10,000 cycles for "S" asphalt type. However, to evaluate the effect of highly modified binder, the test was extended to 90,000 cycles.

It can be seen in the figure that the HPMix test results and the reference mixture results are very similar and both fulfil the requirement of less than 10 % rut depth up to 30,000 cycles as defined for the "H" asphalt type mixture. Extending the test did not provide any added benefit since the trend can be seen already in the phase up to 30,000 cycles.

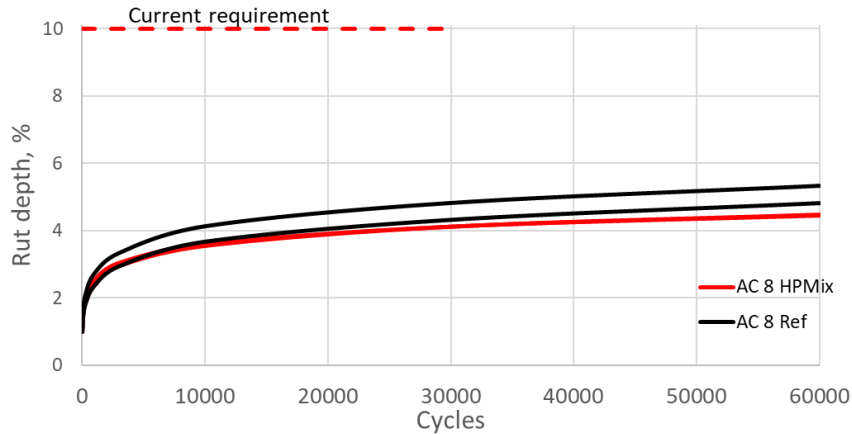


Figure 117: Rutting test results of the AC 8 S mixtures built in the Charnadūra test section. The requirement of "S" type asphalt mixtures is to perform the test up to 10,000 cycles.

4.2.9 Semi-circular bend test

The SCB results, including the Flexibility Index (FI) and the fracture energy, of the plant-produced, lab-compacted AC 8 S mixtures are summarized in Figure 118. The minimum FI of 5.0 for wearing-course mixtures was proposed in an earlier research project titled HighRAP at Empa (Zaumanis, Poulikakos, Boesiger, et al., 2023a). The figure shows that the Reference mixture exhibits slightly higher FI and fracture energy than the HPMix, suggesting a marginally better resistance to crack propagation. However, previous studies have shown that FI is generally not sensitive to the use of polymer-modified binders (Yin, 2023; Zaumanis, Poulikakos, Boesiger, et al., 2023a). Therefore, it is assumed that the observed difference is not due to the polymer content but rather to other factors. Notably, prior research indicates that binder properties and binder content significantly influence FI. The recovered binder content in both mixtures is nearly the same and therefore cannot be the factor that influences the difference between the results. Furthermore, it was shown in the previous subsections that the binder penetration is similar between the two mixtures. The test temperature of penetration and the SCB are the same (25°C) and therefore this is likely the most relevant binder result that relates to the SCB test. Nevertheless, it can be mentioned that other binder properties, including softening point, elastic recovery, and BTSV, and MSCRT showed similar or better performance for the HPMix binder. Of course, the aggregate gradation is also intentionally the same as per design of the study. For these reasons, the cause of the differences in the SCB result is not clear and further testing would be needed to determine it. This was out of the scope of this research.

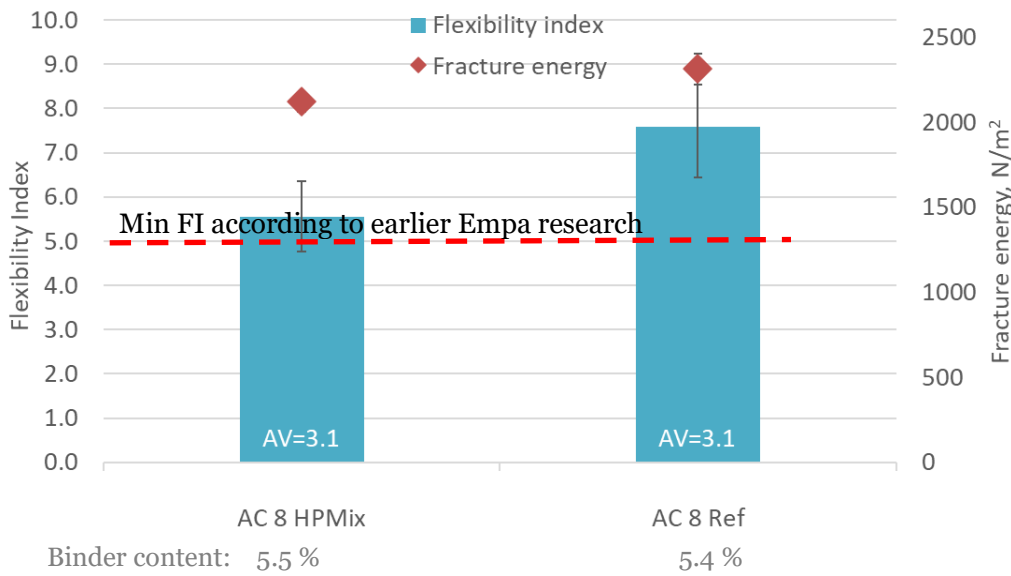


Figure 118: Semi-circular bend test results of the AC 8 S mixtures built in the Charnadūra test section. AV is the air void content of the test samples.

To further analyze the SCB results, the load-displacement curves of all 6 repetitive tests for each material are plotted in Figure 120. It can be seen that the HPMix samples carried a slightly higher maximum load but the post-peak displacement line is slightly steeper compared to the reference sample. Coupled with the smaller fracture energy (the surface area below the curve) this led to a slightly lower Flexibility Index (see Figure 119). For equation to calculate the FI see section 2.2.3.

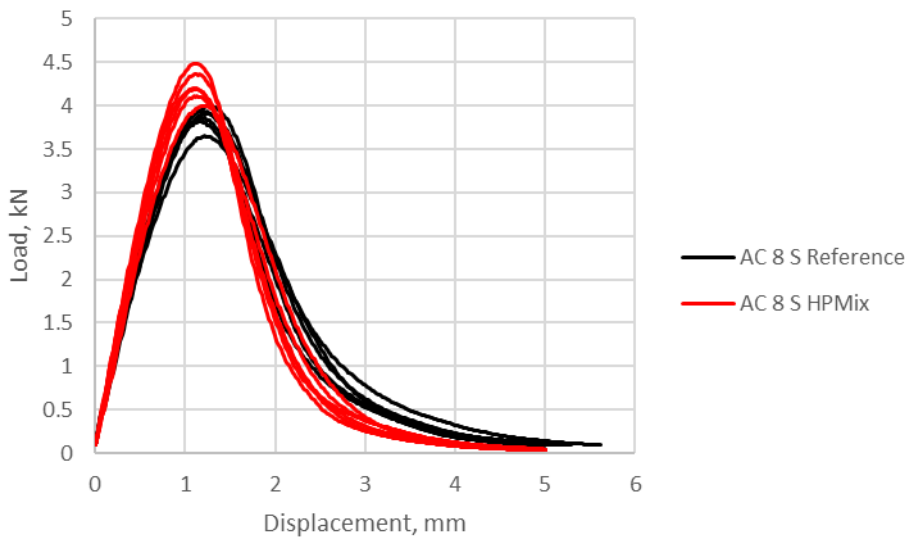


Figure 119: Load-displacement curves of the semi-circular bend test of the AC 8 S mixtures built in the Charnadūra test section.

4.2.10 IDEAL-CT

The IDEAL-CT results of the plant-produced, lab-compacted mixtures, including the CT index and failure energy, are summarized in Figure 120. With other parameters

equal, a higher CT index shows better resistance to crack propagation. The results demonstrate a similar trend to the SCB results discussed in the previous section and show that the Reference mixture has a higher CT index. This indicates a higher resistance to crack propagation. The failure energy of both mixtures is nearly equivalent. Similarly to the discussion of the SCB results, the cause of the differences between the samples is not clear since the binder content, binder penetration and air void content are nearly equivalent for both mixtures. Similar to the SCB Flexibility Index, the CT Index has been shown not to be sensitive toward the polymer content (Yin, 2023).

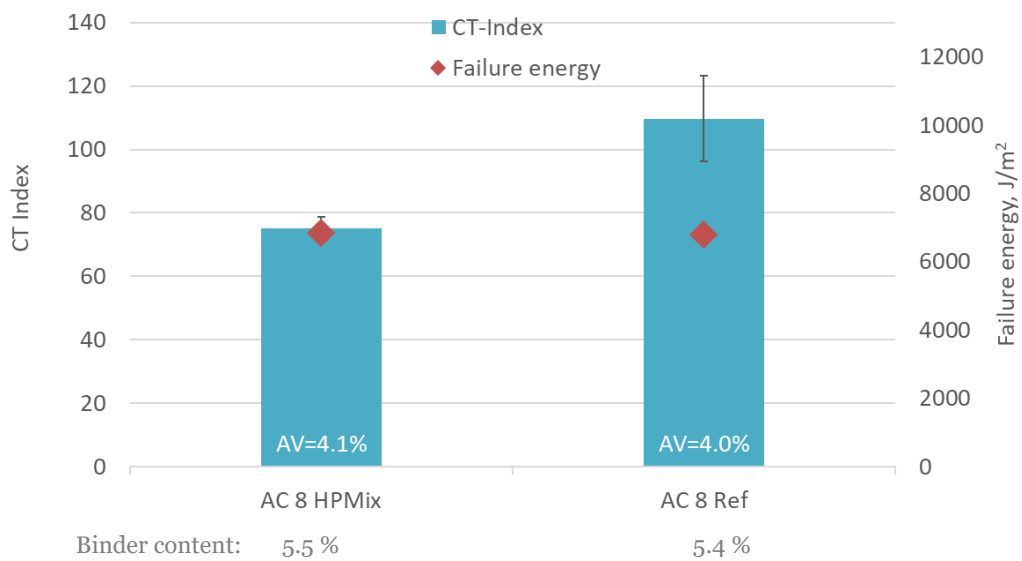


Figure 120: IDEAL-CT results of the AC 8 S mixtures. AV is the air void content of the test samples.

4.2.11 Thermal Stress Restrained Specimen Test (TSRST)

The TSRST results, including the cracking temperature and failure stress, of the of the plant-produced, lab-compacted AC 8 S mixtures are summarized in Figure 121. The air void content for each sample is shown at the top of each column. The error bars demonstrate the range of results for each mix type.

The cracking temperature and the failure stress of the HPMix samples is unknown since the temperature chamber is capable of testing up until -40 °C temperature but the sample had not yet cracked at this temperature. This shows that the mixture has very high resistance to low temperature cracking.

In Switzerland there are no specification requirements for TSRST but in the Alpine region of Austria, the required temperature for mixtures developed using performance-based criteria for wearing courses is -30 °C. This is the requirement for the highest traffic intensity as specified in the Austrian standard ÖNORM B 3580-2:2018-02. It can be seen that both the AC 8 S HPMix and the AC 8 S Ref mixtures clearly fulfil this requirement and therefore both can be considered having high low temperature cracking resistance.

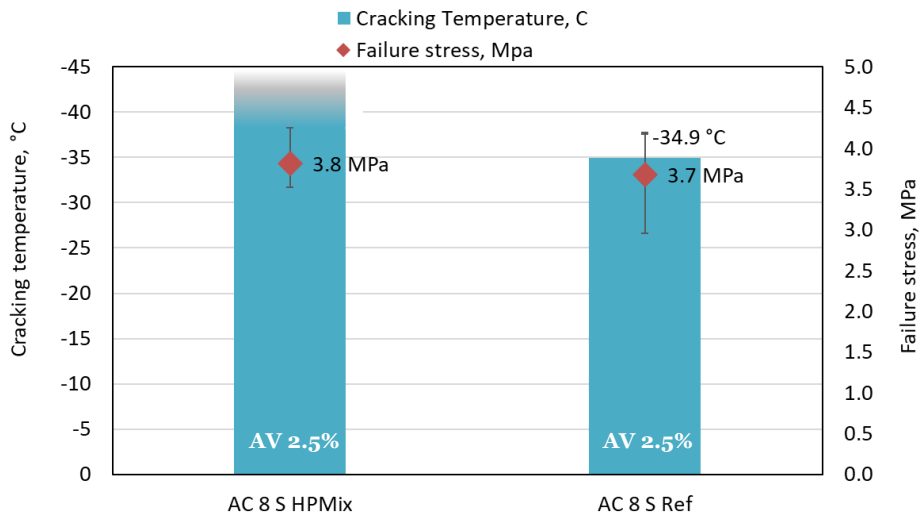


Figure 121: TSRST results of the AC 8 S mixtures. The result of the HPMix samples is not known since was below the temperature range that is supported by the test device (-40 °C). AV is the air void content of the test samples.

4.2.12 Stiffness modulus using indirect tensile test

The stiffness of the plant-produced, lab-compacted mixtures was measured using Indirect Tensile test at 5 different temperatures (-10 °C, 0 °C, 10 °C, 15 °C, and 20 °C). At each temperature, the testing was done at three different frequencies (0.1, 1, and 10 Hz). The samples were prepared from plant-produced asphalt mixtures. This test method was selected since it allows testing both road cores and laboratory compacted samples (which is not possible using the 2-point bending test using trapezoidal specimen).

The samples were prepared by compacting them to 4.5 % air void content (by dimensions) using Gyratory compactor. After cutting to the required height, the sample air voids were measured using the surface-saturated dry method. The final air voids content of the HPMix samples is 2.1 % and for the Reference samples 2.2 %. Since the air void content is nearly equivalent, it is considered that it does not influence the conclusions about the comparison between the two mixtures.

The test results at the five different temperatures and three frequencies at each temperature are demonstrated in Figure 122. It can be seen that the HPMix samples and the reference samples have nearly identical stiffness modulus at all temperatures and frequencies.

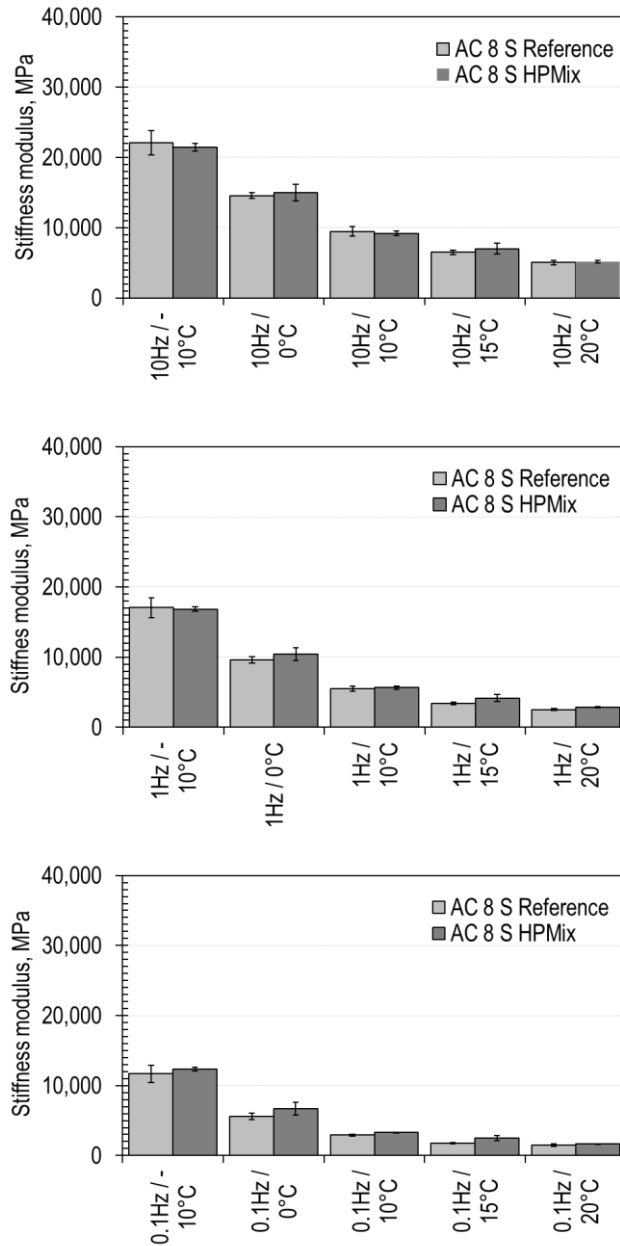


Figure 122: Stiffness modulus of the plant-produced, lab-compacted AC 8 S mixtures at five different temperatures at 10 Hz (top figure), 1 Hz (middle), and 0.1 Hz (bottom)

The testing of stiffness modulus at a range of temperatures and stiffnesses allowed to construct a stiffness modulus master curve. Master curve uses the principle of time-temperature superposition to shift data at multiple temperatures and frequencies to a reference temperature so that the stiffness data can be viewed without temperature as a variable. Further details about the construction of the master curves are provided in the section 4.1.13.

The master curves of the AC 8 S mixtures are shown in Figure 95. The results in this figure are shifted to 15 °C. It can be seen in the figure that the fitting of the mastercurve to the test results is good thus showing the successful application of the time-temperature superposition principle. The results demonstrate that through most of the

frequency range the mastercurves nearly overlap and only at high (frequency which corresponds to low temperature) the reference mixture has a slightly higher stiffness modulus.

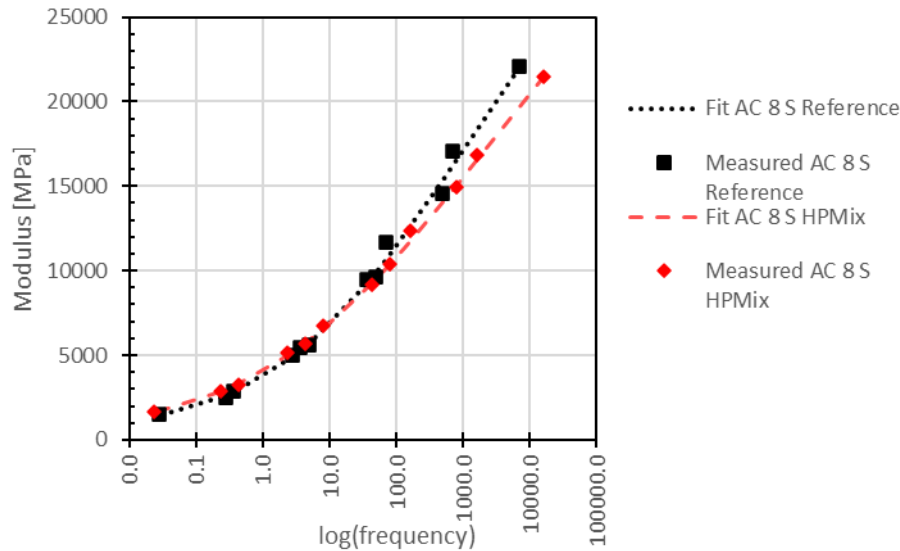


Figure 123: Stiffness master curves of the plant-produced, lab-compacted AC 8 S mixtures. Shifted to 15 °C

Besides plant-produced, lab-compacted specimen test results that were presented above, stiffness modulus was also determined on samples cored from the test section in Charnadüra. The results of the core testing are primarily used for the modelling presented in section 5. However, since the test section was built using the same plant-produced asphalt that was used for producing the lab-compacted samples, it gives an opportunity to compare the stiffness results between these two compaction methods (gyratory compactor and full-scale compaction on a road).

The comparison between the lab-produced ("Gyrator") and road core samples is presented in Figure 95. For each mixture, the results are presented in a separate column. The average air void content for the HPmix road core samples is 5.2 % and for the Reference road core samples - 5.0 %. The difference between these samples can therefore be neglected for the purposes of stiffness evaluation. In comparison, the final air void content of the gyratory-compacted, cut stiffness samples of the HPmix samples is 2.1 % and for the Reference samples - 2.2 %. The difference between the road cores and the lab-produced samples is approximately 3.0 % and can impact the stiffness. Higher air void content typically leads to a significant lowering of stiffness modulus (Zaumanis et al., 2018).

It can be seen in Figure 95 that the gyratory-compacted samples have a higher stiffness modulus compared to the road cores at all temperatures and frequencies. Overall, the relative difference between the samples is slightly higher at low frequencies and lower at high frequencies. The difference is smaller for the reference samples (average 15 % difference across all temperatures and frequencies) as compared to the HPmix samples (average 32 % difference). As mentioned above, one possible cause for the difference is the lower air voids of the gyratory-compacted samples.

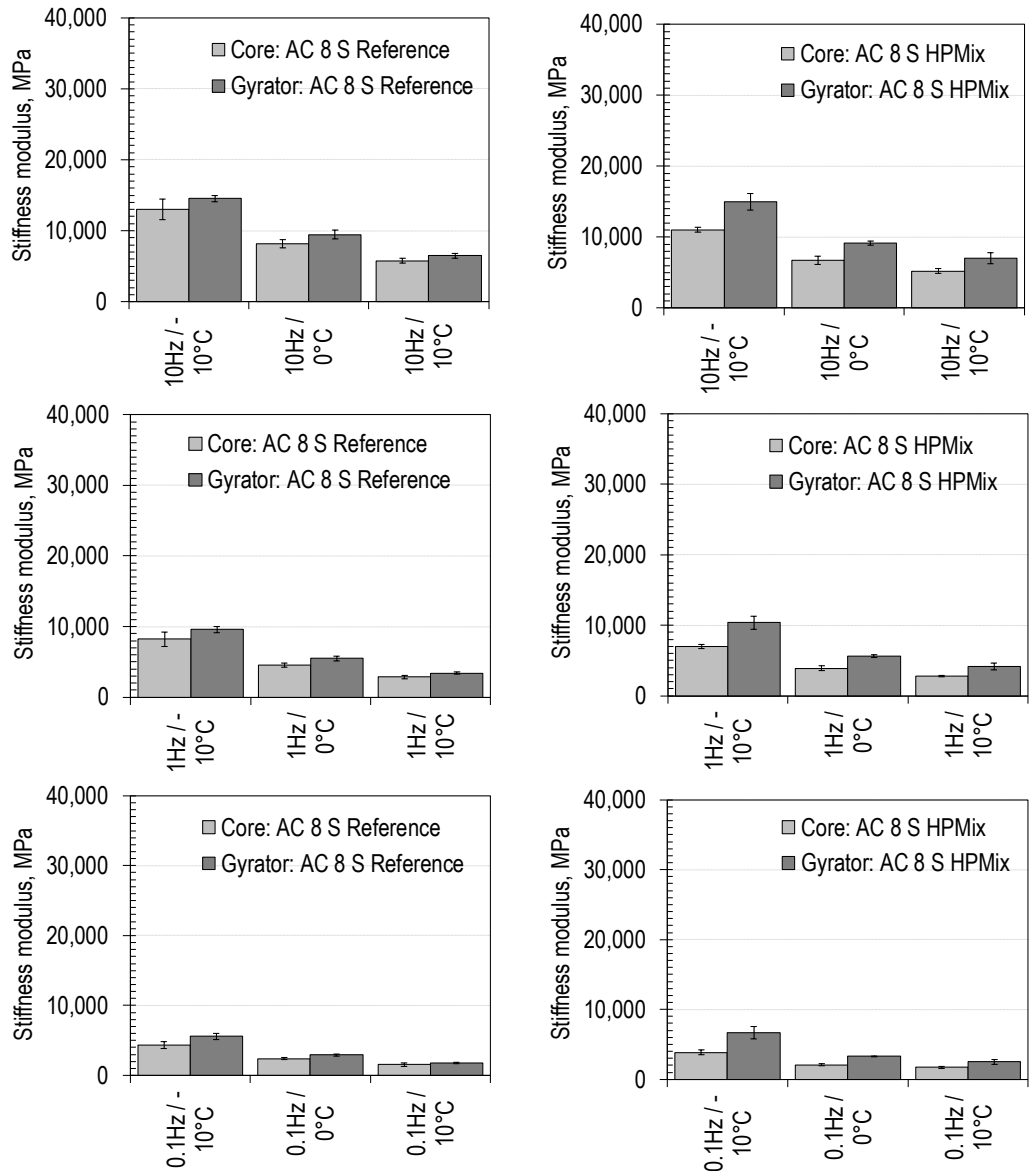


Figure 124: Stiffness modulus of the plant-produced, lab-compacted AC 8 S (denoted as "Gyrator") and road cores from the Charnadūra test section of the same mixtures (denoted as "cores"). Each mixture type is presented in a separate column, and the results are shown for three different temperatures at 10 Hz (top figure), 1 Hz (middle), and 0.1 Hz (bottom). The error bar represents one standard deviation.

4.2.13 Structural capacity with FWD

As already mentioned in section 4.1.16, the structural capacity of the test sections was evaluated through a Falling Weight Deflectometer (FWD) campaign carried out by Infralab SA in September 2024. The left side of Figure 125 show the pavement structure and how they are modelled for the backcalculation using ELMOD software. In this case, the percentage of the layer with high PmB represents 15 % of the total thickness. The backcalculated asphalt layer moduli, corrected to 15°C, are shown the right side of Figure 125 for the RAPMix (RP) and High PmB mix (HP) sections. The average temperature in the pavement during the tests measured by the FWD was 12.7 °C for the Reference pavement and 12.1 °C for HPMix. In this case, the Reference section exhibits slightly higher asphalt stiffness. Correspondingly, the maximum deflections obtained

from the FWD (see Figure 126) are higher for HPMix section. This means that the structural stiffness is slightly less when High PmB is used in the wearing course.

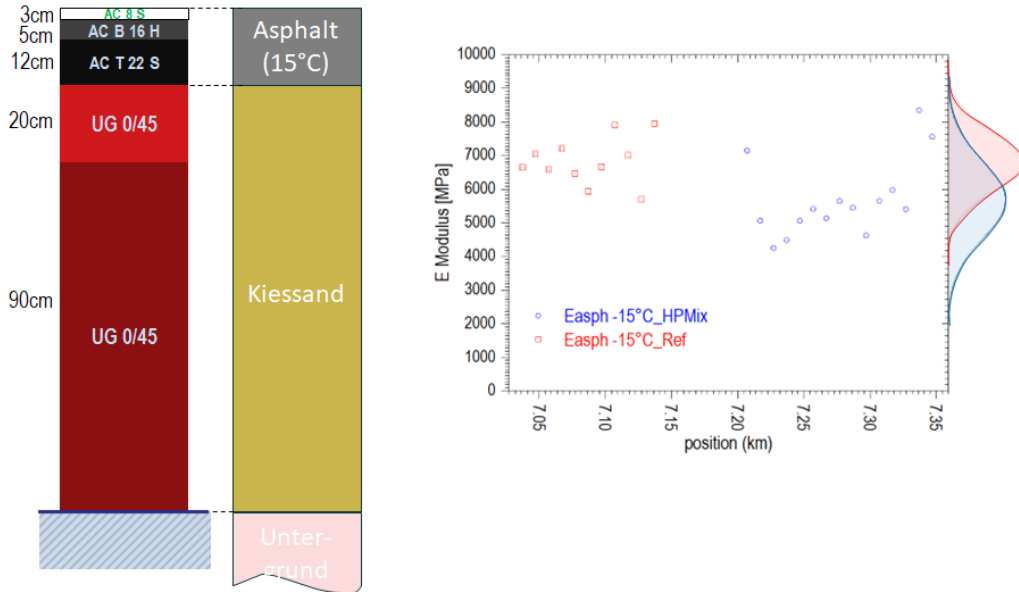


Figure 125: Layer configuration of the test sections and simplification into three layers for backcalculation (left), and backcalculated asphalt layer E-modulus corrected to 15 °C (right).

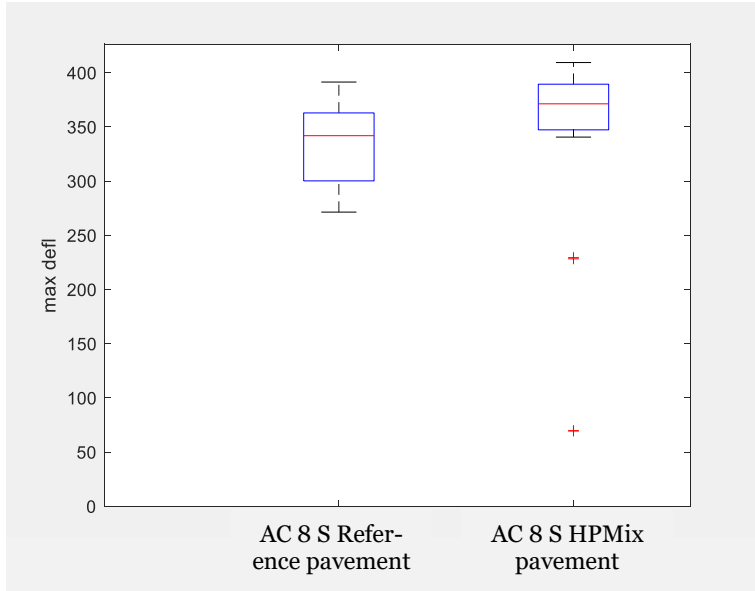


Figure 126: Boxplots showing the maximum deflection measured at the load center for the RP and HP pavement sections.

Figure 127 compares derived FWD indices as explained in section 4.1.16 for both sections. The HPMix section shows slightly higher SCI, BCI, and BDI values compared to the Reference section. A higher SCI indicates a somewhat softer surface response under loading, while higher BCI and BDI values reflect a slightly greater curvature through the base layers, suggesting a more flexible structural behavior. Nevertheless, the overall AREA values are nearly identical, indicating that the general load-bearing capacity and structural efficiency of both sections are comparable.

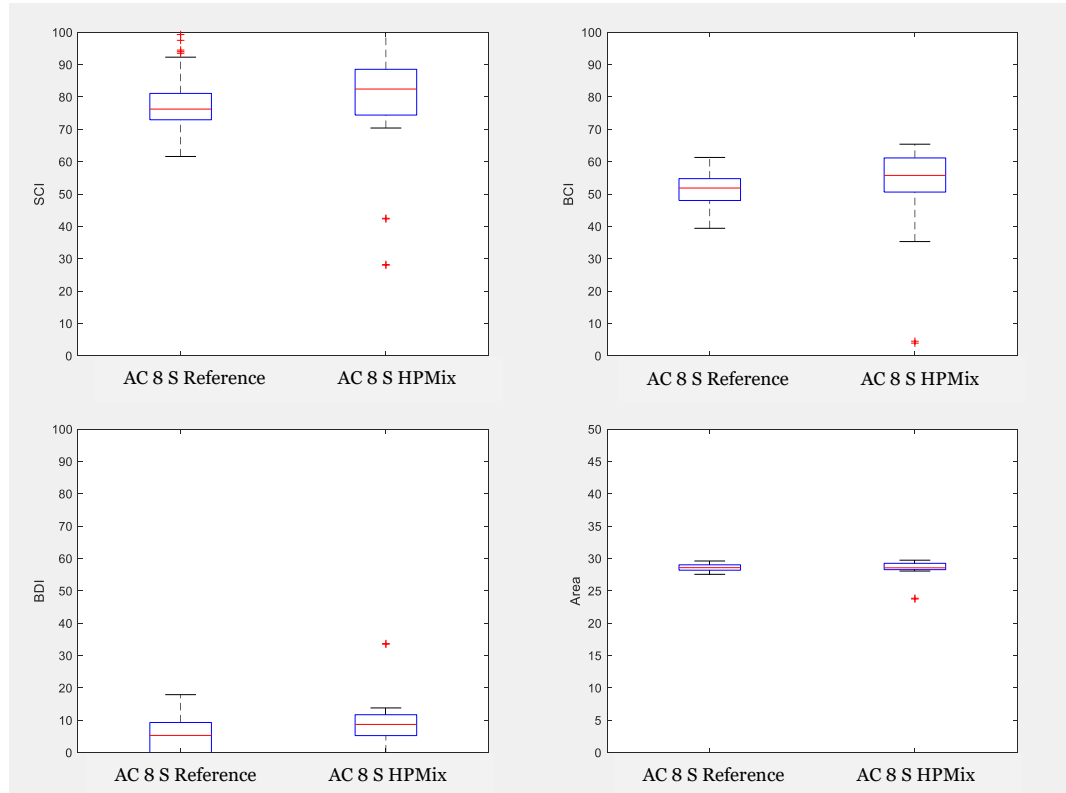


Figure 127: Deflection bowl parameters (SCI, BDI, BCI, AREA) calculated from FWD measurements for the Reference and HPMix sections.

4.2.14 Summary

The results of the AC 8 S test section in Charnadıra are summarized in Figure 128. The table allows to qualitatively compare the results of the HPMix to the reference mixture. The HPMix was produced using a highly polymer-modified binder while the reference mixture was produced using by adding a conventional polymer-modified binder PmB 90/150-60 (CH-E).

Overall, both mixtures provided good performance that corresponds to the current specification requirements. However, as discussed before, the test methods used for quality control do not always offer a reliable way to evaluate the effect of increased polymer content and therefore several performance-based test methods were used in this research.

In can be seen in Figure 128 that the binder tests and low temperature cracking resistance test (TSRST) show superior performance of the highly polymer-modified binder compared to the reference mixture made using conventional polymer-modified binder.

The rutting resistance of both mixtures is similar and very good. Based on the binder test results, it is reasonable to expect better pavement rutting resistance of the HPMix. However, the rutting test conditions were not severe enough to induce significant rutting. Even extending the test did not result in significant damage. Therefore, other changes in test conditions could be considered in the future, for example increasing the test temperature or using another test method (e.g. the cyclic compression test).

The stiffness for both mixtures was similar and the crack propagation resistance was slightly worse for the HPMix compared to the reference mixture. However, based on previous research (Yin, 2023; Zaumanis, Poulikakos, Boesiger, et al., 2023a), it is likely that the differences in the crack propagation are not related to the polymer content since the employed test methods are not sensitive towards polymer content. Overall, the results allow to conclude that the use of highly polymer-modified binder in the wearing course:

- Improves the performance of the wearing course
- Binder characterisation using conventional tests does not fully demonstrate the benefits of using highly polymer modified binder. BTSV and MSCR at 10 kPa are suitable means for binder characterization.
- More severe conditions are required for the rutting resistance test to discriminate between the performance.

Mixture	RAP content	Binder tests			Rutting resistance	Crack propagation resistance		Stiffness	Low temp. cracing resistance	
		ER	BTSV	MSCR	FRT	SCB	IDEAL-CT	ITT	TSRST	
AC 8 S	HPMix	0%	↗	↑	↑	→	↘ ¹	↘ ¹	→	↑
	Reference	0%	●	●	●	●	●	●	●	●

Legend:

- reference mixture result
 - ↑ significantly better performance
 - ↗ slightly better performance
 - similar performance
 - ↘ slightly worse performance
 - ↓ significantly worse performance
 - ER Elastic Recovery (binder)
 - BTSV Binder fast characterisation test
 - MSCR Multiple stress creep recovery test (binder)
 - FRT French Ruting Tester (mixture)
 - SCB Semi-circular bend test (mixture)
 - IDEAL-CT Indirect tensile asphalt cracking test (mixture)
 - ITT Indirect tensile test (mixture)
 - TSRST Tensile stress restrained specimen test
- ¹ SCB and IDEAL-CT tests are not sensitive to polymer content

Figure 128: Summary of the AC 8 S test section test results

4.3 SDA 4-12 test section, K244, Rapperswil IO, Aargau

Semi Dense Asphalt (SDA) is a type of asphalt surface layer that is intended to reduce traffic noise through a relatively high air void content. However, the high air voids also make it prone to raveling (loss of aggregates from the surface). It is hypothesized that highPmB would improve the raveling resistance due to the higher polymer content.

The SDA test section using highly polymer-modified asphalt in Kanton AG was built in 2020 and the relevant test results are included in this report. In 2024 road cores were taken from the built pavement and new lab-produced mixtures were prepared for testing. Provided by the producer, the lab mixture was produced using same mixture recipe and materials from the same sources as in 2020.

Objective

The objective of the test section in Kanton Aargau was to determine the benefits of using high content polymer modified binder in SDA type mixtures, especially focusing on the potential benefits toward raveling resistance.

4.3.1 Mixtures and test section location

The test section is located in K244 Rapperswil IO at the following locations:

- SDA 4-12 Reference section: RBBS D578+70 to D582+65 direction Aarau. Binder PmB 45/80-65 (CH-E) was used for this section.
- SDA 4-12 HPmix 45/80-80 section: RBBS D578+70 to D582+65 direction Brugg. Binder High PmB 45/80-80 was used for this section.

The SDA in both sections are 3cm thick and were built in 2020. The location of the test section and the location of the road cores that were taken after the construction is shown in Figure 129.



Figure 129: Location of the SDA test section in Canton AG and the location of the road cores that were taken after the construction.

4.3.2 Methodology

Since the SDA test site that was constructed in 2020 and this project started in 2023, there are various sample types tested and we also used the test results of the reports from the original construction. In total, four types of results are reported in this section and the following test results are reported from each:

1. **Mixture and binder results from the samples collected during the construction of the test section in 2020.** The results include penetration, softening point, elastic recovery, BTSV, DSR temperature sweep for binder and TSRST for mixture.
2. Mixture and recovered binder test results from the road cores that were cored soon after construction of the test section in 2020. The results include pavement air voids, and Leutner test results.
3. **Mixture and recovered binder test results from the road cores that were cored during the HPmix project in 2024.** These results include penetration, softening point, elastic recovery, BTSV, MSCR, DSR temperature and frequency sweep on recovered binder, as well as pavement air voids, SCB test, Cantabro test, Leutner test on the cores.
4. **Mixture results from the samples produced in the Empa laboratory during the HPmix project in 2024.** The materials and the mixture recipe for these mixtures was obtained from Biturit AG and matched that of the original mixture constructed in 2020. Of course, some deviations in the materials properties are possible even though their origin was the same as during the original construction. For these mixtures, the results include Marshall test and Marshall air voids, rutting test, SCB test, IDEAL-CT, and TSRST. Binder was not recovered from these mixtures.

A complete description of each test method is provided in section 2.

4.3.3 Conventional binder test results

The conventional binder test results are summarized in Table 14. It contains results from the binder recovered from the mixtures in 2020 and recovered binder test results from the road cores obtained in 2024. Thus, effectively these are the same mixtures. It can be seen in the table that both the reference and the HPmix binders have aged during the 4 years after construction: the penetration has reduced while the softening point has increased. The changes are of similar magnitude for both binders. The elastic recovery has slightly decreased for the HPmix binder while it has slightly increased for the reference binder.

Binder test results from the SDA section				
Sampling	Mixture	Penetration, 0.1*mm	Softening point, °C	Elastic recovery, %
Mixture during construction 2020	HPmix 45/80-80	58.0	88.3	95.0
	Reference PmB 45/80-65 CH-E	45.0	63.6	68.0
Road cores 2024	HPmix 45/80-80	23.3	95.2	87.0
	Reference PmB 45/80-65 CH-E	17.7	69.8	72.1

Table 14: Binder test results from SDA test section

4.3.4 BTSV results

The BTSV test results from the SDA test section are summarized in the Figure 130. The figure includes the road core results from 2024 as well as the results from the original construction, including the recovered binder from the mixture and the original virgin binder. The samples from the original construction hold the year "2020" in their abbreviation. The virgin binder samples are shown using crosses while the binders recovered from a mixture are shown using circles.

For comparison, the binders from the HPMix test section in Oberalpstrasse, Canton GR are also included in the figure since these binders have the same grade. Likewise, the HPMix project results from the hard binder grade are also included in the figure. It can be seen in the figure that the reference binder and the HPMix binder can be clearly differentiated based on the phase angle: for the samples with high polymer content the phase angle is considerably lower. The virgin HPMix binder from 2020 as well as the HPMix binder recovered from the 2020 road cores are located in the proposed box for the highly polymer-modified binders.

It can also be seen that the four years of filed aging has caused an around 13-14°C increase in the BTSV temperature and thus the results are not within the proposed boundary box of the hard binder grade. Overall, the aged binder results are located in the same region as the aged laboratory-aged binders thus confirming the validity of the binder aging protocol.

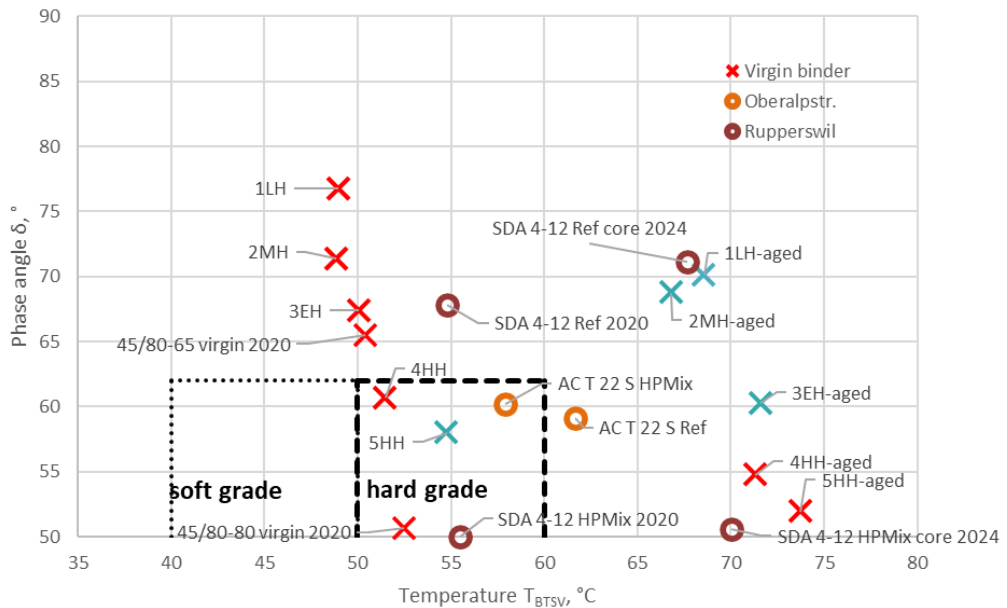


Figure 130: BTSV results from the SDA test section. For comparison, the recovered binder results from the AC T 22 S test section are as well as the virgin hard binder test results are also included in the figure

Figure 131 holds the BTSV results of the binder recovered from the road cores that were sampled in 2024. It can be seen that there is a significant difference in the phase angle between the HPMix binder and the reference binder. Based on the shape of the phase angle line it can be stated that the polymers in the HPMix binder are still active and ensure a highly elastic response over a wide range of temperatures.

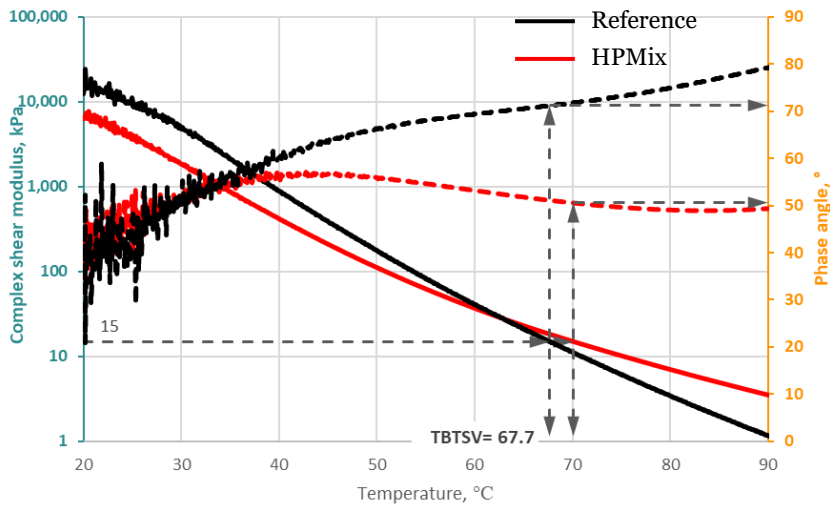


Figure 131: BTVS results of the recovered binder from the road cores (2024) of the SDA sections (dotted line – phase angle, solid line – complex shear modulus)

The BTVS results from the binder extracted from the original mixture in 2020 are shown in Figure 132. These figures are extracted from the report by Consultest AG. It can be seen that also the original binders had a significant "curling" in the phase angle which is evidence of the polymer activity. The curling is slightly less pronounced compared to the binders recovered in 2024 (shown in Figure 131).

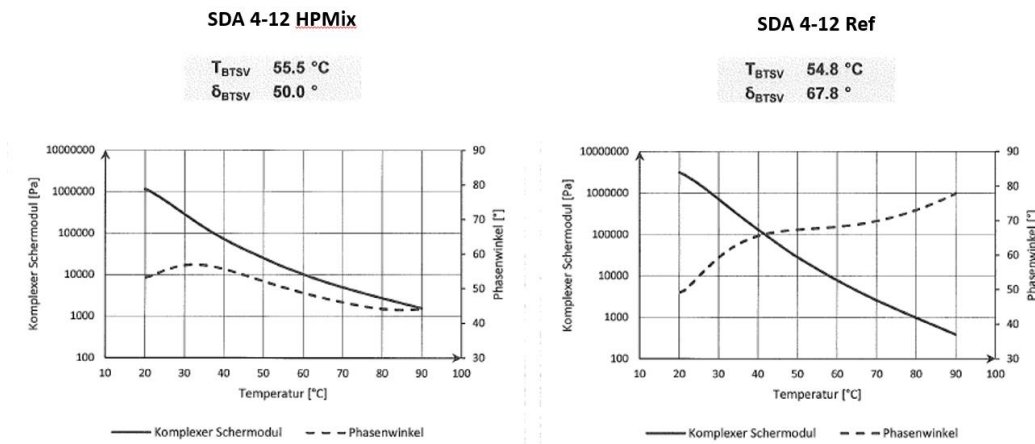


Figure 132: BTVS results of the recovered binder from the mixture (2020) of the SDA sections (from Consultest AG report No. 0953-20-4)

4.3.5 MSCR test results

The MSCR results at 64°C and 10 kPa of the binder recovered from the SDA road cores from 2024 are summarized in Figure 133. For reference the MSCR test results of the hard virgin binders are also included in the table. Likewise, the results from the recovered Oberalpstrasse binder are also included in the figure.

It can be seen in the figure that the HPMix SDA sample even after aging fulfils the proposed criteria for highPmB. The reference binder however has significantly lower recovery and higher creep compliance thus the binders can be clearly distinguished.

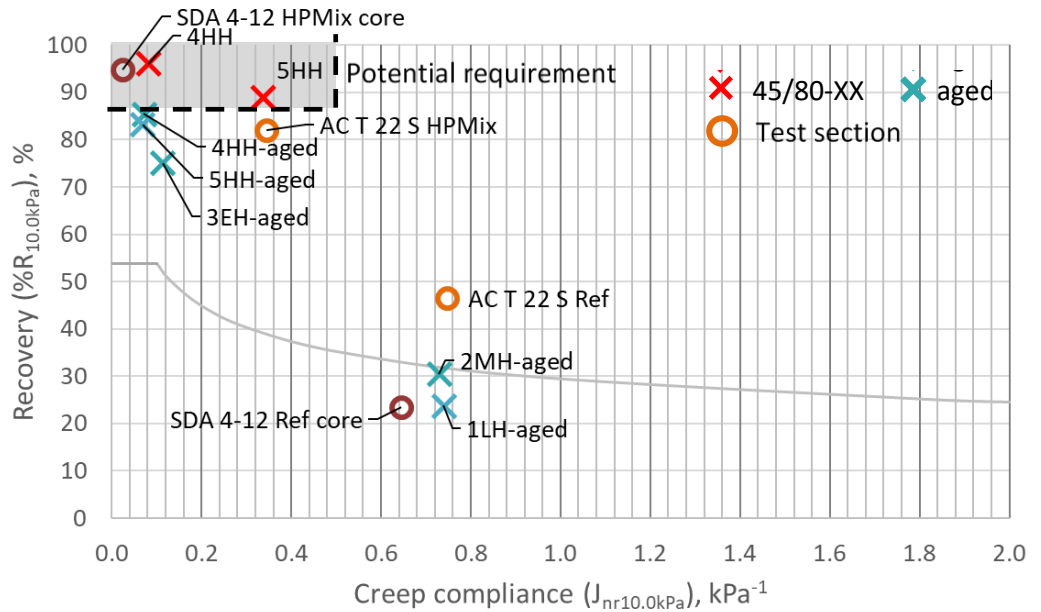


Figure 133: MSCR results of the binder recovered from the SDA road cores in 2024. Test conditions: 10 kPa and 64°C.

Figure 134 presents the MSCR results for each of the recovered SDA binders that were reported in the previous figure. The results show the differences in recovery and strain throughout the ten 10 kPa loading cycles. It can be clearly seen that the reference binder has a higher strain accumulation and lower recovery.

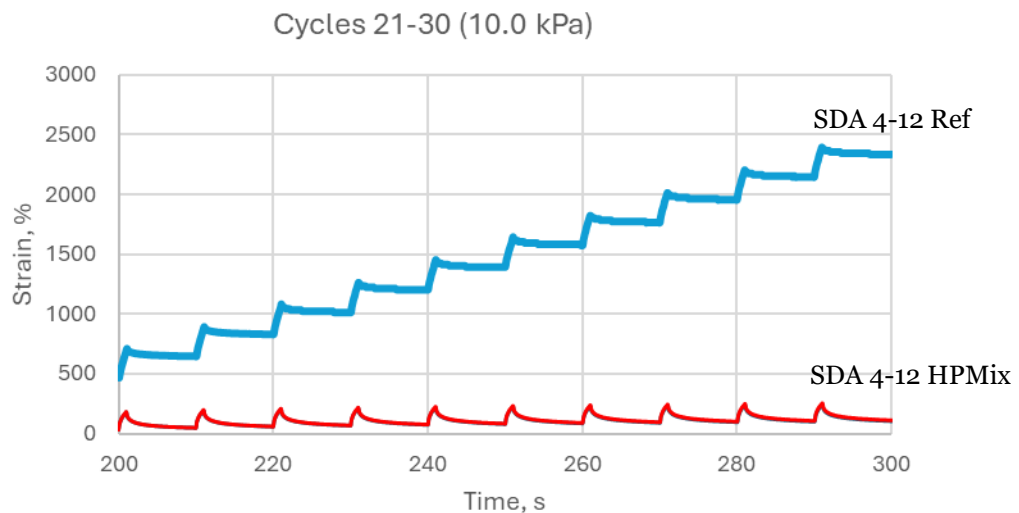


Figure 134: MSCRT cycles for the 10kPa at 64°C

4.3.6 Frequency sweep

The recovered binder test results from the original construction report (Consultest report No.0953-20-4) includes DSR the test results at 1.59 Hz over a range of temperatures. To compare the results from the 2024 road cores, the same testing protocol was repeated.

The results are summarized in Figure 135 and Figure 136. It can be seen that the phase angle is relatively similar between the corresponding samples at construction (2020)

and in 2025. However, due to aging the complex modulus is significantly higher for the binder recovered from the cores.

Based on the test results, a calculation was performed to determine the high Performance Grade (PG) according to ASTM D6373-16. The SDA H had a high PG of 109 °C while the SDA R, a PG of 92°C. As mentioned in the introduction, the PG is not well suited for testing of polymer modified binders therefore these results should be considered only informative.

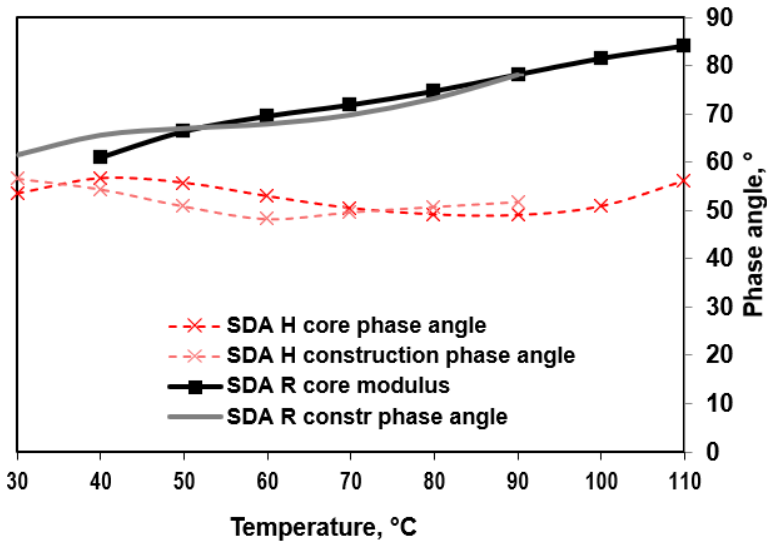


Figure 135: Phase angle at 1.59 Hz test results at various temperatures for the binder from SDA mixtures (H- HPMix, R-Reference)

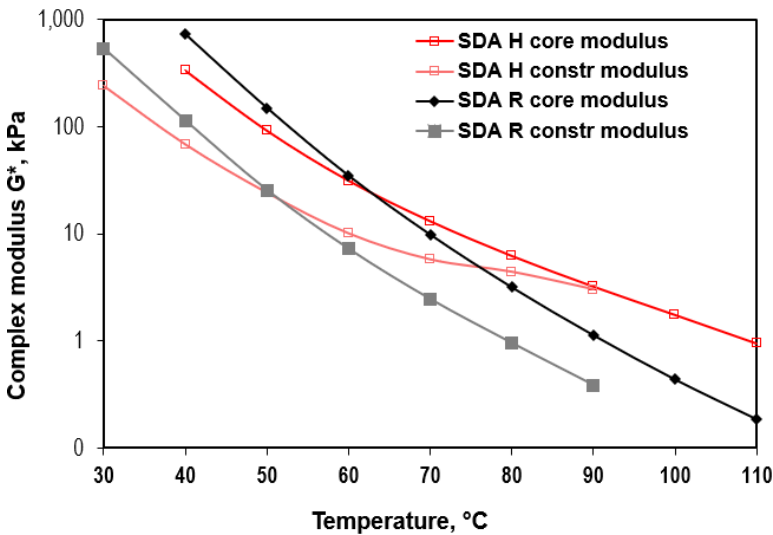


Figure 136: Complex modulus test results at various temperatures for the binder from SDA mixtures (H- HPMix, R-Reference). "Constr" refers to modulus from extracted binder during construction and "Core" refers to the road cores taked in 2024.

A master curve from a frequency sweep, constructed using the time-temperature superposition principle is shown in Figure 137. The results show that the binder from the HPMix is less frequency (or temperature) dependent which in the appropriate climatic conditions would ensure better performance of the mixture.

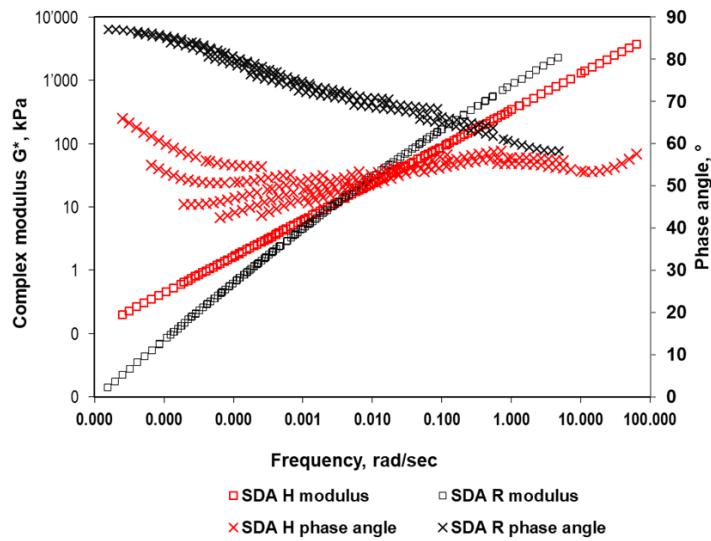


Figure 137: Mastercurve of the SDA binder from the year 2024 road cores (H- HPMix, R-Reference)

4.3.7 Pavement layer tests

The pavement layer air voids and thicknesses are summarized in Table 15. The table holds information from the 2020 Constultest AG report No. 0953-20-4 and the measurements done on the road cores cored and delivered to Empa in 2024.

It can be seen in the table that the highly modified layers have a higher air void content compared to the reference mixtures. The results are also above the requirement from the Swiss norm VSS 40 436. It has to be considered that workability of highPmB mixtures may be lower compared to conventional PmB mixtures due to the high polymer content. Therefore, the compaction energy might need to be higher to reach the same air void content. This could be one possible explanation of the higher air void content in the HPMix layer.

SDA layer properties

Sampling	Mixture	Air voids, %	Layer thickness, mm
Road cores – after construction (2020)	HPMix 45/80-80	16.0	33.5
	Reference PmB 45/80-65 CH-E	14.1	30.0
Road cores – HPMix (2024)	HPMix 45/80-80	15.9	36.0
	Reference PmB	13.5	30.0
	Required PmB 45/80-68 CH-E	10.0...14.0	

Note 1: Maximum density from the Canton AG test results from 2020;

Note 2: For the road cores after construction - average results BK1,3,5,7 for ref. and BK12,14,17,20 for HPMix.

Table 15: SDA layer properties in the Canton AG test section

4.3.8 Marshall air voids and Marshall test

The Marshall samples were compacted using the recipe and materials that were delivered by the asphalt producer to match the recipe of the asphalt in the SDA test section. The results are summarized in Figure 138. The most important parameter in the figure is the air voids and it can be seen that the results fit within the required range for SDA mixtures.

The Marshall stability and Marshall flow values are not required for SDA-type mixtures according to Swiss norms. The results show a slightly higher stability and flow for the HPMix samples.

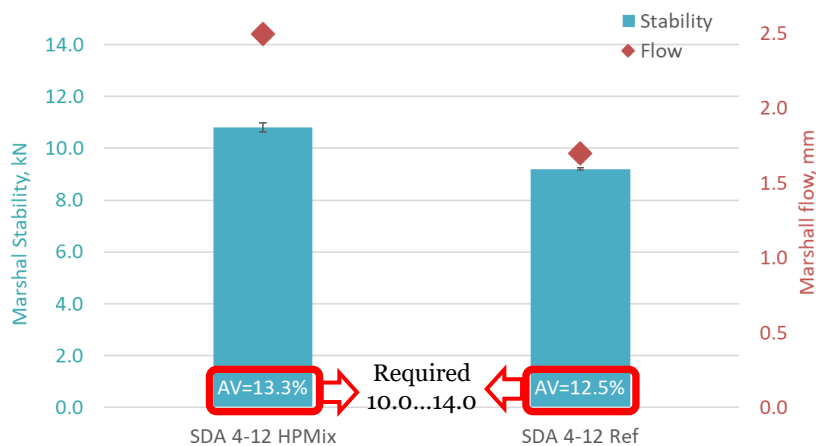


Figure 138: Marshal test results of lab-mixed SDA mixtures

4.3.9 Rutting test

The rutting test on the lab-mixed, lab compacted mixtures was performed according to the standard procedure described in section 2.2.4. However, instead of stopping at 30,000 cycles the test was extended to 90,000 cycles to evaluate if the additional cycles would demonstrate any advantage of the high polymer content compared to the conventional PmB.

The rutting test results are summarized in Figure 139 and show that both mixtures have low rutting that clearly fulfils the requirements. The difference between the mixtures is not significant even after the additional load cycles. There is therefore no advantage of extending the test beyond the current 30,000 cycles.

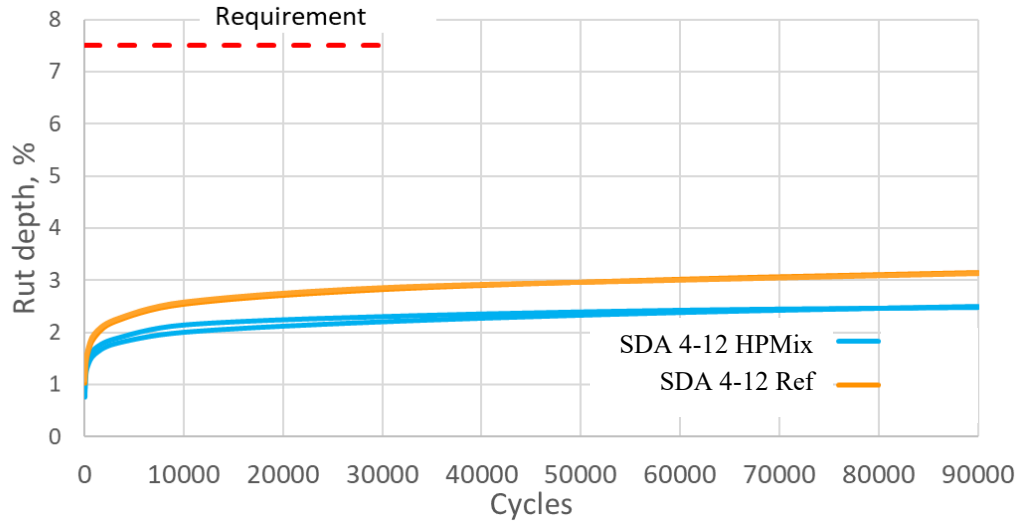


Figure 139: Rutting test results of the lab-mixed SDA mixtures

4.3.10 Semi-circular bend (SCB) test

The SCB results of the lab-produced, lab-compacted mixtures and the road cores from 2024 are summarized in Figure 140. The road cores had a thickness of around 30 mm which is less than the standard 50 mm used for samples prepared in the laboratory. The SCB test is sensitive towards sample thickness and therefore a correction factor was used to estimate the expected flexibility index and fracture toughness if the samples were 50 mm high. The procedure for the correction is borrowed from (Barry, 2016a; Rivera-Pérez et al., 2021) and described in the section 2.2.3.

The test results in Figure 140 show that the Flexibility Index (FI) of the lab-produced mixtures is higher than that of the road cores. Since the test is sensitive to binder properties, this is likely related to the aged binder in the road cores. It has to be noted that the binder was not recovered from the lab mixtures and therefore the properties are not available. It, however, can be assumed that the binder is softer than that in the road cores.

The test results also show that the HPMix samples both for the lab mixtures and the road cores have a higher average FI and a higher fracture energy compared to the corresponding reference mixture. This demonstrates an increased resistance to crack propagation. However, it has to be noted that previous research has suggested that the FI is not sensitive towards the binder polymer modification (Yin, 2023; Zaumanis, Poulidakos, Boesiger, et al., 2023a). Therefore, the improved cracking resistance likely is not related to the polymer content in the mixtures.

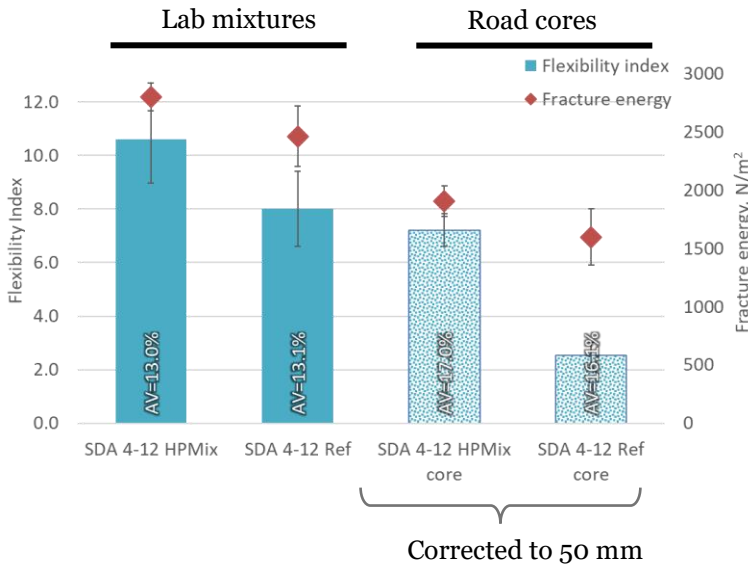


Figure 140: Semi-circular bend test results of the lab-mixed SDA mixtures and the road cores from 2024. AV is the air void content of the test samples.

4.3.11 IDEAL-CT

The IDEAL-CT results of the lab-produced, lab-compacted mixtures are summarized in Figure 141. It can be seen that the mean CT index of the reference mixture is slightly higher compared to the HPMix sample while the failure energy of the reference sample is slightly lower. Similar to the SCB Flexibility Index, the CT Index has been shown not to be sensitive toward the polymer content (Yin, 2023).

The IDEAL-CT test was included in the testing plan mainly to compare the results with the SCB test flexibility index. Comparing the CT index to the results in Figure 140 one can see that the ranking of the results is opposite to the FI results.

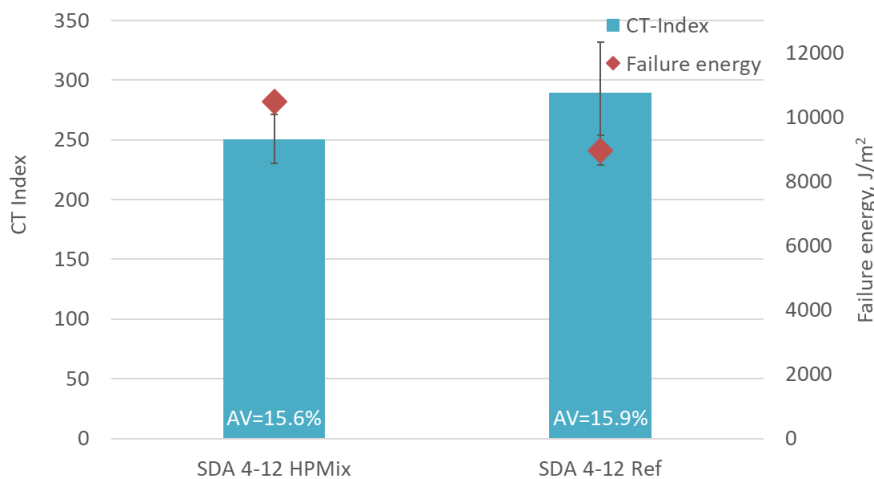


Figure 141: IDEAL-CT results of the lab-produced SDA mixtures. AV is the air void content of the test samples.

4.3.12 Cantabro test

Cantabro test shows resistance to raveling. The test results of the lab-produced, lab-compacted mixtures as well as the road cores are summarized in Figure 142. The figure includes three types of samples tested using two types of procedures:

1. The first two samples in Figure 142 were tested using the standard Cantabro test as described in 2.2.9. It can be seen that the mass loss was very small and the difference between the samples is not substantial.
2. The second pair of samples was tested using a modified Cantabro test. This test was intended to induce higher mass loss. The procedure was modified as follows:
 - 1 standardized metal balls from the LA test were used during the test.
 - Freeze-thaw cycles were carried out as follows: the samples were vacuum saturated with water and frozen in a water bucket at -18°C for 16 h. The temperature was then increased to 60°C for 24 h. Five such freeze-thaw cycles were carried out.

In the Figure 142 second pair of samples show the results of the modified Cantabro test. One can see that here, just like for the first two samples, only small mass has been lost during the test and the difference between the samples is not substantial.

Since the modified test did not induce additional damage, the road cores were without the freeze-thaw cycles while still using the 11 steel balls. The results of the road cores show a higher mass loss compared to the lab-produced samples in Figure 142. However, partially this is due to the fact that the samples were 30 mm high instead of 50 mm like it is for the lab samples. The smaller initial mass means that a similar absolute mass loss would lead to a higher percentage mass loss.

Overall, the Cantabro test did not show a significant difference between the samples with the highly modified binder and samples with conventional polymer modified binder. Photos of representative samples after testing with of the testing procedure is shown in Figure 143. Despite the fact that that the advantage of using highly polymer-modified binder was not demonstrated clearly with these results, it is possible that there is an advantage of using the high PmB which the Cantabro test can not capture. Therefore, other methods for determining the resistance to raveling should be considered.

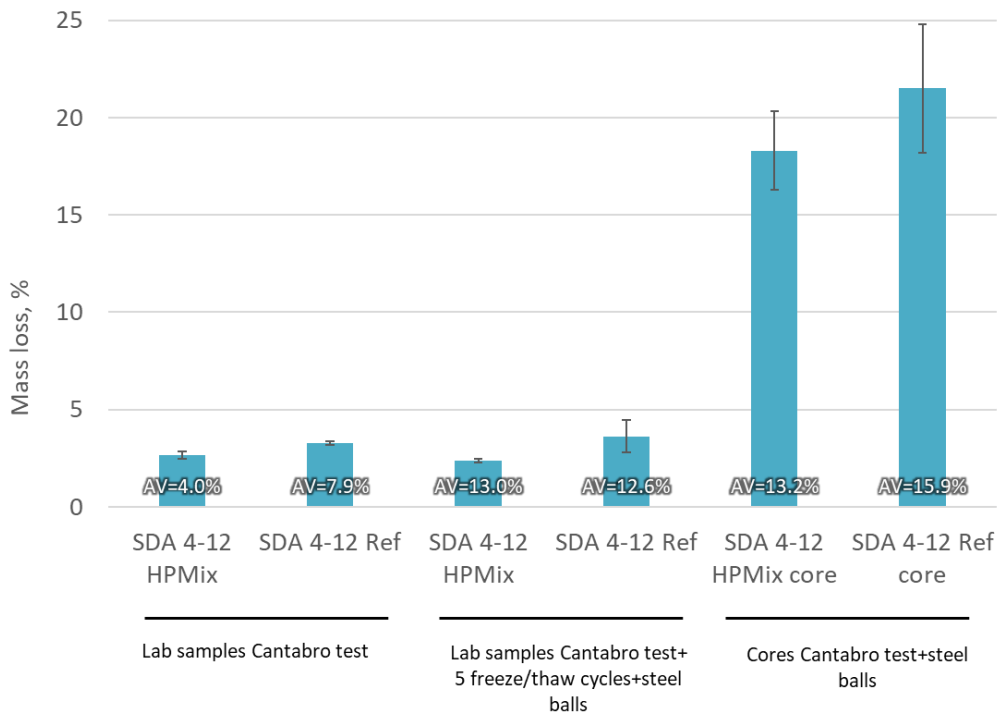


Figure 142: Cantabro test results for lab-produced SDA samples and road cores. AV is the air void content of the test samples.



Lab-prepared samples, tested according to the standard (left: HPMix, right: reference)



Lab-prepared samples, tested after 5 freeze/thaw cycles and steel balls (left: reference, right: HPMix)



Road cores, tested according using steel balls (left: HPMix, right: reference)

Figure 143: Cantabro test samples. Top: laboratory-prepared specimen

4.3.13 Stiffness

The stiffness of the SDA 4-12 road cores was measured using indirect tensile test at 4 different temperatures (-10 °C, 0 °C, 10 °C, 15 °C). At each temperature, the testing was done at three different frequencies (0.1, 1, and 10 Hz). The samples were prepared from road cores that were taken in 2024.

After cutting to the required height, the sample air voids were measured using the surface-saturated dry method. The average air void content of the HPMix samples is 15.9 % and for the Reference samples – 13.5 %.

The test results at the four different temperatures and three frequencies at each temperature are demonstrated in Figure 144. It can be seen that the HPMix samples have a somewhat lower stiffness modulus. Partially this can be attributed to the higher air void content since higher air void content typically leads to lower stiffness.

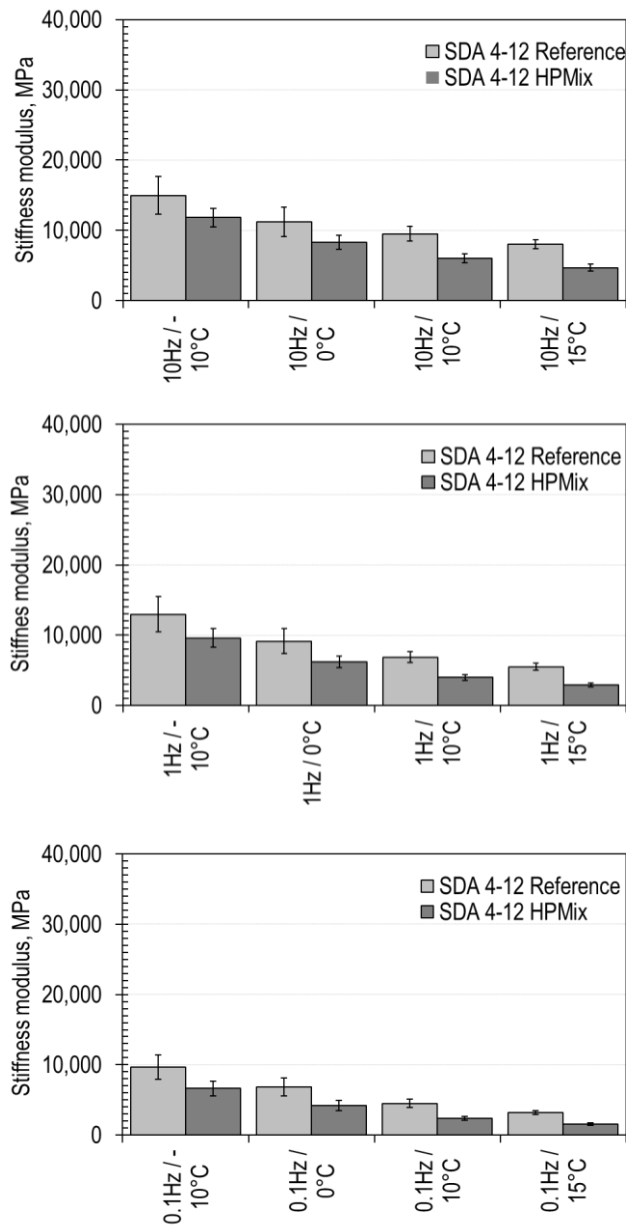


Figure 144: Stiffness modulus of the SDA 4-12 road cores from 2024 at four different temperatures at 10 Hz (top figure), 1 Hz (middle), and 0.1 Hz (bottom)

The testing of stiffness modulus at a range of temperatures and stiffnesses allowed to construct a stiffness modulus master curve. Master curve uses the principle of time-temperature superposition to shift data at multiple temperatures and frequencies to a reference temperature so that the stiffness data can be viewed without temperature as a variable. Further details about the construction of the master curves are provided in the section 4.1.13.

The master curves of the SDA 4-12 mixtures are shown in Figure 145. The results in this figure are shifted to 15 °C. It can be seen in the figure that the fitting of the results to the mastercurve model is good. The results demonstrate that throughout the frequency range the road cores from the reference mixture have a considerably higher stiffness. Like mentioned before, partially this can be attributed to the differences in air void content between the samples.

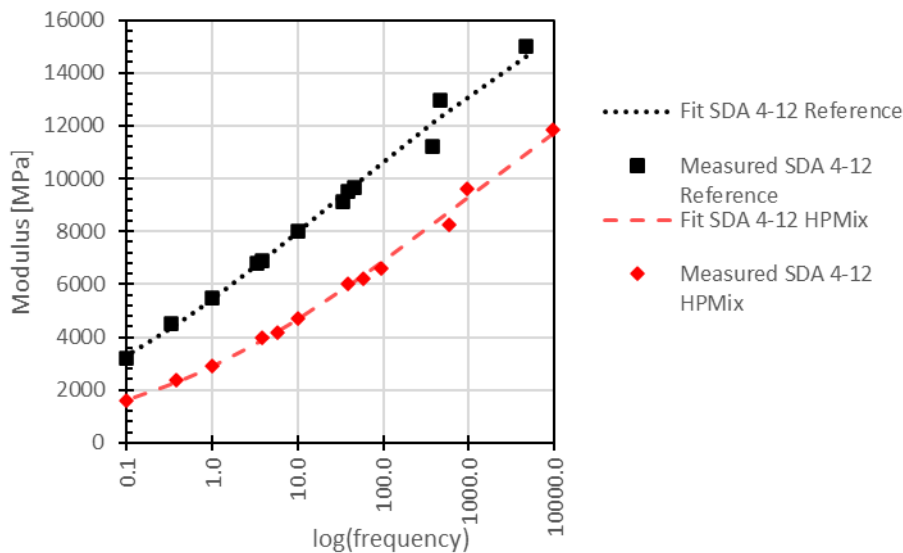


Figure 145: Stiffness master curves of the SDA 4-12 road cores from 2024. Shifted to 15 °C

4.3.14 Thermal stress restrained specimen test (TSRST)

The TSRST results are summarized in Table 16. The figure shows results from the lab mixtures as well as results from the samples that were prepared using the plant-produced mixture from construction of the test section in 2020.

It can be seen in the table that for the lab mixtures the HPmix samples have a lower thermal cracking temperature while the failure stress is similar for both samples.

The cracking temperature of the construction site mixtures is 5-6°C lower compared to the lab mixtures. However, the trend is similar: the HPmix samples have a lower cracking temperature compared to the reference mixture which indicates better resistance to low-temperature cracking. The HPmix samples from the construction exhibit slightly higher failure stress compared to the reference mixtures.

TSRST results of the SDA test section			
Sampling	Mixture	Cracking temperature, °C	Failure stress, MPa
Construction (2020)	HPMix 45/80-80	-30.2	4.2
	Reference PmB 45/80-65 CH-E	-24.0	3.6
Lab mixtures (2024)	HPMix 45/80-80	-35.0	3.6
	Reference PmB 45/80-65 CH-E	-31.5	3.6

Table 16: TSRST results of the SDA mixtures (the construction results are from the Consultest AG report No. 0953-20-4)

4.3.15 Leutner test results

Leutner test results are summarized in Table 17 which include results from the road cores that were gathered soon after construction of the test section in 2020 as well as the results from the road cores that were gathered in 2024. It can be seen that in both cases, the reference samples exhibit higher breaking force between the layers compared to the HPMix samples. Moreover, the HPMix samples do not fulfil the minimum interlayer bond force requirement which is a minimum of 15 kN. Since the construction technology and the tack coat material were equal, one hypothesis is that a chemical reaction between the highPmB and the tack coat reduced the adhesion. Verification of this hypothesis would need further research that is out of the scope of this project.

Leutner results of the SDA mixtures		
Sampling	Mixture	Force, kN
Road cores after construction (2020)	HPMix 45/80-80	14.7
	Reference PmB 45/80-65 CH-E	18.7
Road cores (2024)	HPMix 45/80-80	14.8
	Reference PmB 45/80-65 CH-E	30.3
	Required	≥15

Table 17: Leutner test results of the SDA mixtures (the results after construction are from the Consultest AG report No. 0953-20-4)

4.3.16 Summary

The results from the SDA test section and the lab-produced samples allow to conclude that there appears to be an advantage of using the highly polymer-modified binder over the conventional polymer-modified binder. This is evident in the binder test results in Figure 146. The mixture results also show similar or better performance compared to the reference mixture. The cause of the lower interlayer bond resistance of the HPMix samples is unknown but may be related to the interaction of the binder and the tack coat. The Cantabro test (even after modification to make it more severe) did not allow to conclusively demonstrate the potential advantages of high polymer modification with regard to reducing raveling of SDA mixtures.

Mixture	Binder tests				Rutting resistance	Crack propagation resistance		Raveling resistance	Stiffness	Low temp. cracing resistance	Interlayer bond
	ER	BTSV	MSCR	FS	FRT	SCB	IDEAL-CT	Cantabro	ITT	TSRST	Leutner
SDA	HPMix	↑	↑	↑	→	↗ ¹	→ ¹	↗	↘	↑	↓
	Reference	●	●	●	●	●	●	●	●	●	●

Legend:

- reference mixture result
 - ↑ significantly better performance
 - ↗ slightly better performance
 - similar performance
 - ↘ slightly worse performance
 - ↓ significantly worse performance
 - ER Elastic Recovery (binder)
 - BTSV Binder fast characterisation test
 - MSCR Multiple stress creep recovery test (binder)
 - FS Frequency Sweep (binder)
 - FRT French Ruting Tester (mixture)
 - SCB Semi-circular bend test (mixture)
 - IDEAL-CT Indirect tensile asphalt cracking test (mixture)
 - Cantabro Cantabro test (mixture)
 - ITT Indirect tensile test (mixture)
 - TSRST Tensile stress restrained specimen test
 - Leutner Leutner test (mixture)
- 1 SCB and IDEAL-CT tests are not sensitive to polymer content

Figure 146: Summary of SDA test results

5 Pavement structural design standardization

5.1 Pavement dimensioning according to VSS 40 324

In Switzerland, the pavement design method is described in the standard VSS 40 324. This is an empirical procedure based on the results of the AASHTO design method developed in USA. This method establishes a relationship between loads and the subgrade conditions, pavement strength and expected surface damage conditions. For flexible pavements, this relationship can be described with the following equation:

$$\log(W_{18}) = Z_R \times S_o + 9.36 \log(SN_F + 1) - \dots \quad (16)$$

$$\dots 0.20 + \frac{\log\left(\frac{\Delta PSI}{4.2 - 1.5}\right)}{0.40 + \frac{1094}{(SN_F + 1)^{5.19}}} + 2.32 \log(M_R) - 8.07$$

where

W_{18} is the predicted number of 18-kip (8.16t) equivalent single axle load applications

Z_R is the standard normal deviate

S_o is the combined standard error of the traffic

ΔPSI is the difference between the initial design serviceability index p_o and the design terminal serviceability index p_t

M_R is the resilient modulus of the subgrade (psi)

SN_F is the structural number required to survive future traffic

The empirical relationship among design traffic, pavement structure, and pavement performance for flexible pavements is solved to determine the required structural capacity of the pavement, known in the Swiss standards as "Strukturwert" (SN). The total pavement SN is defined as the summation of the layer thicknesses times the corresponding structural layers as follows:

$$SN = a_1 \times D_1 + a_2 \times D_2 + a_3 \times D_3 + \dots + a_n \times D_n \quad (17)$$

where

a_i also referred as *a-value*, represents the bearing capacity of the layer i

D_i is the thickness of the layer i

Therefore, the terms $a_i \times D_i$ can be interpreted as empirically deduced bearing capacity values of each pavement layer contributing to the structure.

In Switzerland, the values were adapted to correspond to the local conditions and to comply with the metric units. To calculate a pavement SN, it is necessary to add each layer thickness D in cm and the structural coefficient of the layer or a -values obtained from Tab. 7 of the standard VSS 40 324, shown in Figure 147. These values aim to represent the bearing capacity of each material used in road construction relative to the bearing capacity of a round-shaped unbound material with an a -value = 1. The Table has four columns with decreasing a -values for each material, trying to represent the deterioration of the material over time, i.e. their reduction of the bearing coefficient due to damage.

Tragfähigkeitswerte (a -Werte) der Oberbauschichten in Funktion der Schadenbildung Valeurs de portance (coefficient a) des couches de la chaussée en fonction des dégradations					
Oberbauschichten Couches de la chaussée	a -Werte neuer Oberbauschichten Coefficients a de nouvelles couches de la chaussée	a -Werte alter Oberbauschichten in Funktion der Schadenbildung Coefficients a d'anciennes couches de la chaussée en fonction des dégradations			
		Örtliche Schäden Dégradations locales	Ausgedehnte Schäden Dégradations étendues	Strukturelle Schäden Dégradations structurales	
Deck-, Binder- und Tragschichten / Couches de roulement, de liaison et de base					
Asphaltbeton Enrobés bitumineux	AC, AC B, AC T, AC MR	4,0	3,4	2,8	2,4
Asphaltbeton für sehr dünne Schichten Bétons bitumineux très minces	ACVTL				
Hot Rolled Asphalt	HRA				
Splittmastixasphalt Béton bitumineux grenu à forte teneur en mastic	SMA				
Gussasphalt Asphalte coulé routier	MA				
Deck- und Binderschichten / Couches de roulement et de liaison					
Offenporiger Asphalt Bétons bitumineux drainants	PA, PA B	2,6	2,2	1,8	1,6
Tragschichten / Couches de base					
Hochmodul-Asphaltbeton Enrobés bitumineux à module élevé	AC EME 22 C1	4,4 ¹⁾	3,8 ¹⁾	2,8 ¹⁾	2,4 ¹⁾
Hochmodul-Asphaltbeton Enrobés bitumineux à module élevé	AC EME 22 C2	5,6 ¹⁾	5,0 ¹⁾	2,8 ¹⁾	2,4 ¹⁾
Fundationsschichten / Couches de fondation					
Asphaltbeton Enrobés bitumineux	AC F	3,2	2,8	2,2	1,9
Schottertränkung, Stabilisierungen / Pénétration, stabilisations					
Schottertränkung Pénétration		2,6	2,2	1,8	1,6
Stabilisierung mit hydraulischen Bindemitteln Stabilisation aux liants hydrauliques		2,4	2,0	1,7	1,5
Stabilisierung mit bituminösen Bindemitteln Stabilisation aux liants bitumineux		2,7	2,3	1,9	1,6
Ungebundenes Gemisch / Grave non traitée					
Anteil gebrochener Körner: keine Anforderung Proportion de granulats concassés: aucune exigence		1,0 ²⁾	1,0 ²⁾	1,0 ²⁾	0,6 ²⁾
Anteil gebrochener Körner Proportion de granulats concassés	≥ 67%	1,25 ²⁾	1,25 ²⁾	1,25 ²⁾	0,75 ²⁾

- ¹⁾ Überprüfung mit einer analytischen Dimensionierung empfohlen
²⁾ Provisorische Werte basierend auf dem Nationalen Anhang SN 670 119-NA zu EN 13242 [18] und EN 13285 [19], da für ungebundene Gemische noch keine aktualisierten Erfahrungswerte bestehen

- ¹⁾ Vérification avec un dimensionnement analytique recommandée
²⁾ Valeurs provisoires basées sur l'annexe nationale SN 670 119-NA aux EN 13242 [18] et EN 13285 [19], car aucune valeur d'expérience actualisée pour les graves non traitées n'existe encore

Figure 147: a -values proposed in VSS 40 324

As Tab 7 presented in Figure 147 shows, the value for different asphalt concrete mixtures like AC, SMA or MA is 4, i.e. in a new layer of these materials would have 4 times more structural capacity than a layer of unbound round-shaped material. Similarly, for the same structural capacity an AC layer would require 1/4 of the thickness of an unbound round material. Unfortunately, adopting an *a-value* for new material is not a straightforward assumption and no direct method exists for the calculation.

As demonstrated in previous chapters, High PmB mixtures seem to exhibit superior performance compared to standard AC mixtures in many aspects (if not RAP is used). Therefore, in this research, an estimation of a possible *a-value* for High PmB mixtures is presented. Based on the results, it is expected that the actual *a-value* of High PmB will be above 4, allowing to design future pavements with a reduction in the required thickness of High PmB layers. Different experimental studies have already shown that a reduction of 20% to 40% may be attainable (Habbouche et al., 2019; Paul Fournier, 2010; Willis et al., 2016). Alternatively, if the thickness is not reduced, the design durability of the pavement could be increased. This would make it possible to achieve either a longer service life without damage or the capacity to carry higher traffic intensities within the same design period.

Objective

The aim of this part of the work is to find a methodology and propose an *a-value* within the VSS 40 324 framework for mixtures containing High PmB, as projected in WP4 of the project. This would allow a practical implementation of the research output of this project in the construction industry.

5.2 Methodology

As previously explained, the *a-values* in the Swiss standard are of empirical nature, having been established from a combination of experimental studies and calibration against observed pavement performance. Directly repeating the large-scale experimental campaigns that were used to generate these initial values is not feasible due to the associated time, cost, and logistical constraints. Therefore, an indirect methodology must be followed, combining the outcomes of laboratory performance testing with mechanistic considerations derived from structural modelling. A number of research efforts in recent years have estimated structural coefficients of paving materials, particularly when novel mixtures, binders or additives were introduced in the road engineering industry. For this study, two methodologies were identified as particularly relevant:

- Habbouche (2019): *Structural Coefficients of High Polymer Modified Asphalt Mixes Based on Mechanistic Empirical Analyses and Full-Scale Pavement Testing*.
- Perret et al. (2001): *High Modulus Pavement Design Using Accelerated Loading Testing (ALT)*.

After reviewing both approaches, the steps proposed by Perret et al. (2001), which is based on the French design guide, was selected. The justification for this choice is two-fold. First, the *a-values* for High Modulus Asphalt Concrete (EME) included in the Swiss standard were determined following Perret's procedure, which guarantees direct consistency with the framework followed by VSS 40 324. Second, the performance tests

recommended by Perret correspond closely to those specified in both the French and Swiss standards, making the procedure particularly well aligned with Swiss practice. It should be noted that while Perret originally applied this approach to EME, in this study it is adapted to High PmB mixtures with only minor modifications. The selected methodology, which is based in the French pavement design method, consists of the following main steps:

- Evaluation of the engineering properties and performance characteristics of both a standard "reference" mixture and a "target" mixture, i.e. the mixture for which the *a-value* has to be calculated.
- Implementation of these properties into a pavement model, in which one of the layers is first modelled with the "reference" and then with the "target" mixture.
- Simulation of the pavement response under loading.
- Use of strain responses to estimate the expected fatigue life in terms of number of load repetitions to failure, applying the fatigue law of the French design method.
- Verification of rutting resistance, by checking admissible loads against permanent deformation.
- Repetition of the modelling with different thicknesses of the "target" mixture layer, allowing the identification of equivalent thicknesses between "target" and "reference" mixtures for equal fatigue life.
- Calculation of the *a-value* of target mixture by comparing the equivalent thicknesses with those of the reference material.

In this study, the procedure was applied to the plant-produced RAPMix AC B 22 (used as reference) and the HPMix AC B 22 mixtures (see section 4.1). For conciseness, in this chapter the mixtures are identified as RP and HP respectively. A schematic overview of the process is presented in Figure 128, and the detailed steps are summarized in the following list:

1. Laboratory testing of RP and HP, including modulus tests across different temperatures and frequencies, fatigue tests, and rutting tests.
2. Development of a general 3D pavement structural model, incorporating temperature- and frequency-dependent viscoelastic material properties derived from the modulus master curves. Validation of the model was performed using FWD measurements.
3. Simulation of standard Swiss catalogue structures using French reference load (13 ton axle) applied at different speeds and pavement temperatures. The asphalt base layer was alternately modelled using RP and HP parameters. For HP, the simulations were repeated for at least three different thicknesses.
4. Extraction of horizontal tensile strains (ϵ_{11} , ϵ_{22}) at the bottom of the asphalt layers.
5. Application of the French fatigue law, using fatigue parameters derived from laboratory tests (reported in 4.1.14), to calculate the admissible number of load repetitions NE for each model.
6. Development of the thickness–fatigue life relationship for HP and comparison with RP, identifying equivalent thicknesses corresponding to equal fatigue performance.
7. Derivation of the relative structural coefficient (*a-value*) for HP by dividing the equivalent thicknesses of RP and HP.
8. Repetition of the process for multiple temperature and loading conditions, resulting in a range of possible *a-values*.

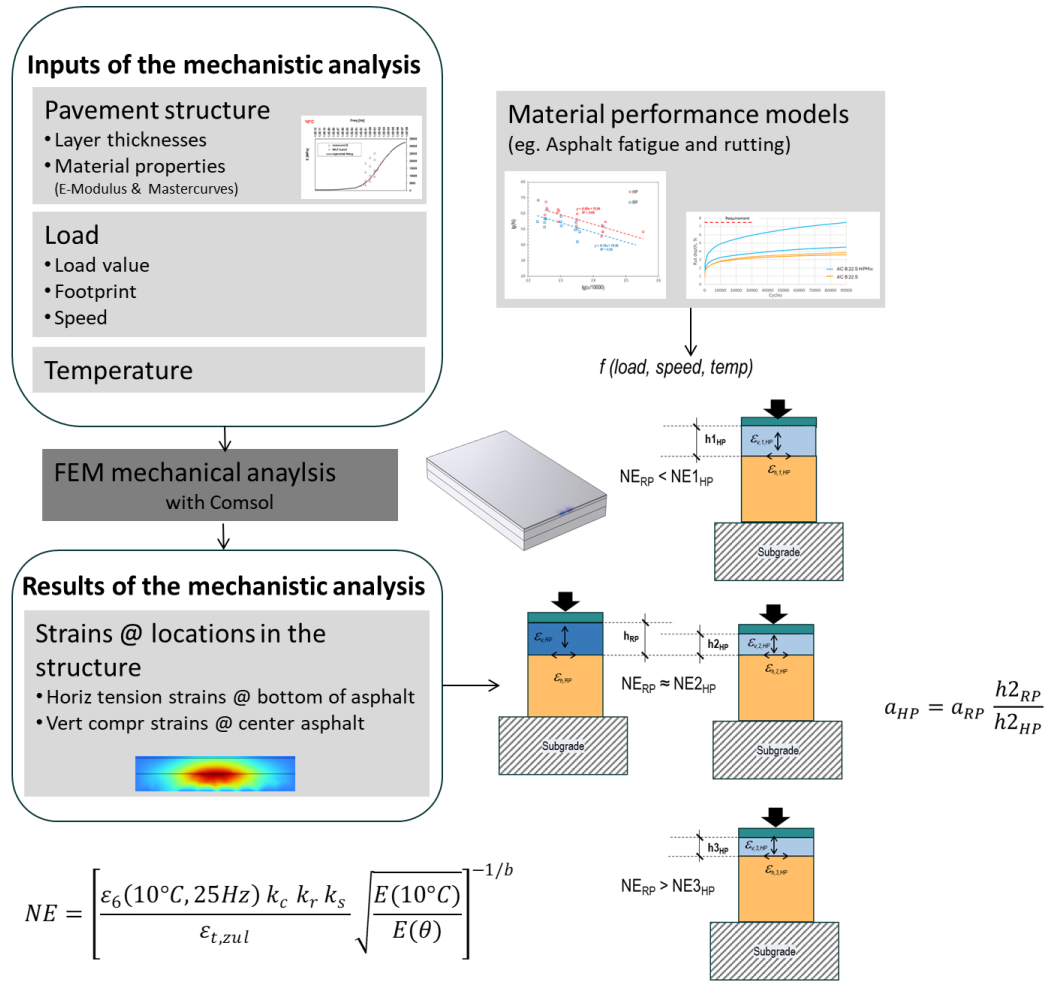


Figure 148: Schematic diagram for the calculation of the a-values for High PmB Mixture

5.2.2 Fatigue design

The French design method relates the fatigue performance of an asphalt material in a pavement layer at temperature θ with the following formula:

$$\varepsilon(NE, \theta, f) = \varepsilon_6(10^\circ C, 25Hz) \left(\frac{NE}{10^6}\right)^b \sqrt{\frac{E(10^\circ C)}{E(\theta)}} \quad (18)$$

where:

- NE is the admissible number of load repetitions
- θ is the temperature of the material, in [°C]
- E is the elastic modulus of the material for a temperature θ , in [MPa]
- $\varepsilon_6(10^\circ C, 25Hz)$ is the fatigue strain at 10^6 cycles using trapezoidal specimens at $10^\circ C$ and $25Hz$
- b is the fatigue slope

The allowable strain in a pavement is then obtained by applying the various correction coefficients defined above:

$$\varepsilon_{t,adm} = \varepsilon(NE, \theta, f) k_s k_r k_c \quad (19)$$

where:

k_s is the support coefficient, which accounts for the different support of the subgrade

k_r is the risk coefficient, takes into account the inhomogeneity of materials and their real layer thicknesses

k_c is the "calage" or adjustment coefficient, which accounts for differences between laboratory and real responses

Then, the equation can be re-written considering all the factors:

$$\varepsilon_{t,adm} = \varepsilon_6(10^\circ C, 25Hz) \left(\frac{NE}{10^6}\right)^b \sqrt{\frac{E(10^\circ C)}{E(\theta)}} k_s k_r k_c \quad (20)$$

Assuming that the admissible strain is equal to the calculated horizontal tension strains from modelling, the admissible number of loads can be cleared, leaving the following equation:

$$NE = \left[\frac{\varepsilon_6(10^\circ C, 25Hz) k_c k_r k_s}{\varepsilon_{t,zul}} \sqrt{\frac{E(10^\circ C)}{E(\theta)}} \right]^{-1/b} \quad (21)$$

This means that with the fatigue parameters ε_6 and b obtained from laboratory tests, with the elastic modulus E obtained from master curves derived from modulus tests at different temperatures and frequencies (shown in section 4.1.13), and with the strains obtained from simulation results, the admissible number of load applications NE for each pavement can be obtained.

Regarding the values of the coefficients used in the calculations, the French design procedure offers different approaches for how to calculate them.

Starting with support coefficient k_s , the standard proposes values ranging from 1.0 and 1.2 depending on the load-bearing capacity of the subgrade considered. In this work, a value of 1 was chosen for all calculations, as this coefficient is not related directly to the material under study and affects the calculations equally for any material.

The risk coefficient k_r instead, depends on the material and is meant to adjust the strain value to the calculated risk, chosen according to a confidence interval around the thickness (standard deviation S_h) and the results of the fatigue test (standard deviation S_N , see section 4.1.14)

$$k_r = 10^{-ub\delta} \quad (22)$$

Where

u is the standard normal variable associated with the chosen risk level. For this work we've chosen 25% for T3 and T4 traffic pavements (see § 5.3), which corresponds to a value of -0.674

b is the slope of the material fatigue load
 δ is the standard deviation of the distribution of $\log(N)$ at failure, calculated as:

$$\delta = \sqrt{S_N^2 + \left(\frac{c \cdot S_h}{b}\right)^2} \tag{23}$$

where

c is the coefficient relating strain variation to random variation in pavement thick-ness (assumed to be 0.02 cm^{-1} for typical structures)

For the materials RP and the HP analyzed here, the k_r are calculated based on parameters summarized in Table 18.

Parameters used for risk coefficient calculation			
Parameter	Material		
	RP		HP
u	-0.674		-0.674
b	-0.162		-0.164
S_N	0.56		0.47
S_h	0.085		0.085
c	0.02		0.02
d	0.56		0.47
k_r	0.87		0.89

Table 18: Parameters used for the calculation of the risk coefficient k_r

Finally, the adjustment coefficient, which reflects the discrepancies between the individual calculation approaches and the real observations of the "in situ behavior" of the roads. Is proposed in the French standard NF P98-086 2021 for several standard materials, ranging from 1 to 1.3. In Perret et al. 2001 (PERRET et al., 2001) however was demonstrated, that the k_c has a strong effect on the resulting NE , meaning that for EME mixtures the value of 1.3 suggested in the French standard "penalizes" the high modulus materials compared to the 1.0 value used in standard in the effect. In the same work, the author finally assigns a value of 1 to every material. Similarly, in this work we selected a value of $k_c = 1$ for both RP and HP, so they can be compared directly.

5.2.3 Rutting verification

The French method also limits the vertical strains in the pavement to prevent failure due to rutting. In particular, the method requires verification of the compressive strain at the top of the subgrade, where permissible compressive strain $\varepsilon_{z,adm}$ is empirically derived from the equivalent traffic load. This relationship, which does not consider rutting in bituminous layers, has the following form:

$$\varepsilon_{z,adm} = A \cdot NE^{-0.222} \tag{24}$$

where:

- A coefficient depending on the traffic level
- NE Number of equivalent axles (13 ton)

The French design standard requires a verification to rutting. However, the goal of our study was to evaluate the fatigue behavior of the layers containing High PmB mixtures. Therefore, rutting check was not carried out.

5.3 Material parameters

To solve Equation (21) of the fatigue design method and calculate the number of equivalent load applications for a given structure under specified temperature and loading conditions, material-specific inputs are required for both the reference mixture (RP) and the High PmB mixture (HP). These include fatigue parameters and stiffness properties.

5.3.1 Fatigue

The fatigue parameters, namely $\epsilon_6(10^\circ C, 25Hz)$ and the slope of the fatigue law $-1/b$ for both mixtures are reported in section 4.1.14, Table 12. These parameters, obtained from trapezoidal beam fatigue tests, provide the basis for evaluating the admissible number of load repetitions (NE) within the French design methodology.

5.3.2 Stiffness

The elastic modulus is required both for solving Equation (21) (terms $E(10^\circ C)$ and $E(\theta)$) also as an input for the pavement modelling. Modulus values for the two mixtures at different temperatures and loading frequencies (reported in § 4.1.13) were used to construct master curves. These were fitted using a sigmoidal function and time-temperature superposition with the Williams-Landel-Ferry (WLF) shift factors (see Figure 149). The parameters of the fitting function can then be used to estimate the elastic modulus at any proposed temperature and loading frequency.

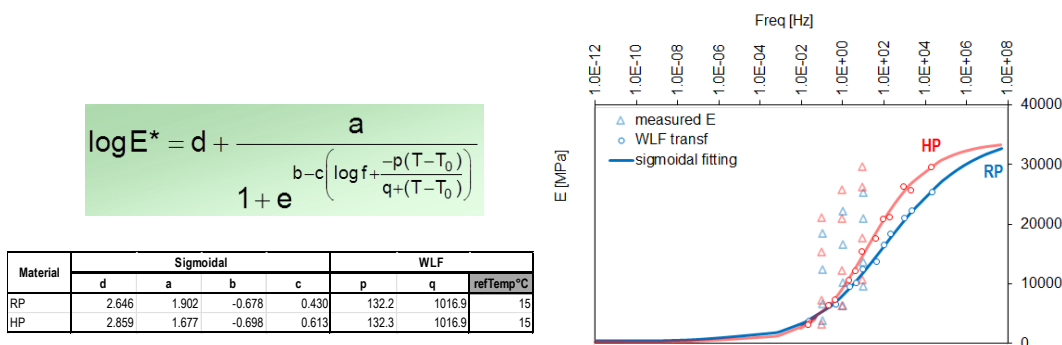


Figure 149: Master curves at 15 °C of RP and HP mixtures based on modulus testing and WLF shift factors.

5.3.3 Viscoelastic characterization

In order to implement advanced viscoelastic material behavior in the pavement models, the modulus and phase angle data from laboratory tests were used to derive a Prony

series representation of the mixtures. This approach, following the procedure described by Arraigada et al. 2009 (Arraigada et al., 2009) allows the material properties in the model to vary realistically with temperature and loading speed. Consequently, the simulations can capture the actual time- and frequency-dependent behavior of the asphalt mixtures. The Prony series parameters for both mixtures are presented in Table 22, and a visual comparison of the real and imaginary parts of the complex modulus, both as measured in the laboratory and as calculated from the Prony parameters, is shown in Figure 150.

Prony series coefficients

Branch	RP		HP	
	Shear modulus (MP)	Relaxation time (s)	Shear modulus (MPa)	Relaxation time (s)
1	9415	0.001	12120	0.001
2	3081	10.6	2112	10.8
3	3302	81.5	3480	74.9
4	1.2E-9	9977	2.2E-10	3614

Table 19: Prony series coefficients for RP and HP mixtures

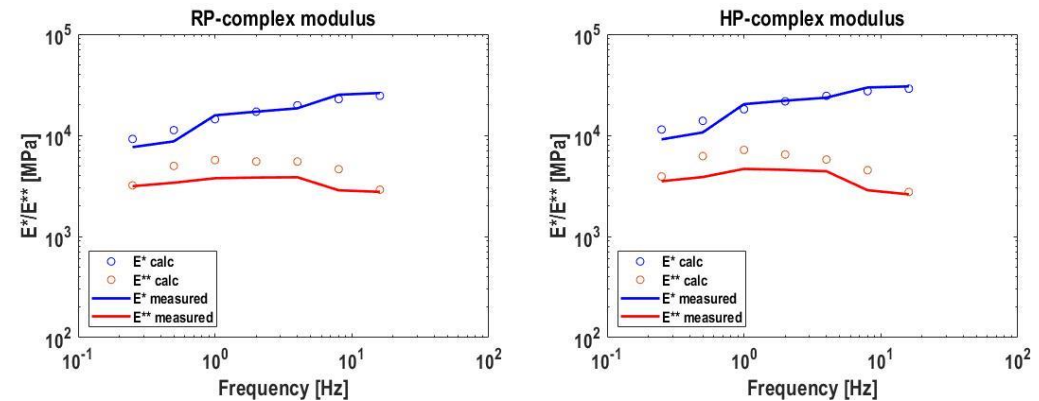


Figure 150: Comparison of measured and Prony-series-calculated complex modulus (real and imaginary components) for RP and HP mixtures

5.4 Pavement modelling

In order to translate the laboratory performance results into structural coefficients (*a-values*), it was necessary to implement the material properties of the tested mixtures into a numerical pavement model. Pavement modelling provides the link between the measured material behavior and the structural response of full-scale pavements under realistic loading and environmental conditions. By simulating representative pavement structures, it becomes possible to predict the critical strains that govern fatigue, and to compare the performance of High PmB mixtures against standard mixtures on an equivalent basis.

The modelling approach adopted here follows the principles of mechanistic–empirical design: the pavement response is first calculated using an advanced viscoelastic model,

and the predicted strains are then translated into performance indicators (fatigue life) using equations from the French design guide previously presented. While the French methodology traditionally relies on 2D elastic layered analysis based on Burmister's theory (implemented in the software Alizé-LCPC), in this study the simulations were performed using the commercial software COMSOL Multiphysics. This choice enables the use of fully 3D, time-dependent finite element models with advanced viscoelastic material laws. As a result, the models provide a more realistic representation of pavement behavior, particularly under varying loads, speeds, and temperatures, thereby increasing the accuracy and applicability of the predictions.

5.4.1 Geometry, material properties and boundary conditions

The simulated structures were based on standard Swiss catalogue pavements, consisting of asphalt surface layers, asphalt base courses, an unbound granular base, and a natural subgrade. Variations were introduced in the thickness of the High PmB (HP) asphalt layer to evaluate its structural contribution relative to the reference mixture (RP). The geometrical configurations correspond to typical Swiss designs for traffic classes T3 and T4, with three different subgrade support conditions (S2, S3, and S4) (see Figure 151).

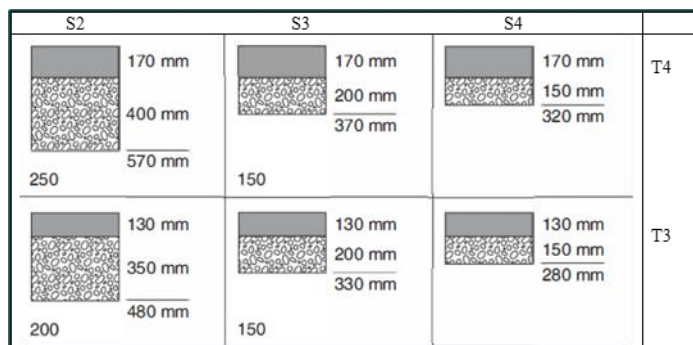




Figure 151: Pavement structure of Type 1 (Oberbautyp 1) from the Swiss design catalogue used for the simulations

The thicknesses and material types of asphalt layers were selected according to VSS 40 430, Table 1 (see Figure 152). For T3 pavements, the surface layer consisted of AC 8 S (30 mm), underlain by a binder/base layer AC B 22 (100 mm) of the reference mixture (RP). The goal was to assess the potential reduction in this base layer thickness when substituting RP with High PmB (HP). For T4 pavements, the structure included a 30 mm AC 8 S surface layer and two AC B 22 base layers of 70 mm each (140 mm total). In all cases, the subgrade was modelled as a 400 mm layer representing the foundation

Walzasphalt, Sollwertbereiche der Schichtdicken in Abhängigkeit der Mischgutsorten und Mischguttypen Enrobés bitumineux compactés, plages des valeurs nominales des épaisseurs des couches en fonction des sortes et des types d'enrobés					
Schichten und Sorten <i>Couches et sortes</i>	Mischguttypen <i>Types d'enrobés</i>				
	L	N	S	H	Ohne Typen <i>Sans types</i>
	[mm]				
Deckschichten / Couches de roulement					
AC 4	15...20				
AC 8	20...35	20...35	25...35	25...35	
AC 11	35...50	35...50	35...50	35...50	
AC 16	45...70	45...70			
SDA 4					25...35
SDA 8					30...40
AC MR 8					25...40
AC MR 11					35...50
SMA 8					25...35
SMA 11					30...45
PA 8					25...35
PA 11					35...50
Binderschichten / Couches de liaison					
AC B 11			35...50		
AC B 16			45...70	45...70	
AC B 22			65...100	65...100	
PA B 16					40...80
PA B 22					60...150
Tragschichten / Couches de base					
AC T 11	30...50	30...50			
AC T 16	45...70	45...70	45...70		
AC T 22	60...100	60...100	65...100	65...100	
AC T 32			90...140	90...140	
AC EME 22 C1					80...120
AC EME 22 C2					80...120
Fundationsschichten / Couches de fondation					
AC F 22					60...150
AC F 32					80...200
Sickerschichten / Couches de drainage					
PA S 16					40...80
PA S 22					60...150
PA S 32					80...200
Sperrschichten im Gleisbau / Couches d'étanchéité pour voies ferrées					
AC RAIL 16					45...70
AC RAIL 22					70...100

 Nicht normierte Typen

 Types non normalisés

Tab. 1
Walzasphalt, Sollwertbereiche der Schichtdicken in Abhängigkeit der Mischgutsorten und Mischguttypen

Tab. 1
Enrobés bitumineux compactés, plages des valeurs nominales des épaisseurs des couches en fonction des sortes et des types d'enrobés

Figure 152: Asphalt layer thicknesses and materials according to VSS 40 430.

The semi-infinite geometry of the structure was modeled as a block with a surface area of 6 m length and 4 m width. This domain size was chosen as a balance between accuracy (minimizing boundary influence) and computational efficiency. A 3D view of the finite element model in COMSOL Multiphysics is shown in Figure 153.

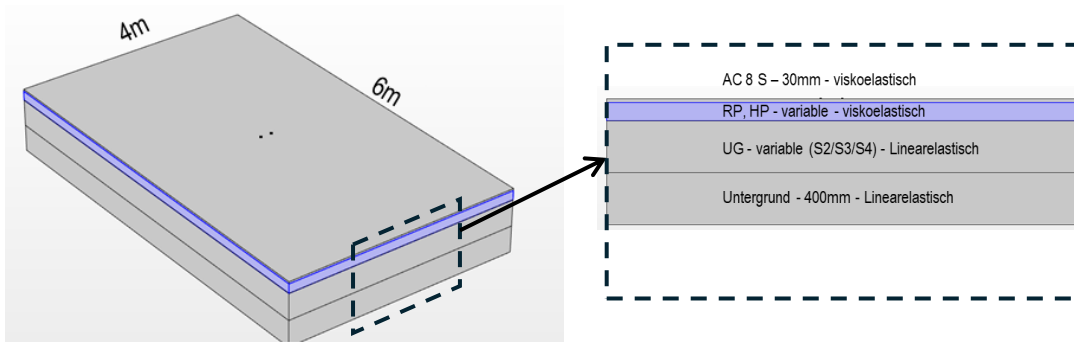


Figure 153: View of the 3D pavement model in Comsol Multiphysics.

The material properties used for each layer are summarized below in Table 20. The viscoelastic parameters of RP and HP mixtures, obtained from Prony series fitting, were described in § 5.3.3. The surface course material (AC 8 S) properties were taken from the Empa database. For the unbound granular base, a Young’s modulus of 170 MPa was applied. The subgrade modulus depended on the support type: 30 MPa for S2, 50 MPa for S3, and 120 MPa for S4. For all unbound and subgrade layers, a Poisson’s ratio of 0.35 was assumed.

Layer thicknesses and properties

str. Type	Subgrade type	S2		S3		S4	
		Thickness	Mat prop	Thickness	Mat prop	Thickness	Mat prop
T4	surface	30 mm	AC 8 S prony	30 mm	AC 8 S prony	30 mm	AC 8 S prony
	base & subbase	140 mm	RP prony	140 mm	RP prony	140 mm	RP prony
		140-120 mm	HP prony	140-120 mm	HP prony	140-120 mm	HP prony
	unbound	400 mm	170 MPa	370 mm	170 MPa	150 mm	170 MPa
subgrade	400mm	30 MPa	400 mm	50 MPa	400 mm	120 MPa	
T3	surface	30mm	AC 8 S prony	30 mm	AC 8 S prony	30 mm	AC 8 S prony
	base	100 mm	RP prony	100 mm	RP prony	100 mm	RP prony
		100-70 mm	HP prony	100-70 mm	HP prony	100-70 mm	HP prony
	unbound	350 mm	170 MPa	200 mm	170 MPa	150 mm	170 MPa
subgrade	400 mm	30 MPa	400 mm	50 MPa	400 mm	120 MPa	

Table 20: Summary of all layer thicknesses and material properties used in the pavement models.

As for the boundary conditions, the bottom surface of the modeled domain was fixed in all six degrees of freedom, preventing both translational and rotational displacements. The lateral boundaries were constrained only in the direction normal to their respective surfaces, allowing free movement in the parallel directions while avoiding unrealistic edge effects. Similarly, the interfaces between the pavement layers were modeled as perfectly bonded, following the same assumption recommended in the French design guide for interlayer behavior when using Alizé-LCPC.

5.4.2 Load

The applied loading conditions were selected according to the French design guide, ensuring consistency with the methodology used to evaluate fatigue life resistance. A standard 130 kN (13 ton) single axle load with dual tires was considered. The load was uniformly distributed over the pavement surface as two circular contact areas, each with a diameter of approximately 12.5 cm, separated by a center-to-center distance of 33.7 cm (see Figure 154). To capture the viscoelastic behavior of the asphalt mixtures, the load was applied as a moving contact across the surface of the model at vehicle speeds of 40 km/h and 80 km/h. This allowed the simulations to account for the time-dependent development of strains and stresses in the pavement structure.

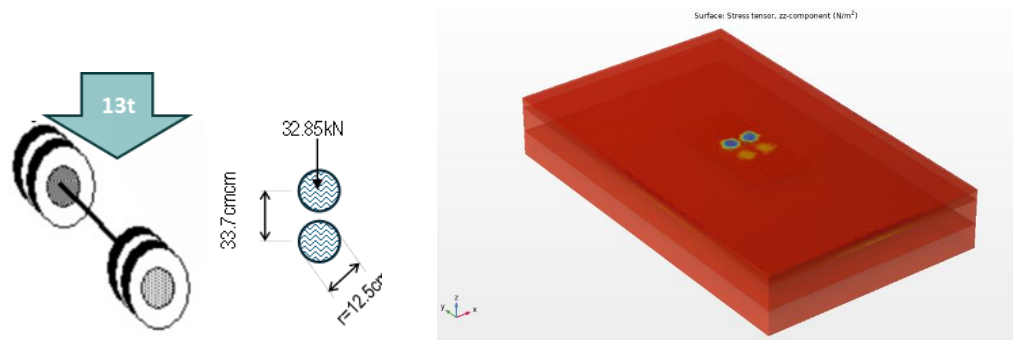


Figure 154: Representation of the dual-wheel axle load applied in the pavement model.

As previously shown, the French pavement design method expresses traffic in terms of the number of standard 13-ton axles expected to travel on the section over its service life. To express the equivalent traffic defined by Swiss standards, which consider ESAL of 8 tons according VSS 40 320, an equivalent factor based on a power law must be applied. The value used for this transformation was 7.1.

5.4.3 Output

The model outputs were established focusing on the critical pavement responses that are related to fatigue. According to the French design guide, the key indicators are the horizontal tensile strains at the bottom of the asphalt base layer, as these are directly associated with fatigue cracking initiation. In the French methodology, which relies on 2D static analytical models, these strains are calculated at a single point directly beneath the applied load, at the interface between the asphalt layers and the unbound base.

In contrast, the present study employs a 3D, time-dependent finite element model, where strain values vary dynamically with both position and time. For a passing wheel load, the strain response at a given point can be represented by its two horizontal components: ϵ_{11} (longitudinal, in the traffic direction) and ϵ_{22} (transversal, perpendicular to traffic), as illustrated in Figure 155. Since both components occur simultaneously, they were combined to obtain the total horizontal strain at the base of the asphalt layer. To avoid bias from a single-point measurement, the analysis was extended over a 1 m \times 2 m rectangular area located at the center of the model (see Figure 156). The maximum combined $\epsilon_{11} + \epsilon_{22}$ strain obtained across this area and over the entire load passage was then used as the input for the French fatigue law and rutting verification criteria described in § 5.2.

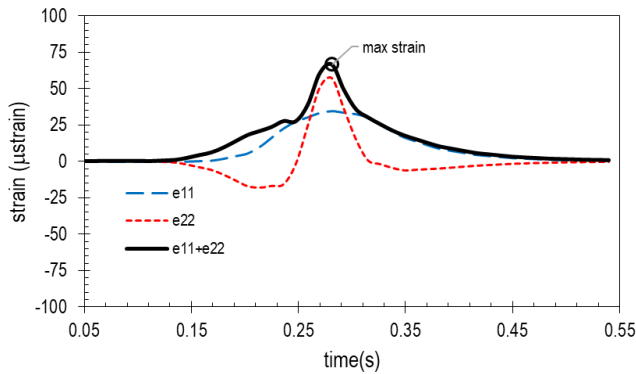


Figure 155: Horizontal strains in the direction and transversal to traffic (e_{11} and e_{22} respectively) and their combination

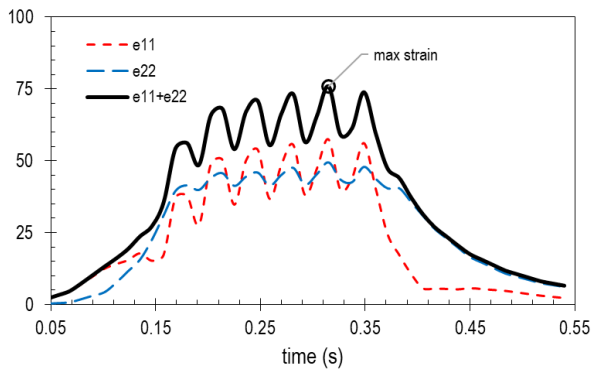
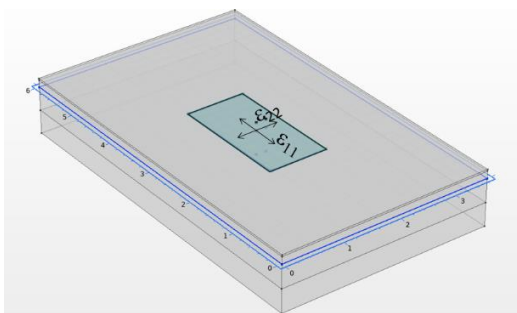


Figure 156: View of the plain to obtain the strains (top) and strain output (bottom)

5.4.4 Summary of the models

In summary, the pavement modelling framework developed in this work consisted of the following elements:

- Pavement structures: Representative Swiss catalogue sections for traffic classes T3 and T4, each evaluated under three different subgrade support conditions (S2, S3, S4).
- Material properties: Viscoelastic characteristics of RAPMix (RP) and HPMix (HP), derived from laboratory testing and implemented in the FEM models using Prony series representations.
- Loading conditions: Standard French design load of a 130 kN dual-wheel axle, applied at two speeds (40 km/h and 80 km/h) and three reference pavement temperatures (5 °C, 15 °C, and 30 °C).

- Model outputs: Maximum combined horizontal tensile strains ($\epsilon_{11} + \epsilon_{22}$) at the bottom of the asphalt base layer, used as input for fatigue and rutting analyses.

In total, 36 model combinations were simulated, covering the range of materials, structures, loading, and environmental conditions. A full overview of these combinations is presented in Table 21.

Scenarios used in the model			
Model No.	Structure	Load speed (km/h)	Temperature (°C)
1	T3_S2	40	5
2	T3_S2	40	15
3	T3_S2	40	30
4	T3_S3	40	5
5	T3_S3	40	15
6	T3_S3	40	30
7	T3_S4	40	5
8	T3_S4	40	15
9	T3_S4	40	30
10	T4_S2	40	5
11	T4_S2	40	15
12	T4_S2	40	30
13	T4_S3	40	5
14	T4_S3	40	15
15	T4_S3	40	30
16	T4_S4	40	5
17	T4_S4	40	15
18	T4_S4	40	30
19	T3_S2	80	5
20	T3_S2	80	15
21	T3_S2	80	30
22	T3_S3	80	5
23	T3_S3	80	15
24	T3_S3	80	30
25	T3_S4	80	5
26	T3_S4	80	15
27	T3_S4	80	30
28	T4_S2	80	5
29	T4_S2	80	15
30	T4_S2	80	30
31	T4_S3	80	5
32	T4_S3	80	15
33	T4_S3	80	30
34	T4_S4	80	5
35	T4_S4	80	15
36	T4_S4	80	30

Table 21: Summary of all numerical simulation scenarios considered in this study

5.5 Validation using FWD test data

Before analyzing the results and to ensure that the numerical model realistically reproduced pavement behavior, simulated deflections were compared against Falling Weight Deflectometer (FWD) measurements carried out on one of the testing sites, namely the H19 Oberalpstrasse (see section 4.1.16). FWD testing is a non-destructive technique commonly used to assess pavement structural condition. It consists of dropping a weight onto a circular load plate, generating an impulse load that simulates a moving wheel. The resulting pavement surface deflections are recorded by a series of geophones, and the deflection basin is then analyzed to evaluate pavement stiffness, estimate layer moduli, design maintenance and rehabilitation strategies, and verify that the pavement can withstand projected traffic loads.

The measurements were performed in September 2024, comprising a total of 25 drops over a section length of approximately 210 m. Drops 1–12 corresponded to the section where the base layer consisted of RAP Mix (RP), while drops 13–24 corresponded to the section constructed with High PmB Mix (HP). A view of the FWD on site, together with the pavement structure and drop locations, is shown in Figure 157. The FWD used a 30 cm diameter loading plate, with an applied load of 110 kN. A total of 14 geophones recorded the surface deflections at distances ranging from 0 m (D0) to 1.9 m (D15) from the load center.

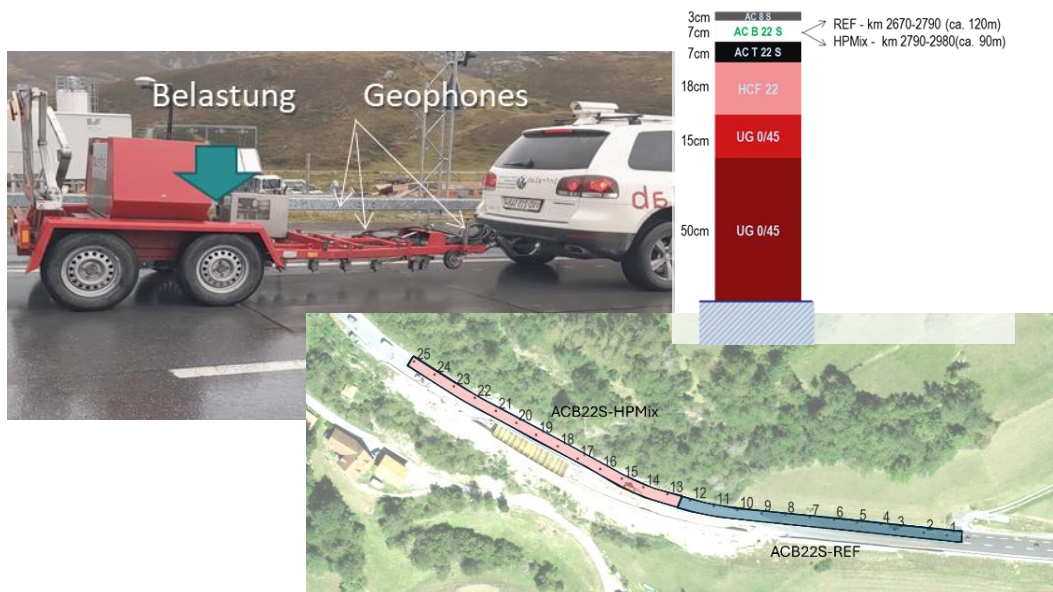


Figure 157: View of the FWD test carried out in the H19 Oberalpstrasse test section.

Instead of applying a moving load, the time-dependent load histories from the FWD tests were directly introduced into the FEM model. Figure 158 a) shows the average, maximum, and minimum transient force histories measured by the load cell of the FWD. Figure 158 b) compares the measured D0 responses for both RP and HP sections, showing that while the average responses were similar, the HP section exhibited slightly higher variability. Pavement temperatures recorded during the tests were very similar between the two sections, with averages of 16.0 °C (RP) and 16.1 °C (HP). These values were used for model validation.

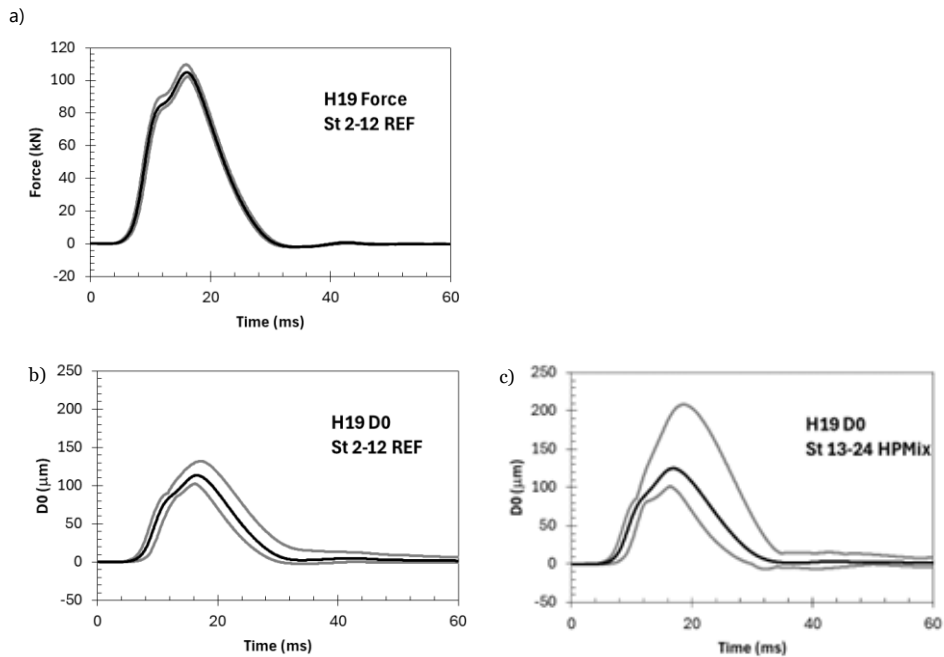


Figure 158: a) average, max. and min. time-dependent load histories used in FEM simulations; b) average, max. and min. measured D0 responses for RP and HP sections of H19 Oberalpstrasse.

For the FWD validation models, the pavement geometry was adapted to reproduce the test conditions. The simulated domain was set to 5 m × 5 m to minimize boundary effects, and the modeled layer thicknesses corresponded to the actual pavement structure. A schematic of the modeled geometry is shown in Figure 159.

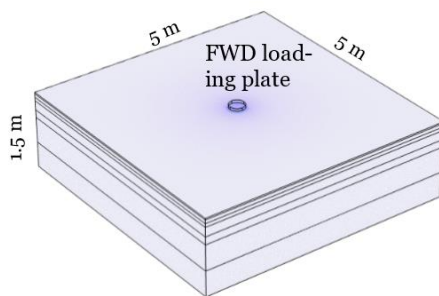


Figure 159: FEM geometry used for FWD validation, with loading plate at the pavement center.

Regarding material properties, all layers were modeled as linear elastic, except for the asphalt base layer and surface layer, which were modeled with Prony series viscoelastic parameters (RP, HP, and AC 8 S) as described in §5.3.3 and in §5.4. Initial modulus values were derived from backcalculation results performed by Infralab SA using the program *Elmod*, based on the FWD deflection basin. Since *Elmod* allows a maximum of three layers, the bituminous layers were combined into a single equivalent layer, the hydraulically bound layer (HCF) and unbound layer were treated as another, and the natural subgrade as a third (see Figure 160). The corresponding backcalculated modulus values at the test temperatures were used as seed values for the FEM calibration.

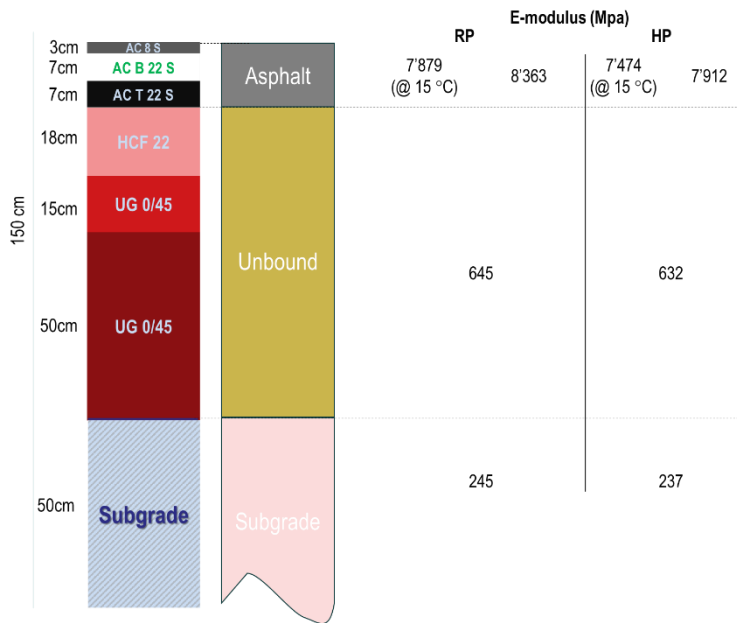


Figure 160: Pavement structure of H19 Oberalpstrasse (left), its 3-layer simplification for Elmod backcalculation (center), and the backcalculated moduli used as seed values in FEM (right).

Layer thicknesses and material properties used for the model

Layer	Thickness	Mat properties
AC 8 S	30 mm	AC 8 S Prony
AC B 22S	70 mm	RP Prony HP Prony
AC T 22S	70 mm	7000 MPa
HCF 22	180 mm	500 MPa
UG 0/45	150 mm	400 MPa
UG 0/45	500 mm	300 MPa
Subgrade	500 mm	100 MPa

Table 22: Summary of layer thicknesses and material properties used for the calibration

Figure 161 compares the time-series of measured and simulated deflections (Do) for both RP and HP pavements. The model predictions follow the measured time histories closely, demonstrating the accuracy of the FEM approach.

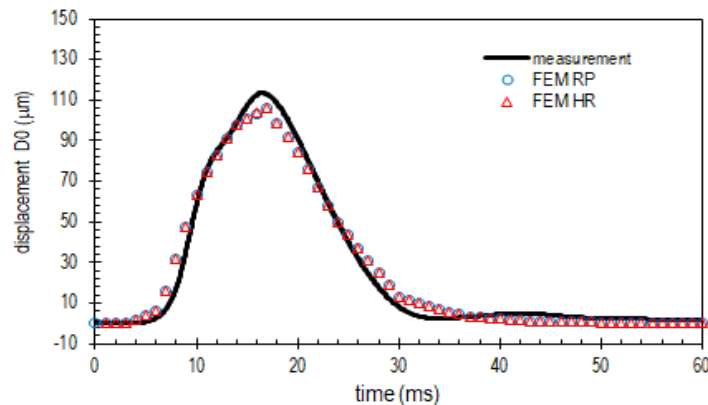


Figure 161: Comparison between measured and simulated D0 deflections under FWD loading for RP and HP mixtures.

This validation confirmed that the viscoelastic properties derived from laboratory testing, when implemented in the FEM, are capable of reproducing field deflection responses with high accuracy. The calibration step provided confidence that the subsequent simulations for fatigue performance under traffic loading would be reliable and consistent with real-world behavior.

5.6 Results and determination of *a-values*

The validated FEM modelling framework described in § 5.5 was applied to the set of 36 modelled combinations defined in Table 34, covering different pavement types (T3 and T4), subgrade conditions (S2, S3, S4), temperatures (5 °C, 15 °C, 30 °C), and loading speeds (40 km/h and 80 km/h). The outputs of the simulations—namely the critical horizontal tensile strains at the bottom of the asphalt base layer—were used as inputs to the French fatigue law (§ 5.2) in order to estimate the admissible number of load repetitions (NE) for each case.

By systematically varying the thickness of the HP mixture in comparison to the reference RP mixture, it was possible to determine the equivalent thicknesses that provided the same performance in terms of fatigue life. The ratio of these equivalent thicknesses directly reflects the relative structural efficiency of HP with respect to RP and thus allows the derivation of an adjusted structural coefficient (*a-value*) for High PmB mixtures within the VSS 40 324 framework.

The complete set of calculated *a-values* for the 36 simulations is presented in Figure 162, where each bar corresponds to one modelling scenario. The results show that the minimum calculated *a-value* was 4.43, while the maximum reached 6.92, depending on temperature, loading speed, and support conditions. Since the introduction of a new material class requires a cautious approach, the conservative lower bound was chosen. Therefore, a rounded value of 4.4 is proposed as a possible structural coefficient for High PmB mixtures in the VSS 40 324 framework. This value remains consistent with the empirical nature of the design method while ensuring that the performance advantage of High PmB mixtures is recognized without overestimating its contribution. In practice, using this *a-value* for the dimensioning using the Swiss design standard would translate into a reduction of the asphalt layer thickness by around 10%, or alternatively into an extension of the theoretical service life, as further detailed in the next

section. It has to be noted that the proposed a -value refers only to mixtures that have no RAP. In case of using high content of RAP, the goal of using high PmB is to achieve similar performance to mixtures that are currently specified in the standard with the existing a -values.

It must be emphasized, however, that while the present approach combines validated laboratory-based material models and mechanistic–empirical pavement simulations, the proposed value remains theoretical. For formal adoption into the Swiss catalogue, the methodology and proposed coefficient require confirmation through either scaled- or scaled accelerated loading tests or long-term field trials, in line with previous procedures followed for the calibration of EME mixtures.

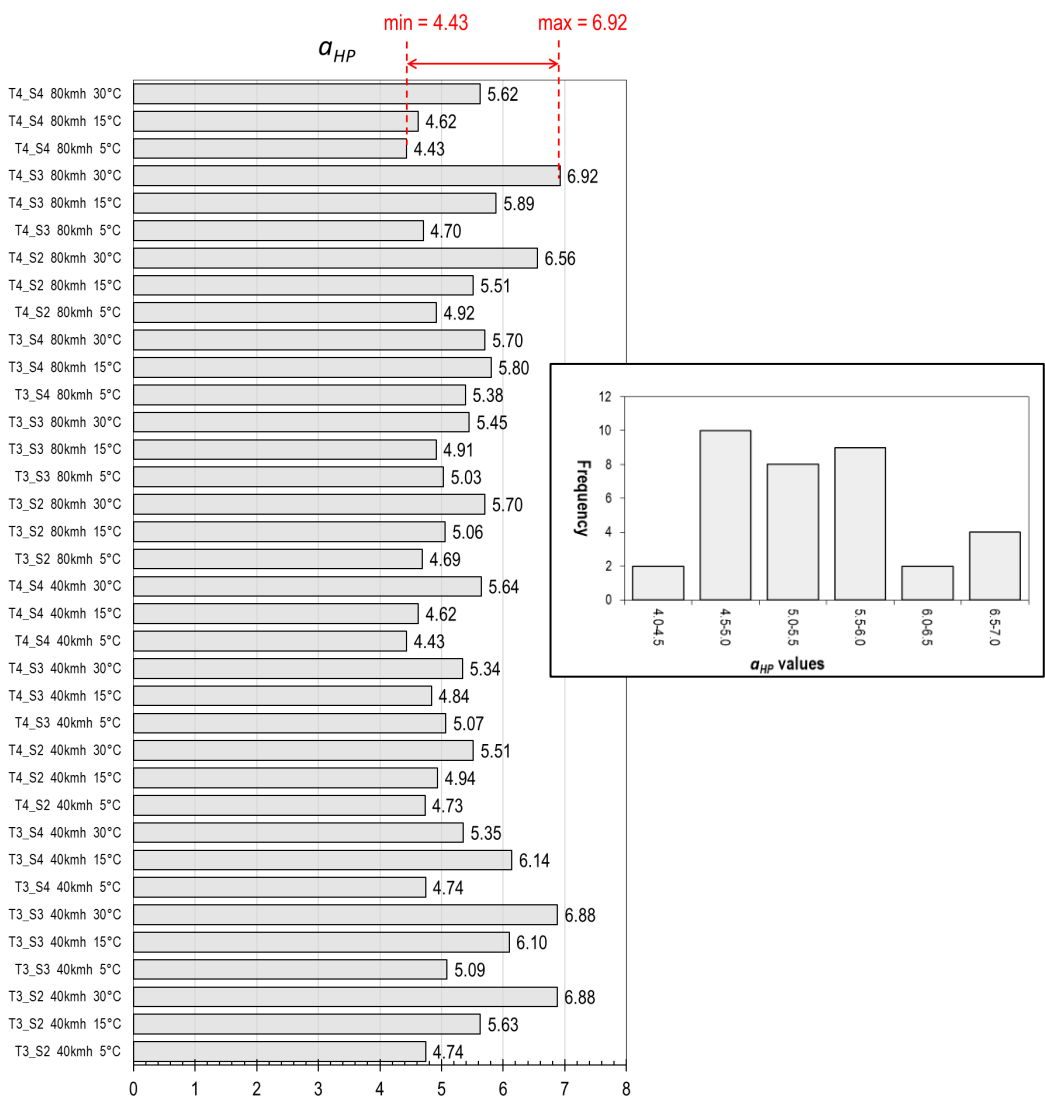


Figure 162: Calculated structural coefficients (a -values) for High PmB mixtures (a_{HP}) from 36 simulations. Values range between 4.43 and 6.92. The inset shows the frequency distribution of the results.

5.7 Impact of the proposed *a-values* in the expected ESALs

To assess the practical implications of the proposed *a-value* for High PmB mixtures in pavement dimensioning, this section illustrates its effect on the calculation of the expected ESALs according to the Swiss dimensioning standard VSS 40 324. For this purpose, the Structural Number (SN) of standard catalogue pavements was recalculated, replacing the current structural coefficient of 4 with the proposed value of 4.4 for all asphalt layers. The results of these recalculations are presented in Table 23 for pavement types T3 to T5. It can be observed that the influence of adopting the proposed *a-value* strongly depends on the total thickness of the asphalt layers. The increase in expected ESALs ranges between 39% and 106%, highlighting the significant structural benefit that High PmB mixtures could provide in practice.

Expected ESALs of the current and High PmB mixtures					
Pavement type	SN		ESAL		Difference
	Standard Mixtures	High PmB Mixtures	Standard Mixtures	High PmB Mixtures	
T3S2	87	92	1'284'450	1'783'273	39%
T3S3	72	77	1'295'911	1'874'636	45%
T3S4	67	72	908'659	1'314'445	45%
T4S2	108	115	4'832'822	7'422'460	54%
T4S3	88	95	4'035'839	6'540'504	62%
T4S4	83	90	9'320'534	16'300'241	75%
T5S2	128	136.8	17'071'844	29'746'473	74%
T5S3	108	116.8	16'696'753	31'187'403	87%
T5S4	103	111.8	48'241'512	99'442'531	106%

Table 23: Comparison of expected ESALs for different standard pavements using current and proposed *a-values*

These results suggest that even a modest increase in the structural coefficient (from 4.0 to 4.4) has a considerable effect on pavement performance predictions. For thicker asphalt structures, the effect is amplified, leading to more than double the number of expected ESALs in the case of T5 pavements. This underlines the potential of High PmB mixtures to extend pavement service life and reduce maintenance needs, provided that the proposed *a-values* are validated in full-scale field applications.

5.8 Summary

In this work, a methodology was applied to estimate structural coefficients (*a-values*) for High PmB mixtures within the Swiss pavement design framework (VSS 40 324). The calculated values ranged between 4.43 and 6.92. From these results, a conservative value of 4.4 is proposed for design. This confirms the expected structural advantage of High PmB mixtures when compared to conventional materials. In practical terms, this could translate into a reduction of around 10% in asphalt layer thickness. Alternatively, if the thickness remains unchanged, an increase in the equivalent single axle load

applications (ESALs) between 39% and 106% can be expected depending on the pavement structure. It has to be noted that the proposed a-value refers only to mixtures that have no RAP. In case of using high content of RAP, the goal of using high PmB is to achieve similar performance to mixtures that are currently specified in the standard with the existing a-values. Nevertheless, the proposed a-value must be validated in real structures, either reduced-scale trials or full-scale pavement testing, before being adopted in practice.

6 Conclusions and recommendations

This research has shown that highly polymer-modified binder can bring definite advantages over conventional polymer-modified binder. During the research this was demonstrated both on the binder and mixture-level. For standardization, however, mostly binder-based test methods and criteria are proposed since on the mixture level, the tests either did not demonstrate a notable difference between the highly polymer-modified binder and a conventional polymer-modified binder or the test execution is too laborious (in the case of the fatigue test). Therefore, even though some of the mixture tests might be beneficial for using in mix design, their use is not necessarily related exclusively to highly polymer-modified binder and therefore no recommendations are provided in this report. Below is a summary of the considerations for proposing or not proposing a certain test for standardization.

6.1 Binder characterisation

It was demonstrated in this research that the currently employed methods for binder characterisation and quality control are not sufficient. The methods do not allow to reliably distinguish between binders containing different polymer content.

Two methods that in Switzerland are currently not used in quality control were evaluated for binder classification: bitumen fast characterisation test (BTSV) and multiple stress creep recovery (MSCR) test. Both test methods provided valuable information about the binder properties and can be successfully used for highly polymer-modified binder characterisation since they allow discriminating between binders having different polymer contents.

To summarize the methods and the temperature at which they were used in this research, Figure 163 is provided. The figure distinguishes between the methods that we consider suitable for routine classification of highly polymer-modified binders and methods that are not.

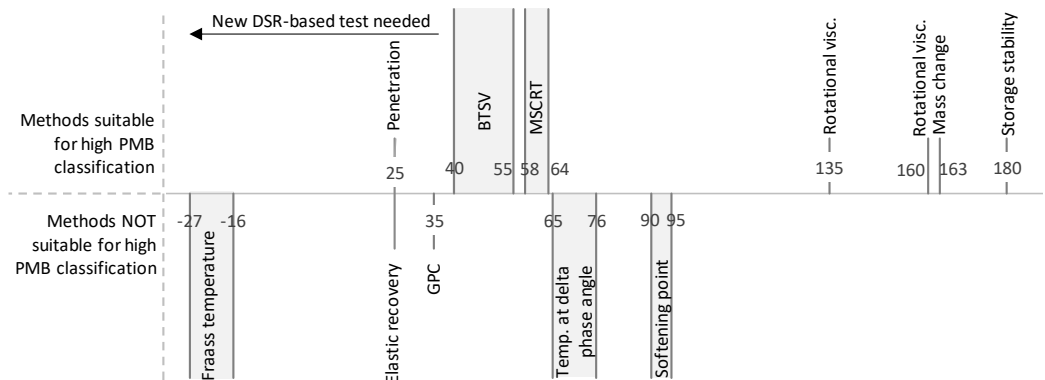


Figure 163: Proposed methods for highly-polymer modified binder characterisation and the temperature for each test as it was used in this research

Table 24 summarizes the methods and the proposed criteria for highly polymer-modified binder classification. The methods are suitable for any PmB and also unmodified binders, but they are especially necessary for highly polymer-modified binder classification since the currently used methods can not adequately distinguish between conventional and highly polymer-modified binders. The two binders included in the table are the ones used in this research. They are named "soft" and "hard".

Proposed methods for High PmB quality control				
Method	Criteria hard binder	Criteria soft binder	Remarks	Standard
Penetration	45-80 0.1mm	90-150 0.1mm	-	EN 1426
Rotational viscosity	≤ 3 Pa·s at 135 °C ≤ 1 Pa·s at 160 °C	≤ 3 Pa·s at 135 °C ≤ 1 Pa·s at 160 °C	Validation of the criteria necessary	EN 13302
Storage stability	$\leq 5^\circ\text{C}$	$\leq 5^\circ\text{C}$	Development of MSCR or BTSV-based criteria recommended	EN 13399
Mass change after RTFOT	$\leq 0.5\%$	$\leq 0.5\%$	-	EN 12607-1
BTSV	$\delta_{\text{BTSV}} \leq 62^\circ$ & $T_{\text{BTSV}} 50-60^\circ\text{C}$	$\delta_{\text{BTSV}} \leq 62^\circ$ & $T_{\text{BTSV}} 40-50^\circ\text{C}$	Validation of the criteria recommended	EN 17643
Aging resistance using BTSV after RTFOT	Reduction in $\delta_{\text{BTSV}} \leq 6^\circ$ Increase in $T_{\text{BTSV}} \leq 8^\circ\text{C}$	Reduction in $\delta_{\text{BTSV}} \leq 6^\circ$ Increase in $T_{\text{BTSV}} \leq 8^\circ\text{C}$	The proposed criteria based on a German pre-norm. Validation recommended	EN 17643 EN 12607-1
Aging resistance using BTSV after RTFOT+2PAV cycles	Reduction in $\delta_{\text{BTSV}} \leq 10^\circ$ Increase in $T_{\text{BTSV}} \leq 23^\circ\text{C}$	Reduction in $\delta_{\text{BTSV}} \leq 10^\circ$ Increase in $T_{\text{BTSV}} \leq 23^\circ\text{C}$	Two PAV aging cycles suggested for more realistic aging state.	EN 17643 EN 14769
MSCR test	$\geq 85\%$ recovery $\leq 0.5\%$ kPa ⁻¹ Test @ 10 kPa stress, 64 °C	$\geq 85\%$ recovery $\leq 0.5\%$ kPa ⁻¹ Test @ 10 kPa stress, 58 °C	10 kPa stress not in standard currently Test temperature should be selected based on climate In this research, testing performed on unaged samples	EN 16659

Table 24: Proposed methods and criteria for highly polymer-modified binder quality control

6.2 Mixture rutting test

All the mixtures fulfilled the rutting test requirements and, in most cases, no more than 5% rut depth was observed up to 30,000 loading cycles. Extending the test to 90,000 cycles did not provide any advantage and did not highlight the potential benefits of the high polymer content in the binder since the results even up to 90,000 cycles were similar between the reference and high polymer content mixture (HPMix) samples. Increasing the test temperature might be an option that allows to better distinguish the mixtures containing highly modified binder in the rutting test.

Based on the test results from the three test sections, it can be stated that lowering the rutting test criteria to a maximum 5 % permitter rut dept would be possible since it was

demonstrated that it is possible to achieve such rut depth both for the AC and AC B type mixtures. Thus a higher resistance to rutting could be expected from mixtures containing highly polymer modified binder. However, it was indicated by some participants of the supervisory committee that there is a risk that such requirements would then be applied even when not fully justified. In other words, even though technically it is possible to achieve rut depth below 5%, it might not be necessary. Moreover, such rutting resistance can be achieved even with conventional polymer-modified binder. Rutting is a particular problem in slow traffic areas exhibiting significant shear forces (e.g. bus stops and roundabouts). Considering the possibility to achieve very high rutting resistance, it can be considered that the highly polymer-modified binders could provide a solution for such locations. It is therefore recommended to evaluate the use of highly polymer-modified mixtures for such locations (possibly through constructing a trial section) and consider developing harsher test conditions or using another test method (for example cyclic compression test) for testing rutting resistance.

6.3 Mixture cracking resistance tests (SCB and IDEAL-CT)

The cracking resistance tests (SCB and IDEAL-CT) are suitable means for mixture design since they are sensitive towards parameters that affect the mixture performance: binder content, binder properties, and RAP content. These methods have also demonstrated relatively high correlation with the field performance and they are simple and quick to perform. For these reasons, the methods can be considered for using in mix design.

However, based on this and previous Empa research, the methods are not sensitive towards the use of polymers in binder. Therefore, they can not be relied upon for mixture characterisation with the goal of evaluating the elastic properties or effect of polymers.

6.4 Mixture fatigue and stiffness tests

The fatigue test demonstrated a distinct advantage of using highly polymer modified binder. However, it is currently not proposed for including in quality control or mixture type testing because the test execution is very laborious and it can reasonably be assumed that the binder characterisation tests are sufficient for assuming sufficient performance of the mixtures, especially for well-established mixture types like AC.

The stiffness test, as expected, did not demonstrate a notable difference between the mixtures containing different polymer contents. Therefore, since the mixture types that were evaluated in this project do not currently require a stiffness test, there is also no need to introduce it when using highly polymer-modified binder.

6.5 Thermal stress restrained specimen test (TSRST)

The TSRST showed that there is possibly an advantage of using higher polymer content for increasing the resistance to low temperature cracking. This was observed also in other studies (Kabir et al., 2023). However, even the conventional polymer-modified

binder ensured high low temperature cracking resistance. Therefore, even though it might be advantageous to include the TSRST as a criteria for approving asphalt mixtures in cold regions, this is not necessarily related to the use of highly polymer modified binder. For this reason, no criteria for standardization is provided for this test as part of this report.

6.6 Pavement dimensioning standardization

In this work, a methodology was applied to estimate structural coefficients (*a-values*) for High PmB mixtures within the Swiss pavement design framework (VSS 40 324). The calculated values ranged between 4.43 and 6.92. From these results, a conservative value of 4.4 is proposed for design. This confirms the expected structural advantage of High PmB mixtures when compared to conventional materials. In practical terms, this could translate into a reduction of around 10% in asphalt layer thickness. Alternatively, if the thickness remains unchanged, an increase in the equivalent single axle load applications (ESALs) between 39% and 106% can be expected depending on the pavement structure. It has to be noted that the proposed a-value refers only to mixtures that have no RAP. In case of using high content of RAP, the goal of using high PmB is to achieve similar performance to mixtures that are currently specified in the standard with the existing a-values. Nevertheless, the proposed a-value must be validated in real structures, either reduced-scale trials or full-scale pavement testing, before being adopted in practice.

6.7 Research needs

During the HPMix project, several specific needs for future research were identified. A follow-up study on these topics would help the implementation of high PmBs:

- During this research, structural coefficient was proposed for mixtures containing high PmB. A validation of these results is recommended by building a test site for loading with MMLS11 according to the dimensions calculated using the new coefficient.
- It was shown that the current rutting test conditions are not severe enough to demonstrate a difference between a conventional PmB and high PmB mixture. Therefore development of new test conditions or validation of another test method, for example cycling compression, is recommended.

Additionally, several areas of shortcomings were identified during the research that are not necessarily related to the implementation of high PmBs but rather could benefit the sector as a whole:

- High PmB can be especially useful in specialty application with high traffic intensity and high shar forces. This includes bus stops, weigh station, roundabouts, intersections and similar locations. A construction of a test section with a corresponding evaluation could show the potential of high PmB mixtures to replace concrete in such applications.

- The storage stability is currently evaluated using softening point test. Since softening point is not recommended for high PmB evaluation, development of new criteria for binder storage stability evaluation using DSR-based test is recommended.
- The proposed DSR-based method are executed at high service temperatures. A new DSR-based method (or methods) should be developed for intermediate and low-temperature binder characterization.
- Calculation of strains and asphalt dimensioning is very laborious but pavement design optimization could save materials and resources as well as allow innovations. A simple, free analytical tool for pavement design can be developed using the approach used in VSS 40 324.

The project revealed potential advantages of using high PmB mixtures. Their use, including their use in combination with asphalt recycling, should also be promoted, considering the sustainability and resource efficiency assessment.

7 Annexes

7.1 FWD report H19 Oberalpstrasse, Infralab SA

infralab

Bericht n° : EMPA24HWDA 05-08-01319 – TS1 Nov. 2024
Version 1.0

Auftrag : Tragfähigkeitsmessungen Trin-Tamins H19 (TS1)
Bestimmung Elastizitätsmoduln

Auftraggeber: Tiefbauamt Kanton Graubünden
Herr Gion Dosch
Loëstrasse 14
CH-7001 Chur

Dieser Bericht umfasst 8 Seiten und 1 Seite Anlagen, d.h. insgesamt 9 Seiten.

Dieser Bericht darf ohne schriftliche Genehmigung von Infralab SA nicht vervielfältigt werden, auch nicht auszugsweise.

Wir weisen darauf hin, dass die Ergebnisse nur für die untersuchten Proben gültig sind.

Infralab SA
Ing. conseils et laboratoire

Rte du Vieux-Collège 4B
CH-1077 Servion

+41 21 544 09 00

info@infralab.ch
www.infralab.ch

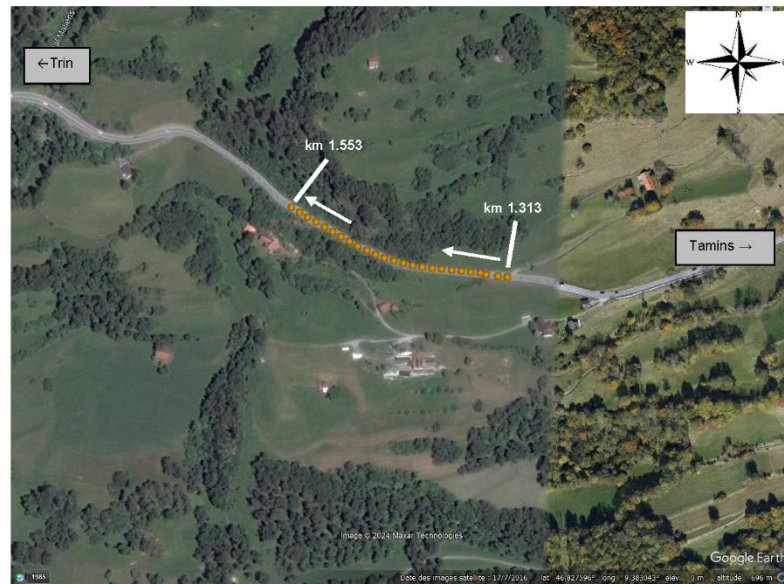
TABLE DES MATIERES

1. BAUSTELLENMESSUNGEN	3
1.1. Lage.....	3
1.2. Ziel.....	3
2. INFORMATIONEN TRAGFÄHIGKEITSMESSUNGEN MIT HWD.....	4
2.1. Beschreibung HWD-Messungen	4
2.2. Das HWD-Gerät.....	4
2.3. Berechnung Elastizitätsmodule	5
2.4. Annahmen für die Elastizitätsmodulberechnung.....	6
3. ERGEBNISSE.....	7
3.1. H19 - Richtung Trin (+)	7
4. ANHANG	9

1. BAUSTELLENMESSUNGEN

1.1. Lage

Die Infralab SA wurde am 10. September 2024 von Tiefbauamt Kanton Graubünden, vertreten durch Herrn Gion Dosch, beauftragt die Elastizitätsmoduln der Asphaltsschicht, der Kiessand und der Untergrund auf die H19 (Trin-Tamins) km 1.313 – km 1.553, Fahrspur Richtung Trin (+), zu berechnen. Um diese Aufgabe zu erfüllen, wurden am 26. September 2024 HWD-Tragfähigkeitsmessungen mit einem Messintervall von 10 m durchgeführt. Der folgende Lageplan zeigt die Lage der HWD-Messpunkte und die untersuchten Bereiche.



Lageplan [Google Earth; 2024]

1.2. Ziel

Ziel dieses Auftrags war es, die Elastizitätsmoduln der verschiedenen Schichten (Asphalt, Kiessand und Untergrund) zu berechnen.

2. INFORMATIONEN TRAGFÄHIGKEITSMESSUNGEN MIT HWD

2.1. Beschreibung HWD-Messungen

HWD-Geräte – seit mehreren Jahren weltweit die zahlenmässig führenden Deflektionsmessgeräte – sind wegen der Qualität der gelieferten Messergebnisse auch bezüglich der Interpretation absolute Spitze.



2.2. Das HWD-Gerät

Das Fallgewichtsgesetz Dynatest (auch kurz HWD-Gerät genannt aus: Heavy Falling Weight Deflectometer) dient der Messung von Deflektionsmulden unter der Impulsbelastung einer auf einer Grundplatte mit 30 cm (oder 45 cm) Durchmesser fallenden Masse. Das Messsystem besteht aus :

- dem Messanhänger mit einem Gesamtgewicht von ca. 2'000 kg mit der Belastungsvorrichtung und den Signalaufnahmesensoren,
- der EDV-gestützten Steuerungsvorrichtung mit der Auswertesoftware, welche im Zugfahrzeug eingebaut ist.

Nach der Einnahme der Messstellung am Messpunkt wird das Fallgewicht aus einer zwischen 2 und 40 cm variabel einstellbaren Höhe ausgeklinkt. Die Fallhöhe und die Belastung werden in Funktion der untersuchten Struktur gewählt. Dabei wird auf die Grundplatte eine Kraft von maximal 320 kN erzeugt. Die Lastübertragung erfolgt über ein Federungselement dessen Konstante die Belastungsdauer vorgibt. Die Deflektionen (in 1/1000 mm) werden mittels 15 seismischen Sensoren (einer davon im Zentrum der Belastungsplatte) registriert – auf einem Träger unter der Deichsel in unterschiedlichem Abstand vom Lastzentrum angebracht – welche die Aufnahme der Deformationsmulde auf einer Länge von ca. 2 m ermöglichen.

2.3. Berechnung Elastizitätsmodule

Mit Hilfe der ermittelten Deflexionsmulde und der Schichtdicken (aus den Kernbohrmentnahme /Sondagen) werden die Elastizitätsmoduln der Schichten (Asphalt, Kiessand und Untergrund) durch Rückrechnung an jedem HWD-Messpunkt bestimmt.

Die Moduln der Asphaltsschicht werden in einem ersten Schritt bei der Temperatur des Asphalts während der Messungen berechnet. In einem zweiten Schritt werden diese Module auf eine Temperatur von 15°C korrigiert. Da keine Informationen über die temperaturabhängigen Moduländerungen für die vorhandenen bituminösen Materialien vorliegen, wird eine Korrektur für Standardmaterialien gemäß der LTPP-Methode (LTPP, Juni 2000) angewendet, die eine lineare Korrektur in einem halblogarithmischen Koordinatensystem [$T^{\circ}\text{C}$, $\log E_{\text{EB}}$] mit einer Steigung von -0,0195 für Messungen in Fahrspuren vorschlägt.

Die folgende Tabelle zeigt eine Klassifizierung der durchschnittlichen Elastizitätsmodule für Standardmaterialien (vorgeschlagen von Infralab):

$E_{\text{Asphalt-15}^{\circ}\text{C}}$ [MPa]	E_{Kiessand} [MPa]	$E_{\text{Untergrund}}$ [MPa]	Klassifizierung [-]
< 3'000	<150	< 30	Sehr schwach
3'000 – 4'700	150 - 285	30 – 60	Schwach
>4'700 – 8'500	>285 - 770	>60 – 120	Genügend
>8'500 – 12'500	>770 – 1'480	>120 – 250	Hoch
>12'500	>1'480	>250	Sehr hoch

Legende:

$E_{\text{Asphalt-15}^{\circ}\text{C}}$	Mittlerer Elastizitätsmodul der Asphaltsschicht bei 15°C und 10 Hz	[MPa]
E_{Kiessand}	Mittlerer Elastizitätsmodul des Kiessandschicht	[MPa]
$E_{\text{Untergrund}}$	Mittlerer Elastizitätsmodul des Untergrunds	[MPa]

Anmerkung :

Die obige Tabelle ist nur für Standardmaterialien gültig. Die vorgeschlagene Klassifizierung basiert auf unserer Erfahrung und ist nur ein Richtwert.

Die Variationskoeffizienten, die für die Elastizitätsmoduln werden, geben Aufschluss über die Homogenität des Materials im untersuchten Gebiet. Die folgende Tabelle zeigt die Klassifizierung der Variationskoeffizienten. Je kleiner der Variationskoeffizient ist, desto homogener ist das Material.

Variationskoeffizient [-]	Klassifizierung [-]	
C.V. < 0.20	Schwach	Sehr homogen
0.20 ≤ C.V. < 0.35	Mittel	Homogen
0.35 ≤ C.V. < 0.70	Hoch	Heterogen
C.V. ≥ 0.70	Sehr hoch	Sehr heterogen

Tragfähigkeitsmessungen Trin-Tamins H19 (TS1)

2.4. Annahmen für die Elastizitätsmodulberechnung

Die Schichtdicken in der nachstehenden Tabelle wurden vom EMPA übermittelt und wurden für die Berechnung der Elastizitätsmodulen verwendet.

Von [km]	Bis [km]	Schichtdicke [mm]		
		Asphalt]	Kiessand	Untergrund
1.313	1.553	100	1'050	∞

Um die konsistentesten Moduln zu erhalten, wurde beschlossen, die ACF-Schicht als Asphaltsschicht (und nicht als Kiessandschicht) zu betrachten.

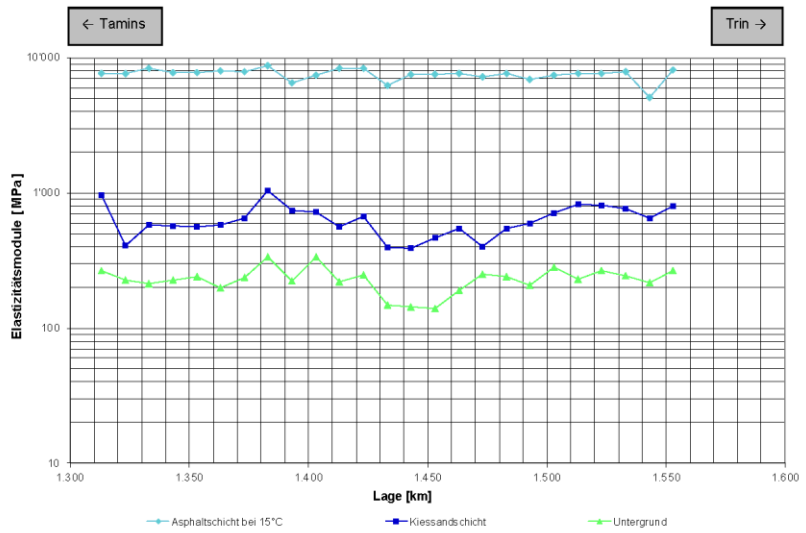
3. ERGEBNISSE

Legende:

$E_{\text{Asphalt-15°C}}$	Mittlerer Elastizitätsmodul der Asphaltschicht bei 15°C und 10 Hz	[MPa]
E_{Kiessand}	Mittlerer Elastizitätsmodul des Kiessandschicht	[MPa]
$E_{\text{Untergrund}}$	Mittlerer Elastizitätsmodul des Untergrunds	[MPa]

3.1. H19 - Richtung Trin (+)

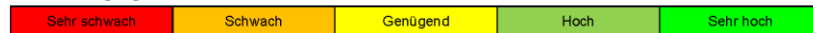
Grafik Elastizitätsmodul



Zusammenfassungstabelle

	$E_{\text{Asphalt-15°C}}$ [MPa]	E_{Kiessand} [MPa]	$E_{\text{Untergrund}}$ [MPa]
Minimum	5'055	392	140
Moyenne	7'565	638	231
Maximum	8'703	1'040	336
Ecart Type	742	169	48
Coef. Var.	0.10	0.26	0.21

Klassifizierungslegende



Tragfähigkeitsmessungen Trin-Tamins H19 (TS1)

Die folgenden Kommentare können in Bezug auf die oben genannten Ergebnisse gemacht werden:

- Der Mittelwert der Elastizitätsmoduln der Asphaltschicht wird mit einem Mittelwert von 7565 MPa als genügend eingestuft;
- Der Mittelwert der Elastizitätsmoduln der Kiessandschicht ist mit einem Mittelwert von 638 MPa genügend;
- Der Untergrund hat hohe Elastizitätsmoduln mit einem durchschnittlichen Wert von 231 MPa;
- Die Eigenschaften der Materialien werden als (sehr) homogen angesehen mit Variationskoeffizienten von 0.10, 0.26 bzw. 0.21;

Servion, den 8. November 2024

INFRALAB SA



Robert Braber
Responsable Département
Auscultation

4. ANHANG

I. Anhang 1 – Ergebnisse HWD-Messungen

Legende:

$E_{Asphalt-15^{\circ}C}$	Mittlerer Elastizitätsmodul der Asphaltschicht bei 15°C und 10 Hz	[MPa]
$E_{Asphalt}$	Mittlerer Elastizitätsmodul der Asphaltschicht bei 10 Hz	[MPa]
$E_{Kiessand}$	Mittlerer Elastizitätsmodul des Kiessandschicht	[MPa]
$E_{Untergrund}$	Mittlerer Elastizitätsmodul des Untergrunds	[MPa]

Anmerkung: Die Werte in Klammern bedeuten, dass es der Software nicht gelungen ist ein theoretisches Deflexionsmulde zu berechnen, das dem gemessenen Deflexionsmulde hinreichend nahekommt. Diese Werte, die dem Messsystem inhärent sind, werden als Ausreißer betrachtet und sind in den untenstehenden Tabellen in Klammern angegeben.

H19 - Richtung Trin (+)

station 17

Lage [km]	$E_{Asphalt-15^{\circ}C}$ [MPa]	$E_{Asphalt}$ [MPa]	$E_{Kiessand}$ [MPa]	$E_{Untergrund}$ [MPa]	Latitude [WGS84 °]	Longitude [WGS84 °]
1.313	7'683	8'185	961	265	46.82686	9.38447
1.323	7'666	8'180	405	226	46.82687	9.38434
1.333	8'329	8'853	580	214	46.82688	9.38418
1.343	7'751	8'230	570	226	46.82690	9.38410
1.353	7'761	8'234	564	240	46.82690	9.38398
1.363	7'950	8'447	581	197	46.82691	9.38385
1.373	7'851	8'316	648	235	46.82692	9.38372
1.383	8'703	9'217	1'040	334	46.82693	9.38358
1.393	6'539	6'940	744	224	46.82694	9.38346
1.403	7'456	7'897	725	336	46.82695	9.38332
1.413	8'329	8'837	565	219	46.82696	9.38320
1.423	8'329	8'840	673	248	46.82698	9.38307
1.433	6'257	6'643	396	147	46.82701	9.38294
1.443	7'571	8'034	392	143	46.82703	9.38281
1.453	7'571	8'011	467	140	46.82706	9.38269
1.463	7'663	8'103	549	189	46.82710	9.38258
1.473	7'227	7'656	398	251	46.82714	9.38245
1.483	7'666	8'131	542	238	46.82719	9.38235
1.493	6'883	7'297	593	207	46.82723	9.38223
1.503	7'458	7'897	712	281	46.82727	9.38212
1.513	7'714	8'155	821	229	46.82732	9.38201
1.523	7'704	8'146	810	266	46.82737	9.38189
1.533	7'912	8'341	763	244	46.82741	9.38178
1.543	5'055	5'320	654	217	46.82745	9.38168
1.553	8'099	8'505	801	266	46.82750	9.38156

Tragfähigkeitsmessungen Trin-Tamins H19 (TS1)

7.2 FWD report H27 Engadinerstrasse, Infralab SA

infralab

Bericht n° : EMPA24HWDA 05-08-01319 – TS2 Nov. 2024
Version 1.0

Auftrag : Tragfähigkeitsmessungen Engadinerstr. H27 (TS2)
Bestimmung Elastizitätsmoduln

Auftraggeber: Tiefbauamt Kanton Graubünden
Herr Gion Dosch
Loëstrasse 14
CH-7001 Chur

Dieser Bericht umfasst 8 Seiten und 1 Seite Anlagen, d.h. insgesamt 9 Seiten.

Dieser Bericht darf ohne schriftliche Genehmigung von Infralab SA nicht vervielfältigt werden, auch nicht auszugsweise.

Wir weisen darauf hin, dass die Ergebnisse nur für die untersuchten Proben gültig sind.

Infralab SA
Ing. conseils et laboratoire

Rte du Vieux-Collège 4B
CH-1077 Servion

+41 21 544 09 00

info@infralab.ch
www.infralab.ch

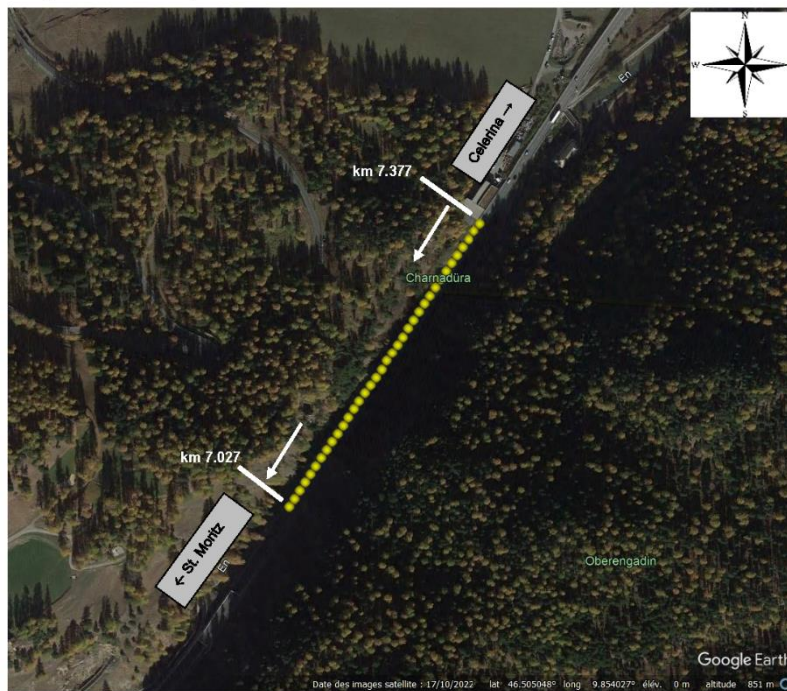
TABLE DES MATIERES

1. BAUSTELLENMESSUNGEN	3
1.1. Lage.....	3
1.2. Ziel.....	3
2. INFORMATIONEN TRAGFÄHIGKEITSMESSUNGEN MIT HWD.....	4
2.1. Beschreibung HWD-Messungen	4
2.2. Das HWD-Gerät.....	4
2.3. Berechnung Elastizitätsmodule	5
2.4. Annahmen für die Elastizitätsmodulberechnung.....	6
3. ERGEBNISSE.....	7
3.1. H27 - Richtung St. Moritz (-).....	7
4. ANHANG	9

1. BAUSTELLENMESSUNGEN

1.1. Lage

Die Infralab SA wurde am 10. September 2024 von Tiefbauamt Kanton Graubünden, vertreten durch Herrn Gion Dosch, beauftragt die Elastizitätsmoduln der Asphaltsschicht, der Kiessand und der Untergrund auf die H27 (St Moritz – Celerina), km 7.377 – km 7.027, Fahrspur Richtung St. Moritz (-), zu berechnen. Um diese Aufgabe zu erfüllen, wurden am 26. September 2024 HWD-Tragfähigkeitsmessungen mit einem Messintervall von 10 m durchgeführt. Der folgende Lageplan zeigt die Lage der HWD-Messpunkte und die untersuchten Bereiche.



1.2. Ziel

Ziel dieses Auftrags war es, die Elastizitätsmoduln der verschiedenen Schichten (Asphalt, Kiessand und Untergrund) zu berechnen.

Tragfähigkeitsmessungen Engadinerstrasse H27 (TS2)

2. INFORMATIONEN TRAGFÄHIGKEITSMESSUNGEN MIT HWD

2.1. Beschreibung HWD-Messungen

HWD-Geräte – seit mehreren Jahren weltweit die zahlenmässig führenden Deflektionsmessgeräte – sind wegen der Qualität der gelieferten Messergebnisse auch bezüglich der Interpretation absolute Spitze.



2.2. Das HWD-Gerät

Das Fallgewichtgerät Dynatest (auch kurz HWD-Gerät genannt aus: **Heavy Falling Weight Deflectometer**) dient der Messung von Deflektionsmulden unter der Impulsbelastung einer auf einer Grundplatte mit 30 cm (oder 45 cm) Durchmesser fallenden Masse. Das Messsystem besteht aus :

- dem Messanhänger mit einem Gesamtgewicht von ca. 2'000 kg mit der Belastungsvorrichtung und den Signalaufnahmesensoren,
- der EDV-gestützten Steuerungsvorrichtung mit der Auswertesoftware, welche im Zugfahrzeug eingebaut ist.

Nach der Einnahme der Messstellung am Messpunkt wird das Fallgewicht aus einer zwischen 2 und 40 cm variabel einstellbaren Höhe ausgeklinkt. Die Fallhöhe und die Belastung werden in Funktion der untersuchten Struktur gewählt. Dabei wird auf die Grundplatte eine Kraft von maximal 320 kN erzeugt. Die Lastübertragung erfolgt über ein Federselement dessen Konstante die Belastungsdauer vorgibt. Die Deflektionen (in 1/1000 mm) werden mittels 15 seismischen Sensoren (einer davon im Zentrum der Belastungsplatte) registriert – auf einem Träger unter der Deichsel in unterschiedlichem Abstand vom Lastzentrum angebracht – welche die Aufnahme der Deformationsmulde auf einer Länge von ca. 2 m ermöglichen.

2.3. Berechnung Elastizitätsmodule

Mit Hilfe der ermittelten Deflexionsmulde und der Schichtdicken (aus den Kernbohrnentnahme /Sondagen) werden die Elastizitätsmoduln der Schichten (Asphalt, Kiessand und Untergrund) durch Rückrechnung an jedem HWD-Messpunkt bestimmt.

Die Moduln der Asphaltschicht werden in einem ersten Schritt bei der Temperatur des Asphalts während der Messungen berechnet. In einem zweiten Schritt werden diese Module auf eine Temperatur von 15°C korrigiert. Da keine Informationen über die temperaturabhängigen Moduländerungen für die vorhandenen bituminösen Materialien vorliegen, wird eine Korrektur für Standardmaterialien gemäß der LTPP-Methode (LTPP, Juni 2000) angewendet, die eine lineare Korrektur in einem halblogarithmischen Koordinatensystem [$T^{\circ}\text{C}$, $\log_{10}E$] mit einer Steigung von -0,0195 für Messungen in Fahrspuren vorschlägt.

Die folgende Tabelle zeigt eine Klassifizierung der durchschnittlichen Elastizitätsmodule für Standardmaterialien (vorgeschlagen von Infralab):

$E_{\text{Asphalt-15}^{\circ}\text{C}}$ [MPa]	E_{Kiessand} [MPa]	$E_{\text{Untergrund}}$ [MPa]	Klassifizierung [-]
< 3'000	<150	< 30	Sehr schwach
3'000 – 4'700	150 - 285	30 – 60	Schwach
>4'700 – 8'500	>285 - 770	>60 – 120	Genügend
>8'500 – 12'500	>770 – 1'480	>120 – 250	Hoch
>12'500	>1'480	>250	Sehr hoch

Legende:

$E_{\text{Asphalt-15}^{\circ}\text{C}}$	Mittlerer Elastizitätsmodul der Asphaltschicht bei 15°C und 10 Hz	[MPa]
E_{Kiessand}	Mittlerer Elastizitätsmodul des Kiessandschicht	[MPa]
$E_{\text{Untergrund}}$	Mittlerer Elastizitätsmodul des Untergrunds	[MPa]

Anmerkung :

Die obige Tabelle ist nur für Standardmaterialien gültig. Die vorgeschlagene Klassifizierung basiert auf unserer Erfahrung und ist nur ein Richtwert.

Die Variationskoeffizienten, die für die Elastizitätsmoduln werden, geben Aufschluss über die Homogenität des Materials im untersuchten Gebiet. Die folgende Tabelle zeigt die Klassifizierung der Variationskoeffizienten. Je kleiner der Variationskoeffizient ist, desto homogener ist das Material.

Variationskoeffizient [-]	Klassifizierung [-]	
C.V. < 0.20	Schwach	Sehr homogen
0.20 ≤ C.V. < 0.35	Mittel	Homogen
0.35 ≤ C.V. < 0.70	Hoch	Heterogen
C. V. ≥ 0.70	Sehr hoch	Sehr heterogen

Tragfähigkeitsmessungen Engadinerstrasse H27 (TS2)

2.4. Annahmen für die Elastizitätsmodulberechnung

Die Schichtdicken in der nachstehenden Tabelle wurden vom EMPA übermittelt und wurden für die Berechnung der Elastizitätsmodulen verwendet.

Von [km]	Bis [km]	Schichtdicke [mm]		
		Asphalt]	Klessand	Untergrund
7.377	7.027	198	110	∞

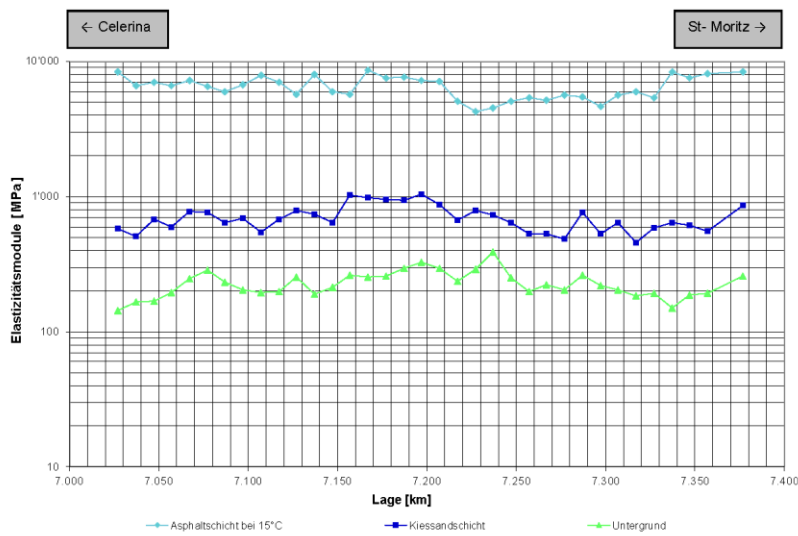
3. ERGEBNISSE

Legende:

$E_{\text{Asphalt-15°C}}$	Mittlerer Elastizitätsmodul der Asphaltsschicht bei 15°C und 10 Hz	[MPa]
E_{Kiessand}	Mittlerer Elastizitätsmodul des Kiessandschicht	[MPa]
$E_{\text{Untergrund}}$	Mittlerer Elastizitätsmodul des Untergrunds	[MPa]

3.1. H27 - Richtung St. Moritz (-)

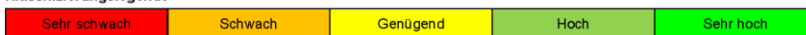
Grafik Elastizitätsmoduln



Zusammenfassungstabelle

	$E_{\text{Asphalt-15°C}}$ [MPa]	E_{Kiessand} [MPa]	$E_{\text{Untergrund}}$ [MPa]
Minimum	4'251	458	143
Moyenne	6'512	699	229
Maximum	8'602	1'039	387
Ecart Type	1'235	157	52
Coef. Var.	0.19	0.22	0.23

Klassifizierungslegende



Tragfähigkeitsmessungen Engadinerstrasse H27 (TS2)

Die folgenden Kommentare können in Bezug auf die oben genannten Ergebnisse gemacht werden:

- Der Mittelwert der Elastizitätsmoduln der Asphaltschicht wird mit einem Mittelwert von 6'512 MPa als genügend eingestuft;
- Der Mittelwert der Elastizitätsmoduln der Kiessandschicht ist mit einem Mittelwert von 699 MPa genügend;
- Der Untergrund hat hohe Elastizitätsmoduln mit einem durchschnittlichen Wert von 229 MPa;
- Die Eigenschaften der Materialien werden als (sehr) homogen angesehen mit Variationskoeffizienten von 0.19, 0.22 bzw. 0.23;

Servion, den 8. November 2024

INFRALAB SA



Robert Braber

Responsable Département
Auscultation

4. ANHANG

I. Anhang 1 – Ergebnisse HWD-Messungen

Legende:

$E_{\text{Asphalt-15°C}}$	Mittlerer Elastizitätsmodul der Asphaltschicht bei 15°C und 10 Hz	[MPa]
E_{Asphalt}	Mittlerer Elastizitätsmodul der Asphaltschicht bei 10 Hz	[MPa]
E_{Kiessand}	Mittlerer Elastizitätsmodul des Kiessandschicht	[MPa]
$E_{\text{Untergrund}}$	Mittlerer Elastizitätsmodul des Untergrunds	[MPa]

Anmerkung: Die Werte in Klammern bedeuten, dass es der Software nicht gelungen ist ein theoretisches Deflexionsmulde zu berechnen, das dem gemessenen Deflexionsmulde hinreichend nahekommt. Diese Werte, die dem Messsystem inhärent sind, werden als Ausreißer betrachtet und sind in den untenstehenden Tabellen in Klammern angegeben.

H27 - Richtung St. Moritz (-)

Lage [km]	$E_{\text{Asphalt-15°C}}$ [MPa]	E_{Asphalt} [MPa]	E_{Kiessand} [MPa]	$E_{\text{Untergrund}}$ [MPa]	Latitude [WGS84 °]	Longitude [WGS84 °]
7.027	8'328	10'330	580	143	46.50238	9.85363
7.037	6'652	8'243	511	165	46.50245	9.85370
7.047	7'048	8'723	678	168	46.50253	9.85377
7.057	6'586	8'119	592	195	46.50260	9.85384
7.067	7'218	8'907	781	246	46.50268	9.85391
7.077	6'481	8'023	768	287	46.50275	9.85398
7.087	5'944	7'366	646	234	46.50283	9.85406
7.097	6'676	8'222	685	203	46.50290	9.85413
7.107	7'919	9'765	547	194	46.50298	9.85420
7.117	7'014	8'643	676	199	46.50305	9.85428
7.127	5'701	7'006	792	254	46.50312	9.85435
7.137	7'955	9'740	737	190	46.50320	9.85442
7.147	5'945	7'278	646	213	46.50328	9.85449
7.157	5'747	7'024	1'027	261	46.50335	9.85456
7.167	8'602	10'539	981	256	46.50342	9.85464
7.177	7'577	9'285	957	259	46.50349	9.85471
7.187	7'613	9'337	943	295	46.50356	9.85479
7.197	7'271	8'966	1'039	324	46.50364	9.85486
7.207	7'146	8'796	877	296	46.50372	9.85493
7.217	5'060	6'224	669	235	46.50379	9.85500
7.227	4'251	5'187	784	290	46.50387	9.85507
7.237	4'486	5'460	728	387	46.50394	9.85514
7.247	5'059	6'125	640	251	46.50402	9.85521
7.257	5'408	6'554	532	198	46.50409	9.85528
7.267	5'134	6'196	531	224	46.50417	9.85536
7.277	5'646	6'764	483	203	46.50425	9.85543
7.287	5'448	6'519	761	260	46.50432	9.85550
7.297	4'623	5'547	533	218	46.50439	9.85558
7.307	5'647	6'827	643	203	46.50447	9.85565
7.317	5'973	7'245	458	184	46.50454	9.85572
7.327	5'404	6'561	587	194	46.50462	9.85579
7.337	8'348	10'165	643	150	46.50469	9.85587
7.347	7'558	9'194	616	187	46.50476	9.85594
7.357	8'120	9'874	554	192	46.50484	9.85602
7.377	8'329	10'232	857	258	46.50498	9.85617

Tragfähigkeitsmessungen Engadinerstrasse H27 (TS2)

Acknowledgements

This work was supported by the ASTRA and VSS under Grant VSS_2022_337 of the project "HPMix". The authors would like to thank the following for financial and in-kind contribution to the project: Swiss Federal Roads Office (FEDRO), Tiefbauamt Kanton Graubunden, and Tiefbauamt Kanton Aargau. We also thank the project's partners and supervisory committee for their valuable input.

Bibliography

- Adriana Vargas-Nordcbeck, & James A. Musselman. (2022). *Highly Modified Asphalt: How-To Document*.
- Alisov, A. (2017). Typisierung von Bitumen mittels instationärer Oszillationsrheometrie. Braunschweig.
- Alisov, A., Riccardi, C., Schrader, J., Cannone Falchetto, A., & Wistuba, M. P. (2020). A novel method to characterise asphalt binder at high temperature. *Road Materials and Pavement Design*, 21(1), 143–155.
<https://doi.org/10.1080/14680629.2018.1483258>
- Arraigada, M., Partl, M. N., Angelone, S. M., & Martinez, F. (2009). Evaluation of accelerometers to determine pavement deflections under traffic loads. *Materials and Structures/Materiaux et Constructions*, 42(6), 779–790.
<https://doi.org/10.1617/S11527-008-9423-5/FIGURES/13>
- Arshadi, A. (2014). Importance of asphalt binder properties on rut resistance of asphalt mixture.
- Barry, M. K. (2016a). An analysis of impact factors on the Illinois Flexibility test. University of Urbana-Champaign.
- Barry, M. K. (2016b). An analysis of impact factors on the Illinois Flexibility test. University of Urbana-Champaign.
- Błazejowski, K., Wójcik-Wiśniewska, M., Peciakowski, H., & Olszacki, J. (2016). The Performance of a Highly Modified Binders for Heavy Duty Asphalt Pavements. *Transportation Research Procedia*, 14, 679–684.
<https://doi.org/10.1016/J.TRPRO.2016.05.331>
- Bucheli, H. P. (2018). HiMA - Bidemittel für die Strassen der Zukunft, HiMA – Bidemittel in der Praxis. . In *Presentation at the Panovo Seminar 2018*.
<https://www.pavono.com/pavonostartseite/seminar/>.
- Chen, J. S., Wang, T. J., & Lee, C. Te. (2018). Evaluation of a highly-modified asphalt binder for field performance. *Construction and Building Materials*, 171, 539–545.
<https://doi.org/10.1016/J.CONBUILDMAT.2018.03.188>
- D'Angelo, J., Kluttz, R., Dongre, R. N., Stephens, K., & Zanzotto, L. (2007). Revision of the Superpave High Temperature Binder Specification: The Multiple Stress Creep Recovery Test (With Discussion). *Journal of the Association of Asphalt Paving Technologists*, 76.
- Edith Arámbula-Mercado, Silvia Caro, Carlos Alberto, Rivera Torres, Pravat Karki, Mauricio Sánchez-Silva, & Eun Sug Park. (2019). *Evaluation of FC-5 with PG 76-22 HP to reduce raveling*.
- Gaspar, M. S., Vasconcelos, K. L., da Silva, A. H. M., & Bernucci, L. L. B. (2017). Highly Modified Asphalt Binder for Asphalt Crack Relief Mix.
<https://doi.org/10.3141/2630-14>, 2630(1), 110–117.
<https://doi.org/10.3141/2630-14>
- Global Highways. (2012). *Modified asphalt trials in Brazil*. <https://www.globalhighways.com/wh6/feature/modified-asphalt-trials-brazil>
- Golalipour, A., Hussain, ;, Bahia, U., & Tabatabaee, H. A. (2017). Critical Considerations toward Better Implementation of the Multiple Stress Creep and Recovery

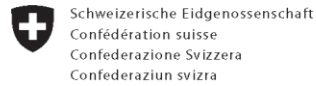
- Test. *Journal of Materials in Civil Engineering*, 29(5).
[https://doi.org/10.1061/\(ASCE\)MT.1943-5533.0001803](https://doi.org/10.1061/(ASCE)MT.1943-5533.0001803)
- Greene, J., Chun, S., & Choubane, B. (2014). Evaluation and Implementation of a Heavy Polymer Modified Asphalt Binder through Accelerated Pavement Testing.
- Habbouche, J., Boz, I., Diefenderfer, B. K., Smith, B. C., & Adel, S. H. (2021). State of the practice for high polymer-modified asphalt binders and mixtures. *Transportation Research Record*, 2675(7), 235–247.
https://doi.org/10.1177/0361198121995190/ASSET/2AE85797-B5DC-4577-BA65-6120013E54B3/ASSETS/IMAGES/LARGE/10.1177_0361198121995190-FIG4.JPG
- Habbouche, J., Hajj, E. Y., & Sebaaly, P. E. (2019). Structural Coefficient for High Polymer Modified Asphalt Mixes.
- Hofer, K., Werkovits, S., Schönauer, P., Mirwald, J., Grothe, H., & Hofko, B. (2023). Chemical and mechanical analysis of field and laboratory aged bitumen. *Road Materials and Pavement Design*, 24(S1), 160–175.
<https://doi.org/10.1080/14680629.2023.2180297>
- Hyung Lee, & Deepak Raghunathan. (2015). *Auburn-Candia Resurfacing Project*.
www.fhwa.dot.gov/hfl.
- Ignacio Kröger, & Carlos Pfeiff. (2019). *Se realizó el primer tramo experimental usando asfalto altamente modificado (HiMA) en Uruguay*.
<https://revistavial.com/se-realizo-el-primer-tramo-experimental-usando-asfalto-altamente-modificado-hima-en-uruguay/>
- Kabir, S. F., Ali, A., Purdy, C., Decarlo, C., Elshaer, M., & Mehta, Y. (2023). Thermal cracking in cold regions' asphalt mixtures prepared using high polymer modified binders and softening agents. *International Journal of Pavement Engineering*, 24(2), 2147523. <https://doi.org/10.1080/10298436.2022.2147523>
- Kluttz, R., Willis, J. R., Molenaar, A. A. A., Scarpas, T., & Scholten, E. (2012). Fatigue performance of highly modified asphalt mixtures in laboratory and field environment. *7th RILEM International Conference on Cracking in Pavements*, 687–696.
- Koyun, A., Büchner, J., Wistuba, M. P., & Grothe, H. (2022). Rheological, spectroscopic and microscopic assessment of asphalt binder ageing. *Road Materials and Pavement Design*, 23(1), 80–97.
<https://doi.org/10.1080/14680629.2020.1820891>
- Koyun, A. N., Büchner, J., Wistuba, M. P., & Grothe, H. (2021). Laboratory and field ageing of SBS modified bitumen: Chemical properties and microstructural characterization. *Colloids and Surfaces A: Physicochemical and Engineering Aspects*, 624(March), 126856. <https://doi.org/10.1016/j.colsurfa.2021.126856>
- Kozłowski, W., & Kucharski, L. (2015). New Road Pavement Technologies – Examples of Applications in Poland. *Logistics and Transport*, 28(4), 67–72.
- Leiva-Villacorta, F., Taylor, A., & Willis, R. (2017). NCAT Report 17-04: HIGH-MODULUS ASPHALT CONCRETE (HMAC) MIXTURES FOR USE AS BASE COURSE.
- Lichtsteiner, F. (2019). HiMA-Bindemittel für die Strassen der Zukunft. https://Catalogs.Spektrumbau.Ch/_pdf/Ausgabe-2016/SpektrumBau_Haupt_1_2016.Pdf.
- Lichtsteiner Felix. (2016, November). Neue Generation polymermodifizierte Bitumen: HiMA Bindemittel für besseren Asphalt. *Strasse Und Verkehr*, 19.
- Liu, H., Zeiada, W., Al-Khateeb, G. G., Shanableh, A., & Samarai, M. (2020). Use of the multiple stress creep recovery (MSCR) test to characterize the rutting potential

- of asphalt binders: A literature review.
<https://doi.org/10.1016/j.conbuildmat.2020.121320>
- Manfro, A. L., de Melo, J. V. S., & Barra, B. S. (2024). Phase Stability Evaluation of Highly Modified Asphalt with High Vinyl Content Copolymer. *Journal of Testing and Evaluation*, 52(4), 2306–2334. <https://doi.org/10.1520/JTE20230407>
- Molenaar, A. A. A., Van de Ven, M. F. C., Liu, X., Scarpas, A., Medani, T. O., & Scholten, E.-J. (2008a). Advanced mechanical testing of polymer modified base course mixes. *4th Eurasphalt & Eurobitume Congress*, 842–853.
- Molenaar, A. A. A., Van de Ven, M. F. C., Liu, X., Scarpas, A., Medani, T. O., & Scholten, E.-J. (2008b). Advanced mechanical testing of polymer modified base course mixes. *4th Eurasphalt & Eurobitume Congress*, 842–853.
- Ohio Asphalt. (2020). HiMA Performs Very Well in High-Stress Applications. *Ohio Asphalt Magazine*. <https://ohioasphaltmagazine.com/OA-Winter-2020/index.html>
- Ozer, H., Al-Qadi, I. L., Lambros, J., El-Khatib, A., Singhvi, P., & Doll, B. (2016). Development of the fracture-based flexibility index for asphalt concrete cracking potential using modified semi-circular bending test parameters. *Construction and Building Materials*, 115, 390–401.
- Pallinen, T. K., Witczak, M. W., & Bonaquist, R. (2004). Asphalt mix master curve construction using sigmoidal fitting function with non-linear least squares optimization. *Recent Advances in Materials Characterization and Modeling of Pavement Systems*, 123, 83–101. [https://doi.org/10.1061/40709\(257\)6](https://doi.org/10.1061/40709(257)6)
- Paul Fournier. (2010). *Georgia DOT Chooses Highly Modified Asphalt For Busy Intersection*. Dixie Contractor. https://www.pavementpreservation.org/wp-content/uploads/2012/05/DXC-Oct2010_feature2-2.pdf
- PERRET, J., A, D., TURTSCHY, J.-, & OULD-HENIA, M. (2001). Evaluation des performances de nouveaux matériaux de revêtement, première partie, Enrobés à haut module (Issue 1000).
- Ping, W. V., & Xiao, Y. (2012). Effect of Polymer Binder Content on Fracture Mechanics Properties of Hot Mix Asphalt Concrete. *Sustainable Transportation Systems: Plan, Design, Build, Manage, and Maintain - Proceedings of the 9th Asia Pacific Transportation Development Conference*, 599–607.
<https://doi.org/10.1061/9780784412299.0072>
- Porot, L., Jellema, E., & Bell, D. (2020). Long Lasting Asphalt Materials with Highly Modified Asphaltic Binder. *Lecture Notes in Civil Engineering*, 76, 517–527.
https://doi.org/10.1007/978-3-030-48679-2_49/FIGURES/9
- Porot, L., Jellema, E., BELL, D., & Gronniger, J. (2019a). Binder and mix evaluation of highly modified asphaltic binder. *AAPA International Flexible Pavements Conference*.
- Porot, L., Jellema, E., BELL, D., & Gronniger, J. (2019b). Binder and mix evaluation of highly modified asphaltic binder. *AAPA International Flexible Pavements Conference*.
- Porot, L., Zhu, J., Wang, D., & Falchetto, A. C. (2022). Multiple Stress Creep Recovery Test to Differentiate Polymer Modified Bitumen at High Temperature. *Journal of Testing and Evaluation*, 51(4), 2168–2178.
<https://doi.org/10.1520/JTE20220306>
- Porot, L., Zhu, J., Wang, D., Falchetto, A. C., Porot, L., Zhu, J., Wang, D., & Falchetto, A. C. (2022). *Multiple Stress Creep Recovery Test to Differentiate Polymer*

- Modified Bitumen at High Temperature Reference.*
<https://doi.org/10.1520/JTE20220306>
- Rivera, C., Caro, S., Arámbula-Mercado, E., Sánchez, D. B., & Karki, P. (2021). Comparative evaluation of ageing effects on the properties of regular and highly polymer modified asphalt binders. *Construction and Building Materials*, 302, 124163. <https://doi.org/10.1016/J.CONBUILDMAT.2021.124163>
- Rivera, C., Caro, S., Arámbula-Mercado, E., Sánchez, D. B., & Karki, P. (2022). Evaluation of the use of a HiMA binder to extend the durability of porous friction courses (PFC). *International Journal of Pavement Engineering*, 24(2). <https://doi.org/10.1080/10298436.2021.2024186>; REQUESTEDJOURNAL: JOURNAL:GPAV20; WGROU: STRING: PUBLICATION
- Rivera-Pérez, J., Ozer, H., Lambros, J., & Al-Qadi, I. L. (2021). Illinois Flexibility Index Test: Effect of Specimen Geometry and Test Configuration on the Asphalt Concrete Damage Zone. *Journal of Transportation Engineering, Part B: Pavements*, 147(1), 04020085. <https://doi.org/10.1061/JPEODX.0000243>
- Roberts, F. L., Kandhal, P. S., Brown, E. R., Lee, D. Y., & W., K. (1996). Hot Mix Asphalt Materials, Mixture Design and Construction. In *NAPA Education Foundation Second Edition*. National Asphalt Pavement Association.
- Scholten, E. J., Timm, D. H., Willis, J. R., Powell, R., Kluttz, R. Q., & Vonk, W. C. (2011). *Accelerated loading test results of two NCAT sections with highly modified asphalt.*
- Southern, M. (2015). A perspective of bituminous binder specifications. *Advances in Asphalt Materials: Road and Pavement Construction*, 1–27. <https://doi.org/10.1016/B978-0-08-100269-8.00001-5>
- Tran, N., Huber, G., Leiva, F., Pine, B., & Yin, F. (2019). NCAT Report 19-08 MIX DESIGN STRATEGIES FOR IMPROVING ASPHALT MIXTURE PERFORMANCE.
- WALAA S. MOGAWER, ALEXANDER J. AUSTERMAN, ROBERT KLUTTZ, & LOUAY N. MOHAMMAD. (2014). Development and Validation of Performance-Based Specifications for High-Performance Thin Overlay Mix. *Application of Asphalt Mix Performance-Based Specifications*. www.TRB.org
- Walther, A., Büchler, S., Cannone Falchetto, A., Wang, D., Riccardi, C., & Wistuba, M. P. (2019). Experimental investigation on asphalt mixtures prepared with reclaimed asphalt pavement and rejuvenators based on the BTSV method. *Road Materials and Pavement Design*, 20(7), 1695–1708. <https://doi.org/10.1080/14680629.2019.1594053>
- Wang, D., Zhu, J., Porot, L., Cannone Falchetto, A., & Damen, S. (2023). Multiple stress creep and recovery test for bituminous binders – influence of several key experimental parameters. *Road Materials and Pavement Design*, 24(S1), 290–308. <https://doi.org/10.1080/14680629.2023.2180992>
- Wasilewska, M., Blazejowski, K., & Pecak, P. (2017). Effect of Type of Modified Bitumen on Selected Properties of Stone Mastic Asphalt Mixtures. *4th International Conference on Road and Rail Infrastructure*, 23–25. <https://cetra.grad.hr/ocs/index.php/cetra4/cetra2016/paper/view/605>
- Williams, M. L., Landel, R. F., & Ferry, J. D. (1955). The Temperature Dependence of Relaxation Mechanisms in Amorphous Polymers and Other Glass-forming Liquids. *Journal of the American Chemical Society*, 77(14), 3701–3707.

- Willis, J. R., Timm, D. H., & Kluttz, R. (2016). Performance of a highly polymer-modified asphalt binder test section at the National Center for asphalt Technology Pavement test Track. *Transportation Research Record*, 2575, 1–9. <https://doi.org/10.3141/2575-01>
- Yin, F. (2023). Impact of Polymer Modification on IDEAL-CT and I-FIT for Cracking Resistance Evaluation of Asphalt Mixtures. <http://mdl.mndot.gov/>
- Zaumanis, M., Poulidakos, L., Arraigada, M., Kunz, B., Schellenberg, U., & Gassmann, C. (2023a). Asphalt recycling in polymer modified pavement: A test section and recommendations. *Construction and Building Materials*, 409(November), 134005. <https://doi.org/10.1016/j.conbuildmat.2023.134005>
- Zaumanis, M., Poulidakos, L., Arraigada, M., Kunz, B., Schellenberg, U., & Gassmann, C. (2023b). Asphalt recycling in polymer modified pavement: A test section and recommendations. *Construction and Building Materials*, 409(November), 134005. <https://doi.org/10.1016/j.conbuildmat.2023.134005>
- Zaumanis, M., Poulidakos, L. D., Boesiger, L., Kunz, B., Mazzoni, H., Bruhin, P., Löttscher, D., & Schellenberg, U. (2023a). *Highly Recycled Asphalt Pavement (High-RAP)*. <https://www.empa.ch/web/s308/highrap>
- Zaumanis, M., Poulidakos, L. D., Boesiger, L., Kunz, B., Mazzoni, H., Bruhin, P., Löttscher, D., & Schellenberg, U. (2023b). *Highly Recycled Asphalt Pavement (High-RAP)*.
- Zaumanis, M., Poulidakos, L. D., & Partl, M. N. (2018). Performance-based design of asphalt mixtures and review of key parameters. *Materials and Design*, 141, 185–201. <https://doi.org/10.1016/j.matdes.2017.12.035>
- Zeida, W., Liu, H., Ezzat, H., Al-Khateeb, G. G., Shane Underwood, B., Shanableh, A., & Samarai, M. (2022). Review of the Superpave performance grading system and recent developments in the performance-based test methods for asphalt binder characterization. *Construction and Building Materials*, 319(December 2021), 126063. <https://doi.org/10.1016/j.conbuildmat.2021.126063>

Project conclusion



Eidgenössisches Departement für
Umwelt, Verkehr, Energie und Kommunikation UVEK
Bundesamt für Strassen ASTRA

FORSCHUNG IM STRASSENWESEN DES UVEK

Version vom 09.10.2013

Formular Nr. 3: Projektabschluss

erstellt / geändert am: 26.11.2025

Grunddaten

Projekt-Nr.: VSS_2022_337

Projekttitel: Standardisation of Highly Polymer-Modified Asphalt Mixtures (HPMix)

Enddatum: 31.03.2026

Texte

Zusammenfassung der Projektergebnisse:

In einem typischen polymermodifizierten Bindemittel (PMB) liegt der Polymergehalt zwischen 2.5 und 3.5 Masseprozent des Asphaltbindemittels, während hochpolymermodifizierte Bindemittel (High-PMB) typischerweise einen Polymergehalt von 6-8 % aufweisen. Im Vergleich zu konventionellen PMBs werden als Vorteile von High-PMB eine längere Lebensdauer des Belags, eine verbesserte Spurrinnen- und Rissbeständigkeit genannt. Ausserdem wird erwartet, dass sowohl eine geringere Belagsdicke als auch ein erhöhter Anteil an recyceltem Asphalt in solchem Mischgut möglich ist. Das derzeitige Fehlen von Kriterien zur Normierung der Verwendung von High-PMBs schränkt deren Anwendung ein und verursacht Probleme bei der Qualitätskontrolle. Das HPMix Projekt bestand aus drei Teilen:

1) Bei der Prüfung von Bindemitteln wurde festgestellt, dass die derzeit verwendeten Prüfverfahren, mit Ausnahme der Penetrationsprüfung, für die Normierung von High-PMB nicht geeignet sind. Stattdessen wird vorgeschlagen, sich bei der Prüfung hauptsächlich auf die DSR-basierten BTSV- und/oder MSCR-Prüfverfahren zu stützen. Es wurden Verbesserungen für die Prüfverfahren sowie neue Qualitätskontrollkriterien vorgeschlagen, darunter Kriterien für die Bindemittelklassifizierung, die Bewertung der Alterungsbeständigkeit und die Verarbeitbarkeit.

2) Bei den Mischgutprüfungen wurden zwei Testabschnitte in Graubünden (AC B 22 S, AC 8 S) erstellt und ein bestehender Testabschnitt in Aargau (SDA 4-12) bewertet. Die Ergebnisse zeigten deutliche Vorteile der Verwendung von High-PmB im Vergleich zu herkömmlichem PMB CH-E-Bitumen. Die Ermüdungs- und Kältebeständigkeit waren laut Mischgutprüfungen besser, während Prüfungen mit rückgewonnenem Bindemittel auch Vorteile in Bezug auf Elastizität und Hochtemperaturverhalten zeigten, die wahrscheinlich zu einer verbesserten Spurrinnenbeständigkeit führen würden. Die Bewertung der Spurrinnenbeständigkeit und des Kornausbruchs ergab keine Vorteile für die Verwendung von High-PmB, was jedoch wahrscheinlich auf die ungeeigneten Standardprüfmethoden zurückzuführen ist. Die Steifigkeit der HPMix- und herkömmlichen PMB-Mischungen war ähnlich. Mit High-PMB war es möglich, mindestens 40 % RAP hinzuzufügen und trotzdem die von CH-E-Bindemitteln geforderte Performance zu erreichen.

3) In der Belagsdimensionierung wurden die Ergebnisse der Mischgut- und Belagsprüfungen (unter Verwendung von Bohrkernen und FWD) verwendet, um ein mechanistisches FEM-Berechnungsmodell zur Bestimmung der Tragfähigkeitswerte für High-PMB zu erstellen. Die Berechnungen wurden mit der FEM-Software Comsol Multiphysics durchgeführt und ermöglichten die Bestimmung der Dehnungen in den Belagsschichten. Je nach Belagsdicke, Temperatur und Verkehrsgeschwindigkeit variierten die berechneten Tragfähigkeitswerte zwischen 4.4 und 6.9. Es wird vorgeschlagen, den Wert 4.4 mit dem mobilen Verkehrslastsimulator zu validieren.



Schweizerische Eidgenossenschaft
Confédération suisse
Confederazione Svizzera
Confederaziun svizra

Eidgenössisches Departement für
Umwelt, Verkehr, Energie und Kommunikation UVEK
Bundesamt für Strassen ASTRA

Zielerreichung:

Im HPmix-Projekt wurden die Projektziele erreicht. Im Einzelnen:

*Es werden neue Prüfmethoden und Kriterien für die Standardisierung von hochmodifizierten Bindemitteln vorgeschlagen. Die Prüfmethoden und Kriterien sind im Bericht zusammengefasst.

*Für die Standardisierung von Mischungsprüfungen wird derzeit empfohlen, keine neuen Prüfverfahren oder Kriterien für HPmix-Prüfungen zu verwenden, da ein Teil der Eigenschaften anhand von Bindemittelprüfungen bewertet werden kann, während für die Bewertung anderer Eigenschaften (wie die Spurrinnenbeständigkeit) das derzeitige Prüfverfahren nicht streng genug ist. Es wird deshalb empfohlen, ein neues Verfahren für die Prüfung der Spurrinnenbeständigkeit zu entwickeln.

*Für HPmix wurde ein neuer Tragfähigkeitswert vorgeschlagen. Damit lässt sich eine potenzielle Verringerung der Belagsstärke oder eine mögliche Verlängerung der Lebensdauer des Belags berechnen. Eine Validierung des vorgeschlagenen Tragfähigkeitswerts wird empfohlen.

Folgerungen und Empfehlungen:

*Im Rahmen dieser Forschung wurde ein Tragfähigkeitswert für Mischgut mit hohem PmB-Gehalt vorgeschlagen. Eine Validierung dieser Ergebnisse wird durch den Bau und die Untersuchung einer entsprechenden Teststrecke empfohlen.

*Es hat sich gezeigt, dass die aktuellen Prüfbedingungen zur Bestimmung der Spurbildung nicht ausreichen, um einen Unterschied zwischen einem herkömmlichen PmB- und einem Mischgut mit hohem PmB-Gehalt nachzuweisen. Daher wird die Entwicklung neuer Prüfbedingungen oder die Validierung einer anderen Prüfmethode, beispielsweise der Druckschwellversuch, empfohlen.

Publikationen:

Zaumanis, M., Arraigada, M., & Hugener, M. (2025). Towards the development of classification criteria for highly polymer-modified binders. Road Materials and Pavement Design, 1–27. <https://doi.org/10.1080/14680629.2025.2481993>

Der Projektleiter/die Projektleiterin:

Name: Zaumanis

Vorname: Martins

Amt, Firma, Institut: Empa

Unterschrift des Projektleiters/der Projektleiterin:

Digitally signed by
Martins Zaumanis
Date: 2025.11.27
17:29:09 +01'00'



Schweizerische Eidgenossenschaft
Confédération suisse
Confederazione Svizzera
Confederaziun svizra

Eidgenössisches Departement für
Umwelt, Verkehr, Energie und Kommunikation UVEK
Bundesamt für Strassen ASTRA

FORSCHUNG IM STRASSENWESEN DES UVEK

Formular Nr. 3: Projektabschluss

Beurteilung der Begleitkommission:

Beurteilung:

Die Forschungsarbeit gibt einen breit abgestützten Überblick über die Eigenheiten von hochmodifizierten Bindemitteln und ihren Verwendung in unterschiedlichen Asphalten, sowohl im Labor als auch auf Teststrecken. Die gesetzten Ziele konnten weitgehend erreicht werden. Wo keine direkten Eigenschaften definiert wurden, wurden entsprechende Prüfverfahren vorgeschlagen. Der Bericht enthält auch Hinweise darauf, bei welchen Prüfmethoden Verbesserungspotential besteht.

Umsetzung:

Die Laborprüfungen wie auch die Teststrecken wurden im vorgegebenen Zeitrahmen realisiert. Der Schlussbericht ist klar strukturiert, die Begleitkommission wurde über die jeweiligen Projektphasen rechtzeitig informiert.

weitergehender Forschungsbedarf:

Um gewisse Bindemittleigenschaften klarer definieren zu können, braucht es einen breiter abgestützten Datensatz. Im Bericht wird vorgeschlagen, den Spurrinntentest zu verbessern, um den Einfluss unterschiedlicher Bindemittel klarer herausarbeiten zu können. Es wird dringlichst empfohlen, die gefundenen a-Werte zur Dimensionierung mit weiteren Versuchen einzuschränken und so einen praktikablen a-Wert herauszuarbeiten.

Einfluss auf Normenwerk:

Der Bericht enthält diverse Hinweise für die zuständige Normkommission Die sind zunächst zu prüfen, bevor normiert werden kann.

Der Präsident/die Präsidentin der Begleitkommission:

Name: Horat

Vorname: Martin

Amt, Firma, Institut: Tiefbauamt der Stadt Zürich

Unterschrift des Präsidenten/der Präsidentin der Begleitkommission:

Horat
Martin

Digital signiert von Horat Martin
DN: cn=Horat Martin,
email=Martin.Horat@zuef.ch
Datum: 2025.11.27 10:57:18
+01'00'